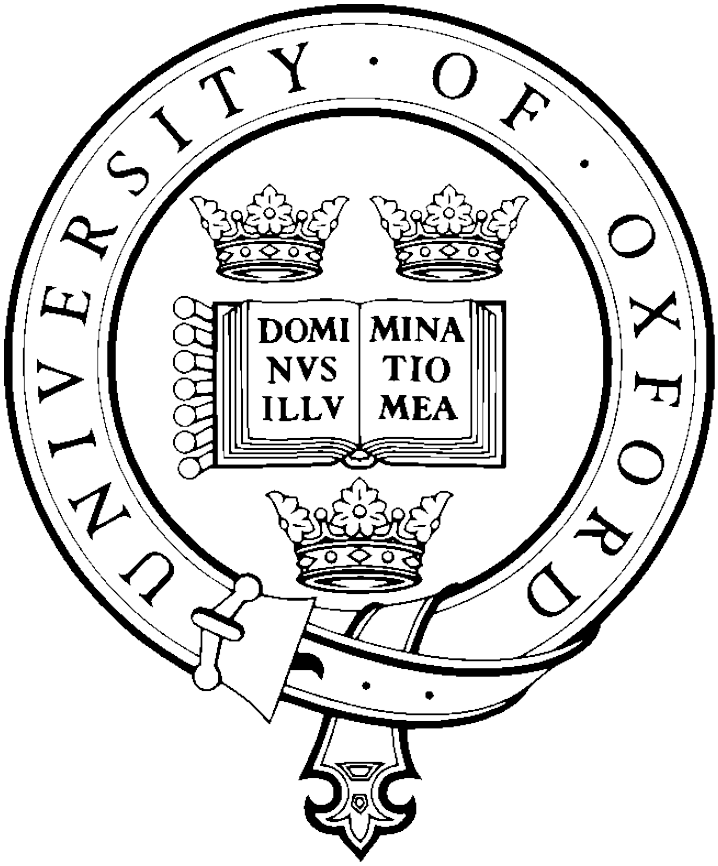
HSV-1 amplicons; a non-integrating, high transgene capacity tool for the generation and differentiation of induced pluripotent stem cells



Thesis submitted to the department of Physiology, Anatomy and Genetics towards the degree of Doctor of Philosophy

Anna Rachel Popplestone,
Brasenose College, University of Oxford
Trinity term 2013

This work was funded by the Medical Research Council.

For my parents, Andrew and Patricia Popplestone.

Abstract

HSV-1 amplicons; a non-integrating, high transgene capacity tool for the generation and differentiation of induced pluripotent stem cells.

Anna Popplestone, Brasenose College. Thesis submission for Doctor of Philosophy degree, Trinity term 2013.

Induced pluripotent stem (iPS) cells are valuable for generating patient-specific disease models. Many reprogramming systems have been developed however some technological concerns remain including insertional mutagenesis caused by integrating viruses, low efficiency and low transgene capacity.
Herpes simplex virus type-1 (HSV-1) amplicons address the main limitations of current reprogramming methods as they are non-integrating and have a large transgene capacity of 150 Kb. In addition HSV-1 amplicons have a high transduction efficiency in both primary fibroblasts and iPS cells. We have developed three sets of HSV-1 amplicons to reprogram fibroblasts to iPS cells, directly differentiate fibroblasts to dopaminergic neurons and aid dopaminergic neuron differentiation from iPS cells.

1) We constructed and characterised a set of HSV-1 reprogramming amplicons, which express the reprogramming factors Oct-4, Sox-2, Klf-4, C-Myc, Nanog and Lin28. These vectors were capable of generating partially reprogrammed colonies as confirmed by RT-PCR analysis of pluripotency factors. We were unable to generate fully reprogrammed colonies and our results suggest that this is due to an induction of the p53 pathway.

2) We constructed an HSV-1 direct differentiation amplicon containing the polycistronic cassette Mash-1, Nurr-1 and Lmx1a. All elements were functional however we were unable to generate dopaminergic neurons.

3) We constructed and characterised a set of HSV-1 neuronal differentiation amplicons expressing the neuronal transcription factors Nurr-1, Lmx1a, FoxA2 and PitX3. We employed a 96 well differentiation protocol and transduced the differentiating cultures with our neuronal amplicons to try and improve dopaminergic neuron efficiency. Transduction at early time points in the protocol resulted in a significant increase in TH positive neurons.

Acknowledgements

This thesis and DPhil could not have been achieved without the intellectual and emotional support provided both at home and in the laboratory. Firstly, I would like to thank my supervisors Dr. Richard Wade-Martins and Professor William James, who were kind enough to take me on and have been a pleasure to work for. I would like to thank Richard for his expert knowledge and advice on vectors and HSV-1 amplicons, which have been integral to this project. I especially appreciate Richard's patience and understanding during the last four years, as he has always supported my decisions and ideas.

Equally, I would also like to thank William for our regular "confessions" which have been invaluable to my scientific development. William's brilliant ideas and expertise have been a great source of inspiration during my DPhil and have kept me motivated when the research has been tough. Many thanks go to James lab members, Dr. Sally Cowley, for her expertise and advice on reprogramming and Jane Vowles, for her endless supply of patient fibroblasts and embryoid bodies for our differentiation experiments.

Special thanks go to Dr. Michele Lufino, whose expertise and daily advice have been essential to my personal development as a scientist. Michele has also been a wonderful friend and his emotional support has helped me through the highs and lows of the DPhil. I would also like to thank Dr. Elizabeth Hartfield for her superb knowledge and guidance on dopaminergic differentiation. Liz has been a role model, a mentor and a great friend and I will miss working with her and discussing ideas.

I would especially like to thank the many past and present members of the Wade-Martins lab who made me feel so welcome when I joined the lab four years ago. The fun and collaborative nature of the lab has been a nurturing and engaging environment to work in and I have enjoyed my time here immensely. Dr. Tara Caffery, in addition to always keeping the lab morale high, she has always been extremely helpful and has been fun to share a lab bench with. Thanks also go to Hugo Fernandes and Dr. Jennifer Badger for kindly feeding my cells on occasions when I was on holiday, Paul Robertson for helping me with the FACs machine, Ana Silva for help with thesis printing. In addition, I would like to thank Rosalind Roberts, Milena Cioroch and Ruxandra Mutihac for their friendship and support during my time here.

I would like to acknowledge my parents, who have always nurtured my academic goals, both emotionally and financially, and I am truly grateful for their support and encouragement. My dad, Andy, has offered many anecdotes and advice based on his own PhD experience and my wonderful mum, Patricia, and my sisters, Emma and Sara, have always been there to listen and help whenever needed. It has been a welcome escape to retreat to Bath and spend quality time with Emma when I have needed a weekend off. In addition, my housemates, Ellie and Siriol, have supplied endless cups of tea during the write-up process and along with my other friends, have been vital to maintaining my mental well-being. Last but certainly not least, I could not have got through my final year without Jake. His love and positivity have kept me in high spirits and his understanding and support through the final phase has made everything so much easier. Thank you!

Table of contents

Abstract		3
Acknowledgements		4
Table of contents		6
List of tables		13
List of figures		14
Chapter 1	General Introduction	20
1.1	Pluripotency and embryonic stem cells	20
1.2	Cellular reprogramming	21
1.2.1	Somatic cell nuclear transfer	21
1.2.2	Cell fusion studies	22
1.2.3	Induction of pluripotency by exogenous expression of transcription factors	24
1.3	Role of reprogramming factors in pluripotency	26
1.3.1	Sox-2	27
1.3.2	Oct-4	28
1.3.3	Klf-4	28
1.3.4	C-Myc	30
1.3.5	Nanog	31
1.3.6	Lin-28	33
1.4	Chromatin states in pluripotent and differentiated cells	35
1.5	Role of reprogramming factors in chromatin regulation and transcriptional changes	36

1.6	Measurable signs of dedifferentiation	38
1.7	Insertional mutagenesis of lentiviral and retroviral vectors	41
1.8	Non-integrating and excisable reprogramming methods	45
1.8.1	Viral vectors	46
1.8.1.1	Non-integrating viral vectors	46
1.8.1.2	Cre-Excision of integrating viral vectors	49
1.8.2	Non-viral vectors	53
1.8.2.1	Transient and episomal plasmid transfection	53
1.8.2.2	Transposons	54
1.8.2.3	Messenger RNA reprogramming	55
1.8.2.4	Protein mediated reprogramming	56
1.8.2.5	Small molecules	57
1.9	A need for an improved reprogramming method	63
1.10	Wild type Herpes Simplex type-1 virus (HSV-1), HSV-1 amplicons and host defence mechanisms	63
1.11	Application of iPS cells to model disease	69
1.11.1	Application of iPS cells to model Parkinson's disease	70
1.11.2	PD patient derived iPSC disease models	71
1.11.2.1	SNCA	71
1.11.2.2	LRRK2	72
1.11.2.3	PARK2	73
1.11.2.4	PINK-1	74
1.11.3	Drug screening using patient derived neurons	75

1.12	Differentiation of dopaminergic (DA) neurons in embryogenesis	76
1.12.1	Midbrain factors – FGF8, Engrailed and Wnt genes	80
1.12.2	DA factors – Pitx3, Lmx1a/b, FoxA1/2, Ascl1 and Nurr1	82
1.12.3	Improving DA neuron differentiation efficiency	84
1.13	Aims	85
Chapter 2	Materials and methods	87
2.1	Vector construction	87
2.1.1	Bacterial culture	88
2.1.1.1	Plasmid DNA purification (Minipreps)	88
2.1.1.2	Plasmid DNA purification (Maxipreps)	89
2.1.1.3	Electrocompetent cells	90
2.1.1.4	Bacterial DMSO stocks	91
2.1.2	DNA manipulation	91
2.1.2.1	Polymerase Chain Reaction (PCR)	92
2.1.2.2	Gel electrophoresis	94
2.1.2.3	Restriction digests	95
2.1.2.4	DNA purification from agarose gels	95
2.1.2.5	DNA purification from other preparations	96
2.1.2.6	Creating cohesive ends	97
2.1.2.7	Dephosphorylation of 5’ ends	97
2.1.2.8	Ligation	98
2.1.2.9	Electroporation	99

2.1.2.10	DNA sequencing	99
2.2	Vector characterisation	101
2.2.1	General cell culture	101
2.2.1.1	Cell counting	103
2.2.1.2	Long term storage of cell lines	103
2.2.1.3	Transfection	104
2.2.1.4	Vector Packaging into HSV-1 amplicons	104
2.2.1.5	Titration of HSV-1 amplicon stocks	105
2.2.1.6	Transduction	106
2.2.2	Transgene expression	106
2.2.2.1	RNA extraction	106
2.2.2.2	Reverse transcription	107
2.2.2.3	Protein extraction	108
2.2.2.4	Western blotting	109
2.2.2.5	Immunocytochemistry	110
2.2.3	Clonal cell lines and Episomal Plasmid Rescue	111
2.2.4	Ganciclovir sensitivity assay	112
2.2.5	MTT assay	113
2.3	Reprogramming, direct differentiation and dopaminergic differentiation experiments	114
2.3.1	Reprogramming experiments	115
2.3.2	Stem cell transduction efficiency	117
2.3.3	FACs staining	117
2.3.4	Direct differentiation	118

2.3.5	Dopaminergic neuron differentiation	118
2.4	Characterisation of reprogramming, direct differentiation and neural transcription factor delivery experiments.	119
2.4.1	RNA extraction from single EBs and reprogramming samples	119
2.4.2	Marker gene analysis	120
2.4.3	Semi-quantitative RT-PCR	121
2.4.4	Quantitative RT-PCR	122
2.4.5	Cell counting analysis of immuno-stained cells	123
		124
Chapter 3	- Construction and characterisation of HSV-1 amplicon reprogramming vectors	124
3.1	Introduction	129
3.2	Vector construction	129
3.3	Vector confirmation	131
3.4	Effect of SOKM expression on amplicon titres	134
3.5	Replacing the immediate early cytomegalovirus promoter (pCMV)	137
3.5.1	Confirmation of correct pCMVTetO2 insertion	139
3.5.2	Functionality of the CMVTetO2 promoter	141
3.6	Vector characterisation	143
3.7	Reprogramming experiments	147
3.8	Summary and conclusions	153

Chapter 4	Improvement of HSV-1 amplicon reprogramming vectors	156
4.1	Introduction	156
4.2	Vector construction	162
4.3	Vector construction validation	165
4.4	Vector characterisation	166
4.5	Cellular reprogramming experiments	168
4.6	Potential reprogramming barriers	174
4.6.1	Candidate reprogramming barrier genes	178
4.6.2	RT-PCR analysis of barrier genes	179
4.6.3	Analysis of barrier genes by qRT-PCR	179
4.6.4	Analysis of barrier genes by Western blot	182
4.6.5	P53 inhibition by Pifithrin-α	184
4.7	Summary and Conclusions	188
Chapter 5	Developing an HSV-1 amplicon vector for direct differentiation.	193
5.1	Introduction	193
5.2	Vector construction	198
5.3	Vector confirmation	200
5.4	Vector characterisation	201
5.5	Direct differentiation experiments	203
5.6	Conclusion and summary	207

Chapter 6	Delivery of HSV-1 neural transcription factor vectors to enhance dopaminergic differentiation.	209
6.1	Introduction	209
6.1.1	Neurotrophic factors	210
6.1.2	SMAD inhibition	211
6.1.3	Neuronal transcription factors	211
6.2	Transduction efficiency of iPS and Neural precursor cells	215
6.3	Vector construction	216
6.4	Vector confirmation	217
6.5	Vector characterisation	220
6.6	NTF vector packaging	221
6.7	Dopaminergic neuron differentiation protocol	222
6.8	DA neuronal cultures HSV-1 amplicon transduction optimisation	224
6.9	Dopaminergic neuron differentiation transduction time points	225
6.9.1	Analysis of cultures transduced at Nim1 time point.	228
6.9.2	Analysis of cultures transduced at Nim2 time point	229
6.9.3	Analysis of cultures double transduced at Nim1 and Nim2 time points	231
6.9.4	Analysis of cultures transduced at BASF time point	232
6.9.5	Analysis of cultures transduced at final differentiation time point	233
6.10	Conclusion and summary	234

Chapter 7	General Discussion	239
7.1	Aims	239
7.2	Summary of findings	240
7.3	HSV-1 amplicons and reprogramming barriers	241
7.4	HSV-1 amplicons and direct differentiation	242
7.5	HSV-1 amplicons and dopaminergic neuronal differentiation experiments	248
7.6	Wild type HSV-1 and p53 induction	255
7.7	Future of iPS technology	257
7.8	Conclusions and future work	257
References		259

List of Tables

Chapter	Table	Table title	Page
1	1	Reprogramming efficiencies of integrating viral vectors.	42
2	1	General laboratory reagents	86
2	2	Expand High Fidelity PCR reagents	91
2	3	Table 3 – AmpliTaq gold reagents	92
2	4	Primers used in cloning transgenes	93
2	5	Sequencing primers used in Chapters 5 and 6	99

2	6	Junction PCR primer sequences	107
2	7	Antibodies used in Western blot	109
2	8	Antibodies used in Immunocytochemistry	110
2	9	Marker gene RT-PCR primers	120
2	10	Semi quantitative RT-PCR primers	121
3	1	Vectors used and constructed in chapter 3	128
4	1	Vectors used and constructed in chapter 4.	162
4	2	Primers designed to amplify the P2A-Oct-4 sequence from the pHGCX+SOKM+EBNA+TK+TetO2 vector	163
4	3	List of pluripotency marker primers used in RT-PCR analysis of partially reprogrammed colonies	172
5	1	Vectors used and constructed in chapter 5	198
6	1	Vectors used and constructed in chapter 6	216

List of Figures

Chapter	Figure	Figure title	Page
1	1	Schematic of “Yamanaka reprogramming” using retroviral vectors expressing the four reprogramming factors Sox-2, Oct-4, Klf-4 and C-Myc (SOKM)	26
1	2	Viral reprogramming methods.	52
1	3	Non-viral reprogramming methods.	62
1	4	HSV-1 amplicon vector packaging by “helper BAC” plasmids	68
1	5	Application of iPS cells.	69

1	6	Inductive signalling of SHH and BMP during ectoderm neuralisation	76
1	7	Factors involved in dopaminergic neuron development	80
1	8	HSV-1 amplicon vectors	86
3	1	Plasmid maps of source vectors containing the expression cassettes used to construct the new iPS HSV-1 amplicon vectors	129
3	2	Construction of HSV-1 amplicon iPS vectors by serial restriction digests and ligations	131
3	3	Restriction enzymes digest analysis of final HSV-1 amplicon vectors	132
3	4	Packaging of HSV-1 reprogramming amplicons	134
3	5	Toxic effect of SOKM expression during packaging results in significantly lower HSV-1 amplicon titres which can be rescued by removal of the CMV promoter	135
3	6	Construction of pCMVTetO2 HSV-1 amplicon iPS vectors by restriction digest and ligation	137
3	7	Restriction enzymes digest analysis of final pCMVTetO2 HSV-1 amplicons	139
3	8	Confirmation of pCMVTetO2-SOKM repression when co-transfected with the tetracycline repressor	141
3	9	Western blot confirmation of Sox-2, Oct-4, Klf-4 and C-Myc protein expression transfected and transduced MRC5-V2 cells	143
3	10	Ganciclovir assay confirmation of thymidine kinase gene function	144
3	11	Episomal rescue and analysis of clonal cell lines transfected with the pHGCX+SOKM+EBNA+TK+TetO2 plasmid after 2 months of continuous cell culture	145

3	12	MTT absorbance assay of HSV-1 amplicons	146
3	13	Timeline of reprogramming protocol	148
3	14	HSV-1 amplicon reprogramming experiments in human donor fibroblasts (MKO82), human fetal fibroblasts (MRC5) and mouse embryonic fibroblasts (MEFs)	150
3	15	Confirmation of ectopic factor expression in transduced primary fibroblasts by RT-PCR	151
4	1	Vector construction of pHGCX+SOKMO+EBNA+TK+TetO2 by PCR, digest and ligation	164
4	2	Vector construction of pHGCX+OSNL+EBNA+TK+TetO2 by restriction digest and ligation	165
4	3	Restriction enzyme digest analysis and corresponding plasmid maps of pHGCX+SOKMO+EBNA+TK+TetO2 and pHGCX+OSNL+EBNA+TK+TetO2	166
4	4	Reprogramming factor expression confirmation in A)pHGCX+SOKMO+EBNA+TK+TetO2 and B)pHGCX+OSNL+EBNA+Tk+TetO2	167
4	5	Morphological analysis of partially reprogrammed colonies	169
4	6	RT-PCR analysis of partially reprogrammed colonies	173

4	7	Effect of HSV-1 amplicons on Sendai virus colony formation	176
4	8	Effect of HSV-1 SOKMO-OSNL amplicons on Sendai virus colony formation	177
4	9	Quantative real time PCR (qPCR) analysis of cells transduced with Sendai virus +/- HSV-1 amplicon	181
4	10	Western blot analysis of phosphorylated p53 and p53	183
4	11	Sendai virus colony formation assay in the presence of Pifithrin-α	185
4	12	Heat inactivation of HSV-1 amplicons and their effect on Sendai virus colony formation	187
5	1	FUW-ANL sequence and primer binding sites	199
5	2	Construction of HSV-1 amplicon iDA vectors by restriction enzyme digest and ligations	200
5	3	Restriction enzyme digest analysis of final HSV-1 amplicon iDA vector	201
5	4	Confirmation of iDA factor RNA expression in pHGCX+ANL+EBNA+TetO2 transfected MRC5-V2 cells	202
5	5	Confirmation of iDA factor protein expression in pHGCX+ANL+EBNA+TetO2 transfected MRC5-V2 cells	203
5	6	Transduction of primary fibroblasts (MRC5) and mouse embryonic fibroblasts (MEFs) with HSV-1 amplicons pHGCX+ANL+EBNA+TetO2 and pHGCX	204

5	7	Immuno staining and quantification of iDA cultures stained with dopaminergic neuron marker Tyrosine hydroxylase (TH) and neuronal marker beta III tubulin (btub)	206
6	1	HSV-1 amplicon transduction of iPS cells and NPCs	215
6	2	Vector construction of NTF HSV-1 amplicon vectors by PCR, digest and ligation	218
6	3	Restriction enzyme digest analysis and corresponding plasmid maps of pHGCX+FoxA2+EBNA+TetO2, pHGCX+LMX1A+EBNA+TetO2, pHGCX+Nurr1+EBNA+tetO2 and pHGCX+PITX3+EBNA+TetO2	219
6	4	Confirmation of LMX1A, PITX3, Foxa2 and Nurr1 protein expression in NTF transfected HEK cells	220
6	5	Immunocytochemistry confirmation of Foxa2, LMX1A, Nurr 1 and PITX3 protein expression in NTF transfected HEK cells	221
6	6	Dopaminergic differentiation protocol and timeline	223
6	7	Transduction of Dopaminergic Neuronal cultures with HSV-1 amplicons	226
6	8	RT-PCR analysis and immunocytochemistry confirmation of neuronal marker expression in dopaminergic neuronal cultures	227
6	9	qPCR analysis of TH and PAX6 expression in neuronal cultures transduced at the Nim1 time point	229

6	10	qPCR analysis of TH and PAX6 expression and quantification of TH positive cells in neuronal cultures transduced at the Nim1 time point	230
6	11	qPCR analysis of TH and PAX6 expression in neuronal cultures double transduced at the Nim1 and Nim2 time points	231
6	12	qPCR analysis of TH and PAX6 expression and quantification of TH positive cells in neuronal cultures transduced at the BASF time point	232
6	13	Quantification of TH positive cells in neuronal cultures transduced at the Final differentiation time point	233
7	1	p53 pathway in response to DNA damage and cellular stress	245
7	2	Action of small molecule inhibitors on p53 homeostasis	246
7	3	Viral structure and gene expression of A) wild type HSV-1 virions and B) HSV-1 amplicon virions	249
7	4	p53 regulation in stressed and unstressed cells	253
7	5	p53 regulation upon wild type HSV-1 and HSV-1 amplicon transduction	254

Chapter 1 – General Introduction

1.1 Pluripotency and embryonic stem cells

Pluripotency is defined as a stem cell's ability to self renew and potentially differentiate into any of the three primary germ layers; mesoderm, endoderm and ectoderm. During mammalian development, the pluripotent stem cells reside in the inner cell mass of the blastocyst in the developing embryo. Embryonic stem (ES) cells were first derived from mouse blastocysts by two independent groups in 1981 [1, 2]. The ES cells were karyotypically normal, grew rapidly in culture, generated embryoid bodies under feeder free conditions and generated teratomas when injected into mice [1, 2].

Human ES cells were later generated from cleavage stage embryos derived from *in vitro* fertilisation in 1998[3]. The resulting ES cells were capable of proliferating continuously in culture for up to eight months without differentiation. The ES cells had a high nucleus to cytoplasm ratio and displayed colony morphology similar to that seen in rhesus monkey ES cells. In addition, the ES cells expressed high levels of telomerase, consistent with the high levels of telomerase activity seen in germ cells and embryonic tissues. Resulting ES cells were karyotypically normal, and express known non-human primate ES-cell surface markers such as SSEA4, TRA-1-60, TRA-1-81 and alkaline phosphatase. The human ES lines generated teratomas containing tissues of all three primary germ layers when injected into severe combined immunodeficient (SCID) mice and generated endoderm and trophoblast differentiation in vitro [3].

1.2 Cellular reprogramming

1.2.1 Somatic Cell Nuclear Transfer

The progressive loss of potency that occurs during cellular differentiation towards a terminal cell fate was thought to be an irreversible process until the Nobel prize-winning discovery by J. Gurdon in 1962 that demonstrated the capacity of adult *Xenopus laevis* cells to dedifferentiate [4]. Gurdon showed that entire feeding tadpoles (1962) and fertile adult frogs (1966) could be generated from the nuclear material of terminally differentiated adult and embryonic intestinal epithelial cells, when transplanted into an enucleated recipient egg. This pioneering discovery showed that adult nuclear material has the potential to reprogram to an embryonic state and generate entire organisms when exposed to the environment of an enucleated egg. In addition this potential was significantly higher when nuclear material from early embryo was used instead, suggesting that immature cells are easier to reprogram than adult tissue (1962).

It was not until 1994 that viable mammalian offspring were established by nuclear transfer to inner cell mass cells [5], which was shortly followed by production of viable offspring from a quiescent embryonic derived cell line [6]. In 1997 I. Wilmut and colleagues were able to derive a live lamb "Dolly the sheep" from adult mammary gland cell nuclear transfer [7] which displayed the phenotypic characteristics of the donor breed (Finn Dorset ewe, all white) and did not reflect the phenotype of the recipient ooctye (Scottish blackface ewe). This advancement was made possible due to advances in understanding of the effect of cell cycle on nuclear transfer. Donor nuclei in the G0 or G1 phase were

found to have a greater chance of developing [6-8] than other cell cycle stages and a greater proportion of the recipient cells develop when they are in the oocyte stage rather than zygote [9].

1.2.2 Cell fusion studies

Following somatic cell nuclear transfer experiments several groups demonstrated that somatic cells can be reprogrammed by fusing with pluripotent stem cells. These experiments were important for uncovering some of the underlying mechanisms of reprogramming such as demethylation of imprinted genes and pluripotency genes such as Oct-4 and Nanog. Resulting hybrids were stringently tested to ensure they were derived from somatic cells and had acquired a pluripotent phenotype cells [10-14].

In 1997 M. Surani and colleagues demonstrated that hybrids of embryonic germ cells and thymic lympohcytes were capable of inducing epigenetic changes in the somatic cell line. Demethylation of several maternal and paternal imprinted genes was detected, as well as demethylation of several non-imprinted genes. Further analysis of the Peg1 paternally imprinted gene using a Peg1-IRES-βneo cassette demonstrated reactivation of the gene and contribution to chimeras in X-gal stained embryos [10]. A later experiment to hybridise adult mouse thymocytes with embryonic stem cells resulted in reactivation of the somatic X chromosome and adoption of the inactive X-specific transcript (Xist) expression pattern, usually found in undifferentiated cells. Activation of transgenic GFP driven by the OCT4 promoter (present in the thymocytes) occurred 48 hours after cell fusion in 97% of the clones. Microinjection of the hybrid cells into

diploid blastocyts resulted in chimeras in 40% of the embryos and chimeric tissue was detected in all three germ layers[11].

Other cell fusion experiments demonstrated dedifferentiation of several cells types including bone marrow, fibroblasts and neural stem cells as described below [12-14]. K. Eggan and colleagues generated ES-like cells by fusing bone marrow cells derived from puromycin resistant, transgenic EGFP mice, fused with ES cells. Cells were cultured under ES conditions and selected under puromycin to generate EGFP expressing ES like colonies. Hybrid cells were capable of generating all three germ layers and forming teratomas in immunocompromised mice. In addition karyotype analysis revealed a tetraploid complement of chromosomes [12].

Pluripotent hybrids were also generated by fusion of puromycin resitant BJ fibroblasts with hygromycin resitant, GFP expressing hES cells. Under dual drug selection colonies were generated after 10 days and analysed for both GFP expression and the presence of the viral vector contained in the BJ fibroblasts to ensure resultant colonies were fusion cells. Resulting colonies were morphologically similar to hES cells, expressed typical hES markers, and karyotype analysis confirmed that the resulting cells were tetraploid. In addition the colonies were capable of generating all three germ layers and forming teratomas. The cell hybrids were transcriptionally similar to the parental hES cells and demethylation of the OCT-4 promoter was demonstrated [13].

Importantly, fusion of Neural stem cells with ES cells overexpressing Nanog improved the generation of hybrid colonies by 200-fold. Comparatively,

overexpression of Nanog in ES-ES cell fusions improved efficiency by 2 fold. Further analysis of the NS-ES fusion confirmed silencing of neuronal specific markers and contribution to all 3 germ layers [14].

1.2.3 Induction of pluripotency by exogenous expression of pluripotency factors

The transcription factors that mediate cellular reprogramming were largely unknown until the discovery in 2006 for which S. Yamanaka won the Nobel Prize alongside J. Gurdon in 2012. Yamanaka and colleagues investigated the genes involved in ES cell maintenance and selected 24 mouse candidate genes as possible factors for reprogramming somatic cells [15]. These genes were chosen based on previous studies highlighting their importance in ES cell pluripotency maintenance (Oct-4, Nanog, and Sox-2) or their contribution of long term maintenance of the ES cell phenotype and frequent upregulation in tumorigenic cells (Stat-3, E-Ras, c-Myc, Klf-4, β-catenin). Other factors were selected as candidates due to their specific expression in ES cells.

Mouse embryonic fibroblasts were generated from transgenic mice containing a β-galactosidase-neomycin resistance fusion cassette inserted into the pluripotency gene Fbx15. This cassette provides a β-galactosidase reporter upon induction of the Fbx15 pluripotency marker and allows selection by neomycin resistance. Neomycin resistant ES cell-like colonies (termed induced pluripotent (iPS) colonies) were generated from mouse embryonic fibroblasts transduced with a pool of retroviruses carrying all 24 of the candidate genes. Individual

factors were then withdrawn from the pool of retroviruses in order to identify critical factors in pluripotency induction. Ten factors were identified from this screen whose withdrawal resulted in no colonies ten days post infection. The combination of the ten factors alone resulted in more iPS colonies than the 24 factors together. By individual withdrawal of these factors from the ten-factor pool the authors were able to identify a combination of just four factors (Sox-2, Oct-4, Klf-4 and C-Myc), which were capable of inducing pluripotent stem cells. Micro-array analysis of the iPS cells revealed a gene expression profile very similar to ES cells. In addition the iPS cells were capable of generating all three of the germ layers *in vitro* and *in vivo.* A schematic of the generation of iPS cells by retroviral delivery of the mouse pluripotency factors Sox-2, Oct-4, Klf-4 and C-Myc is shown in Figure 1 [15].

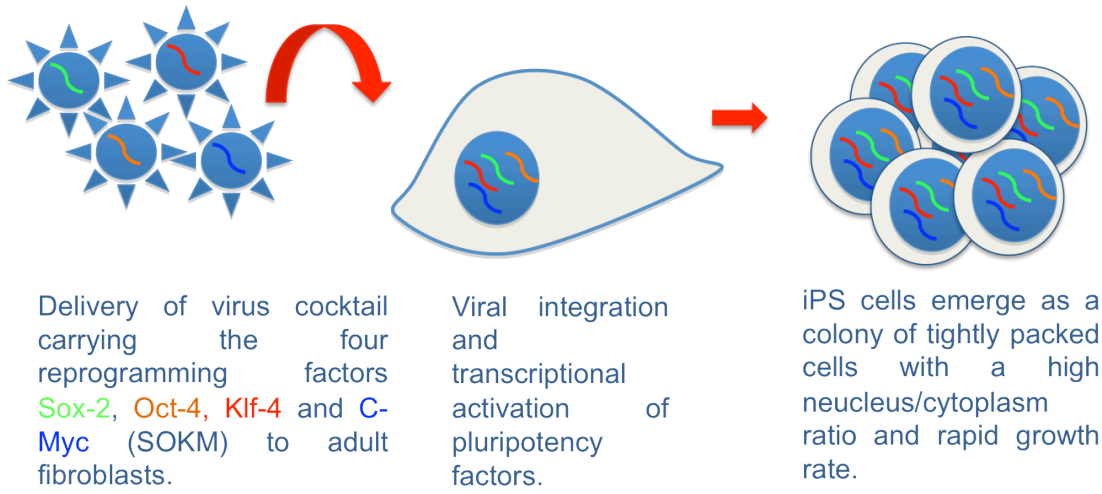


Figure 1 – Schematic of "Yamanaka reprogramming" using retroviral vectors expressing the four reprogramming factors Sox-2, Oct-4, Klf-4 and C-Myc (SOKM). Viral delivery of SOKM to fibroblasts followed by viral integration and transcriptional activation of pluripotency genes and appearance of iPS colonies.

The same group went on to generate iPS cells from adult human fibroblasts by retroviral delivery using the same transcription factors [16]. Shortly afterwards, J. Thomson's group generated iPS cells using a different combination of

transcription factors identified by testing a group of 14 human candidate genes on ES cell derived hematopoietic cells. The factor combination of human SOX-2, OCT-4, NANOG and LIN-28 generated iPS colonies from fetal IMR90 fibroblasts and postnatal human newborn foreskin fibroblasts, via lentiviral delivery of the transcription factors [17]. In each of the iPS papers the resulting colonies expressed key pluripotency markers and were able to generate all three of the primary germ layers [15-17].

1.3 Role of reprogramming factors in pluripotency.

1.3.1 Sox-2

The role of Sox-2 in embryogenesis and pluripotency was investigated by R. Lovell-Badge and colleagues in 2003 by generating Sox2 knock out mice carrying a β-neo reporter ($Sox2^{\beta\text{-}neo}$)[18]. Homozygous $Sox2^{\beta\text{-}neo}$ was lethal and failed to produce viable progeny. The embryos appeared normal at the blastocyst stage however they died shortly after implantation, lacked epithelial cells typical of the epiblast and displayed reduced RNA levels of Oct-4. This lethality was rescued by the transplant of wild type ES cells to blastocytsts as the ES cells contributed to the epiblasts development, allowing the chimeras to survive implantation. These results indicate that Sox2 is essential for epiblast formation [18].

The generation of an inducible Sox-2 null mouse ES cell line resulted in differentiation primarily into tropho-ectoderm like cells [19] as seen previously in Oct-4 nulls [20]. Microarray data of Sox-2 nulls identified significant

upregulation of genes which directly and indirectly upregulate Oct-4 expression levels. Interestingly, the Sox-2 null phenotype is rescued by introduction of the Oct-4 transgene to the Sox-2 null cells [19].

Similar studies investigated the role of SOX-2 in human ES cells [21, 22]. Both groups demonstrated that knockdown in SOX-2 resulted in a loss of pluripotency and differentiation toward the trophoectodermal lineage. P. Donovan and colleagues demonstrated that knock down of SOX-2 in hES cells resulted in the downregulation of several chromatin remodelling genes and eight self renewal and pluripotency genes in addition to NANOG and OCT-4 [21]. In addition, E Kawase and colleagues demonstrated that knock down of SOX-2 results in endodermal differentiation as well as trophoectodermal differentiation. Similar results were obtained when SOX-2 was overexpressed, accompanied by upregulation of the trophoectoderm gene CDX2. Upregulation of CDX2 was not observed when SOX-2 was knocked down [22].

1.3.2 Oct-4

Oct-4 has long been known as a key regulator of pluripotency, dedifferentiation and self-renewal and has been studied extensively [20, 23]. The role of Oct-4 in embryogenesis was investigated by A. Smith and colleagues in 1998. Homozygous Oct-4 knock-out mice were embryonic lethal and the blastocysts did not generate an inner cell mass. In addition, differentiation of homozygous knock out blastocysts *in vitro* generated trophoblast cells only. Down regulation of Fgf4 was observed in Oct-4 null cells however transfection of Fgf4 did not rescue the Oct-4 null phenotype [23].

Oct-4 levels are important in regulating pluripotency status, just a two fold increase in Oct-4 results in differentiation toward endoderm and mesoderm lineages whereas down regulation of Oct-4 in these lines results in dedifferentiation toward trophoectodermal lineages [20].

1.3.3 Klf-4

Krüppel like factor 4 (Klf4) is abundant in epithelial cells of many tissues and is a known oncogene. Microarray analysis of cells hypersensitive to LIF (Shp-2$^{\Delta 46\text{-}110}$ cells) showed that Klf-4 was significantly upregulated by 2-fold increase in response to LIF addition [24]. Analysis of Klf-4 induction in Shp-2$^{\Delta 46\text{-}110}$ cells versus wild type ES cells by Northern blot confirmed a 2 fold increase in Klf-4 expression. In addition, transduction of Klf-4 into ES cell cultures caused a reduced propensity to differentiate to hemangioblasts and primitive erethroid progenitors compared to non-transduced controls, whereas the propensity to generate secondary embryoid bodies was significantly increased. Klf-4 transduction also increased Oct-4 expression by 7-fold, together these results suggest a role in self renewal in pluripotent stem cells [24].

Klf-4 has also been shown to co-operate with Oct-4 and Sox2 to activate the gene Lefty 1 in ES cells. Lefty-1 is driven by Oct-4 in ES cells and the promoter contains conserved Oct-4 and Sox-2 binding sites. However transduction of Oct-4 and Sox-2 in heLa cells was not sufficient to drive the Lefty-1-luciferase (pLefty-1-luc) reporter construct i*n vitro,* suggesting that other factors are present in ES cells that mediate Lefty1 expression [25]. Functional screening of transcription factors to identify genes that could co-operate with Oct-4 and Sox-2

to drive pLefty-1-luc identified Klf as a co-factor. Transduction of Klf-4 alone was capable of increasing luciferase expression by 8.8 fold, whereas together with Oct-4 and Sox-2 expression was increased 25 fold. Luciferase reporter screens using a series of deletion mutants identified that whereas Oct-4 and Sox-2 bind distally to the Lefty1 promoter, Klf-4 binds proximally. Microarray analysis following Klf-4 knockdown by siRNA identified 28 genes down-regulated by Klf-4 which are also targets of Oct-4 and Sox-2 [19].

1.3.4 C-Myc

The Myc family encode a helix-loop-helix/ leucine zipper transcription factors and are involved in many cell functions cell growth and oncongenic transformation. Although c-Myc is depensible for induced pluripotency, its absence results in reduced reprogramming efficiency and slower reprogramming rate [26]. In addition, substitution of c-Myc with the HDAC inhibitors, Valproic acid and trochostatin A, suggests that c-Myc may play a similar role in inducing pluripotency [27].

Elevated levels of c-Myc have been shown to inhibit the differentiation of several cell types and have been shown to play a role in ES cell maintenance [28]. S. Dalton and colleagues demonstrated in 2004 that C-Myc was involved in the LIF/STAT pathway in mouse ES cells. C-Myc RNA transcripts were elevated in mES cells but decreased within two days of embryoid body differentiation which is induced by the withdrawal of LIF from the media. In addition, CHIP analysis demonstrated that the c-Myc promoter is bound by STAT3 and is therefore a direct target of the LIF/STAT pathway *in vivo*. Removal of C-Myc lead to

differentiation of mouse ES cells, indicating that c-Myc is required for self-renewal [28].

Regulation of pluripotency by c-Myc has also been shown to be mediated by micro RNA regulation [29]. Expression of c-Myc mediates differentiatal regulation of microRNAs in differentiated cells, tumour cells and ES cells. Eight miRNAs (miR-124, miR-135A, miR-135B, miR-141, miR-200, miR-302, miR-338, and miR-429) were shown to be significantly upregulated by four-fold in ES cells. Expression of these miRNA's was down regulated upon knock down of c-Myc and repressed miRNA's were upregulated. Direct binding of c-Myc at or near all the upregulated miRNA loci was detected by ChIP analysis, with the exception of miR302, which is thought to be regulated indirectly. Microarray data confirmed that a subset of genes downregulated by c-Myc is mediated by miRNA silencing. In addition, transfection of miRNAs repressed mouse ES cell differentiation upon removal of LIF from media conditions [29].

1.3.5 Nanog

Two groups independantly reported the role of Nanog in mouse ES cell maintenance in 2003. Whereas S. Yamanaka and colleagues identified Nanog while screening candidate genes for factors that maintain pluripotency in the absence of leukemia inhibitory factor (LIF), A. Smith and colleagues undertook a gene library screen approach in order to identify genes involved in ES cell propagation [30, 31].

Nanog is enriched in mouse ES cells [30] and is capable of maintaining mES colonies independently of the stat/LIF pathway, as assayed by generation of colonies in Nanog transfected cells in the absence of LIF [30, 31]. Nanog null ES cells differentiated toward endoderm lineage and showed reduced Oct4 and Rex1 levels. In addition, although homozygous Nanog-null transgenic mice were indistinguishable from wild type embryos at embryonic stage E3.5, the inner cell mass differentiated within 4 days in vitro [30]. Embryo's examined at embryonic stage 5.5 consisted of disorganised extraembyronic tissue and did not develop epiblast. No homozygous embryos were detectable at stage E7.5 [30]. These findings are complementary to the in situ hybridisation studies by A. Smith and colleagues who found that Nanog mRNA was restricted to the inner cell mass early on and later was restricted to the epiblast [31].

Sequence analysis of Nanog cDNA revealed that the protein contains a homeobox domain that is specific to pluripotent cell types and independent from the NK-2 family [30, 31]. DNA binding site analysis revealed a consensus sequence present in the enhancer regions of Gata 6 and Rex 1, genes involved in differentiation and ES maintenance, respectively [30]. S. Yamanaka and colleagues postulated that Nanog may act to repress Gata6 and other differentiation genes, and enhance rex1 and other ES maintenance genes.

Later studies have found that deletion of Nanog in ES cells does not affect the self-renewal capability or multilineage differentiation, indicating that Nanog is dispensible for pluripotency. In addition, deletion of Nanog results in the failure of primordial germ cells to mature in the genital ridge. The authors postulated

that Nanogs role in primordial germ cells and the blastocyst is to regulate the epigenetic reprogramming and methylation during germ cell development [32]. In addition, a later study revealed that Nanog is required for X chromosome reactivation in the ICM of the developing mouse embryo. In Nanog deleted (Δ) embryos the inactivated X chromosome persisted and the embryos were unable to progress to a viable epiblast [33].

Nanog's role in establishing pluripotency has been further investigated in cell fusion studies and molecular reprogramming experiments [33]. Whereas WT ES cells fused with neural stem (NS) cells yielded ~ 40 hybrid colonies, Nanog deleted (Δ) ES cells only produced 2-3 colonies per plate and addition of Nanog (Δ+Ng) yielded ~400 colonies per plate. In addition, in the NanogΔ hybrids the lines expressed Nanog from the NS lines. Fusion of Nanog ΔNS cells with Nanog ΔES cells resulted in hybrid lines with disrupted morphology, which upon ground state culture conditions, (addition of MEKi and GSKi) they either died or differentiated. Comparatively, Δ+Ng hybrids expanded without differentiation under these conditions, indicating that Nanog is required at later stages in order to attain pluripoteny. This was complemented by molecular reprogramming of NanogΔ NS cells and Δ+Ng NS cells under minimal media (media containing serum and LIF), followed by a switch to ground state media conditions (media containing MEKi, GSK3i and LIF). Both NanogΔ NS cells and Δ+Ng NS cells produced ES-like colonies and expressed early markers such as alkaline phosphatase, E cadherin and SSEA1 under minimal media conditions. Following passage of colonies into ground state media conditions the NanogΔ cells died within 7 days and no colonies were formed whereas Δ+Ng cells produced ~100 colonies per plate.

1.3.6 Lin-28

Lin-28 is an RNA-binding protein which regulates non-coding RNAs such as let-7 in embryonic cells [34]. has been shown by serial analysis of gene expression (SAGE) studies to be expressed in human and mouse ES cells in comparison to differentiated cell types and is strongly downregulated during differentiation [35]. Lin28 is also important in development and growth as Lin28 knock out mice are nonviable and weigh only 20% the weight of wild-type mice at birth. Lin28 was also found to be a modulator of ES cell proliferation and maintenance [36].

Knockdown of Lin28 by siRNA treatment resulted in 20% decrease in cell number after 48 hours that was not attributable to cell death and similarly, overexpression of Lin28 in ES cells lead to a 35% increase in cell number after 48 hours. The results were confirmed by BrdU pulse labelling followed by FACs to acertain the number of cells in S phase versus G_2/M phase. A lower number of cells were in G_2/M phase when transfected with Lin28 siRNA and the inverse was seen for cells transfected with Lin28. In addition, Cdk4, Cdk6, Cyclin A, Cyclin B, Cyclin D and Oct-4 mRNA was found by co immunoprecipitation to associate with Lin28 in ribonucleoprotein complexes. No changes in RNA levels due to siRNA treatment were detected when examined by qRT-PCR, however significant decreases in Cdk4, Cyclin A and Cyclin B protein levels were detected by Western blot whereas Oct-4 protein levels were unaffected. This suggests a role for Lin28 in controlling the translation of cell cycle genes in ES cells [36].

Although siRNA knockdown of Lin28 did not affect Oct-4 protein levels, a later publication by the same group showed that siRNA knockdown resulted in a ~40% reduction in Oct-4 protein levels whereas GAPDH levels were unaffected [37]. The contradicting result was postulated to be due to insufficiency of the siRNA in the earlier experiments, which was estimated to induce 70% knockdown of Lin28 compared with ~90% in the later publication. RNA levels were unaffected, suggesting that Lin28 regulates Oct-4 at the translational level. This was confirmed by demonstrating the activity of an Oct-4-luciferase reporter construct in response to Lin28. Further experiments demonstrated that Lin-28 directly binds RNA Helicase A (RHA) and knockdown of RHA results in reduced activity of the Oct-4-luciferase reporter, suggesting a role for the interaction of RHA and Lin28 in controlling Oct-4 translation [37].

1.4 Chromatin states in pluripotent and differentiated cells

The higher order of DNA organisation involves the wrapping of DNA around nucleosomes composed of four histones that are subject to post-translational modifications such as methylation, acetylation and ubiquitination. Transcriptional control of gene expression is maintained by DNA methylation and epigenetic modifications of the histone tails, which control the chromatin organisation. Modifications which allow the chromatin to adopt an open conformation is associated with actively expressed genes, whereas condensed chromatin is associated with gene repression, as reviewed by L. Serrano in 2013 [38].

Chromatin immunoprecipitation sequencing (ChIP-seq), biochemical assays and quantitative imaging experiments have shown chromatin status differs depending on differentiation status. Typically, stem cells possess genome-wide open chromatin status associated with active transcription levels. Active epigenetic histone modifications such as H3/H4 acetylation and histone methylation on lysine 4 and lysine 36 alongside high turnover of proteins that bind to chromatin are observed in pluripotent stem cells. Conversely, differentiated cells have acquired repressive histone modifications such as histone methylation of lysine 9 and lysine 27 and are associated with an inactive, closed chromatin conformation [38]. In addition, important developmental genes in embryonic stem cells possess bivalent histone modifications such as dual methylation of lysine 4(active) and lysine 27 (inactive), which allows the genes to be silenced while in the pluripotent state but poised for activation during the developmental process when the repressive methylation of lysine 27 is lost [38].

1.5 Role of reprogramming factors in chromatin regulation and transcriptional changes

During reprogramming the differentiated cells adopt an epigenetic status similar to ES cells. The role of Oct-4 in transcriptional regulation and induction of pluripotency has been examined in order to elucidate the mechanisms and targets of Oct-4 [39]. Microarray and chromatin immunoprecipitation (CHIP) analysis has shown that Oct-4 associates with hundreds of promoter regions of known protein encoding genes including genes that are highly enriched in ES

cells (Oct4, Sox2, Nanog, Lefty2/Ebaf, Cdx2, Hand1, Dppa4, Gja1/Connexin43, Foxo1a, Cripto/Tdgf1, And Zic3) [40]. Additionally, examination of Sox-2 and Nanog target genes showed that they shared target genes with Oct-4. Oct-4, Sox-2 and Nanog occupy at least 353 shared target genes, over half of the target genes of Oct-4 are shared by Sox-2 and >90% of these are also shared by Nanog. Oct-4, Sox-2 and Nanog were also found to co-occupy at least two miRNA promoters. Transcription factors involved in pluripotency as well as genes involved in the TGF-β and Wnt pathways were found to be transcriptionally active when co-bound by Oct-4, Sox-2 and Nanog whereas transcription factors involved in development and differentiation were found to be transcriptionally inactive. These results suggest that Oct-4, Sox2 and Nanog are autoregulatory and work synergistically to regulate transcription.

The transcriptional and chromatin changes during somatic cell reprogramming was investigated further by comparing binding sites of Oct-4, Sox-2, Klf-4 and C-Myc (OSKM) identified by CHIP sequencing, with microarray data [41]. Interestingly, 90% of genes that are differentially expressed between fibroblasts and iPS cells by more than 2-fold co-bound all OSKM at 48 hours post transgene expression induction. Notably, genes involved in early reprogramming and cell death pathways were bound. Analysis of binding sites revealed that early in reprogramming the transcription factors bind distally to promoters at 48 hours post transduction, compared with binding close to the transcription start site (TSS) in ES cells. Analysis of OSKM binding sites at 48 hours revealed 8 sites where OSKM cooperatively bind and 8 sites where only OSK bind. Further analysis showed that the binding motif in C-Myc allowed engagement of the OSK

transcription factors with chromatin, providing an explanation for the lower reprogramming efficiencies observed in OSK only compared to OSKM transductions [41], which is consistent with previous observations [26]. Binding of OSK was seen in the majority of cases at Dnase-1 resistant regions of chromatin, indicative that the chromatin was in a closed confirmation, whereas binding of C-Myc alone was found to only to bind to open chromatin [41].

1.6 Measurable signs of dedifferentiation

Induction of pluripotency causes morphological changes to the somatic cells resulting in a high nucleus to cytoplasm ratio and the formation of tight compact colonies with a defined border. Detection of iPS markers such as Alkaline Phosphatase and SSEA-4 are detectable early in reprogramming, accompanied by silencing of the exogenous transgenes, followed by expression of endogenous OCT-4 and Nanog and other iPS markers and demethylation of the Oct-4 and Nanog promoters. Several single cell live imaging experiments have been performed in order to elucidate the sequence of events during reprogramming [42-44]. Notably, the most recent reports were able to analyse changes over 5-15 minute periods and track reprogramming back to the original founder cell [44].

In 2009 T. Schlaeger and colleagues performed serial live cell imaging of the same area 40 cm^2 every 2-4 days and analysed the images retrospectively following the generation of iPS colonies in order to determine the temporal expression of markers during reprogramming. In situ staining of the fibroblast marker CD13 and the pluripotency markers SSEA-4 and TRA-1-60 was examined

as well as expression of the proviral reporter EGFP, endogenous Nanog and Hoescht staining phenotype [42]. FACS and automated fluorescence microscopy identified the phenotype of bona fide iPS cells, as well as other partially reprogrammed phenotypes. Typically SSEA-4 positive staining was detected from day 2, followed by TRA-1-60 positive staining in a subset of SSEA-4 positive cells on days 6-10.

The phenotype of bona fide iPS cells originated from clusters on day 8 that were CD13-, GFP^{dim}, SSEA4+ and TRA-1-60+, $Hoescht^{dim}$, however 70% of these clusters would not go on generate iPS colonies. Cluster size correlated with iPS colony generation, where larger clusters of around 35 cells on day 8 were more likely to generate iPS colonies than clusters of around 10 cells. Bona fide iPS colonies stained positive for NANOG by day 16. Characterisation of resulting partially reprogrammed and bona fide iPS colonies revealed that OCT4, SOX2, NANOG, hTERT and GDF3 were expressed in both types whereas expression of REX1, DNMT3B and ABCG2 were specific to fully reprogrammed colonies. In addition, demethyalation of the OCT-4 and NANOG promoters, as well as histone modifications of OCT-4, NANOG and SOX-2 were specific to fully reprogrammed colonies [42].

Other studies that have used single cell live fluorescence microscopy have used dTomato reporter tagged reprogramming factors to reprogram fibroblasts derived from OCT-4-GFP reporter mice to study the kinetics of reprogramming [43]. Activation of the Oct-4-GFP reporter was acquired as little as 3 hours to sixty hours after the emergence of reprogramming factor positive clusters. FACs

analysis detected <2 % double positive cells at early time points and complete absence of double positive cells by day 11, suggesting that vector silencing occurs before or simultaneously with Oct-4-GFP induction. Interestingly, using the time lapse imaging the authors were able to determine that many colonies did not arise from single transduced cells but often originated from several neighbouring cells during the reprogramming progress, resulting in heterogenous colonies [43].

Furthermore, using an enclosed incubator microscope to analyse the kinetics of reprogramming of granulocyte-monocyte progenitors (GMPs), S. Guo and colleagues were able to trace the iPS colonies back to a single founder cell. Serial imaging tracked over 5-15 minute intervals revealed highly dynamic cell migration and division events [44]. In some cases iPS colonies were derived from several founder cells, supporting the previous observations by A. Schambach and colleagues. Conversely, multiple colonies arising from a single founder cell (termed sister colonies and satellite colonies) were also observed [44].

Interestingly, a unique, early morphology change was identified in the early stages of all iPS colonies using this imaging technique. In the very early stage of reprogramming two cells joined by a thin cellular process due to incomplete segregation of the founder cell during division results in a unique dumbbell morphology [44]. This morphology occurs prior to expression of the Oct-4-GFP reporter and in most cases remain joined in this conformation for ~around ten hours before proceeding with subsequent cell divisions. All traceable iPS

colonies displayed this morphology and of 36 dumbell formations identified, 33 went on to generate successful iPS colonies. Knock down of E-cadherin, a pluripotency which mediates mesenchymal to epithelial transition, resulted in abolishment of the dumbbell morphology and subsequent impairment of iPS colony formation [44].

1.7 Insertional mutagenesis of lentiviral and retroviral vectors.

Many groups have successfully derived iPS lines from a variety of cell types using integrating viruses such as lentivirus and retrovirus with a varying efficiency of 0.0001-3.6% depending on cell origin and factors used (Table 1). Reprogramming has been achieved in human embryonic, fetal, and dermal fibroblasts by lentiviral and retroviral delivery of reprogramming factors [16, 45, 46] and other cell types that have successfully been reprogrammed include mononucleated blood cells [47] [48] and human keratinocytes [49].

Table of integrating viral reprogramming methods and efficiencies					
Cell type	**Delivery**	**Factors**	**Efficiency**	**Features**	**Ref**
HDF	Retroviral	SOKM	0.02%		[16]
HDF	Lentiviral	SOKMhT	0.007%		[46]
HEF	Lentivirus	SOKM	0.021%		[46]
HDF	Retroviral	SOKM	0.08%	Polycistronic	[45]
MNC	Retroviral	SOKM	0.5%	P53 knockdn	[47]
MEF	Lentiviral	SOKM	0.001%	Polycistronic	[49]
H keratinocytes	Lentiviral	SOKM	0.0001%	Polycistronic	[49]
MNCs	Retroviral	SOKM	0.006%	+Cytokines	[48]
Mpβ cells	Lentiviral	SOKM	0.1-0.2%		[50]
M NS cells	Retroviral	SOKM	3.6 %		[51]
M NS cells	Retroviral	OK	0.11%		[51]
HFF	Lentiviral	OSNL	0.022%		[17]
HFSF	Lentiviral	OSNL	0.0095%		[17]

Table 1 – reprogramming efficiencies of integrating viral vectors.
S= SOX-2, O= OCT-4, K= KLF4, M= C-MYC, N= NANOG, L= LIN-28, h= hTERT and T= SV40LT; HDF=human dermal fibroblasts, HEF= Human embryonic fibroblasts, HMNC= human mononuclear cells, MEF= mouse embryonic fibroblasts, HK= human keratinocytes, Mpβ cells= mouse pancreatic β cells, MNS= mouse neural stem cells, HFF= human fetal fibroblasts, HFSF= Human foreskin fibroblasts.

The use of integrating viruses to generate iPS cells is concerning due to the possibility of insertional mutagenesis. Retroviruses have long been associated with insertional mutagenesis especially since the occurrence of lympho-cytosis (an increase in the number of lymphocytes in the blood) which lead to hepatosplenomegaly (enlargement of the liver and spleen) during a gene therapy trial to treat X-linked severe combined immunodeficiency [52]. This happened following transcriptional activation of the LMO-2 gene due to retroviral integration within the LMO-2 locus [52]. Another gene therapy trial conducted in 2004 to treat X-linked chronic granulomatous disease (X-CGD) resulted in oligoclonal haematopoiesis, mono-somy 7 and the development of a myelodysplastic syndrome (MDS) due to the integration of retroviral construct within the gene ecotropic viral integration site 1 (*EVI1*) [53].

The development of self-inactivating (SIN) vectors help to prevent trans-activation of neighbouring genes and function due to a deletion within the 3' long terminal repeat (LTR) which includes the enhancer and promoter sequences [54]. The promoter and enhancer sequences are normally only active in the 5' LTR, however during reverse transcription the deletion in the 3' LTR is copied to the 5' LTR, effectively inactivating the transcriptional activity of the pro-virus. Transgene expression in SIN vectors needs to be driven by an internal promoter as the promoter in the LTR is removed during reverse transcription.

Some advances have been made to try and improve retroviral vectors based on studies comparing the Long terminal repeats (LTRs) with self inactivating LTRs (SIN) [55]. Elegant experiments to investigate the effect of LTRs on tumorigenicity were conducted by swapping the LTR and SIN genetic elements between retroviral and lentiviral vectors resulting in reduced tumorigenicity and increased survival in animals transduced with SIN constructs [56].

However, an analysis of the impact of SIN vector design on clonal imbalance and leukemia directly compared a γ-retroviral SIN vector and γ-retroviral vector expressing the potentially therapeutic interleukin-2 receptor common c-chain (IL2RG) or the control DSRed. Both vectors mediated a leukemogenic cascade in secondary mouse bone marrow transplant recipients by upregulating Evi1 and Prdm16 [57]. Additionally, transcriptional activation of the EF2 target genes involved in the retinoblastoma (Rb/p16) tumour suppressor pathway was seen in mouse cells transduced with feline SIN lentiviral vectors, irrespective of integration site [58].

Recent improvements to vector design include integration defective lentiviral vectors and directed integration of lentiviral vectors. Integration defective lentiviral vectors (IDLV), which are packaged using a GAG/POL encoding a mutant integrase (IN), have been used in recent years as expression vectors. Many mutations in the viral IN have been identified which disrupt the catalytic activity of the enzyme, resulting in episomal lentiviral vectors. These lentiviral episomes do not contain an origin of replication and are lost with cell division [59]. These vectors allow a transient pulse of expression with high transduction efficiency and wide cell tropism. Analysis of IDLV transduction followed by cell sorting 3 days after transduction found that less than 0.1% cells were detectable by FACS on day 25 after transduction and no episomal DNA detectable 14 days post transduction nor qPCR detection of Viral DNA in genomic DNA [60]. In addition IDLV vectors were shown to demonstrate rescue of an *in vivo* rodent model of retinal degeneration and episomal expression was detectable 8 weeks after transduction in post-mitotic tissues [61].

Recent work is focused on improving directed integration of the LV vectors by modifying the tethering factor LEDGF/p75 which interacts with the HIV viral integrase. Knockdown of LEDGF/p75 in 293T, Jurkat T cells and osteosarcoma cells signifigantly reduced the number of integrations in transcription units compared to controls [62]. Expression of an engineered LEDGF/p75 in cultured cells can direct integration to heterochromatin regions. This has been achieved by engineering a LEDGF/p75 to contain a chromatin binding domain which recognises the trimethylated Lys-9 of histone H3 (H3K9me3) present in

heterochromatin [63]. The authors confirmed association of the fusion protein with H3K9me3 in transfected 293T cells and integrations of HIV within genes was significantly reduced in transfected 293T cells [63].

Few studies have investigated the effect of viral integration sites on human iPS cell integrity however one HIV-based lentiviral study reported that within 8 iPS clones 75 out of 78 insertion sites mapped to unique chromosomal insertion locations [64]. Whereas no common insertion sites were shared between the 8 iPS cell clones and no adverse effects were reported, a significantly higher number of insertions within 30 kb of oncogenes were detected compared to *in silico* random controls. In addition, significant upregulation of three genes WDR66, MYST2 and KIAA0528in 2 iPS cell clones were detected. WDR66 was recently implicated in esophageal squamous cell carcinoma [65] and overall there was an over representation of proto-oncogene upregulation, consistent with similar studies in mice [66]. In addition tumour formation due to the reactivation of the c-Myc oncogene in chimeric mice derived from iPS cells [67] present a need for alternative methods for deriving iPS cells.

1.8 Non-integrating and excisable reprogramming methods

Alternative non-integrating and excisable reprogramming methods include non-viral reprogramming methods such as plasmid transfection, episomal plasmids, transposons, mRNA, proteins and small molecules (Figure 2). Other non-integrating viral methods include episomal viruses such as adenovirus and RNA based viruses such as Sendai virus. Excisable lentiviral vectors have also been developed using the Cre-Lox P system (Figure 3). However no reprogramming

method is perfect and the limitations of these methods such as labour intensiveness, reprogramming efficiency and transgene capacity are discussed below.

1.8.1 Viral vectors

1.8.1.1 Non-integrating viral vectors

Generation of iPS cells mediated by adenoviral vectors has been achieved in mouse liver cells [68] and human fetal fibroblasts [69], however the efficiency is very low (0.0002%) and requires repeated transductions due to the rapid loss of the vector during cell divisions. Human iPS cell lines generated by adenovirus were free of integrations and confirmed to all be diploid [69] in contrast to the incidents of tetraploidy found in the liver derived mouse iPS cells [68]. It is thought that the tetraploid iPS cell lines were due to the liver origin of the cells, as high incidence of polypoidy has often been observed in this cell type [70, 71]. Further more iPS cells generated from adenoviral reprogrammed adult mice tail tip fibroblasts survived and generated neuronal phenotypes when transplanted into the striatum of immune competent rats [72].

Sendai virus is currently the safest and most efficient method of deriving iPS cells due to its stable expression of a non-integrating RNA vector and ability to erase the vector RNA genome during the reprogramming protocol by siRNA treatment. In addition the virus is not known to cause disease in humans and can deliver polycistronic constructs of the four reprogramming genes [73].

The Sendai virus genome consists of a single stranded RNA genome which encodes 8 Sendai virus proteins (NP, P, C, V, M, F, HN, and L). Initial recombinant Sendai virus vectors developed for gene delivery allowed efficient gene delivery and expression but were replication competent. Later vectors were rendered replication incompetent by removal of the F (fusion) gene essential for replication[74] but these generation of vectors were unable to maintain gene expression for more than 10 days due to the cytopathic nature of the virus and multiple gene deletions were required for complete replication incompetence [75]. Removal of envelope genes from the SeV vector improved cytotoxity issue to some extent [76] and later a persistent and non-cytotoxic vector was developed following the analysis of a temperature sensitive mutant Nagoya strain, Cl.151, which contains 50 nucelotide changes across the 8 genes [75].

Cultured cell lines infected with the Cl.151 strain had a high RNA replicon number of 40,000 replicons per cell and gene expression was persistent for up to 6 months, with a loss rate of less than 0.04% per cell division. In addition, cytopathic assays found that a recombinant vector of this strain had a markedly reduced induction of IFN-βpromoter-luciferase construct when compared with the induction observed in WT Sev infection. By generating chimeric Sev containing the Cl.151 and parental Nagoya strains the authors were able to identify the 5' L region (which contained 4 missense mutations and 1 non-coding mutation) as causative for escaping the interferon pathway and establishing long-term persistence. Transfection of 5' single stranded RNAs into cells infected with the Cl.151 strain resulted in a 10-fold induction of the IFN-β promoter, indicating that the RIG-I/IRF-3 signal transduction pathway is functional in

infected cells. A likely explanation for the reduced cytotoxicity in the Cl.151 strain could be absence of uncapped 5' RNAs, needed to trigger the RIG-I/IRF-3 signal transduction pathway [75]. Further analysis by Nakanishi and colleagues found that one of the four L gene mutations (V1618L) and a miss-sense mutation in the P gene was indespensible for long-term persistence of the virus [75].

Sendai virus was first used as a reprogramming vector in 2009 by using F protein deficient (ΔF), non-transmissible SeV vectors which exhibit low cytotoxity [77]. Sendai virus vectors carrying individual reprogramming genes at different locations within the Sendai virus genome were capable of reprogramming at an efficiency of 1% however expression of the reprogramming genes was persistent in many of the iPS clones [77]. The persistent expression of the virus was overcome by generating temperature sensitive mutants of the virus, which enabled the eradication of viral RNA within 3-5 days at 38 degrees [78].

Sendai virus reprogramming was improved further by increasing the transgene capacity of the Cl.151 strain by removal of the M,F and HN genes without altering long term persistency of the virus. This enabled the delivery of all four reprogramming genes in a single vector [73]. Sendai virus reprogramming vectors were capable of reprogramming mouse embryonic fibroblasts with an efficiency of 0.83% compared with an efficiency of 0.01% by retroviral delivery of the same reprogramming genes. In addition the Sendai virus genome could easily be eradicated by siRNA treatment targeted against the viral RNA polymerase [73].

Sendai virus reprogramming has fast been adopted by many laboratories and used to derive iPS cells from many cell types including fibroblasts [79] [80] and [81], mononuclear cells from peripheral blood [82] and nasal epithelial cells [83]. One reason why Sendai virus may offer a higher reprogramming efficiency than other integration free vectors could be the observed 30-fold down regulation of mitochondria/oxidative stress response and senescence/apoptosis pathway genes in Sendai virus iPS cell clones. Significant downregulation of genes in the INK4/ARF pathway, including $p16^{INK4a}$, $p15^{INK4b}$, and $p21^{CIP1}$ and oxidative stress pathway, including GPX2, PTGS1 and PRNP [79]. Despite the advantages of this vector in terms of safety and efficiency, the main disadvantage is its limited transgene capacity.

1.8.1.2 Cre-Excision of integrating viral vectors

One alternative to using inefficient non-integrating vectors is to deliver reprogramming factors by lentiviral or retroviral vectors followed by Cre-mediated gene excision, which removes the majority of the viral construct. This was first accomplished by R. Jaenisch and colleagues by delivery of individual reprogramming vectors (OCT-4, SOX-2, KLF-4 and C-MYC) under control of an inducible promoter which enabled a reprogramming frequency of 0.01% in human dermal fibroblasts [84]. Cre-excision was mediated by transient transfection of plasmids containing Cre and puromycin resistance or GFP reporter, followed by puromycin selection or FACs sorting for GFP positive cells respectively. Complete excision was observed in 5% of the clones obtained in lines that had 7 or 9 viral integrations prior to excision [84]. Previous attempts

to remove transgenes by Cre-excision is thought to have failed due to the high number of integrations (up to 20) and low transfection efficiency of Cre plasmids in iPS cells [15].

Cre-exision of iPS constructs was improved by modifying the constitutive polycistronic stem cell cassette (STEMCCA), which was utilised due to the reduced number of integrations (mean 2.8 per iPS clone) and relatively high efficiency of 0.5% in mouse tail tip fibroblasts [85]. This lentiviral vector was modified to contain a loxP site in the deleted dU3 region in the vectors 3'LTR. This U3 region is copied into the 5' LTR during reverse transcription of the viral genome prior to integration, creating a loxP flanked (floxed) version of the STEMCCA cassette [86]. Adenoviral delivery of Cre to 90-100% of cells allowed excision of the cassette, as confirmed by southern blot analysis in 5 iPS clones. In addition a second STEMCCA-loxP vector was constructed containing an M-cherry reporter in place of the C-Myc gene. This elegant system allowed cre-excision to be easily visualised and estimated by fluorescence microscopy. Disappearance of M. Cherry expression was observed in 96% of iPS cells [86].

The same group went on to demonstrate transgene-free iPS cells in human fibroblasts using a humanised form of the STEMCCAloxP vector containing human versions of OCT-4, KLF-4, SOX-2 and C-MYC (hSTEMCCA-LoxP). Similar reprogramming efficiencies were observed (0.5%) and Cre-excision was confirmed in 100% of 50 iPS clones [87]. The hSTEMCCA-LoxP vector has subsequently been used by J. Byrne and colleagues to demonstrate differential expression of a gene close to the insertion site before and after cre-excision [88].

The cassette has also been used to generate iPS cells from β-thalassemia patient amniotic fluid cells and fibroblasts with a reprogramming efficiency of 0.33 and 0.02% respectively [89].

Cre-excision methods are promising and have a relatively high efficiency of reprogramming and excision frequency, however the risk of insertional mutagenesis is not completely removed due to the remainder of a 200bp region of the LTR. Although the segment is not transcriptionally active, screening would be needed to ensure the insertion site does not disrupt the genome [90]. Outlines of viral reprogramming methods including integrating methods are shown in Figure 2.

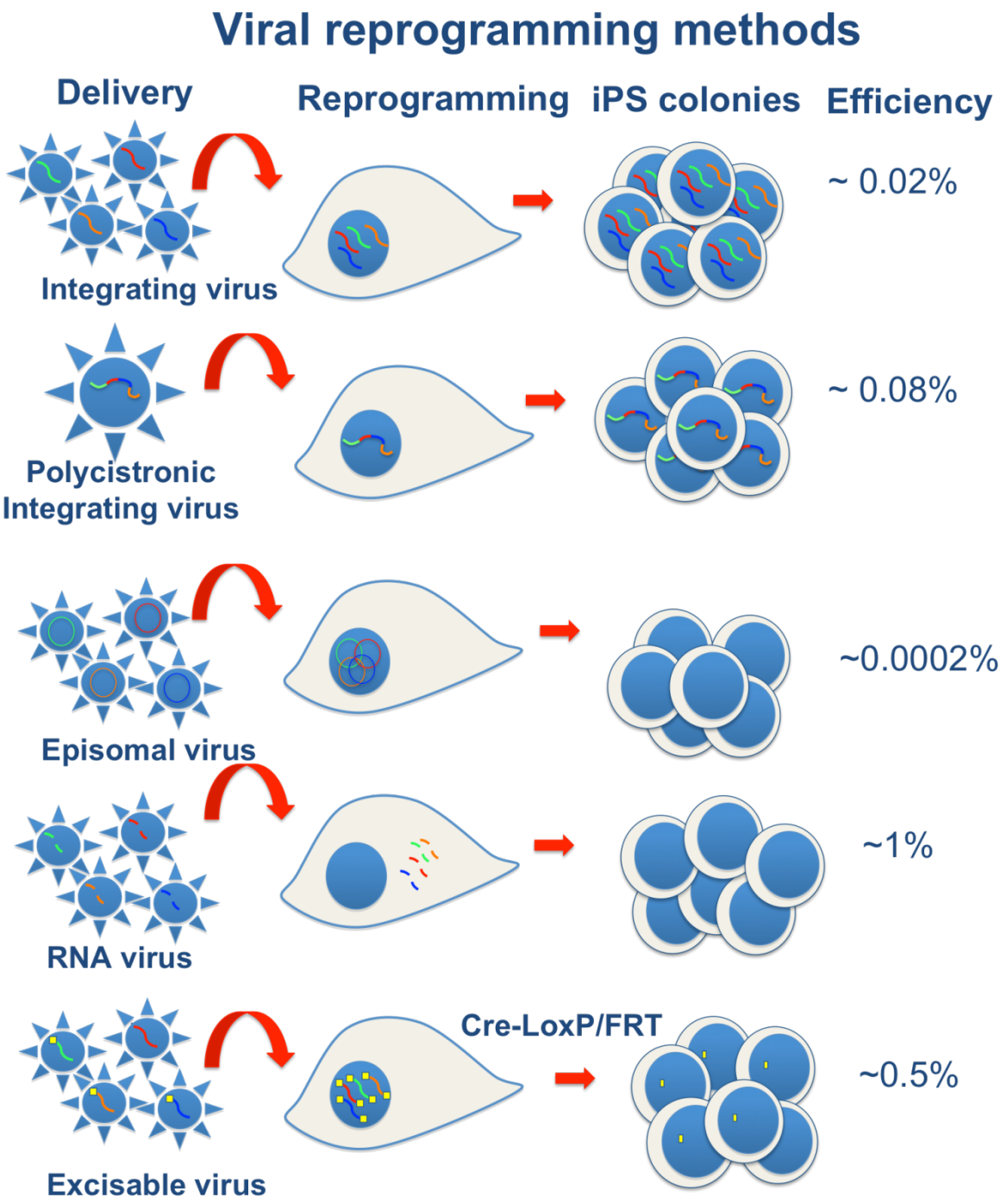


Figure 2 – Viral reprogramming methods. Integrating virus's such as lenti/retrovirus, polycistronic integrating virus's which have fewer integrations, episomal virus's such as adenovirus, RNA virus such as Sendai virus and excisable virus's containing a Cre-LoxP of flip FRT cassette. Relative efficiencies are shown in the right hand column.

1.8.2 Non-viral vectors

1.8.2.1 Transient and episomal plasmid transfection

Plasmid transfections offer a non-integrating method of reprogramming, however the need for repeated transfections due to the rapid loss of the plasmids means that the method is extremely labour intensive [91]. The use of a minicircle vector by J. Wu and colleagues allowed higher transfection efficiency and longer ectopic expression when reprogramming, however multiple transfections were still required. The group reprogrammed human adipose stem cells (hASCs) to iPS cells by delivering a polycistronic minicircle vector expressing OCT-4, SOX-2, NANOG and LIN-28. The group reported a reprogramming efficiency of 0.005% using this system [92]. Alternative routes of plasmid delivery such as liposomal magnetofection (LMF) have proven effective in inducing pluripotency with an efficiency of 0.04% with just one round of LMF [93].

The addition of the episomal retention elements EBNA-1/*oriP* has removed the need for repeated transfections however the efficiency of this method remains low. J. Thomson and colleagues first achieved reprogramming of human foreskin fibroblasts using three EBNA-1/OriP vectors expressing SOX-2, OCT-4, KLF-4, C-MYC, NANOG, LIN-28 and the SV40LT antigen with an efficiency of 0.0003-0.0006% [94]. Yamanaka and colleagues directly compared the Thomson EBNA-1/oriP vectors with a different set of vectors, which replaced NANOG, SV40 and C-MYC with L-MYC and incorporated an shRNA targeting p53. The new combination (SOX-2, OCT-4, KLF-4, LIN-28, L-MYC and p53shRNA) increased

reprogramming efficiency to 0.03% in human dermal fibroblasts [95]. Similar efficiencies were observed by L. Cheng and colleagues when reprogramming cord blood and peripheral blood mononuclear cells (MNCs) (0.05 and 0.001% respectively) when using the five factor combination OCT-4, SOX-2, C-MYC, KLF-4 and NANOG [96].

1.8.2.2 Transposons

Transposable elements, or transposons, are DNA cassettes that contain inverted terminal repeats allowing them to integrate and excise themselves from the genome when catalyzed by the enzyme transposase. Reprogramming was first achieved using the piggyBac (PB) transposon which is derived from the cabbage looper moth *Trichoplusia ni* [97]. PB is capable of integrating large cassettes >100kb in size, and was first utilised in mammalian cell lines and mice in 2005 [98]. The PB reprogramming cassette carries the four mouse reprogramming factors SOKM under the control of a tetracycline/doxycycline inducible promoter. The PB transposon reprogrammed mouse fibroblasts with 0.038% efficiency however excision only occurred in 2% of cells exposed to transposase. Analysis of the integration site confirmed no trace of a transposition event in ten out of eleven subclones following excision of the transposon in the presence of transposase [99].

Few publications have repeated iPS generation using PB transposon however one group used PB to reprogram equine fibroblasts with 0.028% efficiency [100]. A few publications have improved PB reprogramming efficiency; the addition of the HDAC inhibitor Butyrate improved efficiency by 25 fold [101];

and modification of the PB vector to include L-Myc and early transposon promoter and Oct-4 and Sox-2 enhancers (EOS), improved efficiency to 0.27% [102]. Remarkably, in all three of these subsequent publications no mention was made to removal to the PB transposon following reprogramming [100] [101] [102].

The transposon Sleeping Beauty (SB), so named due its long period of inactivation and artificial reconstruction from Tc1/*mariner* transposon fragments [103], has also been utilised for reprogramming of mouse and human fibroblasts [104] [105]. No SB elements exist within the human genome [106], minimising the potential risk of activating endogenous transposable elements. In addition, SB exhibits random integration reducing the risk of insertional mutagenesis [107], unlike PB which tends to target regions near long terminal repeat elements and transcriptional start sites [108]. The utilisation of a hyperactive version of SB capable of transposition into human cells (SB100X) reprograms with an efficiency of 0.02% in human dermal fibroblasts. However, the authors were unable to demonstrate transgene-free iPS cells, despite being able to mobilise transposons by re-expression of the transposase SB100X [105].

1.8.2.3 Messenger RNA reprogramming

Early attempts to reprogram somatic cells by mRNA transfection successfully induced some pluripotency factors such as endogenous OCT4, NANOG, DNMT3b, REX1 and SALL4 in alkaline phosphatase-positive aggregates that emerged during reprogramming. However, these aggregates failed to expand and an

increase in p21 expression was observed. The publication was a proof of principle that reprogramming mRNAs can induce genes required for reprogramming however repeated transfections of mRNA caused cell death [109]. Suppression of innate immune response by transfection of siRNA targeted to interferon-b, Eif2ak2 and Stat enabled frequent transfection with proteins without inducing cell death [110].

Successful reprogramming with mRNA was achieved by incorporation of modified ribonuclease bases such as substitution of 5-methylcytidine (5mC) for cytidine, or pseudouridine (psi) for uridine [111]. Modified transcripts displayed improved viability, increased protein expression and reduction of innate response, as confirmed by qPCR. Daily transfection of five factor reprogramming modified mRNAs (KLF-4, C-MYC, OCT-4, SOX-2 and LIN-28) resulted in a 2% reprogramming efficiency, which was improved to 4% in low oxygen conditions [111].

1.8.2.4 Protein mediated reprogramming

Another alternative method to viral reprogramming is delivery of reprogramming proteins. Overall the efficiency of this technique is poor (0.001%) and takes significantly longer (8 weeks) [112]. In addition, repeated delivery of proteins is required [113]. One suggestion for the lower reprogramming efficiency seen in protein mediated reprogramming is the absence of the TLR3 response normally initiated by integrating vectors. This was elegantly demonstrated by J. Lee and colleagues who directly compared reprogramming efficiencies of proteins on their own versus proteins plus non-

reprogramming lentivirus vectors [114]. The authors observed an increase in reprogramming efficiency in the prescence of lentiviral vectors compared to reprogramming proteins alone. This was accompanied by an increase in TLR3 response, and suggested that TLR3 response was needed to induce the epigenetic changes required for reprogramming.

1.8.2.5 Small molecules

Epigenetic modifications such as DNA methylation and histone modifications are catalysed by DNA methyltransferases (DNMT), histone methyltransferases, methylases and deactylase (HDAC) enzymes. These epigenetic modifications allow transcriptional control of differentially expressed genes such as pluripotency associated genes and developmental genes, genomic imprinting and X inactivation, as reviewed by W. Reik in 2007 [115]. Temporary inactivation of genes typically repressed reversibly by methylation of Histone 3 at Lysine 27 (H3K27), whereas more permanent silencing of genes such as OCT-4 and NANOG during differentiation is due to DNA methylation as well as repressive histone modifications. Agents such as DNMT inhibitors and HDAC inhibitors have been effective in improving reprogramming efficiency.

DNA methyltransferases (DNMT) are highly conserved enzymes, which can be subdivided into two types; 1) DNMT1, a maintenance transferase which maintains existing methylation patterns by copying the methylation on the complimentary strand of hemimethylated DNA and 2) DNMT3a/b, *de novo* transferases, which establish new methylation patterns during embryogenesis,

reviewed by J. Lu in 2013 [116]. DNMTs work by catalysing the transfer of a methyl group from S-adenosyl-L-homocysteine (AdoMet) to the C5 position of cytosine. This interaction causes the target base to "flip out" from the DNA helix, as demonstrated by X-ray crystallography of the bacterial DNMT Hhal I complexed to AdoMet [117].

Binding of pluripotency genes to the regulatory elements of their target genes in itself blocks the interaction with DNMTs, leading to hypomethylation of the pluripotency factors. Efficiency of iPS production can be significantly increased by the use of small molecules and chemicals that target DNMTs. Inhibitors such as 5'azacytidine are incorporated as a nucleoside analogue, which then covalently bind DNMTs, leading to their degradation by the proteosome and the unmethylated daughter DNA. DNMT inhibition by RG108 is non-nucleosidic and works by blocking the active site of DNMTs [116].

Histone modifications such as acetylation, methylation, phosphorylation, ubiquitination and sumyolation allow transcriptional control by altering the conformation of the chromatin, resulting in either a condensed (closed) or uncondensed (open) chromatin structure. Open chromatin is associated with high transcription levels, whereas condensed chromatin is associated with transcriptional repression. Histone tail acetylation neutralizes the positively charged histones, allowing them to adopt an open chromatin structure associated with transcription, whereas deacetylation is associated with condensed chromatin and transcriptional repression. HDAC inhibitors have proven to be very effective in improving reprogramming efficiency. The effect of histone methylation on

transcriptional activity differs depending on which site is methylated. For example hitsone H3 lysine 4 is associated with active transcription whereas histone H3 lysine 9 and histone H3 lysine 27 are associated with transcriptional silencing [116]. Inhibitors of histone methyltransferases and histone demethylases such as BIX01294 and Tranylcypromine, respectively, have also proven to be effective in improving iPS efficiency. The effects of various small molecule inhibitors on reprogramming efficiency are described below.

HDAC inhibitors such as suberolylanilide hydroxamic acid (SAHA), butyrate, trichostatin A (TSA) and valproic acid (VPA) are potent enhancers of reprogramming, in particular VPA, which increased reprogramming efficiency by 100 fold [27]. In addition butyrate was able to reduce the proportion of partially reprogrammed colonies in MEF reprogramming [118] and increased reprogramming efficiency in human fibroblasts 15-51 fold in 4 factor reprogramming or >100- >200 fold in the absence of Klf-4 r C-Myc [101].

Other small molecules that have proven to effective include the DNA methyltransferase inhibitor 5'-azacytidine (5'-azaC) which increased reprogramming efficiency by 10 fold [27] and a G9a histone methyltransferase inhibitor BIX-01294 which increased MEF reprogramming efficiency by 5 fold [119]. The effect of BIX-01294 was further enhanced when used in conjunction with the L-type calcium channel agonist Bay K8644 (15 fold increase) or the DNA methyltransferase inhibitor RG108 (30 fold increase). In addition, BIX-01294 was able to replace Sox-2 in mouse fibroblasts [120] and neural precursor cells (NPCs)

and was also able to replace Oct 3/4 in NPCs, albeit at an extremely low efficiency [119].

Further chemical screens have since been carried out in order to identify more molecules that can replace reprogramming factors in order to try and establish a transgene-free reprogramming method. A screen of small molecules that could replace Sox-2 identified a compound E-616452 (renamed RepSox), which inhibits TGF-β signalling and enables reprogramming through the induction of Nanog transcription [121]. Two groups achieved small molecule substitution of Sox-2, Klf-4 and C-Myc in mouse embryonic fibroblast reprogramming. One group were able to generate iPS cells with 0.02% efficiency by combining lentiviral infection of Oct-4 with the small molecule AMI-5, a protein arginine methyltransferase (PRMT) inhibitor in combination with A-83-01, a TGF- β inhibitor [122]. Similar iPS efficiencies were obtained by combining the HDAC inhibitor (VPA) with two TGF-B inhibitors (CHIR99021 and 616452) and the H3K4 demethylation inhibitor (tranylcypromine). This combination termed VC6T efficiently enhance iPS generation when combined with lentiviral delivery of Oct-4 [123].

Most recently the same authors went on to generate chemically induced pluripotent stem (CiPS) cells from MEFs using a chemical cocktail of seven small molecule enhancers/inhibitors [124]. This combination combined the 4 molecules identified in the previous screen (VC6T) plus Forskolin, the epigenetic modulators [3-deazaneplanocin A (DZNep) and dual inhibition (2i) of glycogen synthase kinase-3 and mitogen-activated protein kinase signalling. This

combination was able to reprogramme MEFs, and adult mouse fibroblasts. However, a small molecule combination has yet to be identified for reprogramming human cells [124]. An outline of non-viral reprogramming methods and efficiencies is shown in Figure 3.

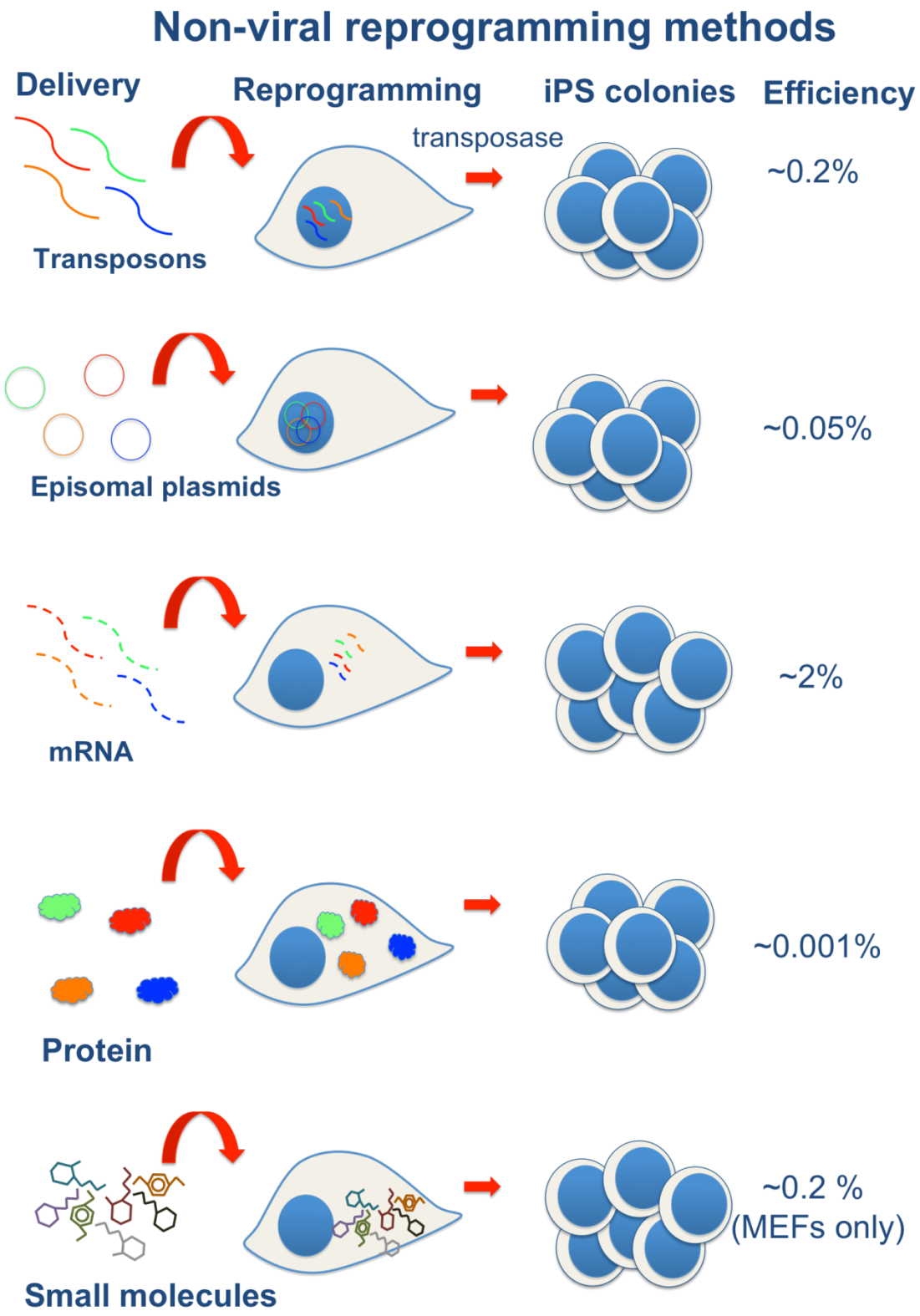


Figure 3 – Non-viral reprogramming methods. Transposons, episomal plasmids, messenger RNA, Protein and small molecules and their efficiencies.

1.9 A need for an improved reprogramming method

Although there are many alternative methods for somatic cell reprogramming, a high efficiency, non-integrating vector which can carry extra genes such as additional safety features is yet to be established. With the exception of Sendai virus and mRNA the non-integrating methods are very inefficient and in addition the Sendai virus vector has a limited transgene capacity. Other promising alternative methods to integrating vectors, such as complete small molecule reprogramming have not been achieved in human cells. In addition to their low efficiency, non-integrating methods such as plasmid transfection and mRNA are laborious and require repeated transfection procedures.

1.10 Wild type Herpes simplex type-1 virus (HSV-1), HSV-1 amplicons and host defense mechanisms.

Wild type HSV-1 viruses are composed of a viral envelope which contains ten viral glycoproteins that facilitate receptor mediated entry and fusion of the viral envelope with the cell membrane. Within the envelope is the tegument, which contains virally encoded proteins including VP16, which is involved in transcriptional up-regulation of the immediate early genes, and VP22, which is involved in viral spread during lytic infection. Within the viral tegument lies the capsid, which surrounds the viral genome and is composed of four proteins, VP5, VP26, VP23 and VP19C, reviewed in [125].

The HSV-1 genome encodes ~85 genes which are involved in nucleic acid metabolism, DNA synthesis and processing of proteins. The HSV-1 genome is under tight temporal control and the genes can be divided into four categories

depending on when they are expressed. These categories are immediate/early genes (α genes, which require no prior viral protein synthesis for expression), early genes (β genes, which are expressed independently of viral synthesis), partial late (γ_1 genes, which are augmented by the onset of viral DNA synthesis) and true late (γ_2 genes, which are totally dependent of viral DNA synthesis) (Fields virology).

The five immediate early genes (infected cell protein 0 (ICP0), ICP4, ICP22, ICP27 and ICP47) are well characterised and are required for induction of the early and late genes and to counteract cellular antiviral responses. The immediate early gene ICP0 has several roles of stabilizing cell cycle regulatory proteins such as cyclin D3, maintenance of protein synthesis and inhibition of interferon (IFN) and interferon stimulated genes (ISG) [126]. The induction of cyclin D3 is likely to induce apoptosis however this is counteracted by the viral US3 gene which blocks apoptosis. ICP27 blocks the splicing of viral and primarily host mRNA and decreases protein synthesis as well as regulating the expression of late genes. Degradation of host and viral mRNA by RNase activity induced by the viral host shut-off down-regulates host protein synthesis (Fields virology).

Anti-viral host defence mechanisms such as the shut off of protein synthesis via the phosphorylation of EIF-2α is evaded in wild type HSV-1 by the expression of the viral partial late gene ICP34.5, which converts phosphatase 1 protein to dephosphorylate EIF-2α, inducing it's expression by 3000-fold. In addition, ICP34.5 also blocks double stranded RNA (dsRNA)-dependent protein kinase (PKR) mediated autophagy by binding Beclin 1, a major activator of

autophagosome formation. Mutant HSV-1 expressing a ICP 34.5 lacking the Beclin 1 binding domain were impaired in their ability to cause encephalitis in mice [127]. In addition PKR mediated autophagy is also blocked by interaction with immediate early protein US11 with PKR [128]. Another way by which wild type HSV-1 averts antiviral defences is by blocking the presentation of antigen peptides by translocation of peptides to the endoplasmic reticulum via the expression of ICP47 (Fields virology).

HSV-1 amplicon vectors are high transgene capacity, non-integrating vectors which have a high transduction efficiency in a wide variety of cells including fibroblasts, iPS cells and neurons. HSV-1 amplicons contain two non-coding *cis*-acting sequences, a viral origin of replication (*Ori S*) and a viral DNA packaging signal (*pac*), which allow them to be packaged into HSV-1 virions [129]. The HSV-1 amplicon does not contain any wild type HSV-1 genes, however the viral proteins that constitute the capsid and tegument can induce cellular responses to HSV-1 transduction.

Theoretically, elimination of the genes which counteract anti-viral host defence mechanisms would mean that cells transduced with HSV-1 amplicons would be more susceptible to host defence pathways such as interferon response, apoptosis and autophagy. Not many publications have detailed the cellular response to HSV-1 amplicons, however a few groups have reported an induction of interferon pathways. Notably, transduction of early passage human fibroblasts (HHFF-2) with HSV-1 amplicons resulted in an antiviral state, characterized by the expression of IFN3 and IFN7 and resistance to vesicular

stomatitis virus [130]. Induction of activated IFN3 was detectable after 8 hours, however degradation of the protein was apparent after 24 hours. Induction of interferon and cytokine pathways were also observed in mice transduced with HSV-1 amplicons by intravenous injection, however interferon and cytokine levels returned to basal levels within 12 hours [131]. Stereotactic injection of HSV-1 amplicons into the striatum of mice resulted in a more modest induction of cytokines, indicative that host response to HSV-1 amplicons differs depending on the cell [132]. These studies show an interferon response is induced in HSV-1 amplicons, however the response is cell type dependent and appears to be transiently induced.

We propose a new reprogramming method based on Herpes simplex-1 (HSV-1) amplicon vectors. We employ a helper bacterial artificial chromosome (BAC) packaging system which enables packaging of the amplicon without contamination of helper virus in the amplicon stocks [133]. The HSV-1 helper BAC (fHSVΔpacΔ27) encodes all the viral proteins required for the HSV-1 virion and has several safety features to prevent the BAC from being packaged into virions.

Firstly, the BAC has been deleted for the DNA packaging signal and therefore can not be packaged into virions. The packaging signal could be acquired via homologous recombination of the the BAC with the amplicon plasmid, however the BAC genome has been modified to contain two additional copies of the ICP0 gene which act as “stuffer” sequences to increase the genome to 178 Kb in size.

This increase in genome size exceeds the amplicon capacity of 150 Kb and so is unable to package into HSV-1 virion.

The second safety feature of the helper BAC is the deletion of the immediate early gene ICP27, which has been shown by deletion mutant studies to be an essential gene for DNA replication and transcriptional control of early and late viral genes [134]. The ICP27 was deleted by homologous recombination from fHSVΔpac, a predessessor of fHSVΔpacΔ27, in order to render any helper virus contaminants replication incompetent. Although deletion of ICP27 rendered the amplicon stocks helper virus free, the titres were severely compromised (<10 transducing units per ml (TU/ml). The titres were restored to ~10^3 TU/ml by packaging the cells into the Vero 2-2 cell line which is stably transfected with the ICP27 gene. Co-transfection of an additional plasmid expressing ICP27 further improved titres to ~10^6 TU/ml. [133].

Generation of helper-virus free stocks that are replication incompetent is important for minimising cytotoxicity of the amplicon stocks. Co-transfection of the amplicon vector with a helper BAC and small plasmid encoding the essential gene ICP27 allows generation of high titre, replication incompetent, helper-virus free, HSV-1 amplicon stocks. The packaging strategy is shown in Figure 4.

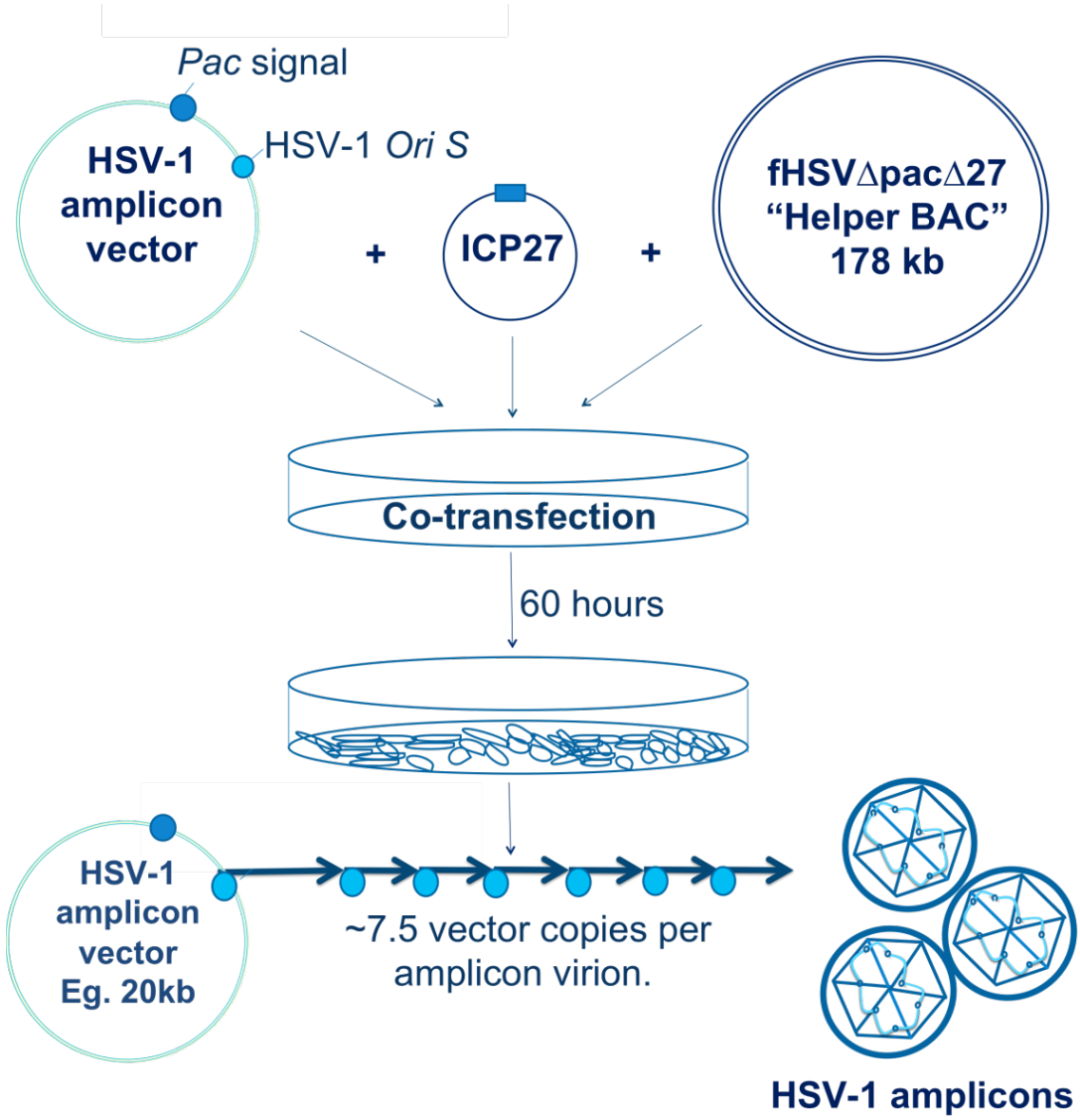


Figure 4 – HSV-1 amplicon vector packaging by "helper BAC" plasmids. Helper BACs contain all the genes of the HSV-1 virion but have deletions in the packaging signal (pac) and essential gene ICP27. HSV-1 amplicon vectors are packaged by rolling circle mechanism into HSV-1 virions, resulting in a concatamer of the plasmid. Copy number depends on amplicon vector size, a 20kb vector is copied into an amplicon virion ~7.5 times.

1.11 Application of iPS cells to model disease

Induced pluripotent stem (iPS) cells are excellent tools for modelling diseases *in vitro* due to the ability to differentiate iPS to most cell types. The differentiated cells can then be used to directly compare diseased cell phenotypes with healthy control cells [135] and can also be used to identify disease markers. Patient derived cells provide an excellent platform for small molecule drug screening and toxicology assays [136] and recent work to transplant differentiated cells to small animal models have yielded promising results [137]. Applications of iPS cells are outlined in Figure 5.

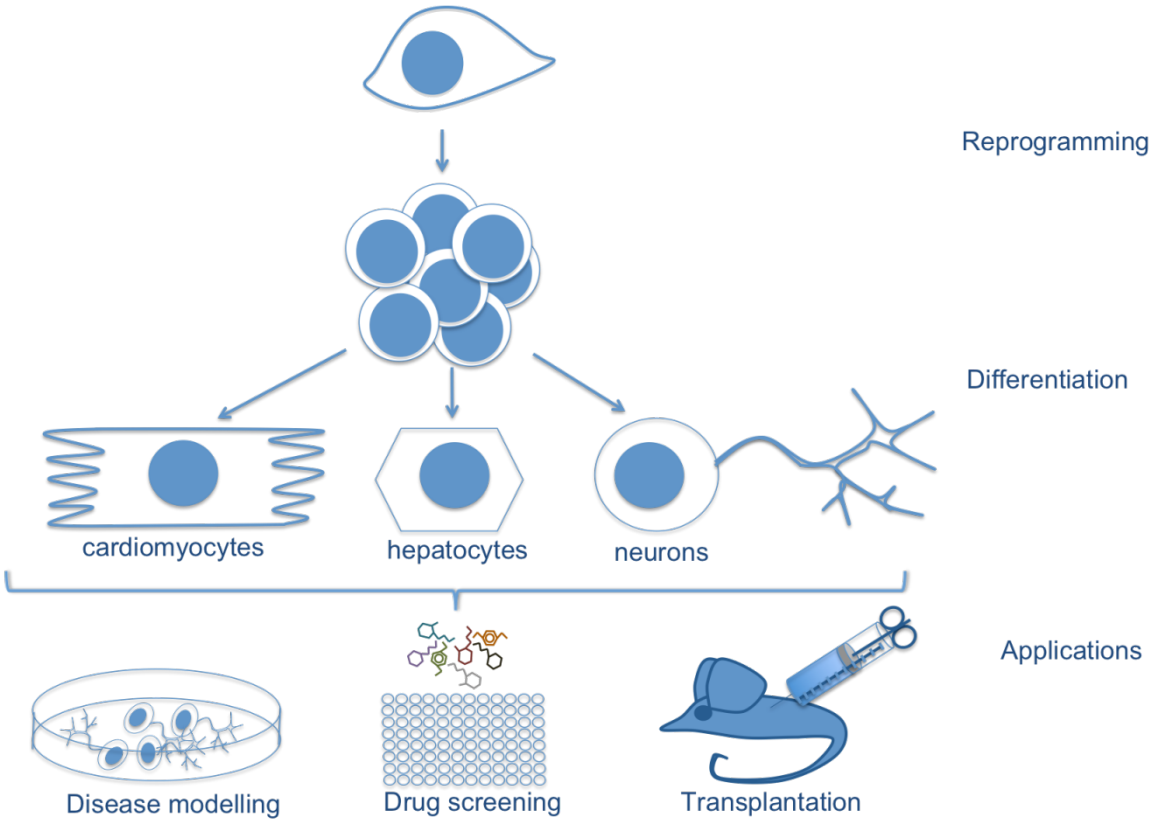


Figure 5 – Application of iPS cells. Reprogrammed fibroblasts can be differentiated to different cell types such as cardiomyocytes, hepatocytes or neurons. Differentiated cells can then be used for disease modelling, drug toxicology or transplantation studies.

In recent years many laboratories have generated iPS cells from patients suffering from many diseases including diabetes, Huntington's disease, Fanconi Anaemia, retinal degeneration, liver disease, and Amyotrophic Lateral Sclerosis [84, 138-140]. Patient specific models provide a platform for studying disease progression in a model carrying the disease-specific genetic background, ultimately increasing understanding of the molecular mechanisms of the disease.

1.11.1 Application of iPS cells to model Parkinson's disease.

Parkinson's disease (PD) patient iPS cells have also been utilised to differentiate dopaminergic (DA) neurons to study PD pathology [135, 141]. PD is a common progressive neurodegenerative disorder, which is thought to be caused by a combination of genetic and environmental factors [142]. There is a strong familial component to PD with the most common mutations occurring in leucine rich repeat kinase 2 (LRRK2). Approximately 90% of PD cases are sporadic, however genome wide association studies (GWAS) found significant associated polymorphisms in alpha-synuclein (SNCA) and microtubule associated protein tau MAPT [143]. Parkinson's disease also has a strong mitochondrial component and mutations in mitochondrial associated genes such as parkin RBR E3 ubiquitin protein ligase (PARKIN) [144], PTEN induced putative kinase 1 (PINK1) [145] and parkinson protein 7 (PARK7 or DJ1) [146] are causative of the disease. Non-motor symptoms of the disease such as anxiety, olfactory impairment and depression are an early indication of PD and can appear up to 20 years before motor symptoms develop [147]. The disease clinically manifests with motor symptoms such as rigidity, tremor and bradykinesia and is linked to the loss of DA neurons in the substantia nigra pars compacta [148].

Differentiation of DA neurons from patient derived iPS cells allows us to study disease phenotypes *in vitro.*

1.11.2 PD patient derived iPSC disease models

1.11.2.1 SNCA

The oligomeric aggregation of α-synuclein (SNCA) protein in the form of Lewy bodies, are the hallmark of PD pathology in post mortem brain tissue [149]. Familial mutations in SNCA are extremely rare, however several laboratories have recruited PD patients with SNCA mutations to identify disease phenotypes *in vitro* [135]. One study on dopaminergic neurons derived from 3 individual iPS lines from a 48 year-old male carrying an SNCA triplication were compared with neurons derived from 3 iPS lines from his unaffected sister [135]. The patient-derived cultures demonstrated over-expression of SNCA and upregulation of oxidative stress markers and displayed sensitivity to hydrogen peroxide. Withdrawal of the antioxidant ascorbic acid from the neuronal cultures resulted in increased proportion of caspase-3/TH double-labeled cells and increased sensitivity to oxidative stress induced cell death. Among the genes upregulated in the SNCA triplication cultures were the ubiquitin chaperone, ubiquitin carboxyl-terminal esterase L1 (UCHL1), which has been implicated in PD and Monoamine oxidases (MAO) which has been implicated in PD models due to increase reactive oxidase species (ROS).. In addition the oxidative stress protein heme oxygenase-2 (HMOX2) and aggregate interacting proteins DnaJ (Hsp40) homolog, subfamily A, member 1 (DNAJA1) and heat shock 27kDa protein 1 (HSPB1) were also upregulated [135].

Another study by R. Jaenisch and colleagues demonstrated zinc finger nuclease (ZFN) insertion of the A53T SNCA mutation into hES clones and the correction of the A53T SNCA mutation from PD patients. This technology allows the development of isogenic controls which contain identical genetic backgrounds and theoretically differ only at the target gene. One limitation of this technology is ZFN off target effects therefore rigorous screening is required to ensure there are no adverse insertions [150].

1.11.2.2 LRRK-2

Several iPS cells from Parkinson's disease patients harboring mutations in LRRK2, have been established [141, 151, 152]. Studies on dopaminergic neuron cultures from patients carrying the G2019S mutation compared with healthy controls displayed an increased sensitivity to caspase-3 activity, proteasome inhibitor MG-132 and peroxide induced cell death [151]. In addition mutant LRRK lines increased expression of six key oxidative stress pathway genes and α-synuclein [151].

Correction of the LRRK2 G1920S mutation *in vitro* using ZFN in two patients iPS lines rescued neurite outgrowth deficit seen in G1920S neurons [152]. The authors also observed a decrease in Caspase-3/TH double positive cells in gene corrected lines compared with G1920S LRRK2 lines. Gene-corrected neuronal cultures also contained 30% less α-synuclein than G1920S LRRK2 cultures. The authors also observed a dysregulation in five genes in G1920S LRRK2 cultures, which was confirmed by knockdown experiments to contribute to

neurodegeneration. Transcriptional dysregulation of three of these genes, calcium-dependent secretion activator 2 (CADPS2), Copine 8 (CPNE8) and ubiquitin-like with PHD and ring finger domains 2 (UHRF2) was dependent on extracellular signal regulated kinase (ERK) activity. Inhibition of ERK activity decreased dopaminergic neuronal degeneration in mouse ES derived neurons, increased neurite outgrowth and decreased cytotoxicity under oxidative stress [152].

Further studies on patient iPS cell harbouring a R1441C mutation in LRRK2 also displayed sensitivity to toxins such as MPP^+. In addition mutant iPS lines resulted in fewer dopaminergic neurons compared with healthy controls [141].

1.11.2.3 PARK2

The PARK2 gene encodes the protein Parkin which is an E3 ubiquitin ligase. Mutations in PARK2 are causative for autosomal recessive juvenile Parkinson's disease. Dopaminergic neurons derived from 2 PARK2 patients displayed increased oxidative stress, impaired mitochondrial homeostasis and abnormal mitochondrial morphology in 80-90% of neurons. In addition the accumulation of α-synuclein was observed in one of the patient lines and post mortem tissue [153].

1.11.2.4 PINK-1

PTEN-induced putative kinase 1 (PINK1) is a mitochondrial kinase, which recruits PARKIN to induce autophagy in dysfunctional mitochondria. Neural cells derived from patients carrying the Q456X mutation in PINK1 were compared with healthy control derived cultures. Mutant PINK1 cultures displayed cellular vulnerability to chemical stressors such as MPP+, hydrogen peroxide and MG132 when compared with control cultures. This increased vulnerability was associated with mitochondrial dysfunction and could be rescued by treatment with coenzyme Q10. Increased levels of mitochondrial reactive oxygen species (mROS) was detected in PINK-1 mutant cultures, which didn't respond to ATP synthase inhibitors, the proton ionophore,carbonylcyanide-p-trifluoromethoxyphenylhydrazone (FCCP) or the mitochondrial complex I inhibitor rotenone. The results demonstrated an increase in the passive leak of protons from the mitochondrial membrane and respiration was ATP independent [141].

Further studies on iPS lines derived from patients carrying several mutations in PINK1 displayed impaired recruitment of lentiviral delivered PARKIN and upregulation in the gene peroxisome proliferator-activated receptor gamma, coactivator 1 alpha (PGC1) that regulates mitochondrial biogenesis. Under treatment with valinomycin control neurons demonstrated mitochondrial translocation of PARKIN, however this was not observed in the patient PINK1 mutant neurons [154].

1.11.3 Drug screening using patient derived neurons

Current drug screens based on immortalised cell lines and animal models often fail when reaching the clinical trial stage due to poor physiological relevance of the disease models used. Patient derived iPS cells provide an ideal platform to screen small molecule compounds and already there have been several publications where promising drug hits have been identified. A screen to identify drugs that prevent motor neuron death identified potential hits including the drug kenpaullone, which outperformed other animal tested drugs that recently failed at the clinical trial stage [136]. Another study has identified a cdk inhibitor that can prevent amyloid β induced toxicity [155].

Drug screening using PD patient DA neurons are currently hampered by the high heterogeneity of DA cultures and low DA generation efficiency. In addition the multifactorial nature of PD makes it difficult to identify potential targets. A recent study in DA neurons derived from several patient iPS lines displaying either LRRK2 mutations (G2019S or R1441C) or PINK1 mutations (Q456X) showed reduced vulnerability when treated with Co-enzyme Q10 and low concentrations of valinomycin and concanomycin A. These results demonstrate that one drug can have multiple targets and improve phenotypes in cell lines derived from different mutations [141]. Improvements in dopaminergic neuron differentiation efficiency need to be made before these can be applied to high throughput drug screens.

1.12 Differentiation of DA neurons in embryogenesis

Development of the vertebrate nervous system in embryogenesis arises from the ectoderm and is controlled by inductive signaling. Neurulation occurs by invagination of the neural plate, which forms a neural groove and subsequently closes to form the neural tube. Brain development can be specified by two axes; the rostrocaudal axis and the dorsoventral axis; which specify the positioning from "nose to tail" and "back to front", respectively. Dorso-ventral patterning of the neural tube is controlled by the secreted glycoprotein Sonic Hedgehog (SHH), which specifies ventral patterning and bone morphogenic proteins (BMPs) which specify dorsal patterning [156]. Development of the neural tube from the neural plate in respone to SHH and BMP signaling is shown in Figure 6.

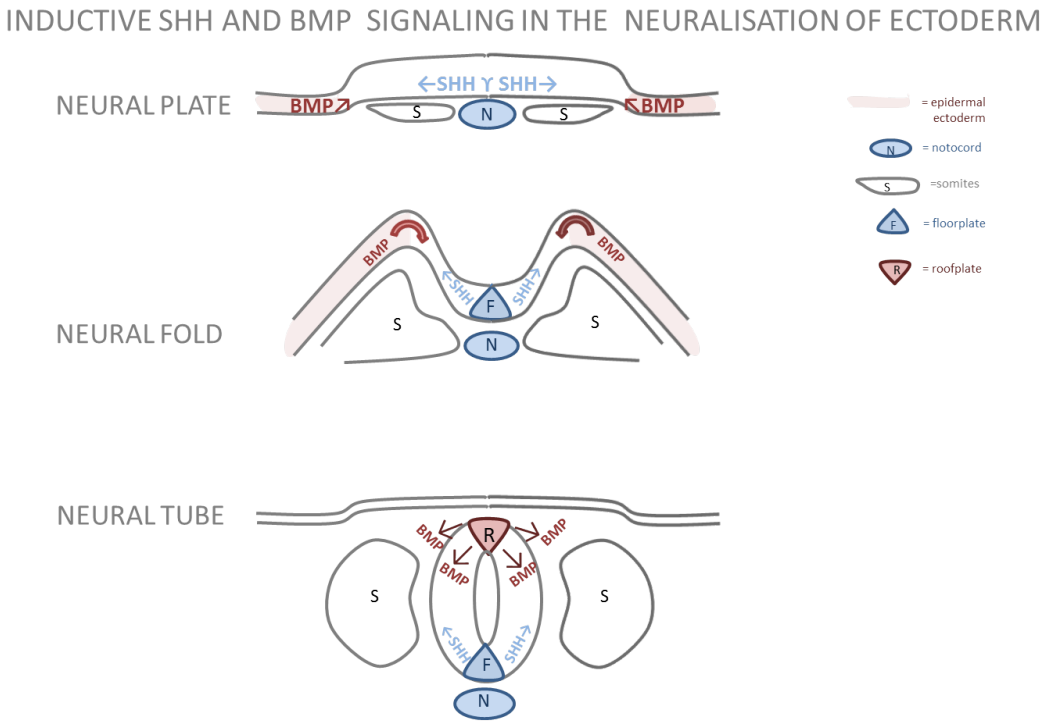


Figure 6 –Inductive signaling of SHH and BMP during ectoderm neuralisation. SHH is secreted from the notochord into the neural plate. BMP signaling is mediated from the epidermal ectoderm. The neural plate buckles to form the neural fold and SHH signaling is maintained in the floorplate cells at the ventral side, following closure of the neural tube BMP signaling is maintained in the roofplate cells in the dorsal side of the tube (adapted from [156]).

SHH is initially secreted from the notochord and by floor plate at later stages. Different cell types arise at different developmental time points depending on exposure to different concentrations of SHH [157]. Whereas low concentrations of SHH induce ventral interneurons, medial concentrations of SHH induce motor neurons and high concentrations induce floor plate cells which subsequently maintain SHH expression. The effect of SHH on neuronal development has been demonstrated in neural explants, which generate different cells dependent on the concentration of SHH exposure. The SHH concentration gradient depends on the rate of diffusion of SHH from the notochord and floor plate and target cells in the neural tube [157].

BMPs are secreted from the epidermal ectoderm at the flanking edges of the neural plate. Following closure of the neural tube, epidermal ectoderm no longer express BMPs and BMP expression is maintained in the roof plate and dorsal neural tube. BMPs are a negative regulator of differentiation and have been shown in culture to promote the differentiation of ectoderm to epidermis, whereas blocking of BMP signals induces neural differentiation. Binding of BMPs to the cell receptors induces phosphorylation of SMADs, which in turn inhibit neural genes from being expressed. This can be counteracted by either; inhibition of BMP receptor binding by three agonists noggin, chordin and follistatin, or, high levels of MAPK which prevent phosphorylation of SMADs. Low BMP levels and high MAPK levels promote neuronal differentiation [158]. Long range patterning of BMPs by gradients and signaling cascades may influence the differentiation of different dorsal cells types such as roof plate cells, neural crest cells and dorsal interneurons [156]

The brain develops at the rostral end of the neural tube and forms three main brain regions, the forebrain, midbrain and hindbrain. Initially the forebrain and midbrain patterning is specified by expression of Otx2 and Gbx2 [159]. The midbrain (mesencephalon) is patterned by signals in the neural organizing centre (isthmus), located at the Otx2/Gbx2 boundary, at the junction of the mesencephalon and metencephalon. Patterning of the hindbrain (metencephalon) is controlled by Retinoic acid (RA) produced by somites in the caudal region of the neural tube. RA activates the expression of the HOX genes (Hoxa1 and Hoxb1) which induce a complex auto and cross regulatory feed back loops between different hox genes that culminates with the segmentation of the hindbrain [160, 161].

Midbrain dopaminergic (DA) neurons of the A9 region of the substantia nigra are the cell type lost during Parkinson's disease. These cells differentiate close to the floor plate of the neural tube and near to the midbrain-hindbrain barrier. Midbrain patterning and development has been studied extensively in order to elucidate the genes involved and temporal expression of these genes. Explant studies and knockout mice have been essential in determining the factors involved and the epistatic relationships between transcription factors and homeodomain genes. Transplantation studies have shown that transplantation of mesencephalon tissue to other parts of the brain result in local tissue differentiation depending on environmental cues. If the isthmus (midbrain hindbrain barrier) is included in the transplant then the mesencephalon develops as normal in the new location and surrounding tissues adopt a

mesencephalon-metancephalon fate [162]. Several transcription factors have been shown to direct midbrain development in vertebrates including SHH, Wnt-1, Fgf8 and engrailed 1 and 2 [163-166].

The interactions of transcription factors and homeodomain proteins in the midbrain are summarised as follows. At early stages of midbrain development many factors have been shown to spcificy midbrain development and DA neuron differentiation. SHH ventralises neural tube, induces Lmx1A, Msx1 and FoxA2 expression. Lmx1B expression arises at E7.5 and regulates Wnt expression and maintains the later expression of PitX3, a DA neuron specific factor via an independent pathway to Nurr-1. FGF8 expression arises early at developmental stage E8.0 and induces Fgf8, En2 and Wnt expression and is involved in Lmx1B maintenence. Wnt signaling also arises at stage E 8.0 and regulates the expression of Engrailed 1 and 2 and inhibits SHH activity. The homeodoamin proteins En 1 and En 2 are involved in maintenance of Fgf8 and patterning of Wnt expression at developmental stage E 8.0. Lmx1A expression arises at developmental stage E 9.0 and regulates Nurr1 and PitX3 and induces Ascl1 (E9.5). Subsequently, Ascl1 induces Ngn2 and downregulates Nkx6.1, the motor neuron factor. Nurr1 expression arises at stage E 10.5 and induces TH expression. Nurr1 has also been shown to regulate the DA markers AADC, VMAT, DAT and cRET [167]. Pitx3 arises at stage E 11.5 and regulates TH expression and induces ADH2 [167]. The interactions of these transcription factors in midbrain embryonic development are discussed in further detail below and in Chapters 5 and 6. An outline of temporal expression of key midbrain and

dopaminergic markers and transcription factors during DA neuron development are demonstrated in Figure 7.

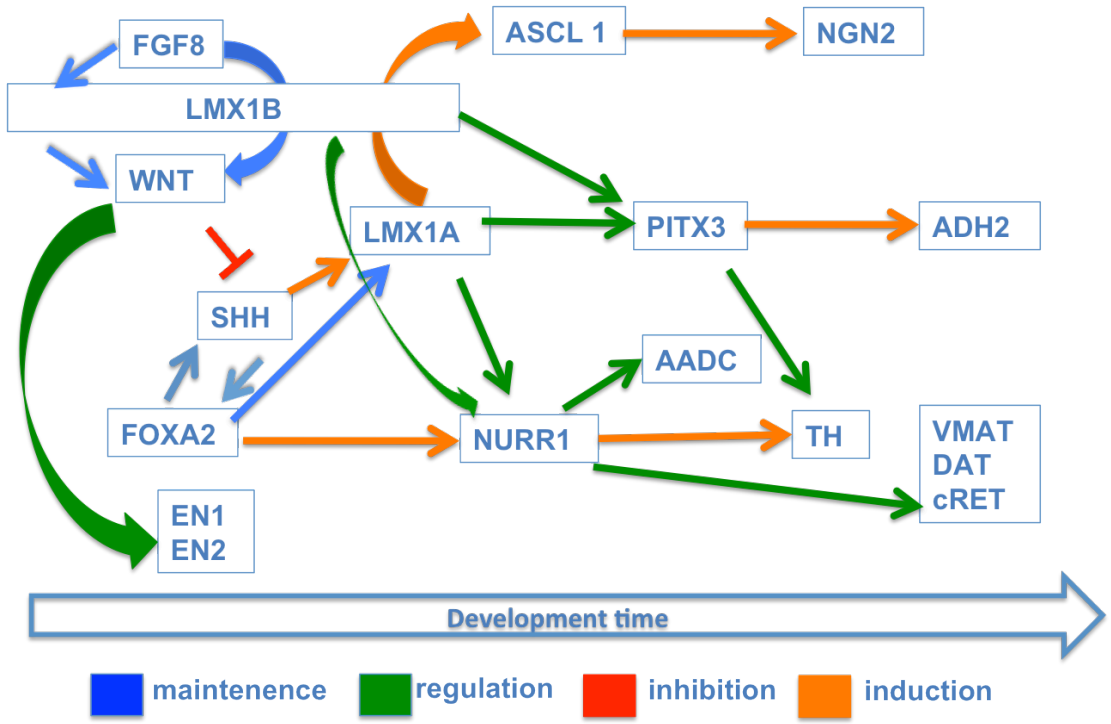


Figure 7 – Factors involved in dopaminergic neuron development. Sequential expression of factors is shown over development time and their actions on other molecules are shown. FGF8 and SHH specify anterior/posterior and dorsal/ventral cues for dopaminergic neuron development. Factors such as FOXA2 and LMX1A regulate and induce later dopaminergic markers such as NURR1 and PITX3. TH expression is directly induced by NURR1 and regulated by PITX3. Mature markers such as VMAT, DAT and cRET are regulated by NURR1. Figure adapted from [167]

1.12.1 Midbrain factors - FGF8, Engrailed and Wnt genes

Fibroblast growth factor 8 (Fgf8) is expressed between the prospective midbrain and hindbrain region at developmental stage E 8.0 in mouse embryos. By developmental stage E 9.0 the expression is restricted to a defined band in the isthmus and the dorsal midline and was detectable up until stage E 12.5 [164].

Histological analysis at stage E 9.5 identified that Fgf8 is expressed immediately caudal to Wnt 1. Midbrain explant cultures cultured with Fgf8 soaked beads showed that the first genes induced were Fgf8, Gbx2 and En2, which showed weak expression after 8 hours of culture and strong induction after 40 hours in culture [165]. Furthermore, exogenous expression of Fgf8 in another part of the brain in the developing chick embryo results in the induction of en2, wnt1 and FGF8 RNA and subsequent development of an ectopic mesencephalon structure [164].

The expression of the homeodomain genes engrailed 1 and 2 and Wnt 1 have been shown to co-localise at embryonic stage E 8.0 in the neural folds, by E 12.0 and E 15.5 the engrailed genes are expressed in the midbrain/hindbrain junction [166]. Further studies have shown that Wnt 1 also regulates midbrain development and is a regulator of the engrailed genes. In Wnt 1 homozygous mutant mice, En1 and En2 RNA and protein expression is diminished in the midbrain and hindbrain regions compared to controls [168].

En 1 and En 2 double knockout mutant mice have deleted midbrain and hindbrain regions at developmental stage E 9.5 and the midbrain genes Pax5, Fgf8, and Gbx2 were not detectable at this stage. Lac Z reporters of the double homozygos knockout identified expression in the midbrain/hindbrain region at stage E 8.0 and expression of Pax5, Fgf8, and Gbx2 was weaker than in $En1^{+/-}$ / $En2^{-/-}$ littermates. By stage E 8.5/ E 9.0 no morphological deletion was detected however weaker and more restricted expression of Fgf8, Gbx2 and Pax5 and altered patterning of Wnt 1 was observed compared to $En1^{+/-}$ / $En2^{-/-}$ littermates

[165]. Furthermore, explant studies using En1/En2 double knockout tissue demonstrated that the engrailed genes are required for induction of Pax5 and inhibition of Pax6 by Fgf8 [165].

1.12.2 DA factors – PitX3, Lmx1a/b, FoxA1/2, Ascl1 and Nurr1

PitX3 is a key transcription factor in DA neuron differentiation. PitX3 expression overlaps with tyrosine hydroxylase (TH) expression in mouse A9 nigrostriatal DA neurons at developmental stage E 11.5. Expression of PitX3 is absent in the injected hemisphere of model rats following unilateral ablation of dopaminergic neurons by the neurotoxin 6-OHDA. In addition, the density of PitX3 expressing neurons in Parkinson's disease patients is reduced compared to non PD controls [169].

Another regulator of dorsoventral patterning is Lmx1b and in situ hybrodization localised Lmx1b to the substantia nigra, suggesting a role in DA neurogenesis. Expression of Lmx1b arises at E 7.5 and is maintained throughout life. In situ hybridisation colocalised with PitX3 and TH and expression was lost following unilateral ablation of DA neurons by 6-OHDA. Absence of the Lmx1b gene in knockout mice resulted loss of PitX3 expression in DA neurons at developmental stage E 12.5, however TH was expressed until developmental stage E 16 and Nurr 1 expression was maintained throughout. Conversely, Nurr1 knockout mice resulted in absence of TH expression at stages E 10.5, E 11.5 and E 12.5 resulted in absence of TH expression whereas expression of Lmx1b and PitX3 was detected. These observations suggest Lmx1b acts in a separate pathway for DA neuron specification to Nurr-1 [170].

The homeodomain proteins Lmx1a and Ascl1 are also important in midbrain dopamine neuron differentiation. Expression of Lmx1a in the developing mouse arises at developmental stage E 9.0 and is expressed in both DA progenitors and Nurr1+/TH+ postmitotic DA neurons. Midbrain explant experiments in developing chick embryos demonstrated that both Lmx1a and Ascl1 are induced in response to SHH and precede the expression of Nurr1 and TH [171].

Retroviral delivery of Lmx1a to developing chick embryos induced ectopic DA neurons, which express Nurr1, Lmx1b and TH. Conversely, siRNA knockdown of Lmx1a resulted in a reduction of Nurr1+/Lmx1b+ post mitotic neurons and abolishment of Ascl1. Ascl1 expression is induced by Lmx1a at developmental stage E 9.5 and correlates with the downregulation of the motor neuron marker Nkx6.1. Unlike Lmx1a, Ascl1 expression is restricted to DA progenitors. Premature expression of Ascl1 in developing embryos resulted in upregulation of the proneural protein Ngn2 and DA markers Nurr1, Pitx and TH at stage E 10.5 and downregulation of the motor neuron marker Nkx6.1. Knockdown of Ascl1 resulted in 40% reduction in the number of Ngn2+ progenitors and Nurr1+ DA neurons [171].

FoxA1 and FoxA2 are expressed in the ventral midbrain of developing mouse embryos at stage E 10.5. FoxA2 was co-expressed with Lmx1a in DA progenitors and co-expressed with Nurr1 and TH in DA neurons. Specific inactivation of FoxA2 and FoxA1 in the CNS at stage E10.5 resulted in a dramatic reduction in Ngn2 but did not affect other DA markers. Further analysis showed that FoxA1

and FoxA2 cooperatively regulate Nkx2.2 expression independently of Shh signalling in the midbrain of E10.5 mouse embryos. At stage E 12.5 double mutants resulted in absence of En1 and a reduction of Nurr1+ /TH+ neurons, indicative of mature DA neuron phenotype [172].

Current protocols to differentiate both iPS cells and fibroblasts to dopaminergic neurons *in vitro* involve artificially inducing midbrain patterning. This is achieved by reproducing the midbrain developmental process by sequential expression/delivery of brain specific factors (described in further detail in Chapters 5 and 6). By mirroring the expression of neuronal transcription factors (NTFs) expressed during *in vivo* DA neuron development DA neuron *in vitro* differentiation protocols have been developed [173].

1.12.3 Improving DA neuron differentiation efficiency

Some research groups have also employed lentiviral delivery of NTFs to enhance DA neuron differentiation efficiency from iPS cells [137, 174] or drive dopaminergic neuron differentiation directly from fibroblasts [175] (described in detail in Chapters 5 and 6) however the same problems with viral integration as described for reprogramming methods remain. The HSV-1 amplicon system provides an attractive alternative to lentivirus for the delivery of neuronal transcription factor delivery to both iPS differentiation protocols and direct differentiation of fibroblasts to DA neurons.

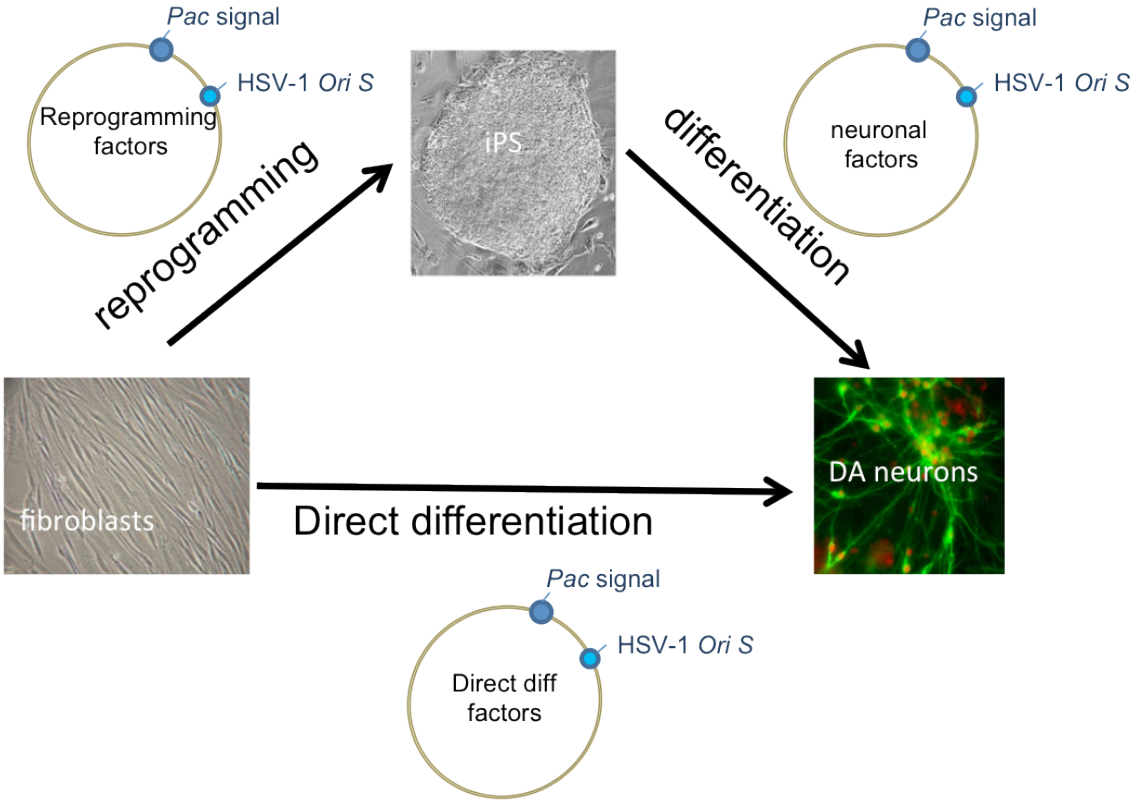
1.13 Aims

HSV-1 amplicons offer a non-integrating alternative to integrating vectors. Their high transduction efficiency and large transgene capacity make them attractive tools for use in iPS technology. We have generated three sets of HSV-1 amplicon vectors in order to develop improved methods for the generation and differentiation of iPS cells. Using these vectors we aimed to:

1) Reprogram human fibroblasts to iPS cells by the delivery of HSV-1 amplicons expressing multiple reprogramming factors.
2) Drive direct differentiation of fibroblasts to DA neurons by delivery of an HSV-1 amplicon expressing multiple neuronal transcription factors.
3) Enhance DA neuron differentiation efficiency by the delivery of HSV-1 amplicons expressing multiple neuronal transcription factors.

In the following chapters we present the construction, characterization and experimental use of these vectors. An outline of the vectors and their use is shown in Figure 8.

.


Pac signal
HSV-1 Ori S
Reprogramming factors
reprogramming
iPS
differentiation
Pac signal
HSV-1 Ori S
neuronal factors
fibroblasts
Direct differentiation
DA neurons
Pac signal
HSV-1 Ori S
Direct diff factors

Chapter 2 - Materials and Methods

2.1 Vector Construction

The vectors were designed using the computer programme Vector NTI. The reprogramming vectors (pHGCX+SOKM+/-EBNA+/-TK+/-TetO2) were constructed by standard bacterial cloning restriction digest, followed by ligation and electroporation into electrocompetent bacteria. The remaining vectors (pHGCX+SOKMO+EBNA+TK+TetO2, pHGCX+OSNL+EBNA+TK+TetO2, pHGCX+ FoxA2/LMX1A/Nurr1/PITX3+EBNA+TetO2 and pHGCX+ANL+EBNA+tetO2) were constructed by PCR amplification followed by restriction digest, ligation and electroporation into electro-competent bacteria. Final vectors were screened by colony PCR and restriction digests to confirm correct insertion and orientation. The techniques and general reagents used to construct the vectors are described in further detail below. The general laboratory reagents are listed in Table 1.

General laboratory Reagents		
Reagent	**Components**	**Preperation**
Phosphate-buffered saline (PBS)	5 tablets of PBS (Sigma), 1 L mQ H2O	Autoclave
Tris-Borate-EDTA (TBE)	4L 10x concentrate TBE (Sigma), 40 L dH2O	x
Tris-EDTA (TE)	10 mM Tris pH 8, 1 mM EDTA	x
Loading Buffer	15% Ficoll 400, 0.25 % xylene cyanol, 0.25 % Orange G (all Sigma)	x
Agarose Gel	0.6 % - 2% agarose (Sigma) dissolved in TBE	Microwave
STET buffer	8 % sucrose, 5 % Triton X-100, 50 mM EDTA, 50 mM Tris.Cl (pH 8)	x
Bacterialalkaline lysis buffer (NaOH-SDS)	1% sodium dodecyl sulfate, 0.2 M NaOH	x
Neutralization buffer	7.5 M ammonium acetate (Sigma)	x
Lysogeny Broth (LB)	25 g LB pellets (Merck), 1 L distilled water	Autoclaved
Lysogeny Broth (LB) agar	14.8 g LB Agar pellets (Merck), 400 mL distilled water	Autoclaved

Table 1 – General laboratory reagents – components and preparation listed.

2.1.1 Bacterial culture

All bacterial cultures were grown on LB agar plates or LB liquid culture containing appropriate antibiotics (Ampicillin (100 μg/mL) for all vectors except fHSVΔpacΔ27 BAC packaging vector which was cultured in Kanamycin (25 μg/mL) and Chloramphenicol (15 μg/mL) and pMSRQ0817831 which was cultured in Streptomycin (100 μg/mL). Cultures were performed using a shaking incubator set to 225 rpm and 37 °C. All minipreps were prepared using a bench top microcentrifuge and maxipreps were prepared using an Avanti J-E centrifuge (Beckman Coulter) using the rotor JA 10.5 for all spins up to 9000 rpm and the rotor JA 17 for the 14000 rpm spins.

2.1.1.1 Plasmid DNA purification (Minipreps)

A single bacterial colony was picked from a LB agar bacterial plate into an overnight 1.5 mL LB culture containing appropriate antibiotics. The next day, the culture was tipped into a 1.5 mL microfuge tube and the bacterial cells pelleted by centrifugation at 5000 rpm for 10 mins. The supernatant was aspirated and the pellet was resuspended by pippetting up and down in 70 μL of STET buffer. 200 μL of NaOH-SDS solution was added to lyse the bacterial cells, immediately followed by 150 μL of 7.5 M ammonium acetate which was inverted 5-10 times to neutralise the lysis reaction. The neutralised lysate was placed on ice for five minutes and then centrifuged at 13,000 rpm for 20 mins at 4 °C. The supernatant was tipped into a fresh 1.5 mL microfuge tube and the DNA was precipitated by adding 250 μL of room temperature isopropanol and mixed by inversion. The DNA was pelleted by centrifugation at 10,000 rpm for 8 minutes

at room temperature. The supernatant was aspirated and 200 μL of 70% ethanol was added to wash the pellet with centrifugation at 10,000 rpm for 8 minutes. The 70% ethanol wash was aspirated and the pellet allowed to air dry for 5 - 10 minutes. Finally, the DNA was resuspended in 50 μL of TE containing 5 mg/mL RNase A.

2.1.1.2 Plasmid DNA purification (Maxipreps)

The DNA plasmid purification kit (QIAGEN) buffers and columns were used for DNA maxiprep extraction. Please refer to the QIAGEN Maxiprep manual for buffer compositions. Single bacterial colonies were inoculated into a 1.5 mL starter LB culture and grown for 8 hours, which were then tipped into a 250 mL LB culture allowed to grow overnight (at least 16 hours). Bacteria were poured into 250 mL centrifuge bottles and pelleted by centrifugation at 6000 rpm for 15 minutes at 4 °C. The pellets were resuspended in 15 mL of Buffer P1 by placing the beakers in the bacterial shaker incubator for 10 minutes. Following resuspension the bacteria were lysed in 15 mL of Buffer P2, swirled thoroughly to mix and left on the bench for 5 minutes, swirling twice more during the time period. After 5 minutres, 15 mL of chilled Buffer P3 was added to neutralise the lysis buffer and mixed by swirling the mixture. The tubes were then placed on ice for 15 minutes and centrifuged for 35 minutes at 9000 rpm at 4 °C to pellet cellular debris and bacterial genomic DNA. During this centrifugation the filtration columns were equilibrated with 15 mL of Buffer QBT by allowing the buffer to flow through by gravity force. In addition, the columns were prepared by inserting a double layer of Kimwipe tissue inside the column to act as a filter

for any cellular debris. The cleared supernatants were passed through the tissue layer and filtration column followed by two washes of 15 mL Buffer QC. After the flow-through was complete the columns were placed above Oakridge tubes and the DNA was eluted with 15 mL of Buffer QF (pre-warmed to 55 °C). Eluted DNA was precipitated with 10.5 mL of isopropanol and subsequent centrifugation at 14000 rpm for 30 minutes at 4 °C. Following centrifugation the isopropanol was carefully tipped off to avoid dislodging the pellet, the pellets were washed by adding 3.5 mL of 70% ethanol followed by an additional centrifugation at 14000 rpm for 30 minutes at 4 °C. The remaining liquid was drained off and the washed pellet were allowed to air-dry for 10-20 minutes and finally resuspended in 250 µL of TE buffer. The tubes were positioned to allow the TE buffer to cover the DNA pellets and allowed to resuspend overnight at 4 °C. The following day the TE buffer was gently flicked and spun at 1500rpm in a JA17 rotor for 5 minutes to collect the resusended DNA solution.

2.1.1.3 Electrocompetent cells

Electrocompetent bacterial cells were prepared in order to transform prepared plasmids and ligations into bacteria by electroporation. All steps in making electrocompetent cells were performed on ice or in the cold room using equipment and reagents (10% glycerol, centrifugation bottles, racks, pipette tips, etc) that were pre-chilled to 4 °C. Single DH10B electroMAX (Invitrogen) bacterial colonies were picked into 1.5 mL LB cultures and grown overnight. The following morning the 1.5 mL culture was tipped into 100 mL LB in the incubator for at least 1.5 hour. After 1.5 hours, the optical density at 600 nm (OD_{600nm}) was measured every 15 minutes until the culture reached a density of 0.35 – 0.36

$OD_{600nm.}$ The flasks were then placed on ice at 4 °C for 40 minutes. The bacteria were then pelleted for 15 mins at 5000 rpm at 4 °C, the supernatant was carefully tipped off and the pellet was resuspended by thoroughly shaking in 100 ml of 10 % glycerol to wash the pellet. The centrifuge and wash steps were then repeated three times using increasing speeds of 6000, 7000 and 75000 rpm. After the final wash, the supernatant was carefully tipped out and the pellet resuspended in the small volume of 10 % glycerol droplets that remained in the centrifuge bottle. 50 μL aliquots were poured into pre-chilled tubes were snap frozen in an ethanol-dry ice bath and stored at -80 ˚C.

2.1.1.4 Bacterial DMSO stocks

At each stage Dimethyl sulphoxide (DMSO) stocks were made of the vector by mixing 0.9 mL of bacterial culture with 75 μL of DMSO, snap freezing in a dry ice and ethanol bath and stored at -80 ˚C.

2.1.2 DNA manipulation

DNA manipulation techniques such as the Polymerase Chain Reaction, restriction digests, removal of 5' overhangs, removal of phosphates, ligation and transformation into electrocompent bacteria is described as follows. All DNA fragments were analysed by gel electrophoresis and quantified using a NanoDrop spectrophotometer.

2.1.2.1 Polymerase Chain Reaction (PCR)

Two main types of reactions have been used in this project. For cloning we used

the kit, Expand High Fidelity PCR System by Roche, due to the proof reading activity of the Taq polymerase, which reduces the probability of generating errors in the final PCR product. Typical reaction components are shown in Table 2, the reaction is prepared on ice as two separate master mixes. First, 24 μL of Master mix 1 is added to 100 ng of DNA (1 μL), then 25 μL of Master mix 2 is added to the total reaction.

Reagents	Volume
Master mix 1	**1x**
40 mM dNTP mix	1 μL
F Primer (10 mM)	1 μL
R Primer (10 mM)	1 μL
Q solution	5 μL
MilliQ Water	16μL
Master Mix 2	**1x**
MilliQ Water	19.25 μL
10x Buffer + Mgcl2	5 μL
High Fidelity Taq Polymerase	0.75 μL

Table 2 – Expand High Fidelity PCR reagents

The second kit that we used was AmpliTaq Gold (Applied Biosystems). This enzyme was preferred when performing colony PCR to screen for correct ligation products. A typical reaction consisted of a final volume of 15 μL, which was combined with 5 μL DNA. The reaction components are shown in Table 3.

Reagents	Volume
Master mix 1	**1x**
10x Buffer	2 µL
MgCl2	1.2 µL
8mM dNTP Mix	2 µL
Taq Gold Polymerase	0.1 µL
F Primer (10 mM)	1 µL
R Primer (10 mM)	1 µL
MilliQ Water	7.7 µL

Table 3 – AmpliTaq gold reagents

All PCR reactions were conducted on an MJ Research PTC 225 Tetrad Gradient Thermal cycler with 4 Alpha Blocks. The programme used was typically a 10 minute denaturation step at 95 °C followed by 30 cycles of (denaturing (95 °C) followed by annealing (50 °C – 65 °C depending on primers melting temperature) followed by elongation (72 °C for 1min/kb)) followed by a final elongation step of 6 minutes. All the primers used for cloning are shown in Table 4.

Primer	Sequence	Annealing Temperature (°C)
Cloning primers Chapter 4		
Myc-2A F1	cttcgaaactctggtgcagctagcggcagcggcgccacaaac	60
OCT4 R1	gcgccgttcgaattagtttgaatgcatgggagagcccagagcagtgacggg	
EGFP-2A	ggcagctgtacaagtaagctagcggcagcggcgccac	60
OCT4 R1	gcgccgttcgaattagtttgaatgcatgggagagcccagagcagtgacggg	
Cloning primers Chapter 6		
Lmx1a F1	gatcgatcggatccatgctggacggcctaaag	63
Lmx1a R1	gcatacgcggccgctcaagatgtgaagtaagaattc	
Pitx3 F1	gatcgatcggatccAtggagttcggcctgctcagcg	63
Pitx3 R1	gcatacgcggccgctcatacgggcctttcc	
rFoxA2 F1	gtacagctggatccatgctgggagccgtgaag	63
rFoxA2 R1	gcatacgcggccgcttaggacgagttcataataggc	
Nurr1 F1	ggatagacttaagatgccttgtgttcagggcgc	63
Nurr 1 R1	ccgtacgctctagattagaaaggtaaggtgtccagg	

Table 4 – Primers used in cloning transgenes. Sequence contains restriction site to enable insertion into the vector.

2.1.2.2 Gel Electrophoresis

Gel electrophoresis was used to separate and analyse DNA fragments of ≤15 Kb. A 0.6 % -2 % (depending on resolution needed) agarose gel was prepared as detailed in Table 1 by dissolving in a microwave for 3-4 minutes. Once the solution had cooled to approximately 50 °C, ethidium bromide was added at a final concentration of 0.25 µg/mL and the agarose mix was poured into a gel tray with appropriate well combs in place. Electrophoresis was performed using a standard electrophoresis tank (Biorad) with a covering volume of 1x TBE. Samples were loaded in wells with 1x sample loading buffer (10 x stock concentration detailed in Table 1). The GeneRuler™ 1 Kb Plus ladder (Thermoscientific) and/or the HyperLadder II (Bioline) 100 bp DNA ladders

were used routinely as size indicators depending of the expected size of the DNA fragments in the DNA sample. The gel was run at ~90 Amps for 1-2 hours or until the bands of interest were resolved. The gel was photographed on a Biorad Gel Dock and the images analysed using Quantity One software from Biorad.

2.1.2.3 Restriction Digests

Digests were carried out using New England Biolabs (NEB) restriction enzymes and all digest buffers were selected by referring to the NEBuffer performance chart with restriction enzymes, available in the NEB catalogue or on the NEB website (www.neb.com). Digests were carried out using 1 unit enzyme per µg DNA in the enzymatic reaction. Typically 200 ng DNA was used in test digests and 3-5 µg DNA was digested for cloning. In addition 1x appropriate buffer was added and was chosen according to the maximum activity of the enzyme and for double digestions a buffer was selected that were compatible for both enzymes. If no compatibility was found, sequential reactions were performed. 1x BSA was added if any of the enzymes required it. If the temperature required for activity were different but the buffers compatible, the mixture was first incubated at the lower temperature and subsequently at the higher. Most digestions were performed at 37 °C for 3 hours for 200 ng DNA or overnight for 3-5 µg DNA. Enzymes used for each of the reactions are detailed in Chapters 3-6.

2.1.2.4 DNA purification from agarose gels

Agarose gels were prepared containing ethidium bromide of 0.25 µg/ml and electrophoresis performed as explained. The band of interest was excised using a

disposable scalpel by placing the gel on top of a long wave UV (365 nm) illuminator and carefully cutting around the correct sized band. Gel extracted bands were purified using a Gene Clean Spin Kit, MP biomedical according manufacturer instructions and all spins were performed at 13,000 rpm on a bench top centrifuge. Briefly, the gel slices were added to 400 µL of the kit component GENECLEAN® SPIN GLASSMILK and melted in a heat block to 55 °C and then the melted solution was added to the SPIN filter and centrifuged for 1 minute and the flow-through discarded. The filter was washed with 500 µL of GENECLEAN® SPIN NEW wash and the flow through was discarded. The spin filter was dried by centrifugation for 1 minute, and then the precipitated GLASSMILK was resuspended in 15 µL GENECLEAN SPIN ELUTION Solution. The SPIN filter was then centrifuged for 15 seconds in order to elute the DNA solution in a fresh DNA catch tube. Please refer to GENECLEAN® manual for buffer compositions and conditions.

2.1.2.5 DNA purification from other preparations

The QIAquick® PCR Purification Kit, Qiagen was used for other purifications according to manufacturer instructions and all spins were performed at 13,000 rpm on a bench top centrifuge. Briefly, 5 volumes of buffer PB was added to 1 volume of DNA and centrifuged in a QIAspin column for 1 minute. The flow-through was discarded and washed with 750 µL buffer PE. After centrifuging for 1 minute, the flow-through was discarded and the column centrifuged again for a further minute. The DNA was eluted in 30-50 µL MilliQ H_2O. Please refer to QIAquick manual for buffer compositions and conditions.

2.1.2.6 Creating cohesive ends

To create cohesive DNA fragments ready for ligation in cloning reactions single-strand overhangs were removed. To fill-in 5' overhangs, DNA (up to 10 µg) was incubated in the following reaction mixture: 1x Klenow buffer (10 mM $MgCl_2$, 1 mM dithiothreitol (DTT), 50 Mm Tris-HCl, pH 7.5, 50 µg/mL BSA), 2.5 mM of each dATP, dTTP, dCTP and dGTP (Invitrogen) and 4 U Klenow enzyme (large fragment of DNA polymerase I, Roche). The reaction mixture was made up to 50 µL in MilliQ H_2O and incubated at 37 °C for 30 minutes.

2.1.2.7 Dephosphorylation of 5' ends

The 5'ends of restriction digested vector fragments were dephosphorylated to avoid religation of compatible ends. Usually 1.5 µL of calf intestinal phosphatase (CIP) (New England Biolabs) were added directly to the digestion reaction, incubated 1 hour at 37 °C.

2.1.2.8 Ligation

Ligations were all carried out at 16 ˚C for 2 hours or overnight. Reactions were set up in a total volume of 10 µL with 1 µL of T4 ligase and 1 µL of T4 buffer, ratios of Vector: Insert depended on the size of the fragments and the relative concentration but typically a ratio of 1:4 was used for standard ligations. A vector only control was included in order to assess background ligation products. Following the ligation reaction the ligation solution was slowly pipetted onto the shiny side of a 0.1 µm Millipore® Durapore® PVDF membrane, which was floating on the surface of Milli Q water. This was left for 30 minutes in order to remove any contaminating salts.

2.1.2.9 Electroporation

In order to transform ligation products into bacteria an electroporation approach was used. Prior to electroporation, the cuvettes, electrocompetent cells and template were pre-chilled on ice. 1 μL of DNA was added to an 18 μL or 50 μL aliquot of electrocompetent cells (fresh DH10B electromax (Invitrogen) or lab-made electrocompetent DH10B cells, respectively. The most suitable concentration of DNA to achieve a good electroporation efficiency ranged from 1 – 10 ng/mL (approximately 1 μL of ligation product). The cells and DNA mixture was added to an electroporation cuvette (Bio-Rad, 0.1 mm Gene Pulser cuvette) and placed into the electroporator (Gene Pulser, Bio-Rad). The electroporator was set to the following parameters: Capacitance: 35 mFD; Resistance: 200; Voltage: 1.8 kV (for 0.1 cm cuvettes). Following the electric pulse, the time constant was noted with values of approximately five being acceptable. Immediately after the pulse, 450 μL of super optimal catabolite repression (S.O.C.) medium (Invitrogen) was added to the cuvette and the entire contents transferred to a test tube. The test tube was then incubated at 37 °C with shaking at 225 rpm for one hour to recover. Following incubation, the culture was plated onto LB agar plates (with antibiotics) and grown for 14 – 16 hours at 37 °C.

2.1.2.10 DNA sequencing

Sequencing templates from PCR reactions were first treated with Exonuclease I (exo I) (NEB) and Shrimp Alkaline Phosphatase (SAP) (USB) to remove residual primers and unincorporated nucleotides respectively. Each PCR reaction was treated with 1 μL SAP, 1 μL SAP reaction buffer, 0.1 μL exo I and 0.9 μL water

and incubated at 37 °C for 30 minutes followed by 80 °C for 15 minutes to inactivate the enzymes. Templates for sequencing were either exo-sap treated PCR products or plasmid preparations. The sequencing reagents were 0.5 μL Big Dye, 1.75 μL 5x sequencing buffer, 1 μL primer (10μM), 40ng of template and MilliQ water to a total volume 10 μL and the following cycling reaction was used (96 °C for 60 seconds) x1 cycle, followed by (96 °C for 10 seconds, 50 °C for 5 seconds, 60 °C for 60 seconds) x 30 cycles. The sequencing primers used are shown in Table 5.

Sequencing primers Chapter 5	
oligoname	**sequence**
FUW forward 1	gggacagcagagatccagtt
FUW forward 2	atccacgctgttttgacctc
ASL I reverse 1	tctccatcttggcagagctt
Asl I forward 1	cggccaacaagaagatga
Asl I reverse 2	gcgcagtgtctccaccttt
Asl I forward 2	agcaggagcttctcgacttc
hNurr1 reverse 1	gtattctcccgaagagtggtaac
hNurr1 forward 1	ccggtgtctagttgccagat
hNurr1 reverse 2	tgcgtgtcgagcagctgag
hNurr1 forward 2	tggagatgacacccagcata
hNurr1 reverse 3	accccattgcaaaagatgag
hNurr1 forward 3	cgccagcaataattgacaaa
lmx1a reverse 1	atcgcgctttggaagttct
lmx1a reverse 4	ggaggagaaaatgaaagccata
Sequencing primers Chapter 6	
Forward pCMV	cgtgtacggtgggaggtcta
R polyA	cgctattgtcttcccaatcc
LMX1A F1	gatcgatcggatccatgctggacggcctaaag
LMX1A R1	gcatacgcggccgctcaagatgtgaagtaagaattc
LMX1A F2	gctctgcaaaggggactatg
LMX1A F2	ctggttttggaaccacacct
LMX1A F3	tggttccaaaaccagagagc
LMX1A R3	atagtccccttttgcagagca
PITX3 F1	gatcgatcggatccatggagttcggcctgctcagcg
PITX3 R1	gcatacgcggccgctcatacgggcctttcc
PITX3 F2	ccttccagaggaaccgctac
PITX3 R2	ccacgttgaccgagttgaa
PITX3 F3	tttccattcgccttcaactc
PITX3 R3	aggtcgcctctagctcctgt
Nurr1 F1	ggatagacttaagatgccttgtgttcagggcgc
Nurr 1 R1	ccgtacgctctagattagaaaggtaaggtgtccagg
Nurr 1 F2	tcgagcagaggaagacacct
Nurr 1 F3	gaccggctctatggagatca
Nurr 1 R2	gaaggtctgcccatccacta
Nurr 1 R3	gatctccatagagccggtca
rFoxA2 F1	gtacagctggatccatgctgggagccgtgaag
rFoxA2 R1	gcatacgcggccgcttaggacgagttcataataggc
rFoxA2 F2	gcagaactccatccgtcatt
rFoxA2 R2	ccggtagaaagggaagaggt

Table 5 – Sequencing primers used in Chapters 5 and 6.

Following the sequencing reaction the DNA was precipitated by adding 2 μL of 125 mM EDTA, 2 μL of 3 M sodium acetate and 50 μL of 100 % ethanol to each well. This was briefly vortexed prior to spinning down at 3000 x *g* (RCF) at 4 °C for 30 minutes. The supernatant was removed by inverting the plates and spinning up to 185 x *g* (RCF) for 15 seconds. The DNA was then washed with 70 μL of 70 % ethanol per well. This was centrifuged at 1650 x *g* (RCF) at 4 °C for 15 minutes. The supernatant was removed by inverting the plate and spinning of 185 *x g* (RCF) for 1 minute. The wells were dried, covered with aluminium foil and taken to the Sequencing Facility, Department of Zoology, University of Oxford. Results were viewed using ContigExpress software (Vector NTI, Invitrogen). All samples were protected from light during drying and storage.

2.2 Vector characterisation

The vectors were characterised by transfection and transduction experiments to ensure that all the elements were functional. Expression of the transgenes was assessed by RT-PCR and/or Western Blot (WB) and/or immunocytochemistry. The TK cassette was assessed by Ganciclovir (GCV) assay and the EBNA-1/*Ori P* element was assessed by generating clonal cell lines and performing episomal rescue.

2.2.1 General cell culture

Cell culture was carried out in a Class II laminar flow cabinet. Cells lines were maintained in saturated humidity incubators at 37 °C with 5 % CO_2. Cells were sub-cultured every three to five days to a maximum of twenty passages. Sub-

culturing of adherent cell lines was performed by application of trypsin-EDTA (Sigma) for five minutes at 37 °C. The trypsin was then neutralised by addition of normal growth media. One-fifth to one-tenth of the cell suspension was then transferred to a new flask and normal growth medium added. All centrifugations were conducted using a Hettich Rotanta 460R centrifuge and all basic cell lines were cultured according to supplier's instructions with the prescribed media formulations as shown below:

- ***Immortalised cell line (MRC5-V2) and Primary lung fetal fibroblasts (MRC5) growth medium, G16.9 seeding medium, Vero 2-2 seeding medium- Complete Dulbecco's Modified Eagles Medium (DMEM)*** – *(High Glucose (4,5g/l), Without L-Glutamine (L-G)); 10% Fetal Bovine Serum (FBS, Gibco®, Cat no: 16000-044), 1% Penicillin-Streptomycin (P/S) (Sigma, Cat. no.: P4458), 1% L-Glutamine (Sigma, Cat no: G7513)*
- ***G16.9 growth medium*** – *Complete DMEM, 10 % FBS, 1 % P/S, 1 % L-G, 200 µg/ml Hygromycin B (Gibco®, Cat. No: 10687-010)*
- ***Vero 2-2 cells growth medium -*** *Complete DMEM, 10 % FBS, 1% P/S, 1 % L-G, plus 500 µg/mL G418 (Invitrogen, Cat no: 10131-027).*
- ***Packaging medium*** *- DMEM, 6 % FBS, 1 % P/S, 1 % L-G, 25 mM HEPES (Gibco®, Cat. No: 15630-056)*
- ***Titration medium*** *– DMEM, 2 % FBS, 1 % P/S, 1 % L-G, 25 mM HEPES*
- ***GCV assay medium*** *– DMEM, 2 % FBS, 1 % P/S, 1 % L-G*

2.2.1.1 Cell counting

In order to seed consistent cell densities for experiments the number of cells per mL of culture cells were counted using a haemocytometer. Cells were trypsinised

as explained above and resuspended in normal growth medium to generate a single cell suspension. Ten µL of the cell suspension was placed in a haemocytometer and the number of cells in a 4 mm^2 grid was counted. The average number of cells counted within four and eight squares was calculated and multiplied by 10,000 to obtain the number of cells per mL of cell culture.

On occasions where large numbers of cells needed to be counted a Scepter 2.0 handheld automated cell counter by Millipore was used to caculate cell density according to manual instructions.

2.2.1.2 Long-term storage of cell lines

Cells were trypsinised as explained above. The cell suspension was centrifuged in a 15 mL falcon tube at 1200 rpm for 5 minutes and the supernatant discarded. Cells were resuspended in 1-3 mL of the growth medium of each cell type and 1 mL added to 1 mL of freezing mix (90% FBS, 10% DMSO). Cells were transferred to a 1.8 ml cryovial (Nunc) and placed within a sealed polystyrene box inside a -80 °C freezer. Cells were transferred within the following week to liquid nitrogen. To thaw frozen cells, vials were placed in a 37 °C water bath until the outer part of the block of ice was defrosted. The cells were then transferred to a new 75 cm^2 flask containing 10 mL of pre-warmed fresh medium.

2.2.1.3 Transfection

MRC5-V2 cells were seeded at 1.3 million cells per 6 cm dish and the following day the cells were washed twice with 2.5 mL of OptiMEM (PAA) before adding

the transfection mix to the cells. Transfection mix contained 2 µg of plasmid maxiprep, 10 µL Plus reagent (Invitrogen), 23 µL of Lipofectamine (Invitrogen) and 500 µL of OptiMEM. OptiMEM was then added to the transfection mix after complexing for 30-40 minutes to reach a final volume of 1.5 mL per transfection and was added to the cells for 4 hours at 37 ˚C. Following the 4 hour incubation period the cells were washed three times with OptiMEM and then replaced with complete DMEM media and left for 60 hours before harvesting or using in down-stream experiments. Cells were viewed on the Nikon inverted microscope prior to harvesting cells in order to confirm EGFP expression.

2.2.1.4 Vector Packaging into HSV-1 amplicons

The vectors were packaged into HSV-1 amplicons using an fHSVΔpacΔ27 BAC system (Chapter 1, Figure 4). The fHSVΔpacΔ27 maxi prep was prepared as described and handled using cut off tips to avoid shearing of BAC DNA. The preps were then analysed on a 1 % TAE pulse field gel alongside a Midrange II PFG ladder.

The iPS amplicon vectors were packaged into Vero -2-2 cells by co-transfection of 2 µg fHSVΔpacΔ27, 200 ng ICP27, 600 ng amplicon vector and 600 ng pcDNA6/TR (repressor plasmid) under the same conditions as described for transfections except Vero -2-2 cells, seeded at 1 million cells per 6 cm dish were used and the vectors were left to package for 60-66 hours in packaging media.

After the 60-hour incubation period the cells were imaged on the Nikon microscope as before and were harvested for viral purification and

concentration. The cells from each dish were scraped into the media using a cell scraper and 6 dishes were pooled together in a 50 mL falcon tube. The cells were then frozen in a dry-ice ethanol bath for 30 minutes and once thawed were sonicated in a tissue culture hood for 30 seconds using a Fisher Scientific Sonic Dismembrator Model 500 set at 50 % amplitude, 2 mm tip. The debris was then spun down in a centrifuge at 3500 rpm and the cleared lysate was loaded into a Beckman ultraclear ultracentrifuge tube. 5 mL of a 25 % sucrose solution was slowly underlayed beneath the lysate and the tubes were filled to the top with cold PBS. The amplicons were concentrated at 22,000 rpm in a Beckmann ultracentrifuge (L70, SW28 rotor) for 1.5 hours. The lysate suspension was then aspirated and the concentrated amplicons were resuspended by manual pipetting in 250 µL complete medium. The suspension was distributed into 50 µL aliquots and stored at -80 ˚C for at least half an hour before titration.

2.2.1.5 Titration of HSV-1 amplicon stocks

Amplicon stocks were titrated on G16.9 cells, seeded on day one at 400,000 cells/well in a 24 well plate (3-4 wells per amplicon prep) in complete DMEM. On day two the amplicon aliquots were titrated by adding a range of different volumes of stock (eg 20 µL, 2 µL and 0.5 µL) in titration media to the G16.9 cells. On day three the cells were imaged using the Nikon microscope and the number of green cells in a single field was counted using the 10 X objective. Six random fields were counted and then the average count from this was multiplied by 151 to calculate the number of cells in an entire well. This was then multiplied by the dilution factor in order to estimate the amount of transducing units/mL (TU/mL).

2.2.1.6 Transduction

Transductions were carried out on a number of different cell lines the day after seeding by calculating Multiplicity of Infection (MOI) (volume of prep needed for an MOI of 1 was calculated by multiplying the total number of cells by 1000 and dividing by TU/mL). The transduction efficiency was determined the following day by counting the number of Enhanced Green Fluorescent Protein (EGFP) positive cells normalised to total number of cells.

2.2.2 Transgene expression

2.2.2.1 RNA extraction

Cell pellets or tissue that was to be used for RNA extractions was snap frozen in liquid nitrogen before being stored at -80˚C before processing. Each sample was transferred into an RNase-free tube and 1 mL Trizol added. The sample was completely homogenised with a pipette tip and left to incubate at room temperature for 5 minutes. Chloroform (200 µL) was added to the tube and shaken vigorously for 15 seconds to mix. The tube was left at room temperature for 5 minutes and then centrifuged at 12,000 x g for 15 minutes at 4 ˚C. Three layers were visible, the bottom layer (pink) contains DNA, the middle layer (white) contains protein and the top layer (clear) contains the RNA. The top layer was transferred to a fresh tube and 500 µL ice cold isopropanol added. The sample was mixed by pipetting and incubated for 10 minutes at room temperature. The sample was then centrifuged for 30 minutes at 12,000 x g at 4 ˚C. The supernatant was discarded and the pellet containing RNA washed with 1 mL 75 % ethanol. This was then centrifuged again for 30 minutes at 12,000 x g at

4 ˚C. The supernatant was discarded and the pellet air-dried prior to resuspension in 30-50 µL RNase-free H_2O.

The RNA was purified using the RNeasy MinElute cleanup kit (QIAGEN) according to manual protocol. The protocol included a DNase step to remove contaminating DNA. The RNA was eluted in 15 µL RNase-free H_2O and the 260/280 absorbance ratio was also used to determine quality of the sample, with ratios in the range of 1.8 - 2.1 being considered high quality.

2.2.2.2 Reverse transcription

In order to examine gene expression levels by PCR, the RNA was reverse transcribed into complementary DNA (cDNA) using the SuperScript III reverse transcriptase kit (Invitrogen). Typically 500 ng RNA was used per 20 µL reaction. To the RNA, 100 ng random primers (Promega), 10 mM of each dATP, dTTP. dGTP, dCTP and RNase-free H_2O up to 13 µL were added. This mixture was incubated at 65 ˚C for 5 minutes then put onto ice for 2 minutes. To the reaction mix, 4 µL First-strand buffer, 1 µL 0.1 M DTT and 40 U RNaseOUT were added. For RT^+ reactions, 1 µL (200 U) SuperScript reverse transcriptase was added to the tubes and for RT^- reactions, 1 µL H_2O was added. The reactions were mixed and incubated at 25 ˚C for 5 minutes, 50 ˚C for 1 hour and 70 ˚C for 15 minutes. The resulting cDNA was stored at -20 ˚C until further use. cDNA was then used in a general PCR reaction. Junction RT-PCR primers were designed in order to flank the 2A sequences and amplify the exogenous transgenes, primer sequences are shown in Table 6.

Junction	Forward	Reverse
Chapter 3 Junction RT-PCR primers		
Sox2 - Oct4	Ggccattaacggcacactg	Gggtgagaaggcgaagtctg
Oct4 - Klf4	Gctctcccatgcattcaaac	Acgcagtgtcttctcccttc
Klf4 - C-Myc	Ccaccttcgccttacacatg	Gggctgtacggagtcgtag
Chapter 4 Junction RT-PCR primers		
C-Myc - Oct4	agcttcgaaactctggtgcag	Gggtgagaaggcgaagtctg
Oct4-Sox2	ctcccatgcattcaaactga	atgttgtacatgcggaatcg
Nanog-Lin28	ctcccatgaacatgcaacctg	cgcacgttgaaccacttaca
Chapter 5 Junction RT-PCR primers		
Ascl1-Nurr1	agcaggagcttctcgacttc	gtattctcccgaagagtggtaac
Nurr1-Lmx1a	tggagatgacacccagcata	atcgcgctttggaagttct

Table 6 – Junction PCR primer sequences.

2.2.2.3 Protein extraction

Protein was extracted from transfected and transduced MRC5-V2 seeded at $1.3x10^6$. Cells were harvested by washing in PBS and scraping into a low volume (1.5 mL) of PBS, followed by centrifugation to pellet cells and resuspension in 100 µL of RIPA (50 mM Tris pH 8, 150 mM NaCl, 2 mM EGTA, 0.5 % sodium deoxycholate, 1 % Igepal 630, 0.1% SDS) plus protease inhibitors (EDTA free tablets, Roche diagnostics, one tablet per 10ml RIPA). Samples were lysed on ice for 30 minutes and then quantified using BCA reagent, 1.25 µL of sample per 100 µL BCA. The samples were prepared in triplicate against protein standards ranging from 0-1000 µg/µL in concentration and quantified using the Genlite programme. Following quantification the samples were then divided into single use aliquots and stored at -80 ˚C. Prior to running on the gel samples were reduced in lamelli buffer at a concentration of 5-50 µg of protein per sample,

reduced samples were stable at -20 ˚C. Samples were denatured for 5 minutes at 95 ˚C prior to loading on an acrylimide gel.

2.2.2.4 Western blotting

Samples were ran alongside a Spectra Multicolour Broad Range Protein Ladder on a 10 % gel (H_2O (1.9 mL), 30 % acrylimide mix (1.7 mL), 1.5 M Tris (pH 8.8, 1.3 mL), 10 % SDS (0.05 mL), 10 % ammonium persulfate (0.05 mL), TEMED (0.002 mL)) in 1X running buffer at 200 V. The gel was then equilibrated in 1X transfer buffer while the Millipore membrane was activated in MetOH, washed in dH_2O and then transferred to 1X transfer buffer. The transfer was assembled in the wet transfer system by Biorad and run for exactly 70 minutes at 100 V. Following the transfer the membrane was blocked in 5 % milk for 1 hour, antibodies were added to 1 % milk (catalogue numbers and antibody dilutions are listed in Table 7) and the membrane was incubated overnight at 4 ˚C. The following day the membrane was washed three X 10 minutes in TBS-Tween (1X TBS plus 0.1 % Tween), the secondary antibody (1:5000-1:10,000) was added in 1 % milk and incubated for 1 hour at room temperature and then the washes were repeated. The membrane was developed in 1 mL developing reagent A and 25 µL reagent B (GE healthcare ECL Western Blotting Detection System). The blot was imaged on a Biorad gel dock after 5 minutes.

Antibody	Species	Supplier	Catalogue No.	Dilution
Anti Sox 2	Mouse	Millipore	ab503	1 in 1000
Anti Oct 3/4	Mouse	Santacruz	sc5279	1 in 200
Anti Klf 4	Rabbit	Santacruz	sc2061	1 in 1000
Anti C-Myc	Rabbit	Santacruz	sc764	1 in 500
Anti Nanog	Goat	R&D Systems	AF1997	1 in 200
Anti Lin28	Mouse	Abcam	ab75483	1 in 200
Anti FoxA2	Goat	R&D systems	AF2400	1 in 500
Anti Lmx1A	Rabbit	Abcam	ab31006	1 in 500
Anti Nurr1	Rabbit	Millipore	Ab5778	1 in 1000
Anti PitX3	Rabbit	Invitrogen	38-2850	1 in 500
Anti Ascl 1	Rabbit	Abcam	ab98557	1 in 500
p53	Mouse	Cell Signalling	2524	1 in 1000
p53 ser15	Mouse	Cell Signalling	9286s	1 in 1000

Table 7 – Antibody used in Western blot – Information regarding antibodies used for Western blot, including supplier, catalogue number, species and dilution factor.

2.2.2.5 Immunocytochemistry

Cells grown as a monolayer on glass coverslips or as single EBs in a 96 well plate were fixed as follows: the medium was aspirated and cells washed with PBS. Cells were incubated with 4 % paraformaldehyde (PFA) for 15 minutes at room temperature. The PFA was removed and cells washed 3 x 10 minutes in PBS. Unspecific binding was blocked in 5 % serum, 1 % bovine serum albumin (BSA, Sigma) in PBS-Triton X100 (PBS-TX100, 0.1 %) for 2 hours at room temperature. The serum used for blocking was from the same species in which the secondary antibody was raised. Primary antibodies (listed in Table 8, all 1 in 500) were diluted in 1 % serum in PBS-TX100 and incubated at 4 ˚C overnight. The cells were washed 3 x 10 minutes in PBX-TX100 and incubated in secondary antibody

diluted in 1 % serum in PBS-TX100 for 1 hour at room temperature. Following a further 3 x 10 minute washes in PBS-TX100. Optional counterstaining of nuclei was performed by incubating in DAPI, 500 ng/mL for 5 minutes at room temperature. 96 well plates containing single EBs were submerged in PBS, wrapped in foil and stored at 4 ˚C in the fridge. Coverslips were mounted onto glass slides in FluorSave Reagent (Calbiochem) and left to dry for at least 1 hour before imaging.

Antibody	Species	Supplier	Catalogue No.
Anti FOXA2	Goat	R&D systems	AF2400
Anti LMX1A	Rabbit	Abcam	Ab31006
Anti Ascl I	Rabbit	Abcam	Ab98557
Anti Nurr 1	Rabbit	Millipore	Ab5778
Anti PitX 3	Rabbit	Invitrogen	38-2850
Anti TH	Rabbit	Millipore	AB152
Anti Tuj 1	Mouse	Covance	MMS-435P

Table 8 – Antibodies used in Immunocytochemistry. List includes the spcies, supplier and catalogue number. All antibodies were used at a 1 in 500 dilution.

2.2.3 Clonal cell lines and Episomal Plasmid Rescue

Clonal MRC5-V2 cell lines were established following transfection with pHGCX+SOKM+EBNA+TK+tetO2 as described. Transfections were passaged to 10 cm dishes and maintained in media containing Hygromycin 200 µg/mL. After 7-14 days most cells had died but resistant colonies had started to appear on the dish. Clones were isolated using cloning cylinders (Fisher) and transferred to 24 well plates in the same media composition. Expanded clones were frozen at the 6 well stage and harvested for episomal rescue from a 10 cm dish.

The episomal rescue protocol is based on alkaline lysis to rescue supercoiled DNA from mammalian cells and uses the same buffers as described in materials and methods 1.1. Cells were harvested in 1.5 mL of PBS and spun down at 5000 rpm to pellet the cells. The cells were then resuspended in 60 µL STET, lysed in 130 µL lysis buffer and 110 µL ammonium acetate. The lysates were chilled on ice and spun at 13000 rpm for 30 minutes at 4 ˚C. The supernatant was then phenol-chloroform extracted 2X and chloroform extracted 2X using heavy phase-lock gel tubes (5 PRIME). The product was then precipitated in 2.5 X volume 100 % EtOH at 13000 rpm, washed in 70 % EtOH and resuspended in 20 µL TE plus 5 µg/mL RNaseA.

The DNA product was then electroporated into DH10B cells as described in materials and methods 1.6 and plated on agar containing appropriate antibiotics. Colonies were then innoculated for minipreps and digested as in materials and methods 1.3 with *Eco RI*, *Mbo I* and *Dpn I* using 200 ng of the original pHGCX+4genes+EBNA+TK+TetO2 maxi prep as a positive control.

2.2.4 Ganciclovir sensitivity assay

The day following transduction of G16.9 cells with pHGCX+SOKM+TetO2 and pHGCX+SOKM+TK+TetO2 (Table 3) cells were imaged on an inverted Nikon microscope and the number of green and total cells / well were counted as described previously to get an estimation of transduction. GCV (Sigma, catalogue number G2536, resuspended in 0.1 N HCL) was added in triplicate at 10, 30 and 50 µg/mL per well and HCL alone was added to wells as a negative control at the

same volume as the 50 µg/mL well. On day 5 the cells were viewed on an inverted Nikon microscope and the number of green cells/well were counted as described previously. Counts for each condition were normalised against HCL only and a two-way Anova was performed on normalised values.

2.2.5 MTT assay

Viablity of transduced and untransduced MRC5 cells was determined using an 3-[4,5-dimethylthiazol-2-yl]-2,5-diphenyl tetrazolium bromide (MTT) kit from Sigma®, Catalogue number CGD1. The assay measures mitochondrial activity by the reduction of soluble MTT to insoluble purple MTT formazan crystals, measured by spectrophotometry. Cells were grown on a 24 well plate and transduced in triplicate according to conditions listed in Table 3. The following day the cells were incubated in MTT solution (0.5 mg/mL) for 3 hours at 37 ˚C. The resulting formazan crystals were dissolved in MTT solvent and 200 µL was transferred to a 96 well plate in duplicate for each well. Absorbance of the resulting solution at 570 nm was measured using a Multiskan EX microplate reader (Thermo Scientific). Background absorbance was subtracted at 690 nm. A student's T-test was performed on normalised results to determine weather the results were significant.

2.3 Reprogramming, direct differentiation and dopaminergic differentiation experiments

Cell culture was carried out under the conditions described previously. The following cell lines and cell culture media were used.

- ***Primary lung fetal fibroblasts (MRC5) and donor fibroblasts (MKO 82 and JRO 53) growth medium -*** *Complete Dulbecco's Modified Eagles Medium (DMEM), 10% FBS, 1% P/S 1% L-G*
- ***Mouse embryonic fibroblast (MEF) medium*** *– Advanced DMEM (Gibco, Cat no: 12491-015), 10 % FBS, 1 % Glutamax, 0.1 % 2-Mercaptoethanol*
- ***Human embryonic stem (hES) cell medium*** *- KnockOut DMEM (Gibco, Cat no: 10829-018), 20 % KnockOut Serum Replacement (Gibco, Cat no: 10828010), 1 % Gluta-MAX (Gibco, Cat no: 35050038), 0.1 % 2-Mercaptoethanol (Gibco, Cat no: 31350010), 1 % Non-Essential Amino Acids (PAA, Cat no:), 10ng/mL Basic Fibroblast Growth Factor (R&D, Cat no: 4114-TC-01M)*
- ***Mouse embryonic stem (mES) cell medium*** *- KnockOut DMEM, 20 % KnockOut Serum Replacement, 1 % Gluta-MAX, 0.1 % 2-Mercaptoethanol, 1 % Non-Essential Amino Acids, 0.1 % Leukemia Inhibitory Factor (Millipore, Cat no: ESG1106)*
- ***Basic Nueronal media*** *- DMEM/F12 (Invitrogen, Cat. no: 12500-062), 1% penicillin/streptomycin and 1% N2 supplement (insulin 500 mg/L, transferrin 10,000 mg/L, Sodium Selenate 0.003 mM, progesterone 0.002 mM and puterescine 0.002 mM – R&D systems, Cat no: AR003)*

- ***Neural induction Media 1*** *- DMEM/F12, 1 % penicillin/streptomycin and 1 % N2 supplement, 1 % L-Glutamine, 2% BSA, 10 μM Rock inhibitor (Merck, Cat no: 688001) 10 μM SB431542 (Tocris, Cat no: 1614), 200 ng/ml noggin, 1% antimycotic/antibiotic*
- ***Neural Induction Media 2 -*** *DMEM/F12, 1 % penicillin/streptomycin and 1 % N2 supplement, 1 % L-Glutamine, 2% BSA, 10 μM Rock inhibitor, 1% antimycotic/antibiotic, 200 ng/mL SHH (R & D systems, Cat no; 1845-SH).*
- ***BASF media*** *- DMEM/F12, 1 % penicillin/streptomycin and 1 % N2 supplement, 1 % L-Glutamine, 2% BSA, 10 μM Rock inhibitor, 20 ng/ml BDNF, 200 ng/mL sonic hedgehog , 100 ng/mL FGF8a (R & D Systems, Cat no: 745-F8), 5 μg/mL heparin, 200 μM ascorbic acid, 1 % antimycotic/antibiotic*
- ***Final differentiation media*** *- DMEM/F12, 1 % penicillin/streptomycin and 1 % N2 supplement, 1 % L-Glutamine, 2% BSA, 20 ng/ml BDNF, 200 ng/mL, 20 ng/mL GDNF, 1 mM cAMP, 200 μM ascorbic acid, 1 % antimycotic/antibiotic*

2.3.1 Reprogramming experiments

The following fibroblast cell lines were used in reprogramming experiments - MRC5 (obtained from AATC cell bank repository) or mouse embryonic fibroblasts (MEFs) or the donor primary fibroblast lines MKO82 and JRO53 (obtained through the Oxford Parkinson's Disease Centre iPS cell recruitment program). The fibroblasts were seeded into empty 12 well plates at a density of 100,000 cells per well. The following day the cells were transduced at an MOI of

10 with either the HSV-1 reprogramming amplicons (pHGCX+SOKM+EBNA+TK+TetO2 /pHGCX+SOKMO+EBNA+TK+tetO2 /pHGCX+OSNL+EBNA+TK+tetO2) or negative control (pHGCX/pHGCX+EBNA+tetO2) or defective persistent Sendai virus vector. In the case of HSV-1 amplicon transduced cultures the media was replaced the following day and allowed 48 hours to recover from the transduction (total 72 hours post transduction). At 48 hours post transduction 6 well plates were coated with gelatin (0.1 %) at 1 mL/well and transferred to the incubator for 1 hour. Mitomycin C treated MEFs were then thawed and split onto the gelatin coated 6-well plates at a density of 4 million cells per plate. The following day the transduced fibroblasts were trypsinised, counted and split onto the mitomycin C treated MEFs in hES media (or mES media in the case of mouse embryonic fibroblast transductions) at a density of 8000 cells per well. A 50 % change of media with hES/mES media supplemented with 0.1 % Vitamin C and 0.1 % Valproic acid (VPA) was made every two days until MEFs were ten days old. Thereafter the media was changed to MEF conditioned hES media supplemented with βFGF (5 ng/mL) and Vitamin C. The experiment was maintained up until 40 days following transduction or until iPS colonies appeared. A schematic of the protocol is shown in Chapter 3, Figure 13.

In the case of transduction with the positive control Sendai virus transduction the protocol was the same as detailed above except that following transduction the cultures were maintained at room temperature inside a laminar flow cabinet for two hours prior to moving to the incubator. The transduced cultures were transferred onto MEFs 24 hours after transduction instead of 72 hours. Resulting

colonies were micro-dissected in a laminar flow cabinet using a 26 gauge needle and transferred onto fresh MEFs in hES media.

In order to assess whether HSV-1 amplicon's were preventing complete reprogramming the reprogramming experiments were set up as above except 48 hours following amplicon transduction the cultures were transduced with Sendai virus vectors. Colony formation was quantified blind by a colleague by microscopy.

2.3.2 Stem cell transduction efficiency

The hES cell line HUES 2 and iPS line NHDF1 were transduced with pHGCX to determine whether they were tolerant to HSV-1 amplicon infection and to determine the transduction efficiency. Transductions were imaged after 24 hours and FACs stained to determine the transduction efficiency.

2.3.3 FACs staining

To fix the cells pipette up and down in accutase and passed through a needle syringe to obtain a single suspension. Cells were centrifuged for 1 minute at 10,000 rpm on a microcentrifuge, the accutase was removed and the cells were resuspended in 100 μL PBS and pippetted up and down to obtain a single cell suspension. Samples were mixed with 400 μL 4% PFA and incubated for 10 minutes at room temperature. Samples were run on a FACSCalibur (BD biosciences) machine to analyse fluorescence.

2.3.4 Direct differentiation

Primary lung fibroblasts (MRC5), mouse embryonic fibroblasts (MEFs) or donor fibroblasts from the Oxford Parkinson's disease centre were trypsinised and seeded onto geltrex coated coverslips at a density of 50,000 cells per well. The next day cells were transduced with HSV-1 amplicons at an MOI of 10 in 250 μL of complete DMEM. The following day a 100 % change of media was made to basic neuronal media (N2 media). The cultures were maintained for 22 days and a 50 % media change was made every day, at the end of the experiment the cultures were fixed in 4 % PFA and stained for tyrosine hydroxylase (TH), β III tubulin and DAPI.

2.3.5 Dopaminergic neuron differentiation

Embryoid bodies (EBs), generated from the iPS lines derived from NHDF1 or NHDF2 fibroblasts using the AggreWell™ methodology, were obtained from the Oxford Stem Cell Institute. 96 well plates, single cloning cylinders and 12 well plates were coated with 0.1 % geltrex, 150 μL, 150 μL or 500 μL, respectively and incubated for 1 hour in a 37 ˚C incubator. Afterwards EBs were plated at a density of 10 - 15 EBs per well in a 12 well plate, or 1 EB per well in a 96 well plate/cloning cylinder. Cells were incubated in neural induction media 1 (Nim1) for 5 days, followed by neural induction media 2 (Nim2) on days 5-9, BASF media on days 10-17 and Final differentiation media for a further 2-4 weeks. In the case of 12 well plates and cloning cylinders, neuronal cultures were dissected into small pieces using a 26-gauge needle and transferred to geltrex-coated 96 well plates on day 17. Transductions were made at four individual time points

during the protocol and MOI of 10 was calculated based on the cell count from a single trypsinised EB. Transductions were made in 100 μL (for 96 well plates/cloning cylinders) or 400 μL (for 12 well plates) in the appropriate media. A 100 % media change was made the day following transduction. Throughout the experiment a 50 % change in media was made every 2-3 days. At the end of the experiment the cultures were fixed in 4 % PFA and stained for tyrosine hydroxylase (TH), β III tubulin and DAPI. A protocol schematic is shown in Chapter 6, Figure 6.

2.4 Characterisation of reprogramming, direct differentiation and neural transcription factor delivery experiments.

2.4.1 RNA extraction from single EBs and reprogramming samples

RNA was extracted from single EBs for use in RT-PCR and qRT-PCR experiments. RNA was extracted using the Ambion RNA extraction protocol according to manufacturers instructions. In brief, cells EBs were harvested with a pipette tip, pipetted up and down and centrifuged to pellet the cells. Pellets were resuspended in 100 μL lysis solution by vortexing and 50 μL of 100 % EtOH added. The mixture was loaded onto a microfilter cartridge assembly filter and centrifuged to pass through the filter followed by 3 x 180 μL washes with wash solution 2/3. The flow through was discarded and the filter centrifuged to dry the filter and then transferred to a new elution tube. The RNA was eluted in 20 μL elution solution followed by optional DNase treatment according to manufacturers instructions.

2.4.2 Marker gene analysis

RT-PCR analysis was performed on cDNA purified from single reprogramming samples and single EBs obtained from dopaminergic differentiation experiments. RT-PCR was performed as described in section 2.2.2.2 using the primers shown in Table 9.

Chapter 4 RT-PCR primers		
Gene name	Forward Sequence	Reverse Sequence
hTERT	tgtgcaccaaacatctacaag	gcgttcttggctttcaggat
REX 1	tcgctgagctgaaagaaatg	cccttcttgaaggtttacac
GDF3	aaatgtttgtgttgcggtca	tctggcacaggtgtcttcag
OCT4 endogenous	cctcacttcactgcactgta	caggttttctttccctagct
SOX2 endogenous	cccagcagacttcacatgt	cctcccatttccctcatttt
FGF4	ctacaacgcctacgagtcctaca	gttgcaccagaaaagtcagagttg
ESG1	atatcccgccgtgggtgaaagttc	actcagccatggactggagcatcc
DPPA2	ccgtccccgcaatctccttccatc	atgatgccaacatggctcccggtg
DPPA4	ggagccgcctgccctggaaaattc	tttttcctgatattcttattcccat
DNMT3B	ataagtcgaaggtgcgtcgt	ggcaacatctgaagccattt
CYCLIN B1	cgggaagtcactggaaacat	aaacatggcagtgacaccaa
E CADHERIN	acgaagacacaagagagattgg	cgatgatggagatgttcatgg
NANOG endogenous	gatttgtgggcctgaagaaa	aagtgggttgtagtcat
ALP	ggtgaaccgcaactggtact	cccaccttggctgtagtcat
Chapter 6 RT-PCR primers		
Gene name	Forward Sequence	Reverse Sequence
PAX6	aacagacacagccctcagactcc	cgggaacttgaactggaactgac
NESTIN	accaagagacattcagactcc	cctcatcctcattttccactcc
ENGRAILED 1	ctgggtgtactgcacacgttat	tactcgctctcgtctttgtcct
GIRK2	ggaactggaaattgtgggtcat	catcaccatttctttctttctgttt
DAT	cccactacggagcctacatctt	caatggcgtaggccagtttc
TH	gcggttcattgggcgcagg	caaacaccttcacagctcg
BETA III TUBULIN	gcctcttctcacaagtacgtgcctcg	ggggcgaagccgggcatgaacaagtgcag
PITX3	ggactaggccctacacacaga	tccgcgcacgtttatttc
GAPDH	gtggacctgacctgccgtct	ggaggagtgggtgtcgctgt

Table 9 – Marker gene RT-PCR primers.

2.4.3 Semi-quantitative RT-PCR

Semi-quantitative PCR was performed on cDNA samples as described for general PCR with the exception that 25 PCR cycles were used. Samples were then ran on a 2 % gel and imaged on a Biorad Gel Dock. Images were analysed by the program Image J and the relative intensity of each primer pair was normalised to a gapdh reference gene control. The primers used are shown in Table 10.

Chapter 4 semi-quantitative RT-PCR primers		
Gene Name	Forward Sequence	Reverse Sequence
p53	gctcgacgctaggatctgac	gctttccacgacggtgac
p21	catgggttctgacggacat	agtcagttccttgtggagcc
p38	gatcagcgactggaaggg	cgcctacggctccgtct
IP3	gtccggatcttctgccagt	ctgctgagcgacagtgagag
Aurora A kinase	gggcatttgccaattctgt	tggaatatgcaccacttgga
GAPDH	gtggacctgacctgccgtctcg	ggaggagtgggtgtcgctgt

Table 10 – semi-quantitative RT-PCR primers. Forward and reverse primer sequences used to analyse gene expression by semi quantitative RT-PCR in Chapter 4.

2.4.4 Quantitative RT-PCR

The relative level of gene expression was determined by real-time PCR using the relative standard curve method. Five-fold dilution standards were prepared to generate a standard curve for each primer. RNA samples were analysed in duplicate using the SYBR Green PCR Master Mix (Applied Biosystems). The assay was performed using the StepOnePlus Real-Time PCR system (Applied Biosystems) with the following protocol: 10 min at 95 ˚C for enzyme activation, followed by 40 cycles of denaturation at 95 ˚C for 15 s and primer annealing and extension at 60 ˚C for 1 min. Specificity of amplification was monitored with a final dissociation stage which generates a melting curve Mean data from each

primer pair was normalised to the geometric mean of the three reference genes GAPDH, ACTB and HPRT. All statistical analysis was conducted using Prism Graph Pad.

2.4.5 Cell counting analysis of immuno-stained cells

Immuno-stained cells were imaged using the 20 x objective on a Nikon inverted microscope and each field of view was imaged under the Far-Red, Red, Green and DAPI filters. 4-6 fields were imaged per well and were quantified using the cell count plug in on Image J software. Cell images were quantified blind and normalised to the total cell count (DAPI) and statistically analysed using Prism Graph Pad software.

Chapter 3 - Construction and characterisation of HSV-1 amplicon reprogramming vectors

3.1 Introduction

In 2006 S. Yamanaka and colleagues first achieved somatic cell reprogramming in mouse fibroblasts via the delivery of retroviral vectors harbouring the embryonic transcription factors Sox-2, Oct-4, Klf-4 and C-Myc [15]. Since then induced pluripotency has been repeated using numerous methods including viral vectors, plasmid transfection, RNAi knockdown, small molecule enhancers, transposons and delivery of reprogramming proteins. In addition, reprogramming has been achieved in humans and many other species from a wide range of somatic cell types. Induced pluripotent stem (iPS) cells are a valuable tool for generating patient-specific disease models, however some technological concerns still remain, including the potential for the integrating virus to cause insertional mutagenesis[176] and the relatively low efficiency for the non-integrating alternatives to the retroviral system[91].

In order to address the obstacles associated with somatic cell reprogramming methods, we chose herpes simplex virus type-1 (HSV-1) amplicon vectors to generate iPS cells. These amplicons provide a non-integrating, high titre, helper virus free system; enabling high transduction efficiency, without contamination of replication-competent HSV-1 viruses [177]. Since the beginning of the project Sendai virus has emerged as a highly efficient non-integrating reprogramming method, however its transgene capacity is limited[73]. HSV-1 amplicons have a

transgene capacity of up to 150 kilobases, enabling the inclusion of several unique design features that improve their safety and efficiency.

The first design feature is the inclusion of a polycistronic reprogramming cassette pioneered by R. Jaenisch and colleagues in 2008 to enable the equimolar expression of the four mouse reprogramming factors Sox-2, Oct-4, Klf-4 and C-Myc (SOKM) [49]. The cassette contains individual 2A oligopeptide sequences which were first identified in the foot and mouth disease virus (FMDV) in 1991 by G. Thomas and colleagues [178] and were later employed by the authors to separate a single artificial polyprotein transcript encoding chloramphenicol acetyl transferase (CAT) and beta-glucuronidase (GUS) into individual proteins [179].

The incorporation of these ~20 amino acid 2A peptides allow the generation of several peptides from a single open reading frame. 2A peptides were originally thought to mediate a proteolytic cleavage event, resulting in two proteins in equimolar quantities. However, a study by D.Ryan and colleagues in 2001 demonstrated non-equimolar ratios of the N-terminal-2A peptide in comparison with the C-terminal protein. This was observed even if the order of proteins were reversed, indicating that the difference was due to the presence of the 2A peptide, not due to individual proteins. This observation suggested a different mechanism for discrete translation products rather than proteolytic cleavage. The authors proposed that the 2A peptides act by promoting hydrolysis of the peptidyl(2A)-$tRNA^{gly}$ ester linkage, allowing the first translation product to be released at the C-terminus of the 2A peptide and allowing the ribosome to

proceed translation of the following amino acid without the formation of a peptide bond. This has been termed a ribosomal skipping event which occurs between the glycine and proline residues in the highly conserved D(V/I)EXNPGP motif [180] [181]

This proposal was supported by a study which analysed translation in the presence of puromycin, which resulted in puromycin terminated products of the same size as the N-terminal-2A peptide product, consistent with the ribosome pausing at the 2A site. Time course translation experiments also identified the accumulation of the N-terminal-2A peptide at early time points consistent with a release of the product during translation rather than proteolytic cleavage [181].

Following translation the N-terminus product includes the protein and the 2A sequence up until the C-terminus Glycine residue (~18 amino acids in addition to the first cistron protein). The downstream product contains the following gene preceded by an additional Proline residue. Presence of the 2A peptide results in a ~2 kDa shift in protein size, however no deleterious effects have been reported for either of the products. Incorporation of a GSG linker sequence at the N terminal of the 2A sequence improved the cleavage efficiency to close to 100 %, allowing equimolar ratios of translation products [182]. The GSG sequence is a feature of the 2A peptides used in our polycistronic SOKM cassette.

Three different 2A sequences were used in the polycistronic SOKM cassette to prevent unwanted recombination events from occurring between matching sequences. The 2A sequences used were derived from foot and mouth disease

virus (FMDV) equine rhinitis A virus (ERAV), porcine teschovirus-1 (PTV-1) and were termed F2A, E2A and P2A, respectively. In addition, all of the 2A sequences used in our constructs contain the GSG linker sequence, reducing the chances of incomplete cleavage products and ensuring that equimolar expression is enabled in our construct.

In our reprogramming vectors the polycistronic cassette was originally driven with an immediate-early cytomegalovirus promoter/enhancer (pCMV), which provides a strong transient pulse of expression before being silenced due to methylation[183, 184]. Due to toxic effects caused by over expression of the reprogramming factors during HSV-1 amplicon packaging we were unable to attain high titre amplicon stocks using this promoter. Thus we replaced the CMV promoter with the immediate-early cytomegalovirus type-2 tetracycline operator (tetO2) promoter/enhancer (pCMV-TetO2) to allow us to control expression of the polycistronic cassette during HSV-1 amplicon packaging. This promoter is repressed when co-transfected with the tetracycline repressor (Tet R), which binds to the TATA element of the tetracycline operator, blocking activity of the pCMVTetO2 promoter [185].

The second design feature is the *trans*-acting Epstein-Barr virus Nuclear Antigen-1 (EBNA-1) protein and the *cis*-acting *oriP* origin of replication (EBNA-1/*oriP*). The EBNA-1/*oriP* element is derived from Epstein-Barr virus and enables the viral chromosome to be maintained as a plasmid *in vivo* and *in vitro*. The *cis*-acting origin of plasmid replication (*oriP*) is an 1800bp segment that was identified and mapped in 1984 [186]. The *trans*-acting EBNA-1 element was

identified a year later and binds to two cluster sites on the *oriP* [187, 188]. Both elements are required for chromosomal maintenance and together act by associating the plasmid close to the condensed chromosomes during mitosis and replicate during S phase [189].

Vectors containing the EBNA-1/*oriP* cassette enable episomal retention of the vector in the transduced cells for a number of weeks but are eventually lost from the cells at a rate of 1-6% per cell division [190]. J. Thomson and colleagues successfully generated iPS cell lines using EBNA-1/*oriP* based vectors, confirming that EBNA-1/*oriP* maintain vectors for sufficient enough time to allow cells to reprogram [94].

The final feature utilised by our HSV-1 amplicon iPS vectors is the Thymidine Kinase (TK) cassette, which causes cell death upon the addition of the prodrug Ganciclovir (GCV) [191]. Ganciclovir is an analogue of guanosine, which is monophosphorylated by the thymidine kinase suicide gene, effectively converting GCV to a toxic metabolite. The toxic metabolite interferes with replication, effectively killing cells expressing the TK transgene [192]. Incorporation of the TK cassette into our HSV-1 amplicon iPS vectors will allow us to selectively kill any iPS cells, which still contain the vector, preventing future reactivation of the transgenes.

Since the beginning of this DPhil, A. Xiang and colleagues reported that the TK/ganciclovir system is effective at killing iPS lines infected with the TK transgene [193]. Subsequently K. Leong and colleagues developed a Cre-

excisable-TK lentiviral reprogramming construct Cre-loxP/HSV-tk/gan, which allows transgene excision and negative selection of the reprogramming vector [194].

3.2 Vector construction

For reference all the vectors used in this chapter, including information on the type of vector, the transcription factors carried and their species origin, the promoter driving the transcription factors and presence of the EBNA-1/oriP and thymidine kinase cassettes are presented in Table 1.

Vectors used in Chapter 3

Vector name	Type of vector	Promoter	Factors	EBNA	TK	Size	Constructed by
pHGCX	HSV-1 amplicon	pCMV	no	no	no	6.7 Kb	R. Wade-Martins
FUW-SOKM	Lentiviral	pCMVTetO2	mouse SOKM	no	no	12.3 Kb	R. Jaenisch
pMS-RQ		x	no	no	yes	5.3 Kb	W. James
p7157.1	HSV-1 amplicon	x	no	yes	no	12.2 Kb	R. Wade-Martins
pHGCX+SOKM	HSV-1 amplicon	pCMV	mouse SOKM	no	no	11.8 Kb	A. Popplestone
pHGCX+SOKM+TetO2	HSV-1 amplicon	pCMVTetO2	mouse SOKM	no	no	11.8 Kb	A. Popplestone
pHGCX+SOKM+TK	HSV-1 amplicon	pCMV	mouse SOKM	no	yes	13.5 Kb	A. Popplestone
pHGCX+SOKM+TK+TetO2	HSV-1 amplicon	pCMVTetO2	mouse SOKM	no	yes	13.6 Kb	A. Popplestone
pHGCX+SOKM+EBNA	HSV-1 amplicon	pCMV	mouse SOKM	yes	no	18.3 Kb	A. Popplestone
pHGCX+SOKM+EBNA+TetO2	HSV-1 amplicon	pCMVTetO2	mouse SOKM	yes	no	18.4 Kb	A. Popplestone
pHGCX+SOKM+EBNA+TK	HSV-1 amplicon	pCMV	mouse SOKM	yes	yes	20.1 Kb	A. Popplestone
pHGCX+SOKM+EBNA+TK+TetO2	HSV-1 amplicon	pCMVTetO2	mouse SOKM	yes	yes	20.1 Kb	A. Popplestone

Table 1 – Vectors used and constructed in chapter 3. The table indicates the type of vector, promoter used, species of factor and factors carried, presence of EBNA-1/oriP and TK elements, Size (Kb) and who constructed the vector. SOKM= Sox-2, Oct-4, Klf-4 and C-Myc reprogramming factors.

The iPS HSV-1 amplicon vectors were constructed by isolating the SOKM polycistronic cassette, TK cassette and EBNA-1/*oriP* retention element from the vectors FUW-SOKM, pMS-RQ0817831 and p7157.1 by restriction digest. The 5.08 Kb polycistronic SOKM cassette was excised from the FUW-SOKM vector by *Eco RI* digest. The TK cassette was isolated from pMS-RQ0817831 using the restriction enzyme *Asl I* that generated a 1.7 Kb fragment. A fragment containing

the EBNA-1/*oriP* cassette, hygromycin resistance gene and EGFP reporter gene was digested from the p7157.1 vector using the enzymes *Bgl II/Nru I* generating a 7.6 Kb fragment. The vector plasmid maps and restriction sites are shown in Figure 1.

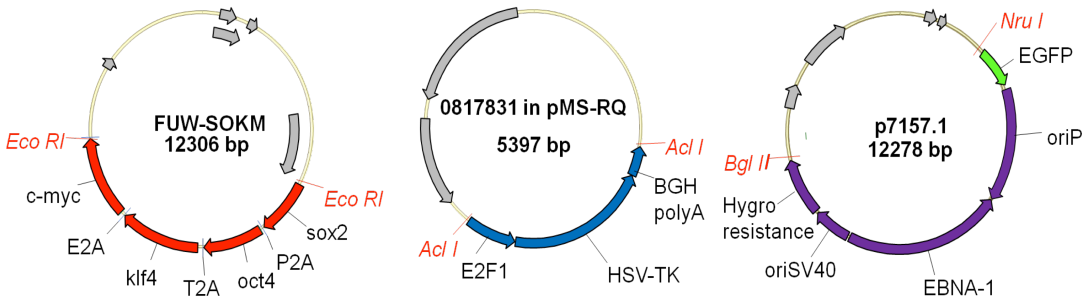


Figure 1 – Plasmid maps of source vectors containing the expression cassettes used to construct the new iPS HSV-1 amplicon vectors. The SOKM polycistronic cassette was isolated by *Eco RI* digest from FUW-SOKM. The TK cassette was isolated by *Acl I* digest from pMS-RQ0817831 and the EBNA-1/*oriP* element, hygromycin resistance and EGFP cassette were isolated from p7157.1 by *Bgl II* and *Nru I* digest.

The SOKM, TK and EBNA-1/*oriP* elements were cloned into the pHGCX HSV-1 amplicon vector which contains the HSV-1 packaging signals (pac) and origin of replication (Ori S) required for packaging into HSV-1 amplicons. The pHGCX vector was digested with the restriction enzyme *Eco RI*, treated wth calf intestinal phosphatase (CIP) and ligated to the purified SOKM cassette to generate the vector pHGCX+SOKM. Next the pHGCX+SOKM vector was digested with the restriction enzymes *Bgl II* and *Nru I* to remove the EGFP cassette. This fragment was CIP treated and ligated to the EBNA-1/*oriP*-hygromycin resistance-EGFP fragment to generate the vector pHGCX+SOKM+EBNA. Finally the pHGCX+SOKM+EBNA and pHGCX+SOKM vectors were each digested with *Pac I* to linearise the vectors. The fragments were then treated with Klenow

exonuclease followed by CIP and ligated with the TK cassette to generate the vectors pHGCX+SOKM+TK and pHGCX+SOKM+EBNA+TK. The cloning strategy detailing the plasmid maps and restriction sites is shown in Figure 2.

3.3 Vector confirmation

The resulting plasmids pHGCX+SOKM, pHGCX+SOKM+EBNA, pHGCX+SOKM+TK and pHGCX+SOKM+EBNA+TK were screened by restriction digest to ensure they were correct. Digestion of mini-prep DNA with restriction enzymes determined whether the insert was present and in the correct orientation. The first plasmid pHGCX+SOKM was screened by *Pci I* restriction digest, which yielded two possible digests indicating both orientations of the insert were present. A plasmid map and corresponding gel of the correct orientation is shown in Figure 3A. The pHGCX+SOKM+EBNA plasmid was screened by *Eco RI* to check for the correct insert and was further digested by *Eco RI/Nru I* as shown in Figure 3B. The vectors pHGCX+SOKM+TK and pHGCX+SOKM+EBNA+TK were digested with *Eco RI/Nde I* and *Eco RI/Bgl II* respectively, as shown in Figure 3 C and D.

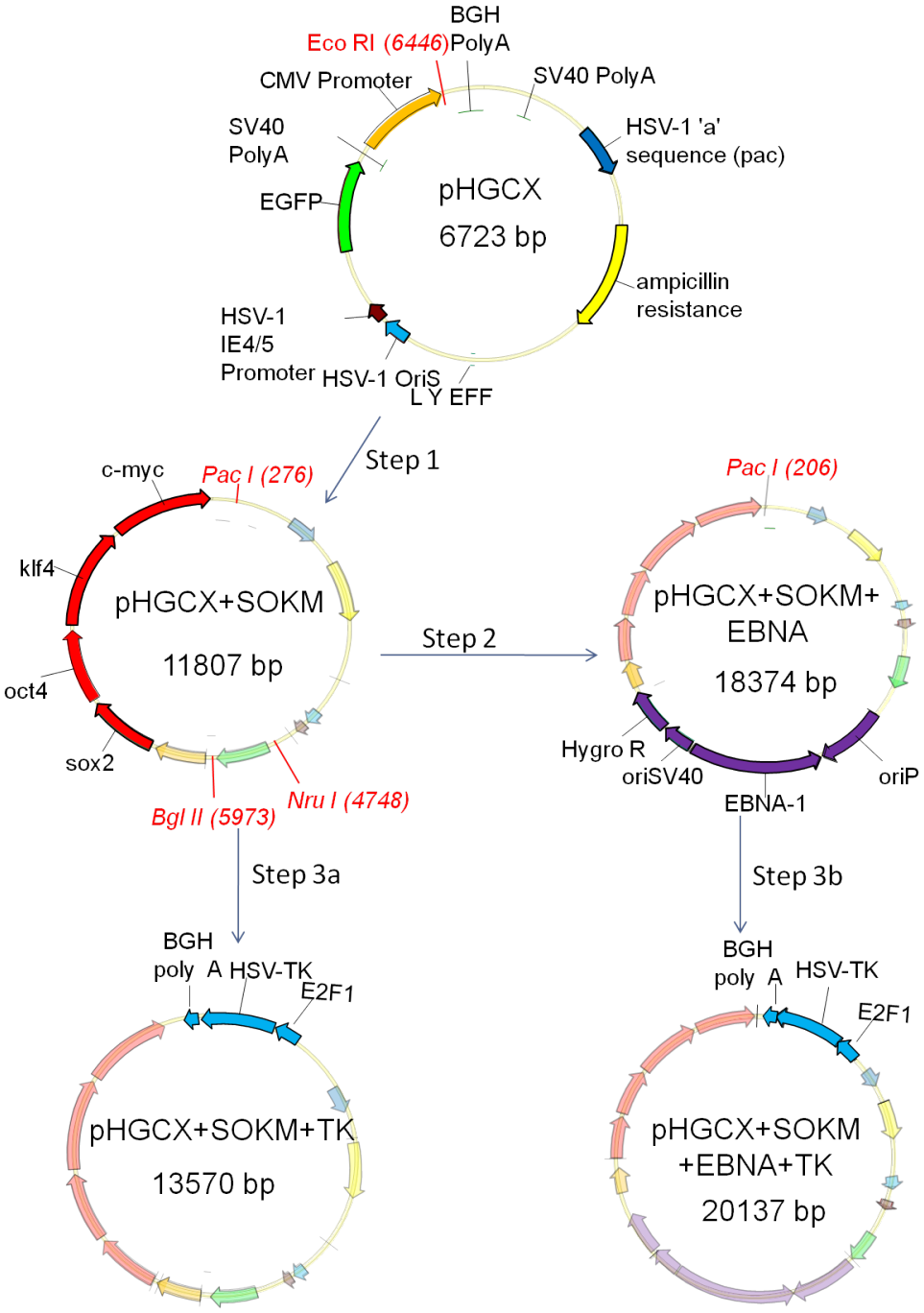


Figure 2 – Construction of HSV-1 amplicon iPS vectors by serial restriction digests and ligations. Step 1) The polycistronic cassette (Sox-2, Oct-4, Klf-4 and C-Myc) was ligated into pHGCX vector at the *Eco RI* site, resulting in pHGCX+SOKM. Step 2) The EBNA-1/OriP cassette, Hygromycin resistance and EGFP titration cassette were inserted at the *Bgl II* and *Nru I* site in pHGCX+SOKM, replacing the existing EGFP cassette. Step 3a and 3b) The TK cassette was inserted into pHGCX+SOKM and pHGCX+SOKM+EBNA vectors at the *Pac I* site resulting in two vectors; pHGCX+SOKM+TK and pHGCX+SOKM+EBNA+TK.

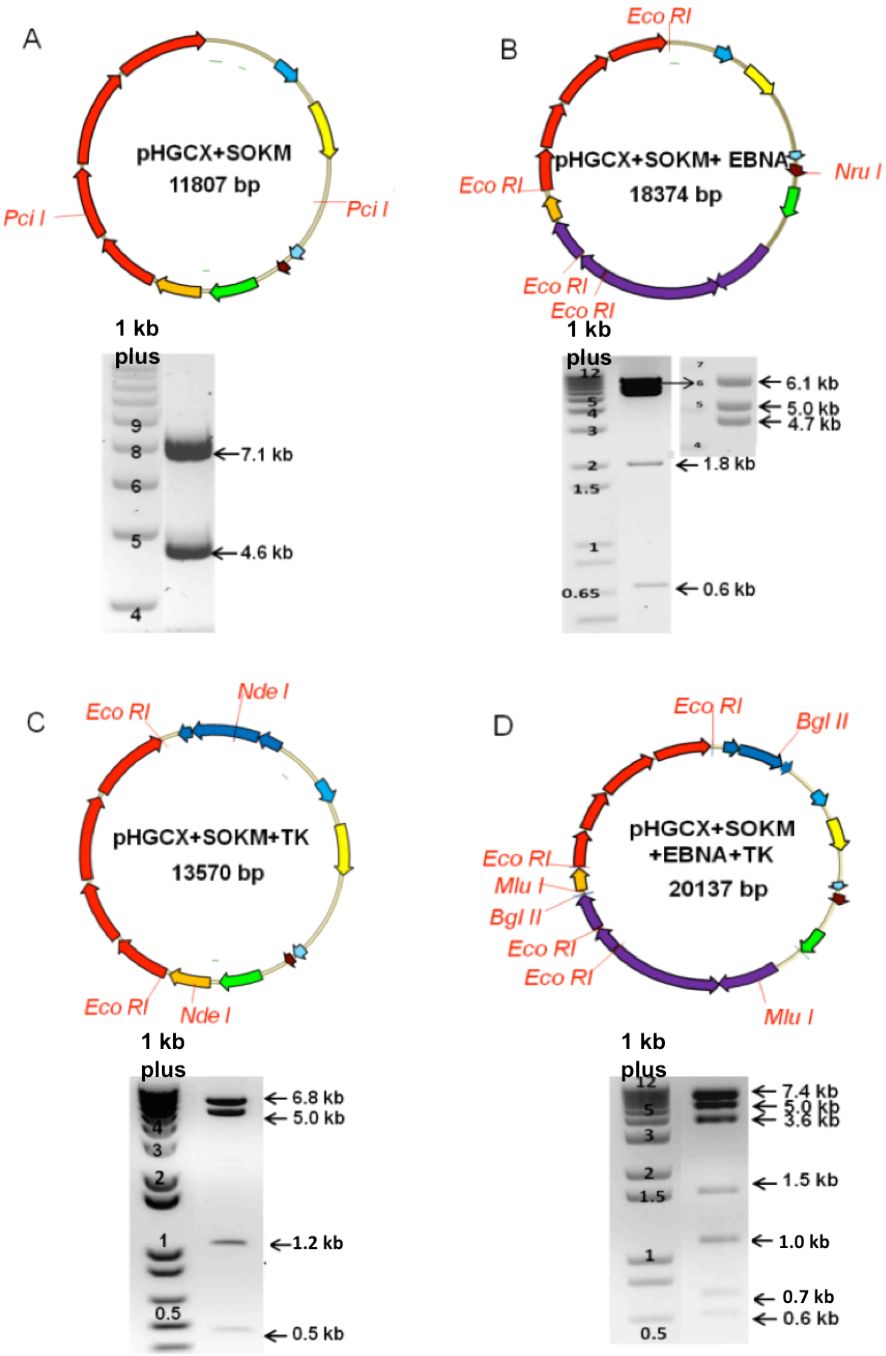


Figure 3 – Restriction enzymes digest analysis of final HSV-1 amplicon vectors. At each stage of vector construction test digests were carried out to ensure the fragments were inserted correctly and in the right orientation. Plasmid maps and corresponding digests are shown in panels A-D. **(A)** pHGCX + SOKM - *Pci I* (7.1 and 4.6kb) **(B)** pHGCX+SOKM+EBNA - *Eco RI, Nru I* (6.1, 5.0, 4.7, 1.8 and 0.6kb) **(C)** pHGCX+SOKM+TK - *Eco RI* and *Nde I* (6.8, 5.0, 1.2, 0.5) **(D)**pHGCX+SOKM+EBNA+TK – *Bgl II, Eco RI, Mlu I* (7.4, 5.0, 3.6, 1.5, 1.0, 0.7, 0.6, 0.02*NB fragment run off the gel).

3.4 Effect of SOKM expression on amplicon titres

Packaging of the HSV-1 reprogramming amplicons was performed using the Helper BAC system as described in Chapter 1 (Figure 4). During packaging of the HSV-iPS vector very low titres of vector stock were obtained. Whereas our control vector pHGCX consistently gave titres of $1x10^7$ - $1x10^8$ transducing units (TU) per ml, the HSV-iPS vector titres were often in the range of $1x10^2$ – $1x10^5$ TU/ml. Furthermore, Vero 2-2 cells packaged with pHGCX+SOKM had very few replicating foci in comparison to pHGCX and many dead cells were observed suggesting that SOKM may have a toxic effect on the Vero 2-2 cells (Figure 5).

Initially the lower titres were thought to be due to the size difference of the vectors. However, packaging of the smaller vector pHGCX+SOKM resulted in significantly different titres in comparison to pHGCX despite being only 5 kb larger (Figure 5). To verify this hypothesis without markedly changing the size of the vector, the SOKM immediate/early CMV promoter (689bp) was removed from pHGCX+SOKM, effectively shutting off expression of the four genes. This resulted in a complete rescue of the viral titres to pHGCX levels, in three independent experiments (Figure 5D) indicating that expression of SOKM during packaging compromises HVS-1 amplicon titres.

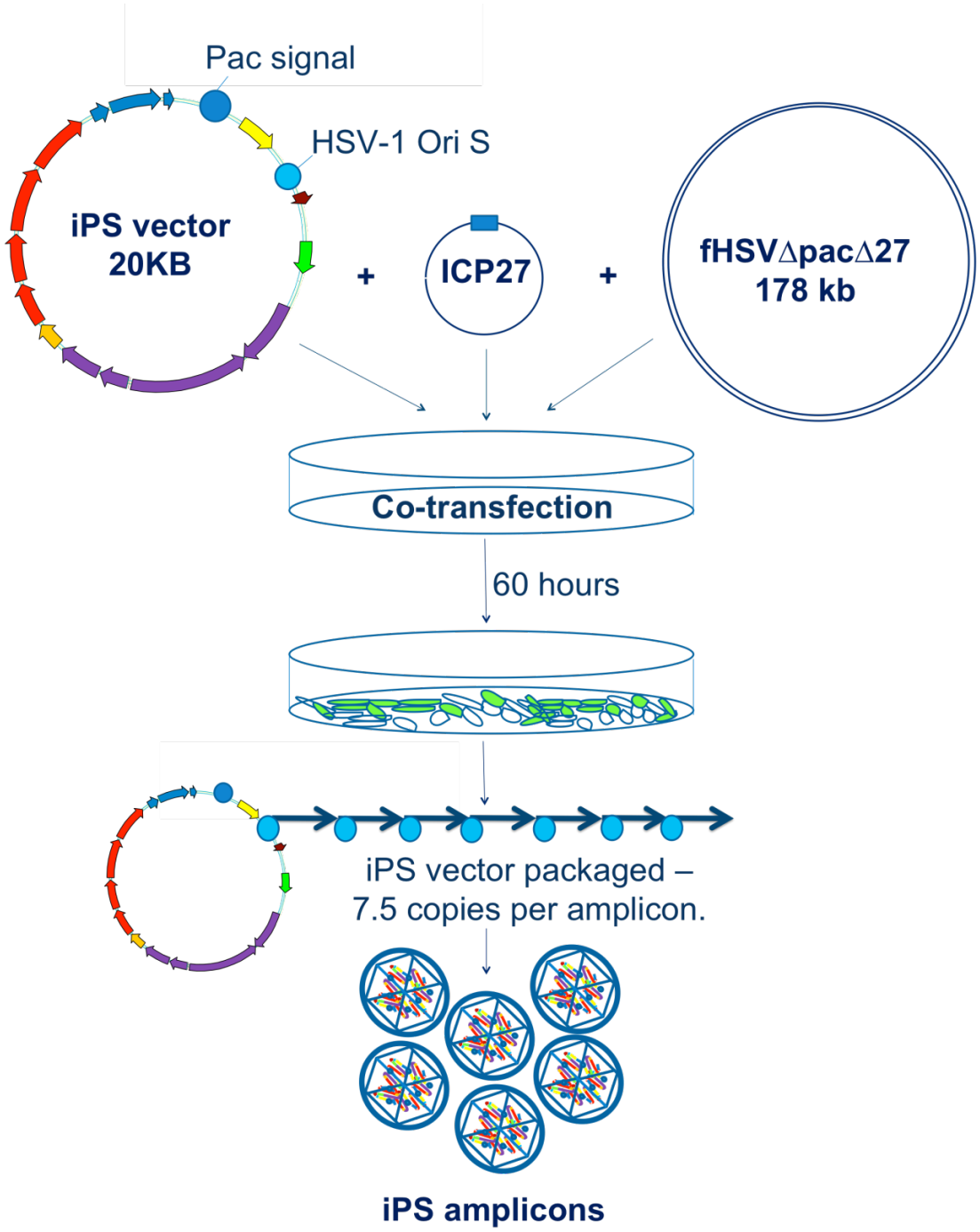


Figure 4 – Packaging of HSV-1 reprogramming amplicons. The iPS vector was co-transfected with fHSVΔpacΔ27, a BAC encoding the viral envelope genes but which has deletions in the packaging signal (supplied by the iPS vector) and essential gene ICP27 (supplied by a 3rd plasmid helper plasmid). The iPS vector was packaged into the virion by rolling circle mechanism resulting in concatamers of the vector. HSV-1 iPS amplicons are ready to purify and concentrate after 60 hours.

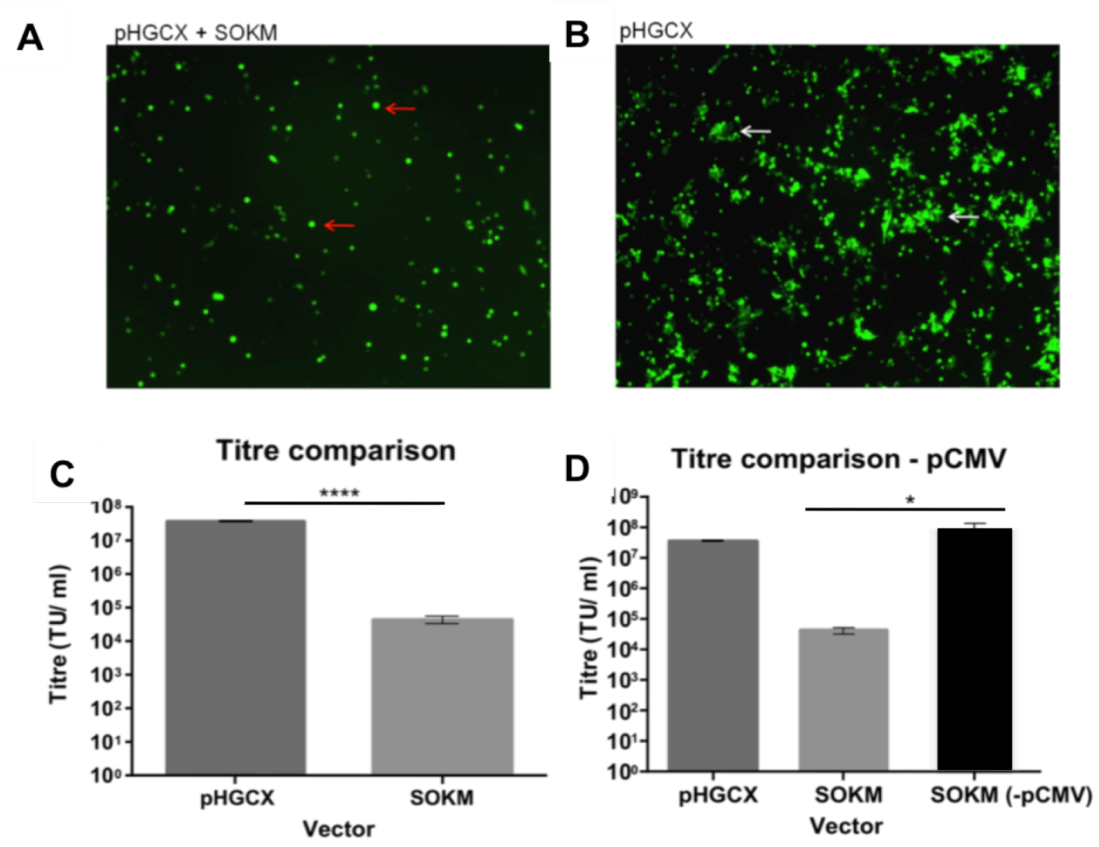


Figure 5- Toxic effect of SOKM expression during packaging results in significantly lower HSV-1 amplicon titres, which can be rescued by removal of the CMV promoter. A) Toxicity observed during packaging of SOKM vector in Vero-22 packaging cell line, detached cells indicated by red arrows. **B)** Replicating foci observed in packaging of pHGCX vector, indicated by white arrows. **C)** Significant differences in amplicon titres observed in pHGCX+SOKM (SOKM) compared with pHGCX (analysed by unpaired students t-Test). **** $p<0.0001$. **D)** Comparison of pHGCX amplicon titre with SOKM and SOKM (-pCMV) with deleted promoter (analysed by one way Anova, Dunnett's multiple comparison test, *$p<0.05$), n=3).

3.5 Replacing the immediate early cytomegalovirus promoter (pCMV)

Subsequently the immediate early cytomegalovirus promoter/enhancer (pCMV) was replaced in the existing constructs with the immediate-early cytomegalovirus type-2 tetracycline operator (tetO2) promoter/enhancer (pCMV-TetO2), which contains the TATA box TetO2 sequence. The Tetracycline repressor (TetR) represses gene expression from the CMVTetO2 promoter by binding to the TATA box.

To clone in the CMVTetO2 promoter the existing CMV promoter was removed from the pHGCX+SOKM and pHGCX+SOKM+TK vectors using the enzymes *Kpn I, Mlu I*. The enzymes *Kpn I, Bgl II* were used to digest the promoter from pHGCX+SOKM+EBNA followed by Klenow exonuclease treatment to blunt the restriction site. The CMVTetO2 promoter was digested from the source vector pcDNA4/TO/myc-His A using the enzymes *Kpn I* and *Mlu I*. The digested fragments were gel purified, the vectors were CIP treated and ligated with new promoter together in parallel to generate the three vectors pHGCX+SOKM+TetO2, pHGCX+SOKM+TK+TetO2 and pHGCX+SOKM+EBNA+TetO2. The TK cassette was digested with *Asl I* and cloned into the pHGCX+SOKM+EBNA+TetO2 vector at the *Pci I* site as described previously generating the vector pHGCX+SOKM+EBNA+TK+TetO2. The promoter insertion in all vectors is shown in Figure 6.

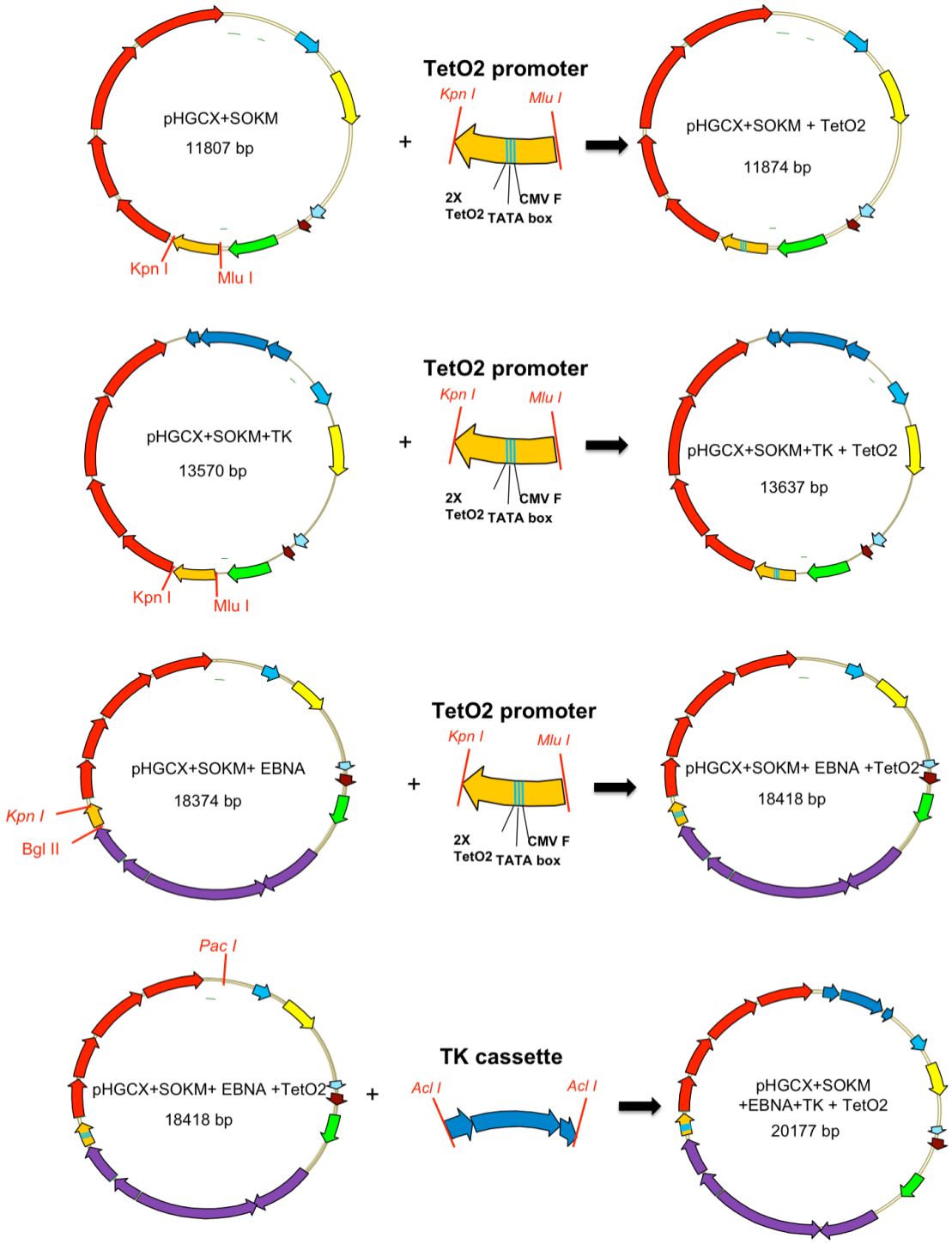


Figure 6 – Construction of pCMVTetO2 HSV-1 amplicon iPS vectors by restriction digest and ligation - The TetO2 promoter was isolated from pcDNA4/TO/myc-His A by Kpn I and Mlu I digest and inserted into pHGCX+SOKM, pHGCX+SOKM+TK and pHGCX+SOKM+EBNA replacing the pCMV promoter. The TK cassette was inserted into the *Pac I* site in the pHGCX+SOKM+EBNA+TetO2 vector.

3.5.1 Confirmation of correct pCMVTetO2 insertion

The resulting plasmids pHGCX+SOKM+TetO2, pHGCX+SOKM+EBNA+TetO2, pHGCX+SOKM+TK+TetO2 and pHGCX+SOKM+EBNA+TK+TetO2 were screened by restriction digest to ensure they were correct. Digestion of mini-prep DNA with restriction enzyme *Ase I* was used to screen the correct insertion of CMVTetO2 promoter as the enzyme cuts twice in the CMV promoter and once in the CMVTetO2 promoter. A digest pattern of three bands confirms correct insertion of the CMVTetO2 promoter and two bands indicate the promoter has not inserted and the original vector would yield four bands. Insertion of the TK cassette into the pHGCX+SOKM+EBNA+TetO2 was confirmed by *Eco RI* digest.

Minipreps with the correct digest pattern were further digested with different restriction enzyme combinations to confirm the vector conformation was correct. The following double digests from the 4 final vectors and their corresponding plasmid maps are shown in Figure 7. The pHGCX+SOKM+TetO2 plasmid was digested with *Asc I* and *Sph* yielding five bands 4.6, 3.6, 1.6, 1.4 and 1.1 kb in size. The pHGCX+SOKM+TK+TetO2 was digested with *Bam HI* and *Sph I* yielding six bands 4.0, 3.3, 2.5, 1.7, 1.1, 0.9 kb in size. The pHGCX+SOKM+EBNA+TetO2 was digested with *Eco RI* and *Mlu I* yielding five bands 7.0, 5.5, 3.6, 1.8 and 0.62 Kb in size. Finally insertion of the TK cassette in the plasmid pHGCX+SOKM+EBNA+TK+TetO2 was confirmed by *Apa LI* and *Bam HI* double digest, yielding seven bands 5.9, 5.3, 2.3, 1.8, 1.4, 1.2, and 1.1 kb in size.

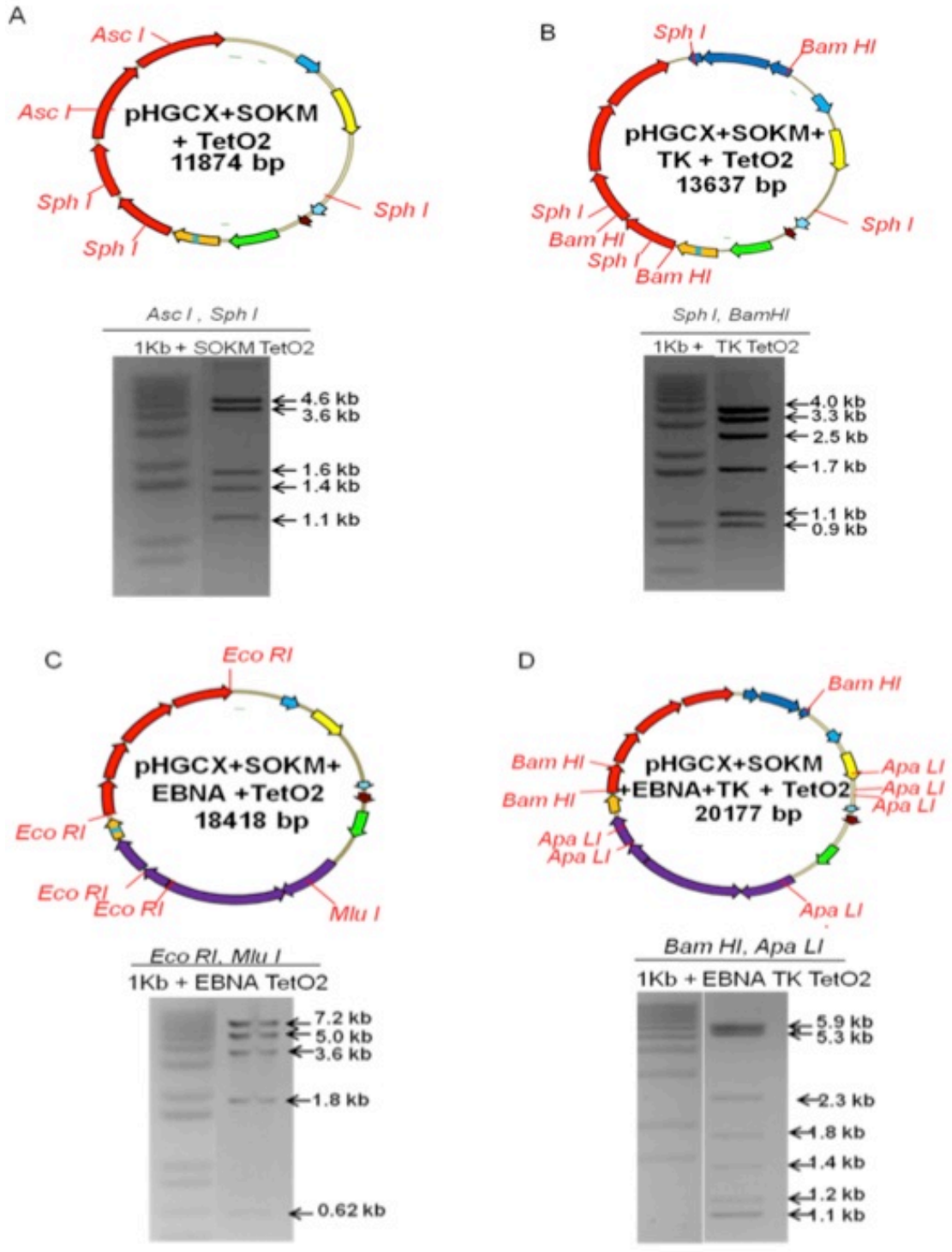


Figure 7 – Restriction enzymes digest analysis of final pCMVTetO2 HSV-1 amplicons. Restriction maps and diagnostic digests gels are shown of the four HSV-1 amplicon TetO2 iPS vectors A) pHGCX+SOKM+TetO2 – *Asc I* and *Sph I* B) pHGCX+SOKM+TK + TetO2 – *Bam HI* and *Sph I* C) pHGCX+SOKM+EBNA+TetO2 - *Eco RI* and *Mlu I* D) pHGCX+SOKM+EBNA+TK+TetO2 – *Bam HI* and *Apa LI.*

3.5.2 Functionality of the CMVTetO2 promoter

The new TetO2 iPS vectors were co-transfected with a plasmid (pcDNA6/TR) containing the tetracycline repressor (TetR) into the immortalised lung fetal fibroblast MRC5-V2 cell line to check for repressor functionality. The CMVTetO2 promoter enables SOKM silencing during packaging by co-transfection of the pcDNA6/TR plasmid with the packaging vectors fHSVΔpacΔ27 and ICP27 (Figure 8A). Co-transfection of the pcDNA6/TR plasmid during packaging rescued the TetO2 iPS amplicon titres to pHGCX levels. Titres generated from the three Tet02 iPS vectors pHGCX+SOKM+TetO2, pHGCX+SOKM+TK+TetO2 and pHGCX+SOKM+EBNA+TK+TetO2 packaged in presence and absence of the pcDNA6/TR plasmid were statistically compared by student t-Test and found to be significantly increased, **** $P<0.0001$(Figure 8B) Western blotting of the TetO2 iPS vectors co-transefected with pcDNA6/TR confirmed repression of the SOKM transgenes, whereas TetO2 iPS vectors transfected alone expressed SOKM as normal (Figure 8C).

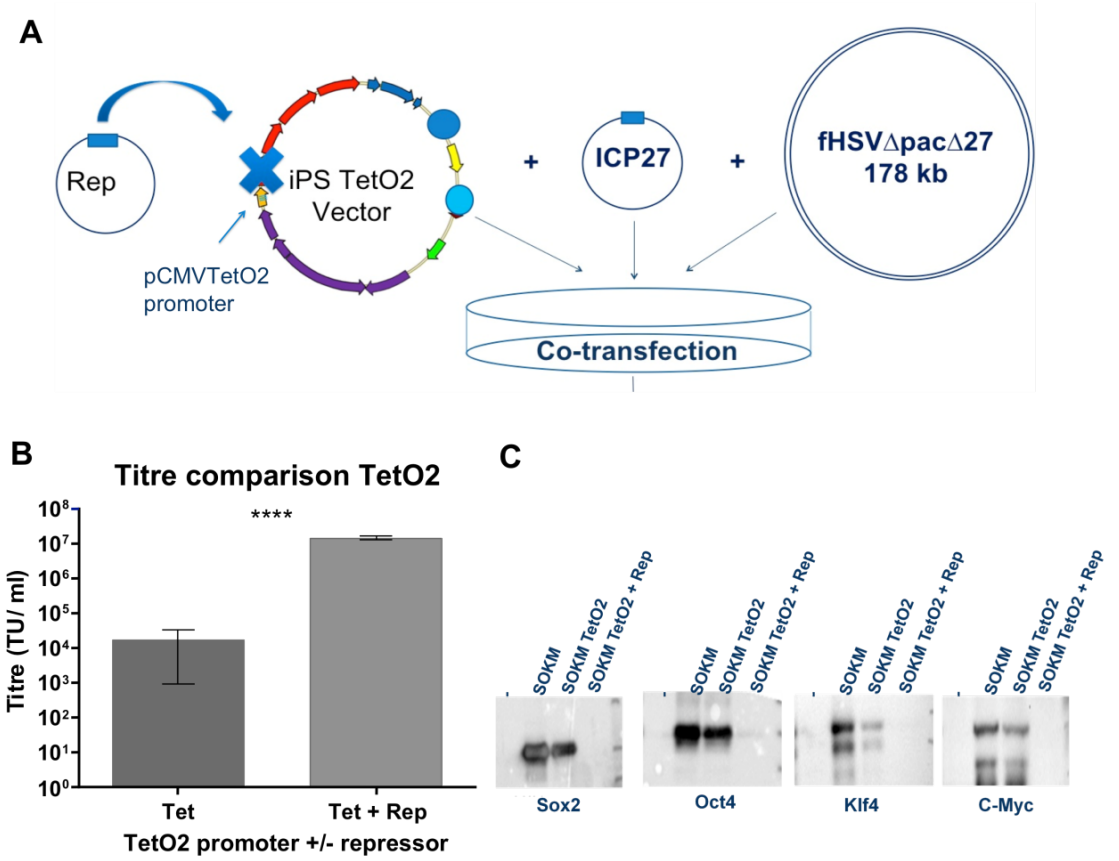


Figure 8 – Confirmation of pCMVTetO2-SOKM repression when co-transfected with the tetracycline repressor A) Schematic of iPS TetO2 vector co-transfected with packaging vectors and an additional TetO2 repressor plasmid**. B)** Titres achieved by TetO2 vector packaged in presence/absence of repressor plasmid pcDNA6/TR. A significant increase was observed in plasmids packaged with the repressor. P<0.0001 (unpaired student t-Test). **C)** Western blot of iPS vector (SOKM) and SOKM TetO2 vector co transfected in presence/absence of the pcDNA6/TR plasmid.

3.6 Vector characterisation

The iPS vector elements were fully characterised to confirm functionality before use in reprogramming experiments. Confirmation of the four reprogramming factors protein expression was determined by Western blot analysis of MRC5-V2 cells transfected with HSV-1 iPS vectors and the negative control pHGCX. Cells were harvested and lysed 48 hours after transfection and analysed by Western blot. Confirmation of Sox-2, Oct-4, Klf-4 and C-Myc protein expression was confirmed by the presence of bands approximately 40, 45, 70 and 65 kDa in size respectively when probed with corresponding primary antibodies. With the exception of Sox2, the SOKM proteins were slightly larger than their calculated sizes of 41.9, 42.0, 56.1, 50.1 kDa respectively, inclusive of the additional amino acids of the 2A sequences. Protein sizes were calculated using UniProt software.

Enhanced protein expression was observed in iPS vectors containing the EBNA-1/*oriP* cassette most likely due to EBNA-1 binding to a 30 bp family repeat region and acting as a transcriptional enhancer [195]. Expression of SOKM in MRC5-V2 cells transduced with iPS vector and pHGCX amplicons at a multiplicity of infection (MOI 3) was also confirmed by Western blot (Figure 9).

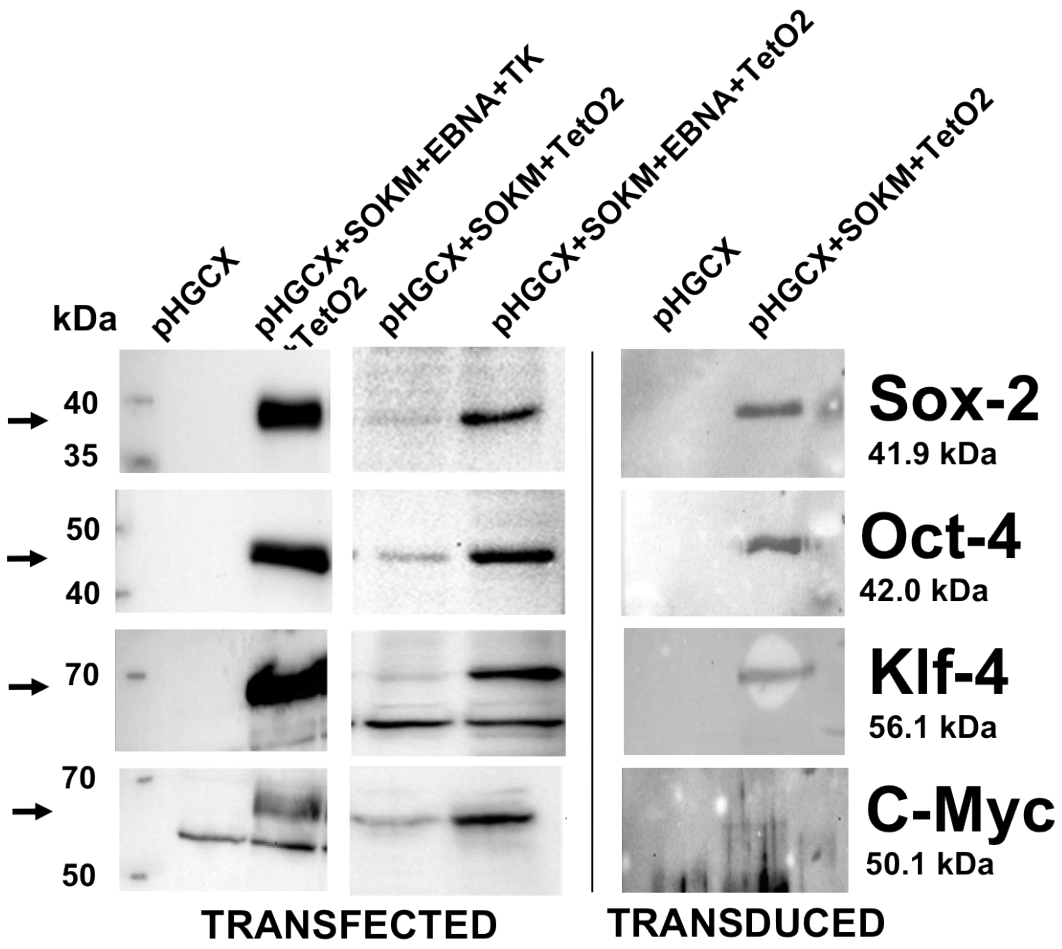


Figure 9 – Western blot confirmation of Sox-2, Oct-4, Klf-4 and C-Myc protein expression transfected and transduced MRC5-V2 cells. The left hand column shows cells transfected with pHGCX (negative control) and pHGCX+SOKM+EBNA+TK+TetO2. The middle column shows comparative increase in expression seen in the vectors containing the EBNA-1/ori-P element. The right hand column shows MRC5-V2 cells transduced with pHGCX and pHGCX+SOKM+TetO2 amplicons.

To assess whether the thymidine kinase suicide gene (TK) was functional; G16.9 cells were transduced with pHGCX+SOKM+TetO2 or pHGCX+SOKM+TK+TetO2 at an MOI of 3 in triplicate. The day after infection ganciclovir GCV reconstituted in 0.1 N HCl was added to the wells at 10 and 25 μg/ml using an equal volumes of

0.1 N HCl as a negative control. Five days after drug addition the number of EGFP positive cells was counted in each well to analyse whether there were any differences in the number of transduced cells. The number of EGFP positive transduced cells treated with GCV was normalised with the number of EGFP positive cells treated with HCl only. A significant reduction in the number of EGFP+ cells was observed in cells transduced with pHGCX+SOKM+TK+TetO2 (~60% reduction at both concentrations) in comparison to cells transduced with pHGCX+SOKM+TetO2 (no difference at both concentrations). Cell counts were analysed by two way Anova assay, where **** p<0.0001 (Figure 10).

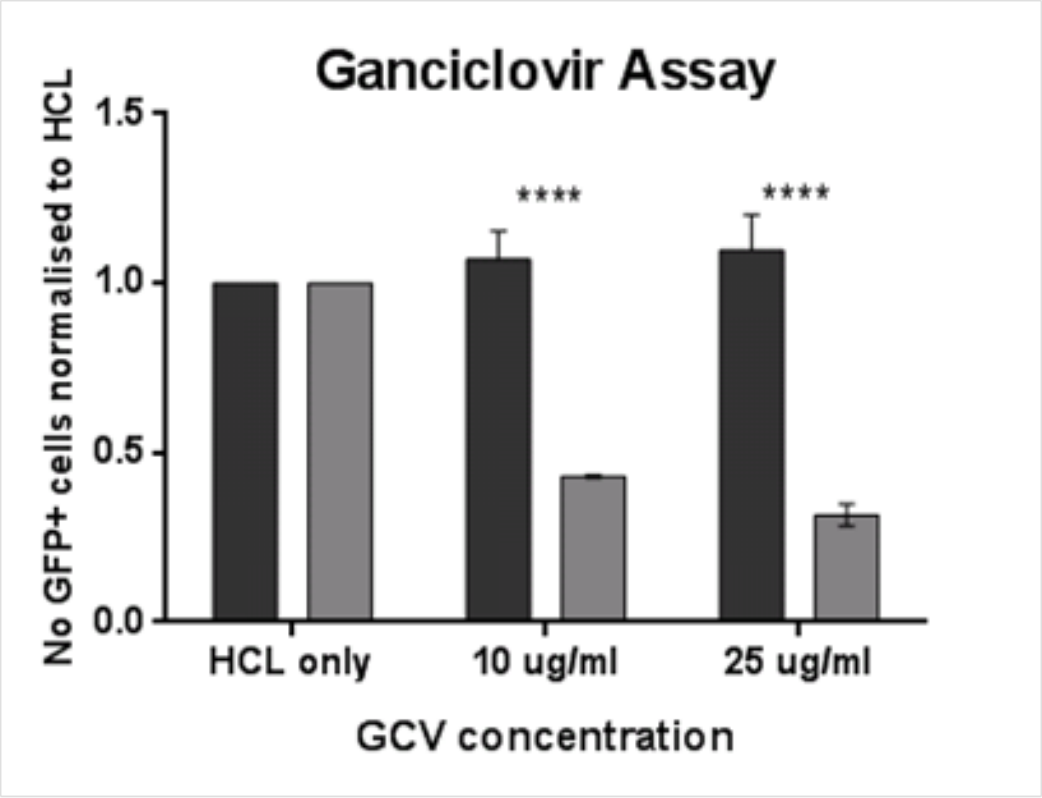


Figure 10 – Ganciclovir assay confirmation of thymidine kinase gene function. Cells were transduced with the HSV-1 amplicon pHGCX+SOKM+TK (light grey bars) and compared with the pHGCX+SOKM control (dark grey bars), which does not contain the TK cassette. G16.9 ells were treated with ganciclovir at 10 and 25 μg/ml and assayed by counting the number of surviving GFP positive cells normalised to the HCL only control. The data was statistically analysed by two-way Anova assay and significant decrease in cell survival was found in the cells transduced with pHGCX+SOKM+TK (**** p<00001), the experiment was performed in triplicate, n=1.

EBNA-1/*oriP* function was assessed by establishing stable SOKM transfected MRC5-V2 clonal cell lines. Cells were transfected with pHGCX+SOKM+EBNA+TK+TetO2 and incubated in 200 µg/ml Hygromycin to selectively kill any untransfected cells. Single clones started to appear after 7-10 days of antibiotic selection. Thirty-three clones were isolated and transferred to a ninety-six well plate and gradually expanded to a 10 cm dish over a period of two months. Twenty-four clones survived and were harvested and treated with alkaline lysis to rescue supercoiled plasmid DNA.

Fourteen of the twenty-four alkaline lysis preparations of episomal plasmid DNA generated bacterial colonies when electroporated into electrocompetent E. coli, confirming the presence of intact episomal plasmids. The bacterial colonies were miniprepped and digested alongside the untransfected pHGCX+SOKM+EBNA+TK+TetO2 plasmid with the restriction enzyme *Eco RI* to compare digest patterns. Four of the mammalian clones analysed had non re-arranged plasmids present (Figure 11).

A

clone	Frequency
24	1/10
39	1/3
44	4/14
45	7/28

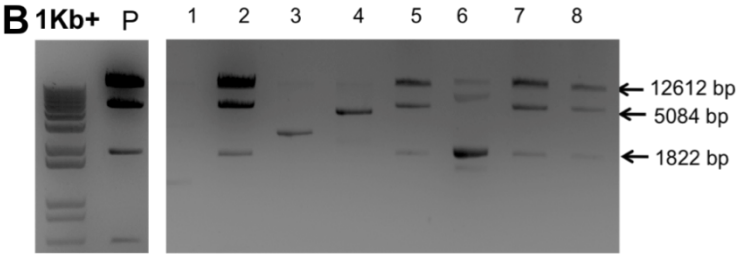


Figure 11 – Episomal rescue and analysis of clonal cell lines transfected with the pHGCX+SOKM+EBNA+TK+TetO2 plasmid after 2 months of continuous cell culture. A) Table of intact plasmid frequencies obtained from episomal rescue of plasmids **B)** *Eco RI* restriction digest of minipreps obtained from MRC5-V2 clone number 45 compared with the non-cultured plasmid control (P). Intact plasmids can be seen in lanes 2,5,7 and 8.

3.7 Reprogramming experiments

The primary lung fetal fibroblasts (MRC5) cells were initially chosen for reprogramming experiments due to the high transduction efficiency (~90%) in their immortalised counterparts (MRC5-V2) with HSV-1 amplicons [196]. In addition MRC5 cells have been reprogrammed previously making them an excellent cell line to use [46]. Transduction efficiency of the primary cell line MRC5 was assessed by pHGCX amplicon transduction at MOI 1,5,10 and 20 and a transduction efficiency of 10-20% was observed at MOI 10. An MTT assay of MRC5 cells transduced with pHGCX or pHGCX+SOKM+EBNA+TK+TetO2 showed no significant changes in MTT absorbance in the majority of conditions (when transduced with pHGCX, MOI 1 and MOI5 or pHGCX+SOKM+EBNA+TK+TetO2, MOI5), however a significant reduction in MTT absorbance was observed in cells transduced with SOKM at MOI 1 (*$p<0.05$) as shown in Figure 12.

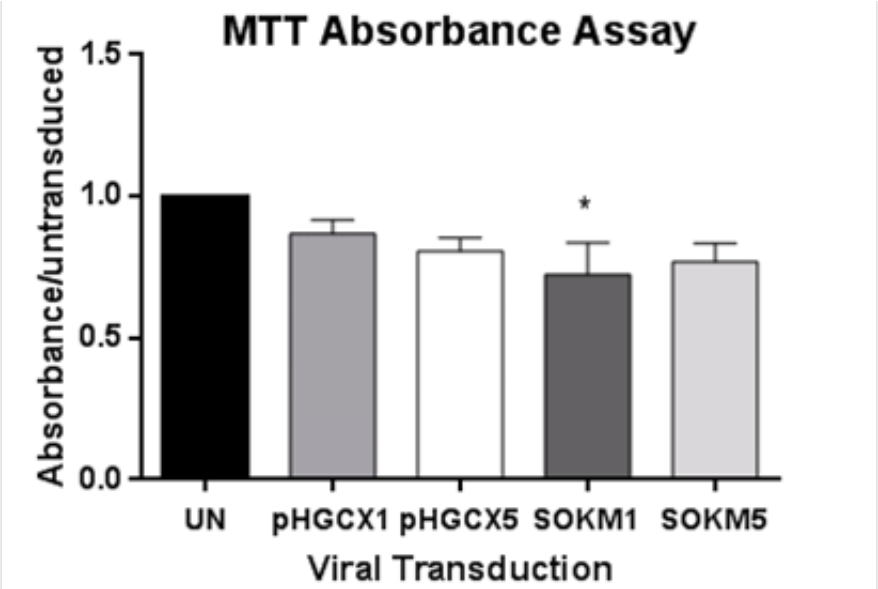


Figure 12 – MTT absorbance assay of HSV-1 amplicons – Viability of MRC5 cells transduced with pHGCX and pHGCX+SOKM. Cells were analysed by MTT assay of MRC5 cells transduced at an MOI of 1 and 5. A significant decrease in cell viability was found in cells treated with SOKM, MOI 1 in comparison to untransduced cells (* $p<0.05$, analysed by one-way Anova) however no significant changes were observed in any of the other conditions (pHGCX MOI 1 and 5 or SOKM MOI 5). The experiment was performed in triplicate, n=1.

The absorbance of the MTT assay relates to cell viability, given that three out of the four conditions do not significantly effect absorbance the conclusion can be drawn that HSV-1 amplicons do not have a significantly adverse effect on cell viability. The experiment was performed in triplicate at an MOI of 1 and 5 and compared with untransduced MRC5 cells and the results were analysed by one-way Anova, Dunnett's multiple comparison test.

Transduction of donor primary fibroblast lines (MKO82 and JRO53) obtained through the Oxford Parkinson's Disease Centre iPS cell recruitment program had a similar transduction efficiency of 30% GFP positive cells at an MOI of 10 and 45% at MOI 30. Initial reprogramming experiments were carried out on both primary MRC5 cells and control donor fibroblast lines (MKO82 and JRO53). Primary fibroblasts were transduced with pHGCX+SOKM+EBNA+TK+TetO2, the negative control pHGCX or a Sendai virus positive control at an MOI of 10. The day after transduction the media was replaced with fresh media and left to recover from transduction. After 48 hours (72 hours after initial transduction) the cells were trypsinised and seeded on to irradiated mouse embryonic fibroblasts (iMEFs) at a density of 8000 fibroblasts per well.

The following day the media was changed to human embryonic stem (hES) cell media supplemented with vitamin C (Vit C) and Valproic acid (VPA). Valproic acid is an HDAC inhibitor which can increase reprogramming efficiency 100 fold, Vitamin C has been reported to accelerate mouse and human reprogramming, increase efficiency, and counteract senescence [27] [197, 198]. A 50% hES media change was made every second day up until 10 days after seeding. After 10 days

the media was replaced with MEF conditioned hES media due to the inactivation of iMEF feeder layer. The MEF conditioned media was supplemented with basic fibroblast growth factor (FGF2) due to the rapid degradation of the molecule at 37°C during MEF conditioning. A 50% MEF conditioned hES media change was made every other day and cultures were maintained for up to 40 day and analysed frequently for the appearance of iPS colonies. The reprogramming protocol is outlined in Figure 13.

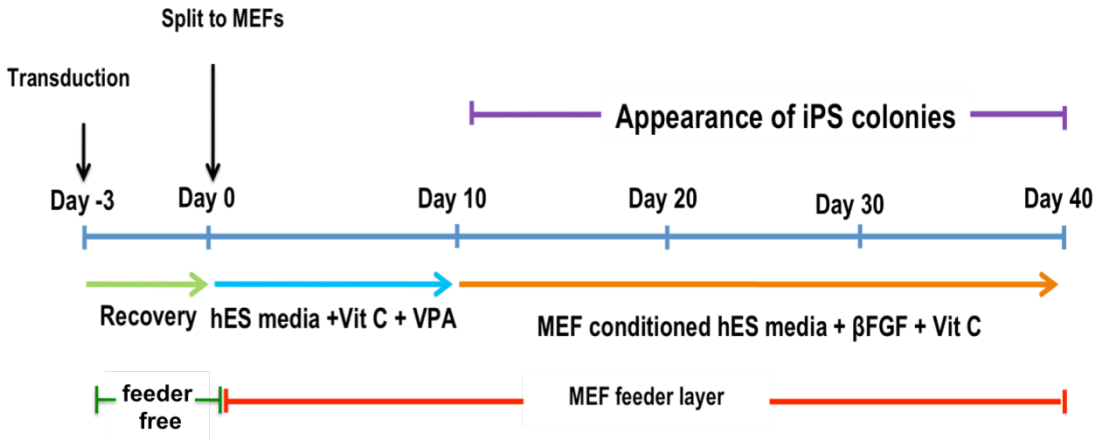


Figure 13 – Timeline of reprogramming protocol. The media conditions and timings of transduction, transfer to MEF feeder layer and change to MEF conditioned media are indicated. Appearance of colonies typically happen from day 12 onwards.

We observed fibroblast morphology changes and the appearance of small colonies, which arose 12 days after transfer of SOKM transduced fibroblasts to iMEFs. The colonies were distinct from fibroblasts however these colonies did not have typical iPS morphology. True human iPS cells have a high nucleus-cytoplasm ratio, are tightly packed and the colony is flat with a defined edge with more differentiated cells in the centre of the colony. Typical iPS colonies emerge around 1-2 weeks into the differentiation protocol and grow rapidly and are usually ready to isolate and passage onto fresh MEFs around 20 days into the

protocol. Colonies derived from Sendai virus differ from human iPS cells as they have a more three dimensional appearance and resemble mouse iPS colonies. We did not observe any colony like cultures in our pHGCX+EBNA+TetO2 transduced control wells.

We were unable to improve the reprogramming outcome despite experimenting with seeding densities, starting cell population number, MOI, media components and cell lines. We attempted reprogramming on several cell lines including MRC5 (lung fetal fibroblasts) JRO53 and MKO 82 (donor fibroblasts) and mouse embryonic fibroblasts. Initial experiments were performed on MRC5 fibroblasts due to their high transduction efficiency, however we observed a growth deficiency in untransduced MRC5 fibroblasts cultured in hES media, which was not observed in our normal human dermal fibroblasts (NHDF) control. We optimised culture conditions and found that a gradual change from DMEM to hES media rescued the growth deficiency. Addition of VPA and Vitamin C to the culture condition had no adverse affects on cell morphology or growth. Further experiments using early passage (p5-8) donor fibroblast lines JRO53 and MKO82 did not require the gradual change to hES media.

We also tried reprogramming mouse embryonic fibroblasts (MEFs) due to their relatively higher reprogramming efficiency. We obtained a transduction efficiency of 50% and observed a few colony like structures similar in morphology to those seen in our human fibroblast reprogramming experiments. We consistently saw iPS colonies in our positive control Sendai virus in each of these cell lines, indicating that experimental technique and viability of cells was

not compromised. Images of transduction, observed morphology changes and colonies are shown in Figure 14.

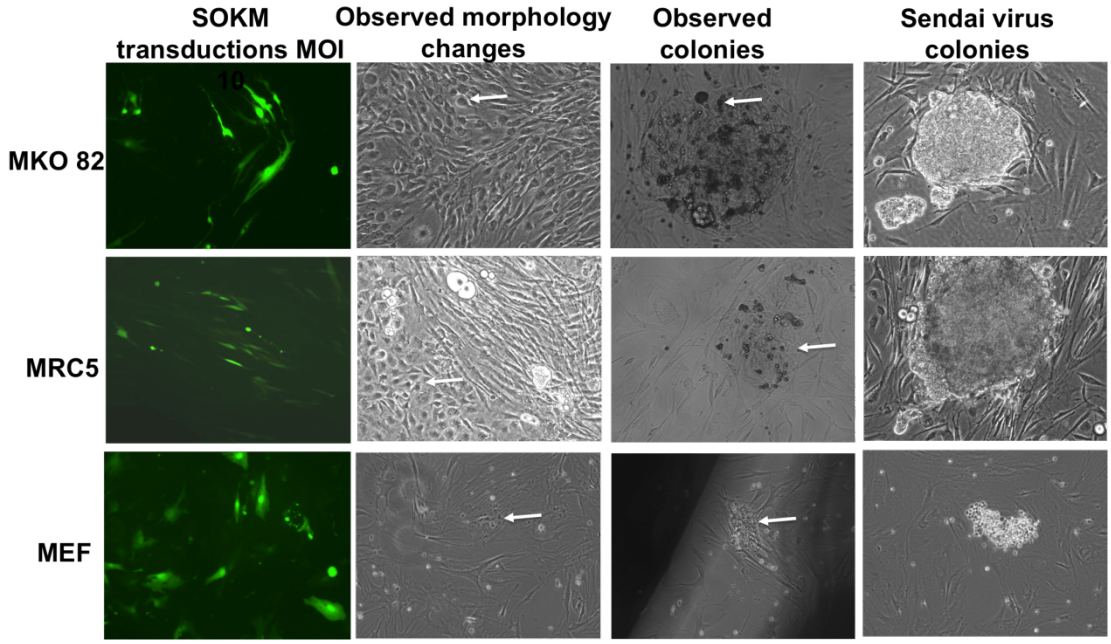


Figure 14 – HSV-1 amplicon reprogramming experiments in human donor fibroblasts (MKO82), human fetal fibroblasts (MRC5) and mouse embryonic fibroblasts (MEFs). The first column of images shows the three cell lines transduced with pHGCX+SOKM+EBNA+TK+TetO2 at an MOI of 10. Observed fibroblast morphology changes and colonies are shown in the second and third columns and are indicated by white arrows. Control colonies derived from Sendai virus are shown in the fourth column.

We increased starting cell population from 100,000 to 1,000,000 to improve the chances of generating iPS cells and experimented with the following cell seeding densities; 1000, 2000, 8000, 16,000, 24,000 and 72,000 cells per well. Transductions were performed at MOI 5, 10, 20 and 30 using filtered (0.22 μm and 0.45 μm) and unfiltered virus preps however no differences were observed in the number of colony like structures and no true iPS colonies were observed.

Transgene expression of the SOKM transgenes in the transduced fibroblasts was confirmed by RT-PCR. Primers were designed to amplify the exogenous Sox-2 to Oct-4, Oct-4 to Klf-4 and Klf-4 to C-Myc junctions and not amplify endogenous reprogramming factor sequences. The correct sized products of 151 bp, 200 bp and 223 bp was observed, confirming the expression of transduced factors. A control sample produced during cDNA conversion without the reverse transcriptase enzyme (RT-) was included to ensure there was no DNA contamination. A pHGCX negative control transduction was also analysed to ensure the primers were binding specifically to the SOKM cassette. The RT-PCR gel is shown in Figure 15.

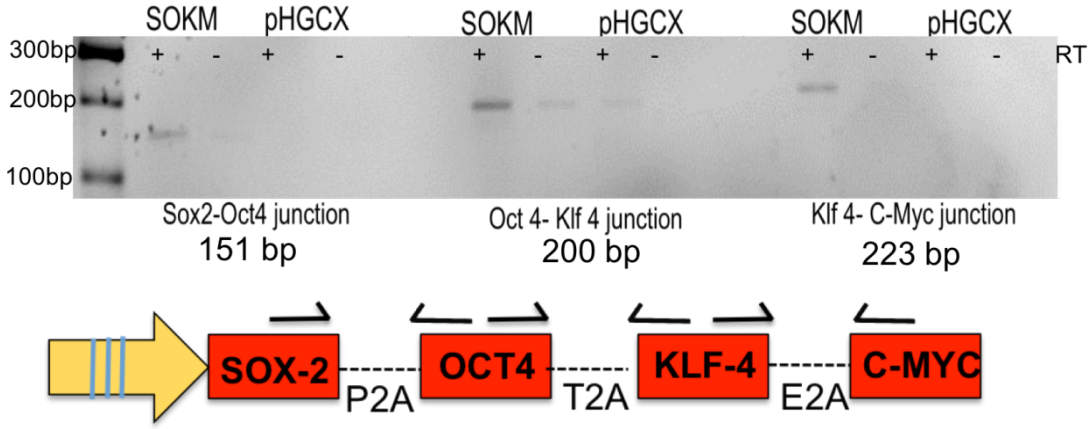


Figure 15 - Confirmation of ectopic factor expression in transduced primary fibroblasts by RT-PCR. RT-PCR was performed on transduced MRC5 fibroblasts and ectopic gene expression was confirmed using primers that flank the 2A junctions in the vector. Primer pairs were designed to bind to either side of the Sox-2 to Oct-4, Oct-4 to Klf-4 and Klf-4 to C-Myc junctions, avoiding amplification of endogenously expressed genes. Non-RT controls did not amplify confirming expression was from cDNA and not DNA contamination. No expression was seen in the pHGCX negative control. The primer binding sites are shown on the polycistronic cassette schematics (black arrows).

3.8 Summary and conclusions

Despite successful construction and characterisation of our HSV-1 amplicon iPS vectors we were unable to generate true iPS colonies, which were

morphologically similar to ES cells. The main obstacle we encountered before starting our reprogramming experiments was the consistently low titres observed in all our iPS vectors compared to our pHGCX control. This was overcome by replacing the pCMV promoter with a pCMVTetO2 promoter that can be repressed during packaging by co-transfecting the repressor. We suspect the SOKM cassette had a negative effect on viral titres due to the high levels of overexpression of the reprogramming factors during packaging having a toxic effect on the Vero 2-2 cells. Although toxicity was observed during packaging of SOKM vectors compared with pHGCX we did not observe this toxic effect in transduced MRC5 (assayed by MTT, Figure 12).

Characterisation of our vectors confirmed that all elements were functional. In particular expression of the four genes was confirmed by both Western blot (transfected and transduced MRC5) and RT-PCR (donor fibroblasts used in reprogramming experiments). The 2A peptide system should confer equimolar expression of the four genes in comparison with other polycistronic systems such as IRES elements. We did not observe any overt differences in gene expression between the four genes, however this was not confirmed by QRT-PCR. Confirmation of equimolar expression may not be essential, however as recent literature suggests that in fact a higher Oct-4 ratio is optimal for reprogramming [199].

Increased transgene expression was observed at the protein level in vectors containing the EBNA-1/OriP element compared with versions not containing the episomal maintenance cassette. This is consistent with reports that the Family

Repeat (FR) elements, present in the Ori/P sequence, transcriptionally enhance gene expression. Western blot confirmed expression in transfected and transduced cells, compared with untransfected/untransduced or pHGCX transfected/transduced controls. However, with the exception of Sox-2 a noticeable shift in protein size was detected in Oct-4 (3-5 kDa), Klf-4 (~10-15 kDa) and C-Myc (~10 kDa).

Although non-optimal gel pH can cause protein shifts, it's unlikely that this is the cause as the same protein sizes were observed on both hand cast gels and pre-cast gels. The relative charge can influence protein migration, as well as protein aggregation however given the relative shift in size it is most likely to be due to post-translational modifications such as glycosylation, phosphorylation or acetylation. There are several types of glycosylation and these have been demonstrated to cause similar protein shifts to that seen in our transcription factors [200]. The three most common glycosylations are N- linked glycosylations, O- linked GalNac Glycosylations and O-linked GlcNac glycosylations. N-linked glycosylations are found in membrane and secreted proteins and are adjoined to the Asaparagine within the Aparagine, X, Threonine/Serine consensus sequence. O-linked GalNac glycosylations are attached to surface and secreted proteins and GlcNac are found on cytosolic and nuclear proteins, however there is no consensus sequence for O-glycosylation but they are always on Threonine or Serine residues and usually near to Proline residues [201]. Recently, O-linked-N-acetylglucosamine (O-GlcNAc) was identified as an important regulator of pluripotency [202]. Inhibition of O-

GlcNAc can disrupt ES cell self-renewal, inhibit reprogramming and O-GlcNAc has been identified in Oct-4 [202] and Sox-2 [203] and c-Myc [204].

To assess whether the larger protein sizes observed in Klf-4 and c-Myc could theoretically be due to O-GlcNac I used the prediction software YinOYang 1.2 Server. The predictions were calculated based on promixity of Serine tract residues to Valine and Proline and an absence of Leucine and Glutamine. The prediction server also identifies probable Yin/Yang sites (sites which can undergo O-GlcNac as well as phosphorylation) by cross-referencing with NetPhos. Using this software thirty-six possible O-Glycosylation sites were predicted for both Klf-4 and C-Myc, sixteen and twenty one of these sites respectively could also undergo phosphorylation. Given that the high number of predicted sites and the large 10-15 kDa shift seen in both these proteins, it is likely that the higher molecular weight could be due to O-linked GlyNac glycosylation, which has been demonstrated to cause similar shift in protein size [200]. Comparatively, five and fifteen O-Glycosylation sites were predicted in Oct-4 and Sox-2 using this software, however no shift in protein size was detected in Sox-2 and the 3-5 kDa shift observed in Oct-4 could be due to phosphorylation or O-glycosylation as previously reported.

Given that this type of glycosylation is highly dynamic and has been shown to be recipricol with phosphorylation in the control of a number of proteins including c-Myc, these proteins could conceivably be in a unmodified, phosphorylated or glycosylated state. In future it would be useful to test for O-GlcNac modification by Western blot. Antibodies are available for this however appropriate controls

such as treatment with specific inhibitors to prevent addition/removal of the O-GlcNAc, resulting in elevated/inhibited O-GlcNac levels are needed [205].

We were unable to reprogram from a starting population of 1 million cells despite generating many colonies from the same cell line and passage number using the Sendai virus control. This suggests that if our HSV-1 amplicons do work then they have an efficiency of <0.0001% compared with ~0.02% for lenti virus [17], 0.001% for protein [112] and 0.0003% for episomal plasmids [94]. We observed a number of small granulated colonies suggesting that our amplicon vectors are inducing morphological changes, however, given the extremely low estimated efficiency we hypothesise that four genes alone may not be sufficient to fully reprogram the fibroblasts. Other low efficiency systems such as the episomal vectors by J. Thomson required additional genes such as Lin-28 and Nanog for successful generation of colonies. Given the similarity of episomal vectors with our reprogramming vectors we hypothesise that additional reprogramming factors would also be needed for HSV-1 amplicons.

Chapter 4 – Improvement of HSV-1 amplicon reprogramming vectors

4.1 Introduction

In Chapter 3 I described the development and characterisation of an HSV-1 amplicon reprogramming vector (pHGCX+SOKM+EBNA+TK+TetO2). The vector was able to generate small colony like structures, however these were morphologically distinct from fully reprogrammed iPS colonies. Whereas fully reprogrammed iPS cells have small tightly packed cells, a defined colony edge and rapid growth rate, the HSV-1 colonies were granular in appearance and senesced shortly after emerging.

Additionally, I estimated the reprogramming efficiency of the pHGCX+SOKM+EBNA+TK+TetO2 amplicon, based on the starting population number of cells, to be less than one in a million. Together these observations suggested that although the pHGCX+SOKM+EBNA+TK+TetO2 amplicon was capable of generating partially reprogrammed colonies, reprogramming efficiency was extremely low. We hypothesised that extra transcription factors would be needed to drive complete reprogramming and improve HSV-1 amplicon reprogramming efficiency.

When developing the EBNA-1 plasmid episomal vectors J. Thomson and colleagues were unable to generate iPS cells using their original lentiviral reprogramming factor combination (OCT-4, SOX-2, LIN28 and NANOG) [17]. To improve the reprogramming efficiency of the EBNA-1 vectors additional

transcription factors were optimised using the existing lentiviral vectors. The authors discovered that C-MYC and KLF-4 in addition to OCT-4, SOX-2, NANOG and LIN-28 increased lentiviral reprogramming efficiency by 100 fold.

This combination was repeated in their EBNA-1 plasmid episomal vectors however the authors were unable to generate iPS colonies. This was overcome by addition of the p53 inhibitor SV40LT, allowing the successful generation of iPS colonies using EBNA-1 vectors [94]. Using this set of transcription factors the same group then tested different vector combinations to find the optimal transcription factor ratios. All successful vector combinations had a relative ratio of 2x OCT-4 and SOX-2 compared to other factors. This was concurrent with other reports in the literature that comparatively high Oct-4 levels were needed for successful reprogramming[206].

In 2009 M. Sadelain and colleagues investigated the effect of relative reprogramming factor stoichiometry on reprogramming efficiency. Using a combination of fluorescence microscopy and flow cytometry, the authors found that Oct-4 levels were critical for enhancing efficiency in comparison to any of the other reprogramming factors. Whereas increasing Sox-2, C-Myc and Klf-4 decreased iPS efficiency by more than 5 fold, elevating Oct-4 increased the efficiency by 1.5 fold. Conversely decreasing Sox-2, Klf-4 and C-Myc levels had no effect on reprogramming efficiency whereas decreasing Oct-4 was severely detrimental. In addition, the relative increase of Oct-4 was critical as although a 3-fold increase enhanced reprogramming, higher relative ratios of 9-fold were detrimental[206].

The finding was complemented by a publication by T. Canz and colleagues in 2011, which investigated the effect of reprogramming factor stoichiometry on reprogramming efficiencies, the proportion of fully reprogrammed colonies and differentiation capabilities. Using similar experimental methods the authors confirmed that a high Oct-4 ratio generated higher numbers of alkaline phosphatase positive colonies. A higher proportion of cells stained positive for the pluripotency marker SSEA1 (77%) when generated with high Oct 4 ratio in comparison to lines with higher Sox-2 and Klf-4 ratios (20%). In addition they investigated the quality of iPS lines obtained and found that although lines high in Sox-2 and Klf-4 expressed substandard levels of endogenous Oct-4 and Sox-2, their differentiation capabilities were not compromised [199].

Furthermore R. Jaenisch and colleagues compared the epigenetic status of iPS cells derived from two different transgenic systems and their ability to generate "all-IPSC" chimeric mice. The authors directly compared iPS derived from a polycistronic 2A system expressing Oct-4, Sox-2, Klf-4 and C-Myc (OSKM) in equimolar quantities with a polycistronic 2A/internal ribosomal extry site (IRES) system expressing high levels of Oct-4 and Klf-4 and lower levels of Sox-2 and C-Myc (OKsm). The ability of iPS cells to generate "all-IPSC" mice was compromised when reprogrammed using the OKSM system compared with OKsm[207].

The IRES system employed by these vectors operate by a different mechanism to 2A peptides. Initiation of translation of eukaryotic mRNA is largely dependent on the 7-methyl guanosine triphosphate cap which binds to the cap binding complex (eIF4F) which in turn recruits other initiating factors, RNA helicase and the 40S ribosomal unit. The complex then tracks along the mRNA until the first AUG initiation codon is recognised, at which point a 60S ribosome subunit joins the complex to make an elongation competent ribosome, as reviewed by A. Komar in 2011 [208]. Many viral mRNAs such as picornaviral mRNA lack the conventional 7-methyl guanosine triphosphate cap and contain unusually long 5' untranslated regions encoding several AUG initiation codons. The mechanism of translation in these viral mRNAs was discovered by several studies in the late 1980's to be due to an internal ribosome entry site (IRES) mRNA sequence located within the 5' UTR [209, 210].

In order to address whether picornaviruses inititiate translation of mRNA by a mechanism independent of 5' cap initiation, a bicistronic cassette of two transgenes separated by a truncated 5' UTR was constructed and characterized [209]. Translation of both cistrons was observed and analysis of translation kinetics strongly indicated that translation of the second cistron was independent of the first. Serial deletions of the UTR region also identified a critical region for efficient translation. Independently, similar experiments were performed by N. Sonenberg and colleagues, who constructed a bicistronic cassette expressing thymidine kinase (TK) and chloramphenicol acetyl transferase (CAT) separated by the poliovirus UTR mRNA sequence. Deletion studies also identified the critical region of the IRES which was confirmed by the

insertion of Xba I linkers immediately following this region, which caused a hairpin structure, effectively inhibiting translation [210]. IRES have since been discovered in at least 39 viral mRNAs and 85 cellular mRNAs. The sequences are diverse and viral IRES can be subdivided into 4 groups, 2 of which are known to directly bind the 40S ribosomal subunit, the other 2 bind via other initiating factors, as reviewed by J. Kieft in 2008 [211].

The advantage of IRES sequences over 2A peptides are that they do not give rise to fusion proteins. However the main disadvantage is that expression between the cistrons is not equivalent and often the proteins proceeding the IRES have a lower level of expression. This could be considered an advantage if, like in the case of our reprogramming factors, a relatively higher expression was desired of the protein preceeding the IRES. Several recent studies have directly compared IRES and 2A linkers to discern differences in expression levels and efficiency [212, 213]. The first group analysed mouse knock-in lines expressing EGFP preceded by SOX9-IRES/F2A or Bagpx1-IRES/F2A. Expression of EGFP in F2A constructs was significantly higher than in the IRES constructs by 6 fold in Sox9 constructs and 2 fold in Bagpx1 constructs. Despite the addition of a GSG linker that was previously reported as having 100% cleavage, the observed cleavage efficiency in both the Sox9 and Bagpx1 constructs were 42.2% and 49.4% respectively. In addition, the RAKR sequence which cleaves off the residual 2A sequence proved to be ineffective in this system as the Sox9-2A and Bagpx1-2A fusion proteins were detectable by Western blot [212].

A later report compared three different IRES and 2A vectors expressing RFP linked to GFP were analysed by fluorescence and WB in 3 transfected cells lines (HEK 293, M3 and HT 1080). Two different IRES linkers were compared i) IRES-2 which closely resembles the WT IRES sites which contained two modifications shown to improve IRES activity and ii) IRES*att* which is a shortened version which lacks the native initiation codon and was expected to exhibit lower levels of expression. These IRES sites were compared to a porcine teschovirus 2A peptide, which contained several modifications to improve cleavage efficiency. The P2A vector yielded higher expression of both transcripts in all three cells lines in comparison to the IRES vectors and contrary to the report by T. Lufkin and colleagues [212] had a high cleavage efficiency of 99% [213].

Based on these publications, we decided to modify our existing reprogramming vector to express an additional copy of Oct-4. In addition due to the similarity of our system with the Thomson EBNA-1 reprogramming vectors, we designed a second HSV-1 amplicon-reprogramming vector, which would express the human factors OCT-4, SOX-2 LIN-28 and NANOG using two IRES-2 linkers. The use of an IRES instead of a 2A peptide would enable a relatively higher expression level of OCT-4 in comparison to the other reprogramming factors. We decided to avoid the use of the SV40LT due to it being a known proto-oncogene and its role in p53 suppression. Together these vectors provide a relative factor expression of 3x Oct-4, 2x Sox-2 and 1x (Klf-4, C-Myc, LIN-28 and NANOG). This is consistent with the factor ratios that proved most efficient by J. Thomson and colleagues with the exception of higher Oct-4 levels and the omission of the SV40LT gene.

4.2 Vector construction

For reference all the vectors used in this chapter, including information on the type of vector, the transcription factors carried and their species origin, the promoter driving the transcription factors and presence of the EBNA-1/oriP and thymidine kinase cassettes are presented in Table 1.

Vectors used in Chapter 4

Vector name	Type of vector	Promoter	Factors	EBNA	TK	Size	Constructed by
pHGCX	HSV-1 amplcion	pCMV	no	no	no	6.7 Kb	R. Wade-Martins
pEP4 EO2S EN2L	Episomal vector	EF1A	human OSNL	yes	no	15.4 Kb	J. Thomson
pHGCX+EBNA+TetO2	HSV-1 amplicon	pCMVTetO2	no	yes	yes	13.3 Kb	A. Popplestone
pHGCX+SOKM+EBNA+TK+TetO2	HSV-1 amplicon	pCMVTetO2	mouse SOKM	yes	yes	20.1 Kb	A. Popplestone
pHGCX+SOKMO+EBNA+TK+TetO2	HSV-1 amplicon	pCMVTetO2	mouse SOKMO	yes	yes	21.3 Kb	A. Popplestone
pHGCX+OSNL+EBNA+TK+TetO2	HSV-1 amplicon	pCMVTetO2/pEF1a	human OSNL	yes	yes	22.7 Kb	A. Popplestone

Table 1 – Vectors used and constructed in chapter 4. The table indicates the type of vector, promoter used, species of factor and factors carried, presence of EBNA-1/oriP and TK elements, Size (Kb) and who constructed the vector. SOKMO= Sox-2, Oct-4, Klf-4, C-Myc and Oct-4 mouse reprogramming factors. OSNL= OCT-4, SOX-2, NANOG and LIN28 human reprogramming factors.

We modified the existing pHGCX+SOKM+EBNA+TK+TetO2 vector to express an additional copy of mouse Oct-4 at the end of the polycistronic SOKM cassette, generating the vector pHGCX+SOKMO+EBNA+TK+tetO2. To construct the vector we amplified the P2A sequence followed by Oct-4 from the existing pHGCX+SOKM vector by high fidelity PCR. Both primers contained the *Bst BI* restriction site in order to clone the P2A-Oct-4 fragment into the *Bst BI* site near the 3' end of the C-Myc gene.

The left hand primer was designed to complement the last eighteen bases of the C-Myc gene, with the exception of the TAA stop site, followed by a twenty-four base sequence complementary to the P2A. The right hand primer contained the

reverse sequence for Oct-4 followed by the TAA stop site (Table 2). Together these primers amplified the P2A-Oct sequence, flanked by the 3' C-Myc sequences and *Bst BI* restriction sites.

Primer	Sequence	key
Myc-2A F	cttcgaaactctggtgcagctagcggcagcggcgccacaaac	Bst BI site C-Myc end P2A sequence
Oct4 R	Gcgccgttcgaattagtttgaatgcatgggagagcccagagcagtgacggg	Bst BI site TAA STOP Oct-4 reverse

Table 2 – Primers designed to amplify the P2A-Oct-4 sequence from the pHGCX+SOKM+EBNA+TK+TetO2 vector. The forward and reverse primers for cloning Oct-4 from pHGCX+SOKM vector are shown. Sequences are colour coded for which region they are complementary to. The key for these regions are detailed in the key column on the right hand column of the table. The Myc-P2A forward primer is a long primer, which is complementary to the P2A sequence preceding the Oct-4 in the pHGCX+SOKM vector. The primers include a *Bst BI* restriction site and a region complementary to the distal C-Myc sequence. The Oct-4 reverse primer binds to the reverse Oct-4 sequence and includes a *Bst BI* restriction site and TAA stop site.

Next the PCR fragment was purified by column purification and digested with *Bst BI*. The vector was also digested with *Bst BI*, column purified and treated with calf intestinal phosphatase (CIP) to remove phosphates from the 5' end of the DNA fragment to prevent self-ligation. The linearised vector and digested PCR product were then ligated together alongside appropriate controls to generate a ligation mixture containing the pHGCX+SOKMO+EBNA+TK+TetO2 vector (Figure 1).

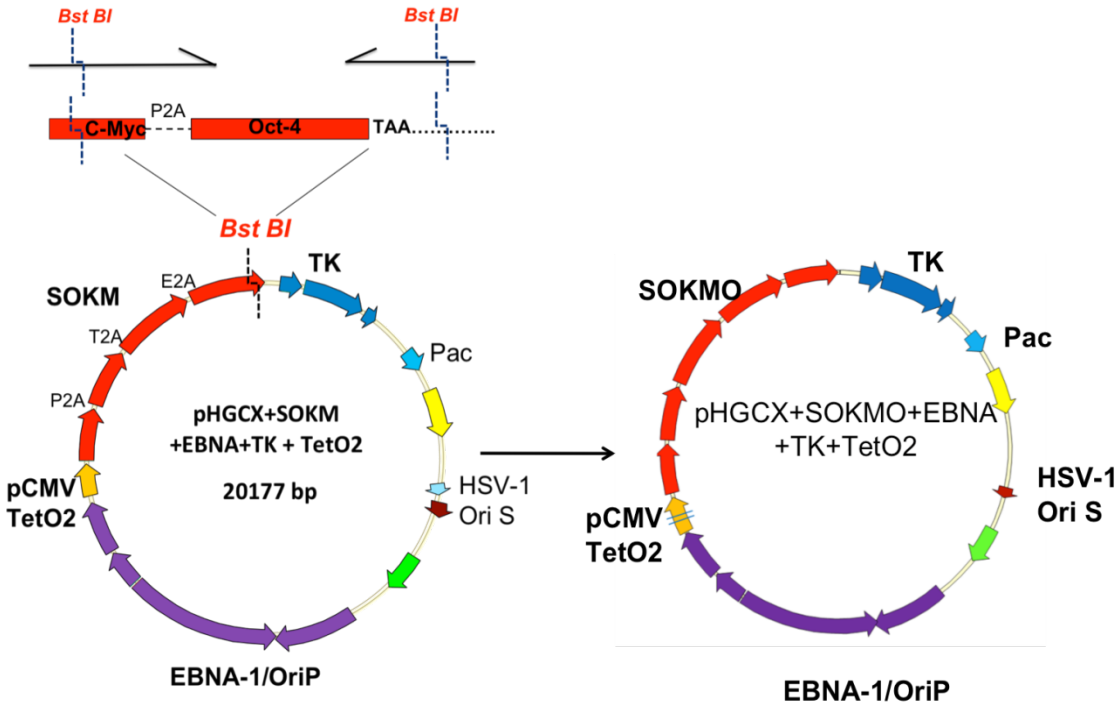


Figure 1- Vector construction of pHGCX+SOKMO+EBNA+TK+TetO2 by PCR, digest and ligation. Oct-4 was amplified from the pHGCX+SOKM vector using PCR primers engineered to include the *Bst BI* restriction site, the P2A sequence, a TAA stop site and the 5' end of C-Myc. The PCR product and pHGCX+SOKM+EBNA+TK+TetO2 vector were digested with *Bst BI* and ligated together to generate the pHGCX+SOKMO+EBNA+TK+TetO2 vector.

A second HSV-1 amplicon reprogramming vector was constructed containing the human OCT-4, SOX-2, NANOG and LIN-28 genes. First the SOKM cassette was removed from the existing pHGCX+SOKM+EBNA+TK+TetO2 vector using the restriction enzymes *Afl II* and *Xba I,* leaving the CMVTetO2 promoter intact. Next we digested the OCT-4-IRES-SOX-2-polyA cassette and pI/Ea NANOG-IRES-LIN-28-polyA cassette from the pEP4EO2SEN2L vector using the restriction enzymes *Spe I* and *Eco RV*. The vector and insert were purified and ligated to generate the pHGCX+OSNL+EBNA+TK+TetO2 vector (Figure 2). A new control vector pHGCX+EBNA+TetO2 was made in parallel by digesting SOKM from the pHGCX+SOKM+EBNA+TetO2 vector and religating without an insert.

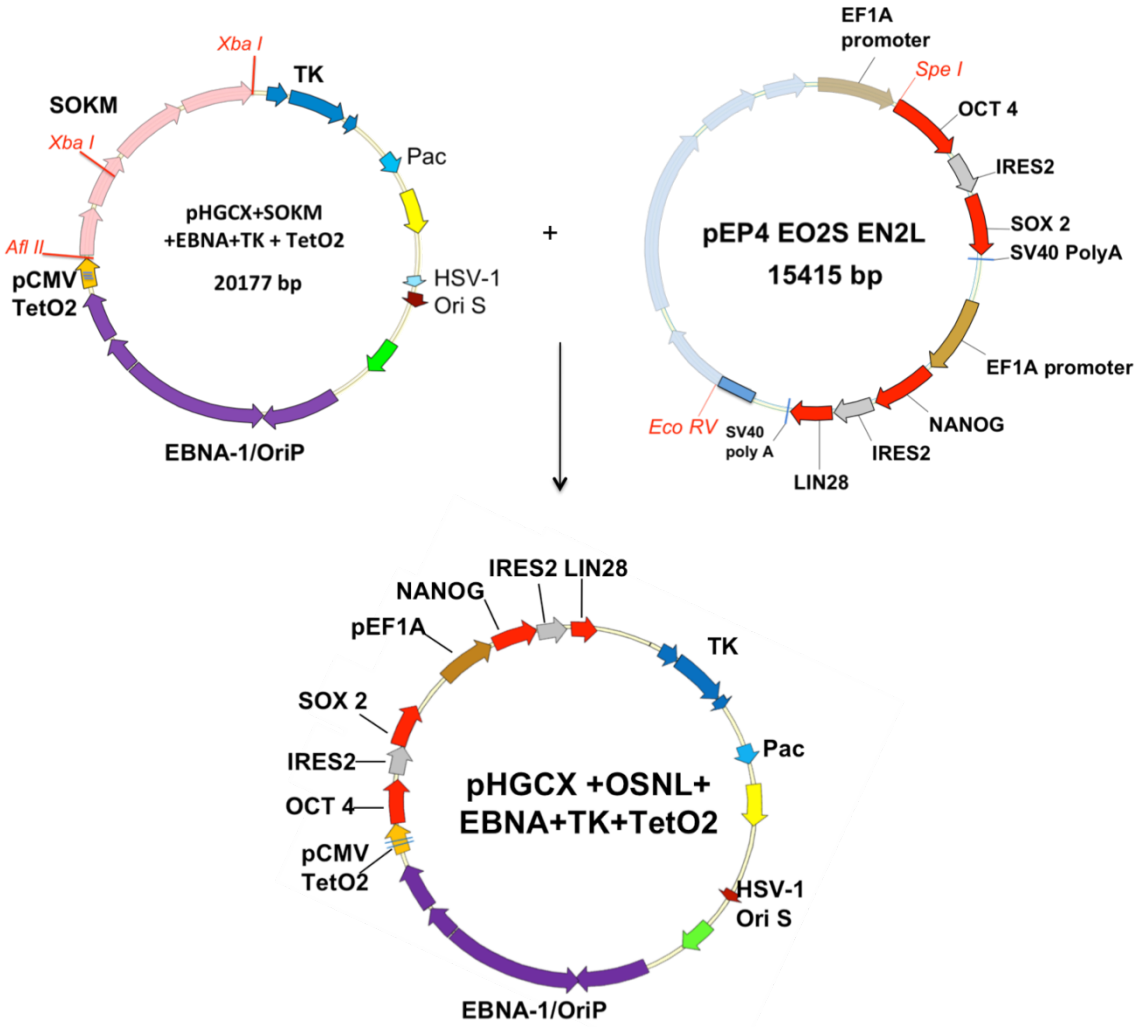


Figure 2- Vector construction of pHGCX+OSNL+EBNA+TK+TetO2 by restriction digest and ligation. The OSNL insert was digested out from the PEP4-EO2S-EN2L vector by *Spe I* and *Eco RV* restriction enzymes and ligated into the pHGCX+SOKM+EBNA+TK+TetO2 vector at the *Afl II* and *Xba I* site, replacing the SOKM cassette.

4.3 Vector construction validation

Ligation reactions included vector only and insert only controls in order to check for background ligation products. A fairly high frequency of background ligation products was observed therefore the bacterial colonies were screened by colony PCR for the correct ligation products followed by restriction digests to confirm the insert and orientation were correct. The *Bam HI, Not I* double digest and

corresponding plasmid map of pHGCX+SOKMO+EBNA+TK+tetO2 vector is shown in Figure 3A. The *Bam HI, Mlu I* double digest and corresponding plasmid map of pHGCX+OSNL+EBNA+TK+TetO2 is shown in Figure 3B.

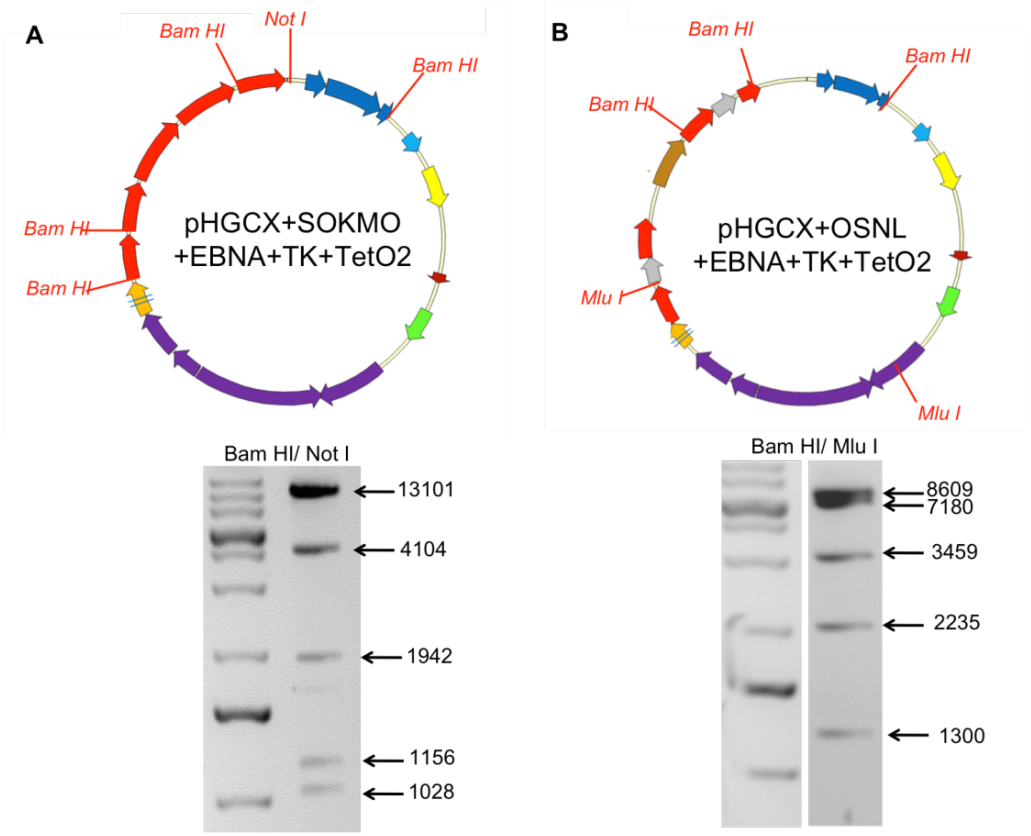


Figure 3 – Restriction enzyme digest analysis and corresponding plasmid maps of pHGCX+SOKMO+EBNA+TK+TetO2 and pHGCX+OSNL+EBNA+TK+TetO2 A) pHGCX+SOKMO+EBNA+TK+TetO2-plasmid maps indicating where *Bam HI, Not I* restriction enzymes cut the vector. Gel Electroporation of *Bam HI, Not I* digest products(1028, 1156, 1942, 4104, 13101). **B)** pHGCX+OSNL+EBNA+TK+TetO2 – plasmid maps indicating where *Bam HI, Mlu I* restriction enzymes cut the vector. Gel Electroporation of *Bam HI, Mlu I* digest products (1300, 2235, 3459, 7180, 8609)

4.4 Vector characterisation

To confirm functionality of the additional reprogramming factors MRC5 primary fibroblasts were transfected with pHGCX+SOKMO+EBNA+TK+TetO2 and pHGCX+OSNL+EBNA+TK+TetO2. After 48 hours the cells were harvested for RNA extraction and RT-PCR was performed. In the

pHGCX+SOKMO+EBNA+TK+TetO2 vector gene expression was confirmed using primers flanking all four of the factor junctions (Sox-2-Oct-4, Oct-4-Klf-4, Klf-4-c-Myc, c-Myc-Oct-4). Transduction with pHGCX+EBNA+TK+TetO2 vector was included as a negative control as well as untransduced cells.

In the pHGCX+OSNL+EBNA+TK+TetO2 vector OCT-4 and SOX-2 expression was confirmed using primers flanking the OCT-4 to SOX-2 junction. NANOG and LIN-28 expression were confirmed using primers flanking the NANOG to LIN-28 junctions. A non-reverse transcriptase (RT-) control was included for all samples to ensure there was no plasmid DNA contamination (Figure 4).

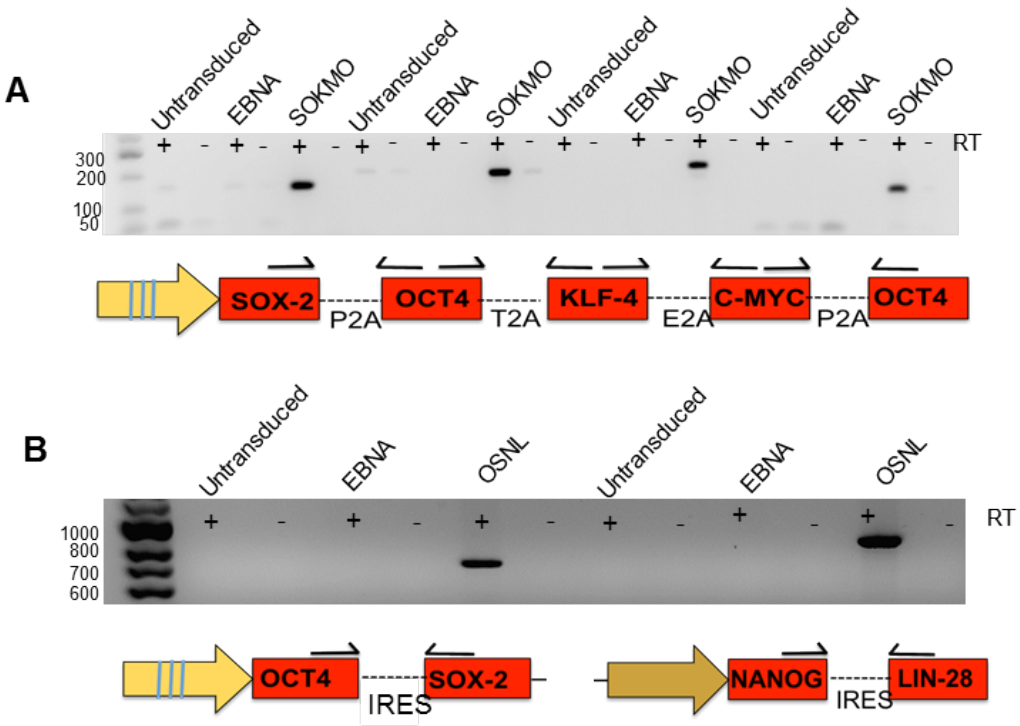


Figure 4 – Reprogramming factor expression confirmation in A)pHGCX+SOKMO+EBNA+TK+TetO2 and B)pHGCX+OSNL+EBNA+Tk+TetO2 – **A)** Confirmation of factor RNA expression in SOKMO transduced MRC5-V2 cells, all four junctions; Sox-2-Oct-4 (151 bp), Oct-4-Klf-4 (200bp), Klf4-C-Myc (223 bp) and C-Myc-Oct-4 (136 bp) were amplified by RT-PCR using primers flanking each junction. **B)** Confirmation of OCT-4, SOX-2, NANOG and LIN-28 expression in OSNL transduced MRC5-V2 cells. Assayed by RT-PCR using primers flanking the OCT-4 to SOX-2 (709 bp) and NANOG to LIN-28 (846 bp) junctions. No expression was detected in the negative control (untransduced or EBNA) non-RT control (-) for any of the primer pairs. The primer binding sites are shown on the polycistronic cassette schematics (black arrows).

4.5 Cellular reprogramming experiments

Reprogramming experiments were performed on the control donor fibroblast line JRO-53 as described in Chapter 3. One million JRO-53 fibroblasts per well were seeded on day one into empty wells of a 6 well plate. The following day the cells were double transduced with pHGCX+SOKMO+EBNA+TK+TetO2 and pHGCX+OSNL+EBNA+TK+TetO2 at a combined MOI of 20. In parallel the fibroblasts were also transduced with the negative control amplicon pHGCX+EBNA+TetO2 or the positive control Sendai virus to check the JRO-83 fibroblast line was viable for reprogramming.

After 48 hours the fibroblasts were seeded onto MEFs and as described previously, partially reprogrammed colonies began to emerge 12 days into the reprogramming protocol in the SOKMO OSNL transduced cultures. Contrary to previous observations the colonies also expressed EGFP and no colonies were observed in the negative control cultures (Figure 5). The colonies were morphologically distinct from iPS colonies and over the following two weeks the colonies did not increase in size.

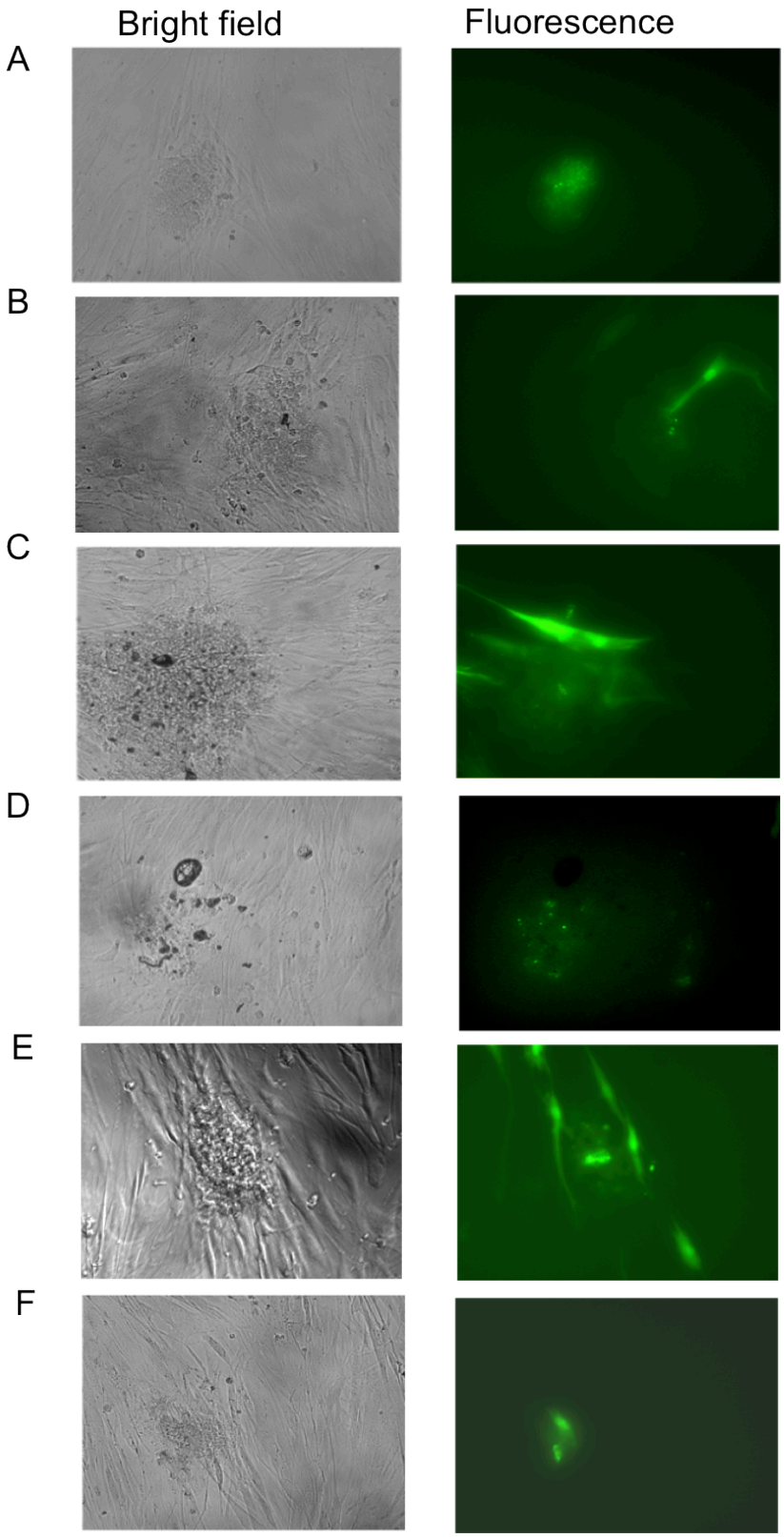


Figure 5 – Morphological analysis of partially reprogrammed colonies. Bright field and fluorescent images of observed EGFP+ colonies observed during reprogramming of JRO-53 fibroblasts (10x objective). Colonies are distinct from fully reprogrammed colonies and have a granular appearance.

I manually dissected eight of the SOKMO OSNL transduced colonies and transferred them together onto a single well on top of fresh irradiated MEFs to attempt colony expansion. We manually dissected the same number of Sendai virus colonies and transferred them into a second well to provide a positive control for the procedure and RT-PCR analyses. We also trypsinised pHGCX+EBNA+TetO2 transduced cells and transferred them onto MEFs in parallel to provide a negative control for RT-PCR analysis.

The SOKMO OSNL partially reprogrammed colonies failed to expand on fresh irradiated MEFs whereas the positive control Sendai virus colonies successfully adhered to the MEFs and grew rapidly in size. In order to validate the hypothesis that the SOKMO OSNL colonies were partially reprogrammed we extracted RNA from each of the wells and assessed pluripotency markers by RT-PCR.

We chose pluripotency markers based on several publications, which specifically analysed intermediates of reprogramming and insufficient markers of pluripotency as they were more likely to be expressed in partially reprogrammed colonies [16, 42, 214]. A report by T. Schlaeger and colleagues in 2009 used live cell imaging to distinguish fully and partially reprogrammed cell populations. The authors determined that expression of growth and differentiation factor 3 (GDF3), telomerase reverse transcriptase (hTERT), NANOG and alkaline phosphastase were insufficient as pluripotency markers on their own. Conversely reduced expression 1 (REX-1), DNA (cytosine-5-)-methyltransferase 3 beta (DNMTB3) and tumor related antigen -1-60 (TRA-1-60) distinguishes fully reprogrammed colonies [42].

Further reprogramming factors were chosen based on another report by K. Hochedlinger and colleagues, who employed a cell sorting strategy to investigate reprogramming intermediates and determined gene expression profiles. E-cadherin was confirmed to be expressed early in reprogramming followed by a steady increase in Alkaline phosphastase and Fbx15 and finally Cyclin B1, endogenous OCT-4 and SOX-2 transcripts were detectable later in reprogramming [215].

We also chose pluripotency factors based on the factors screened in early publication as robust and specific pluripotency markers were not established until later. Pluripotency markers such as; fibroblast growth factor 4 (FGF4), embryonic stem cell specific gene 1 (ESG1), developmental pluripotency associated gene 2 (DPPA2), DPPA4, endogenous Oct-4, endogenous Sox-2 and endogenous Nanog were investigated in early reprogramming publications [16].

Based on the literature findings we chose to analyse NANOG, hTERT, GDF3 and alkaline phosphatase as they were likely to be expressed in partially reprogrammed populations. We also chose to investigate whether endogenous SOX-2, endogenous OCT-4, Cyclin B1, DPPA2, DPPA4, FGF4, ESG1 and E-Cadherin were upregulated as these were possible candidates for partially reprogrammed markers. We did not expect to see expression of DNMT3B and Rex-1, however we included them as negative controls for the partial reprogramming hypothesis. Primers sequences and sources are shown in Table 3.

Gene name	Forward sequence	Reverse sequence	reference
hTERT	TGTGCACCAACATCTACAAG	GCGTTCTTGGCTTTCAGGAT	Chan et al
REX1	TCGCTGAGCTGAAACAAATG	CCCTTCTTGAAGGTTTACAC	Chan et al
GDF3	AAATGTTTGTGTTGCGGTCA	TCTGGCACAGGTGTCTTCAG	Chan et al
OCT 4 END	CCTCACTTCACTGCACTGTA	CAGGTTTTCTTTCCCTAGCT	Chan et al
SOX 2 END	CCCAGCAGACTTCACATGT	CCTCCCATTTCCCTCGTTTT	Chan et al
DNMT3B	ATAAGTCGAAGGTGCGTCGT	GGCAACATCTGAAGCCATTT	Chan et al
FGF4	CTACAACGCCTACGAGTCCTACA	GTTGCACCAGAAAAGTCAGAGTTG	Takahashi et al
ESG1	ATATCCCGCCGTGGGTGAAAGTTC	ACTCAGCCATGGACTGGAGCATCC	Takahashi et al
DPPA2	CCGTCCCCGCAATCTCCTTCCATC	ATGATGCCAACATGGCTCCCGGTG	Takahashi et al
DPPA4	GGAGCCGCCTGCCCTGGAAAATTC	TTTTTCCTGATATTCTATTCCCAT	Takahashi et al
E-cadherin	ACGAAGACACAAGAGAGATTGG	CGATGATGGAGATGTTCATGG	Tang et al
Cyclin B1	CGGGAAGTCACTGGAAACAT	AAACATGGCAGTGACACCAA	Gao et al
NANOG END	GATTTGTGGGCCTGAAGAAA	AAGTGGGTTGTTTGCCTTTG	primer 3
ALP	GGTGAACCGCAACTGGTACT	CCCACCTTGGCTGTAGTCAT	primer 3

Table 3 – List of pluripotency marker primers used in RT-PCR analysis of partially reprogrammed colonies. The table details the forward and reverse sequences and the source reference where the primer sequences were published. Primer 3 refers to the online program for primer design.

Of the fourteen genes that we tested we observed robust expression of endogenous OCT-4 and endogenous NANOG in our partially reprogrammed colonies. In addition, we also observed weaker expression of Cyclin B1, hTERT and DPPA4. No expression was observed in the remaining candidate markers or the fully reprogrammed marker controls (Figure 6).

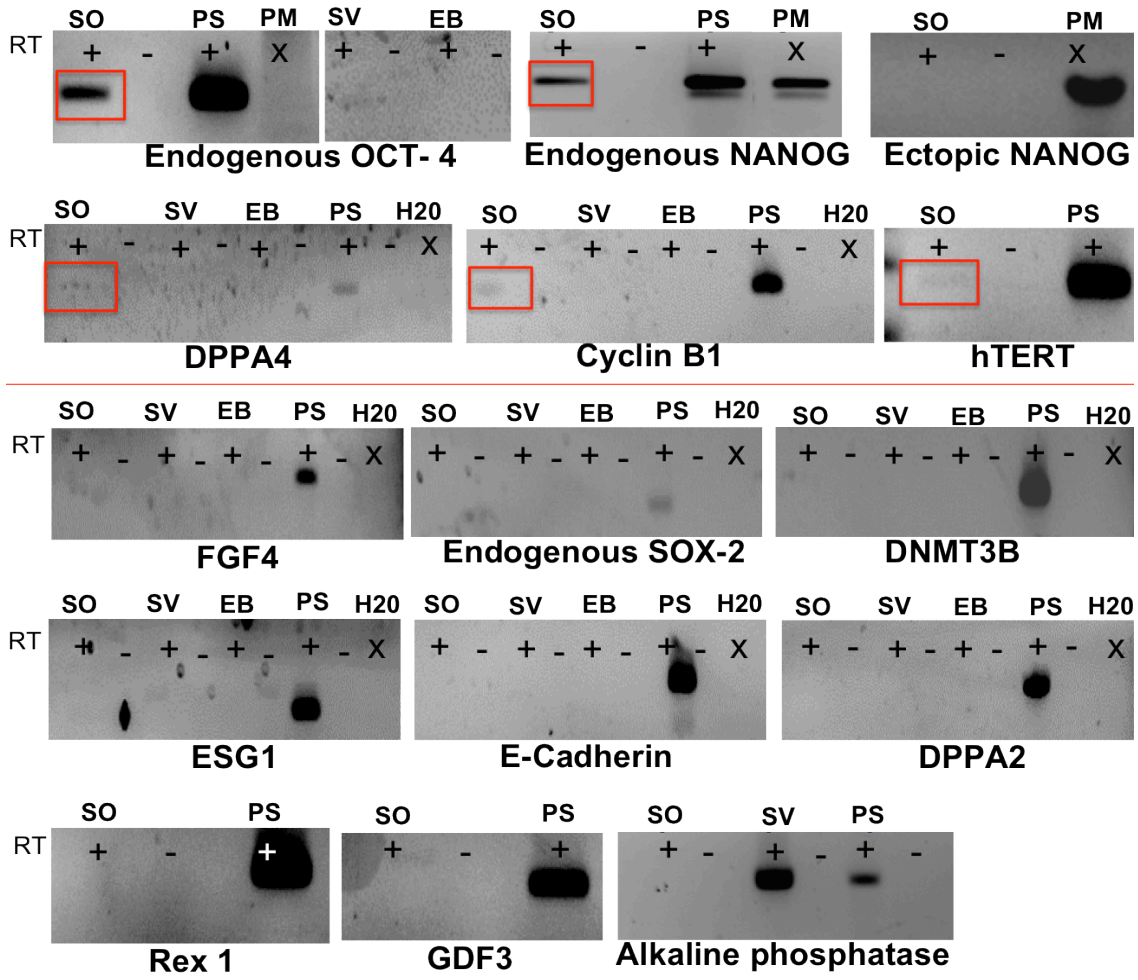


Figure 6 –RT-PCR analysis of partially reprogrammed colonies. RT-PCR analysis of known pluripotency markers. Colonies that emerged from pHGCX+SOKMO+EBNA+TK+TetO2 and pHGCX+OSNL+EBNA+TK+TetO2 (SO) transduced cells are compared with Sendai Virus (SV) colonies, a control iPS line (PS), negative control EBNA transduced cells (EB) and plasmid control (PM). Expression of five pluripotency markers (endogenous OCT-4, endogenous NANOG, DPPA4, Cyclin B1 and hTERT) was seen in SO transduced colonies.

The pHGCX+SOKMO+EBNA+TK+TetO2 and pHGCX+OSNL+EBNA+TK+TetO2 plasmids were included as negative controls to ensure the primers did not amplify the OCT-4 or NANOG transgenes from the transduced vectors. Whereas no expression was seen in OCT-4, the NANOG primers did amplify DNA from the plasmid control suggesting that expression could be exogenous.

An additional control to amplify of the NANOG to LIN-28 junction in the partially reprogrammed colonies was negative, confirming that expression of NANOG was from genomic RNA, not the vector. No Expression was seen in our non-RT controls or in the EBNA transduced control confirming that there was no genomic DNA contamination and amplification must be from cDNA.

4.6 Potential reprogramming barriers

HSV-1 reprogramming amplicons are capable of generating partially reprogrammed colonies but we did not observe any true iPS colonies, even from a starting population of one million fibroblasts. The efficiency was extremely low (< 0.0001%) and the addition of extra reprogramming factors did not improve this (0.0008% partially reprogrammed colonies < 0.0001% true iPS colonies).

We hypothesised that the HSV-1 amplicons could have inhibited the reprogramming progress by inducing a cellular response that is detrimental to cellular reprogramming. To investigate whether the HSV-1 amplicons were inhibiting the reprogramming progress we designed an experiment to assess colony numbers generated from cells transduced with Sendai virus alone or Sendai virus + HSV-1 amplicon (pHGCX+EBNA+TetO2 or pHGCX+SOKMO+EBNA+TK+TetO2 and pHGCX+OSNL+EBNA+TKL+TetO2).

Cells were seeded at a density of 50,000 cells per well into three empty wells of a 12 well plate on day one. On the second day one of the wells was left

untransduced and a second well was transduced with pHGCX+EBNA+TetO2 and a third well was double transduced with pHGCX+SOKMO+EBNA+TK+TetO2 and pHGCX+OSNL+EBNA+TK+TetO2. The media was replaced with DMEM the following morning on day three and on day four the three wells were transduced with Sendai virus and split onto irradiated MEFs the next day. Cells were fed hES media every other day and colonies were counted eight days after transfer.

Interestingly, we observed that whereas Sendai virus generated an average of 100 colonies per well over three wells, Sendai virus + EBNA generated an average of 7 colonies per well over three wells and Sendai + SOKMO OSNL did not generate any colonies over three wells, data is represented as number of colonies per 1000 cells (Figure 7). Statistical analysis by one-way Anova, Dunnett's multiple comparison test confirmed that this was a significant difference with a p. value of $p<0.0001$.

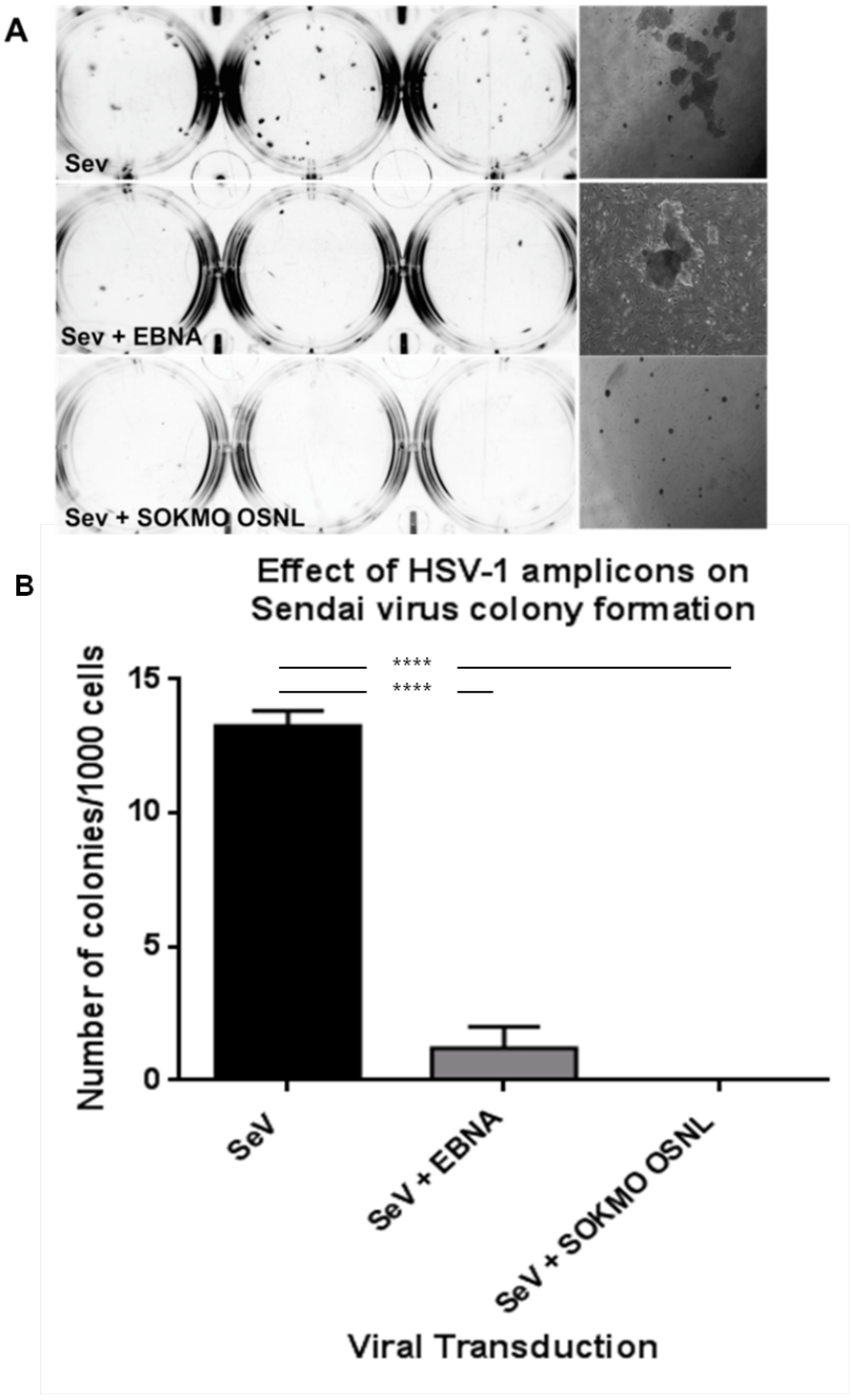


Figure 7 – Effect of HSV-1 amplicons on Sendai virus colony formation. A) 0.5x and 4x brightfield images of colony clusters seen in Sendai virus transduced fibroblasts +/- EBNA/SOKMO OSNL amplicons. **B)** Quantification of observed colonies in 3 wells per condition (Sendai virus +/- EBNA/SOKMO OSNL) data is represented as number of colonies per 1000 cells and was analysed by one-way Anova, Dunnett's multiple comparison test, **** $p<0.0001$.

This experiment was repeated an additional four times with Sendai virus compared with Sendai virus plus SOKMO OSNL and no colonies were observed in the SOKMO OSNL condition (Figure 8). A significant difference in colony formation was observed with a p. value of $p<0.0006$ when analysed by unpaired Student's *t*-test, indicating that HSV-1 amplicons inhibit Sendai virus mediated reprogramming.

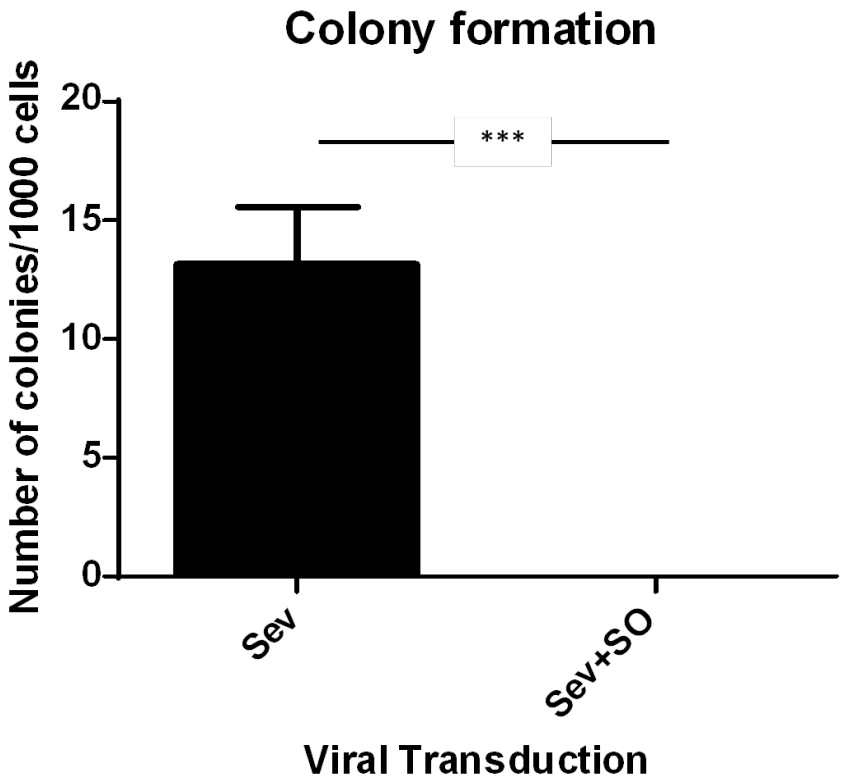


Figure 8 – Effect of HSV-1 SOKMO OSNL amplicons on Sendai virus colony formation Quantification of observed colonies in 3 wells per condition in 4 independent experiments (Sendai virus +/- SOKMO OSNL) analysed by Student's *t*-test, *** $p<0.0006$, n=4. Data is represented as number of colonies per 1000 cells.

4.6.1 Candidate reprogramming barrier genes

In order to assess the mechanism by which HSV-1 amplicons were inhibiting colony formation in Sendai virus reprogramming we harvested RNA from the colony formation assay (Sendai virus +/- EBNA or SOKMO OSNL) at two time points, two days and 12 days after transfer to MEFs.

We investigated whether the known inhibitory factors (Aurora A kinase, IP3, p53, p21 and p38) of reprogramming were upregulated at the transcript level. We also tested whether the known enhancer TLR3 was expressed. The kinases Aurora A Kinase, inositol trisphosphate 3-kinase (IP3K) and p38 were identified as potential barrier genes in reprogramming as a result of a small molecule kinase inhibitor screen [216]. The inhibition of p38, inositol trisphosphate 3-kinase, and Aurora A kinase by small molecule inhibitors and their specific knockdown by RNAi potently enhanced reprogramming efficiency and cells were able to reach a fully reprogrammed state [216]. The tumour suppressor p53 gene and its primary target gene p21 have been well documented as inhibitors of reprogramming for since 2009 and early reprogramming efforts were improved by reducing signalling to p53, or by knocking down p53 and p21 expression [95, 217, 218]. We also tested whether TLR3 was expressed in response to amplicon transduction due to a recent report that inducing its activation by lentiviral infection boosts reprogramming in protein mediated reprogramming [219].

4.6.2 RT-PCR analysis of barrier genes

To investigate whether Aurora A kinase, IP3, p53, p21, p38 or TLR3 were expressed after amplicon transduction we performed RT-PCR on samples harvested on day 12 after transfer to MEFs to see whether any of the inhibitory markers were expressed. All of the markers were detected by RT-PCR in all of our transduced samples (Sendai virus (SV), Sendai virus plus EBNA (SV+EB), Sendai virus plus pHGCX+SOKMO+EBNA+TK+TetO2 and pHGCX+OSNL+EBNA+Tk+TetO2 (SV+SO) or SO alone). We performed semi quantitative RT-PCR with 25 cycles on all genes and analysed differences in PCR band intensity in comparison to the reference gene GAPDH using Image J software. A 2.5 - 3 fold increase in p21 expression was detected between the Sendai virus and Sendai virus plus SOKMO OSNL samples (data not shown). These results promted us to investigate p21 expression and expression of it's activator p53 further.

4.6.3 Analysis of barrier genes by qRT-PCR

We analysed expression of p53 expression levels by q-PCR on cDNA samples harvested 2 days after splitting onto MEFs. The expression of p53 levels were normalised to the reference genes ACTB and GAPDH and to the geometric mean of these reference genes (Figure 9A). A significant difference was found between Sendai virus compared with; EBNA (**), SOKMO OSNL (***), Sendai virus plus EBNA (***) and Sendai virus +SOKMO OSNL (*) for p53/geomean where *$p<0.05$, ** $p<0.01$, ***$p<0.001$, as analysed by one-way Anova assay (Dunnett's multiple

comparison test). This result demonstrated that two days after transfer to MEFs p53 was upregulated at the transcript level in amplicon transduced samples.

We also analysed p21 expression levels at a later time point (12 days after transfer to MEFs) and p21 expression was upregulated in amplicon transduced samples in comparison to Sendai virus only. A significant increase was found for p21/ACTB (Sendai virus compared with SOKMO OSNL = ** $p<0.01$; Sendai virus compared with Sendai virus plus SOKMO OSNL = * $p<0.05$). This result was not significant when normalized to GAPDH or the geomean, however a clear trend in p21 upregulation is seen in the amplicon transduced samples (Figure 9B) (analysed by one-way Anova, Dunnett's multiple comparison test).

In conclusion we see a significant increase in p53 RNA expression in amplicon transduced cultures compared to Sendai virus in samples harvested two days after transfer to MEFs. This is complemented by an increase of p21 RNA expression (downstream target of p53) 12 days after transfer to MEFs when normalised to the reference gene ACTB.

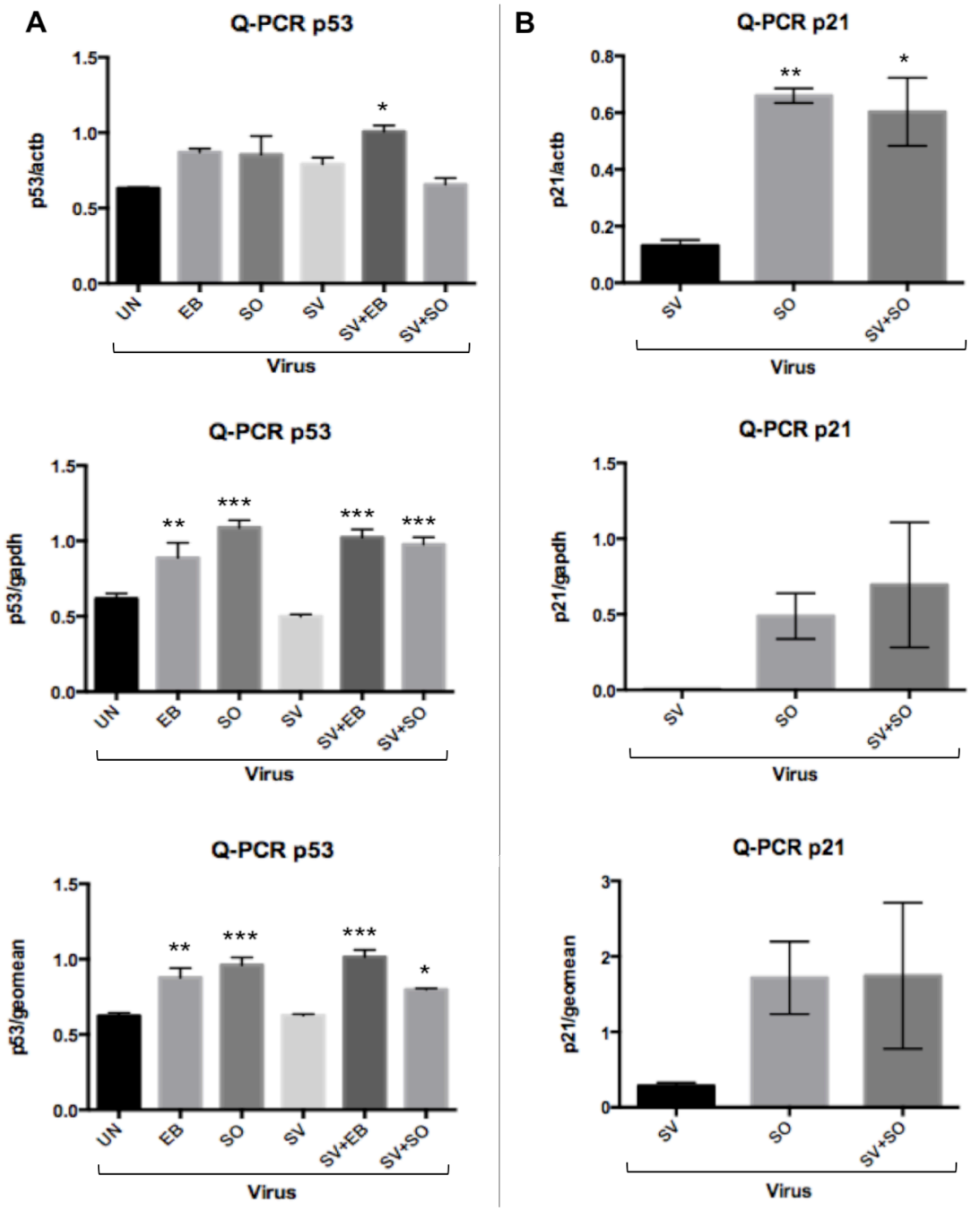


Figure 9 –Quantitative real time PCR (qPCR) analysis of cells transduced with Sendai virus +/- HSV-1 amplicon. (Sendai virus (SV), Sendai virus + EBNA (SV+EB), Sendai virus + SOKMO OSNL (SV+SO), SOKMO OSNL alone (SO), EBNA alone (EB) or untransduced) **A)**Amplification of p53 and **B)** downstream marker p21 were normalised by the reference genes ACTB, GAPDH and the geometric mean of ACTB and GAPDH. Quantifications of all samples were compared with SV in a one-way Anova, Dunnett's multiple comparison test assay where *p<0.05, ** p<0.01, ***p<0.001, experiments were performed in triplicate, n=1 for both data sets.

4.6.4 Analysis of barrier genes by Western blot

Phosphorylation of p53 at the Serine 15 residue occurs in response to DNA damage and results in increased transcriptional activity due to enhanced association with the co-activator p300 [220]. Phosphorylation at this residue prevents the degradation of p53 by inhibiting the interaction between p53 and it's negative regulator HDM2, resulting in accumulation of the protein [221]. In order to follow up our qRT-PCR results we analysed untransduced, EBNA transduced, SOKMO transduced and SeV transduced JRO53 fibroblasts (48 hours post transduction) by Western blot for total p53 and phosphorylated p53 protein expression (Figure 10A). Surprisingly, a second band was detected in the SOKMO transduced sample, which has been previously reported by M. O'Reilly and colleagues in 2005, and is thought to be due to proteolytic processing of the protein [222].

We quantified the upper bands only of p53 and phosphorylated p53 using Image J software analysis and both sets of data were normalized to quantified ACTIN. We then normalised phosphorylated Serine 15 to p53 to determine the phosphorylated/unphosphorylated ratio (Figure 10B). We observed an increase of phosphorylated p53 in the EBNA and SOKMO transduced fibroblasts compared to levels induced by Sendai virus transduction. This demonstrates that HSV-1 amplicons induce phosphorylation of the protein, leading to an accumulation of transcriptionally active p53.

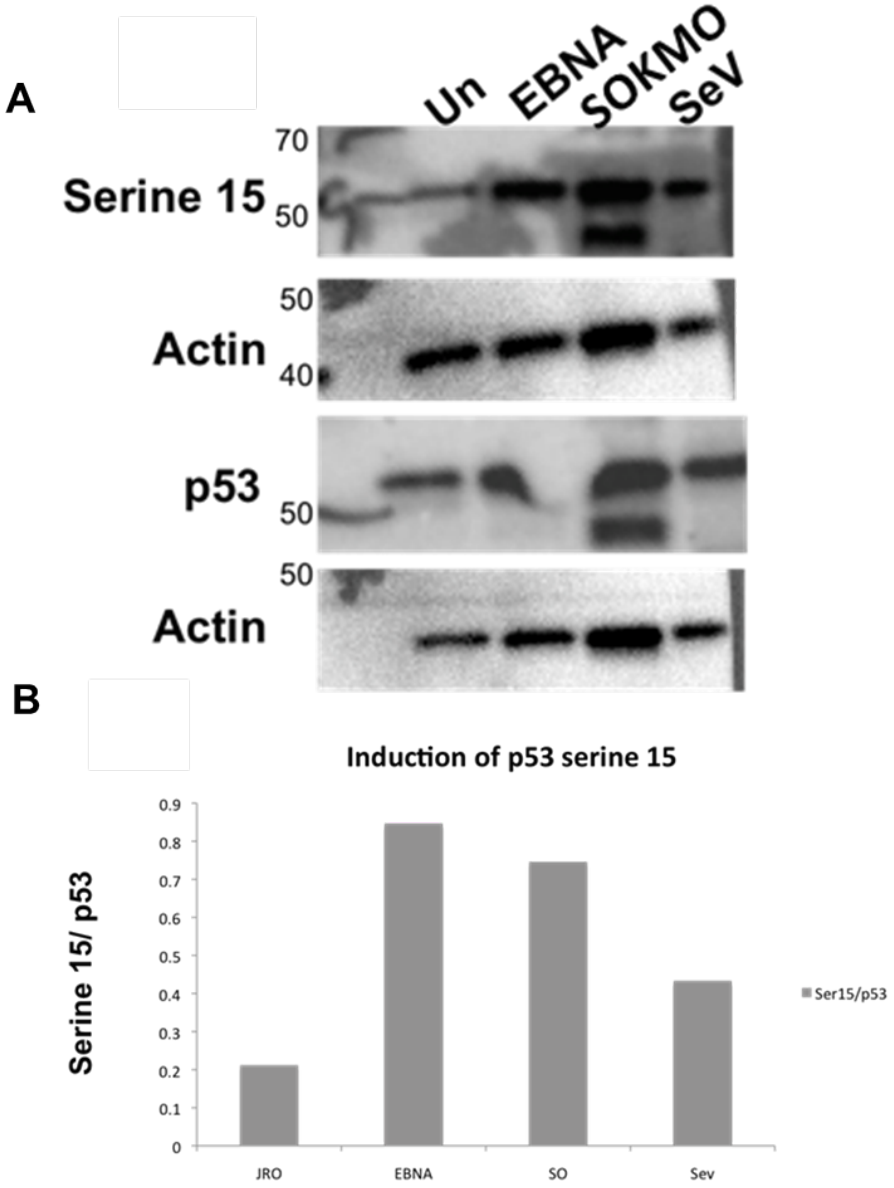


Figure 10 – Western blot analysis of phosphorylated p53 and p53.
A) untransduced, EBNA transduced, SOKMO transduced and Sendai virus transduced cells were analysed by Western blots for expression of phosphorylated p53 (serine 15) and p53 and their corresponding β actin loading controls. **B)** Quantitative analysis of Serine 15 normalised to p53, n=1. Pixel intensity was quantified on a small area of each band in order to be representative of total band intensity across all wells.

4.6.4 p53 inhibition by Pifithrin-α

To confirm whether p53 activation by phosphorylation was the cause of reprogramming inhibition we repeated the Sendai virus plus amplicon colony formation experiment in the presence of the p53 inhibitor Pifithrin-α on JRO 53 fibroblasts (passage 4). Pifithrin-α is a small molecule that inhibits the ability of p53 to activate transcriptional targets such as Cyclin D1 and p21, possibly by modulating the nuclear export/import pathway [223].

We transduced JRO 53 fibroblasts with the following conditions; untransduced, SOKMO OSNL alone, Sendai virus alone, Sendai virus + SOKMO OSNL and transferred to a MEF feeder layer the day after Sendai virus transduction. Reprogramming media plus 5 μM or 10 μM of Pifithrin-α, or equal volumes of DMSO as a negative control, was added following transfer of fibroblasts onto a MEF feeder layer at 4000 cells/ well of a 12 well plate. A significant increase $p<0.0001$ in the number of colonies in the Sendai virus control was observed upon addition of Pifithrin-α in comparison to DMSO controls (~3 fold increase). In addition, a small number of colonies were generated in the SeV + SOKMO OSNL + Pifithrin-α conditions, compared with zero colonies under DMSO conditions, however difference in colony numbers were not significant (Figure 11).

This demonstrates that Pifithrin-α is capable of enhancing reprogramming efficiency in the Sendai virus only controls and partially alleviating colony inhibition mediated by HSV-1 amplicons. Analysis of the literature shows that inhibition of p53 by Pifithrin-α is optimal when added during genotoxic stress, suggesting that we should apply the drug during amplicon transduction in order

to prevent p53 transactivation and subsequent inhibition of colony formation [223].

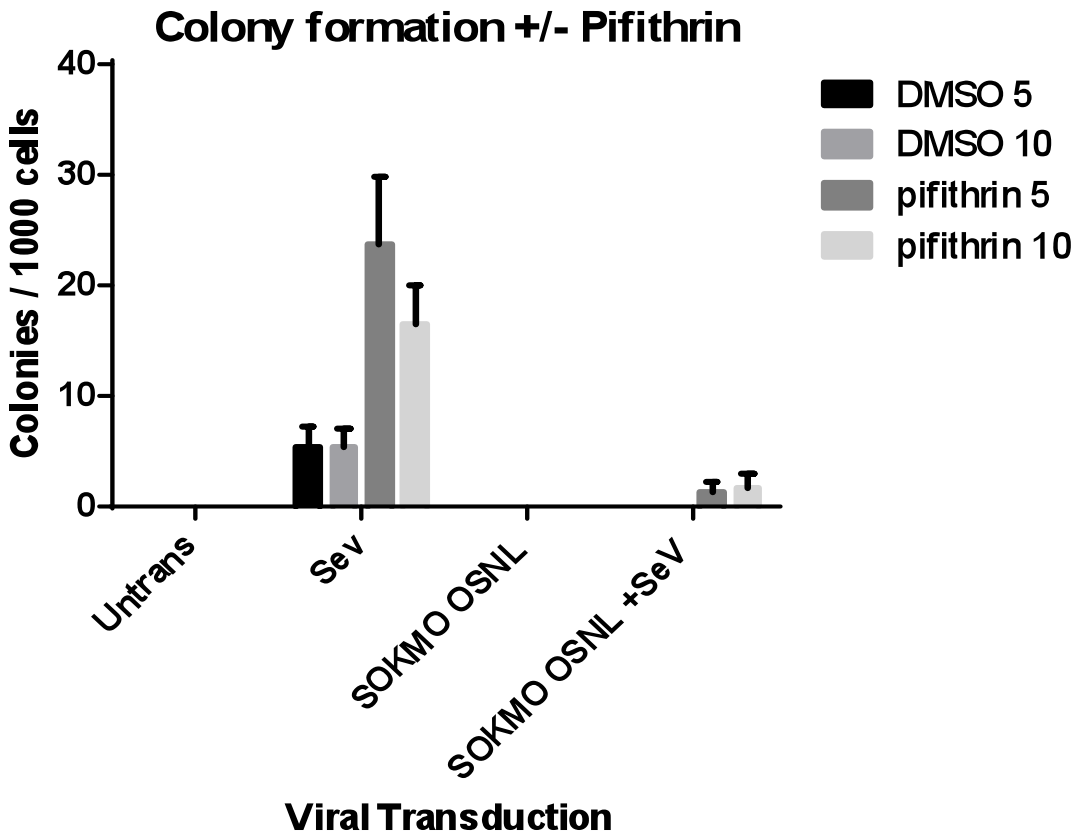


Figure 11 – Sendai virus colony formation assay in prescence of Pifithrin-α
Colony counts in the presence of 5 or 10 μM Pifithrin-α, or equal volumes of DMSO. Colony counts were performed blind by a colleague in triplicate, n=1, and are represented as /1000 cells. Pifithrin-α addition significantly increased the number of colonies in the SeV only condition compared to all other conditions(****), analysed by two way Anova, Tukey's multiple comparison test, $p<0.0001$.

We repeated the experiment three more times, performed as three independent sets of transductions, set up in parallel on JRO53 fibroblasts (n=3). This time we cultured the fibroblasts in DMEM plus 5 μM Pifithrin-α or DMEM plus an equal volume of DMSO prior to amplicon transduction. We also included an additional control of heat inactivated EBNA in order to address whether the colony

knockdown observed is triggered by components of the amplicon virion such as glycoproteins, or due to cellular debris and contaminants in the amplicon preparation that are acquired during purification and concentration of the virus. pHGCX+EBNA+TetO2 was heat inactivated at 60 °C for one hour on a heat block and assessed for EGFP expression in transduced G16.9 cells, compared with an equal volume of the same unheated amplicon preparation. Whereas robust EGFP expression was observed in the unheated amplicon transductions, transduction with heat inactivated amplicons resulted in absence of EGFP expression, Figure 12A.

The number of colonies generated in all conditions, including the SeV positive control was much lower than in previous experiments, with a high standard deviation. No significant differences were observed when analysed by one-way Anova. The passage number of the fibroblasts was high (passage 9) by the time we had grown enough cells to set up the experiment in triplicate and is the most likely cause for the low colony numbers observed. Interestingly, although no significant differences were observed between any of the transductions, under DMSO conditions the number of colonies generated in the heat inactivated EBNA condition was increased compared to non-heated transduction and generated a similar number of colonies to the Sendai virus only control (Figure 12B). This strongly suggests that the colony inhibition that we observe is induced by phospholipids and/or glycoproteins of the amplicon virion, rather than due to contaminants of the amplicon preparation.

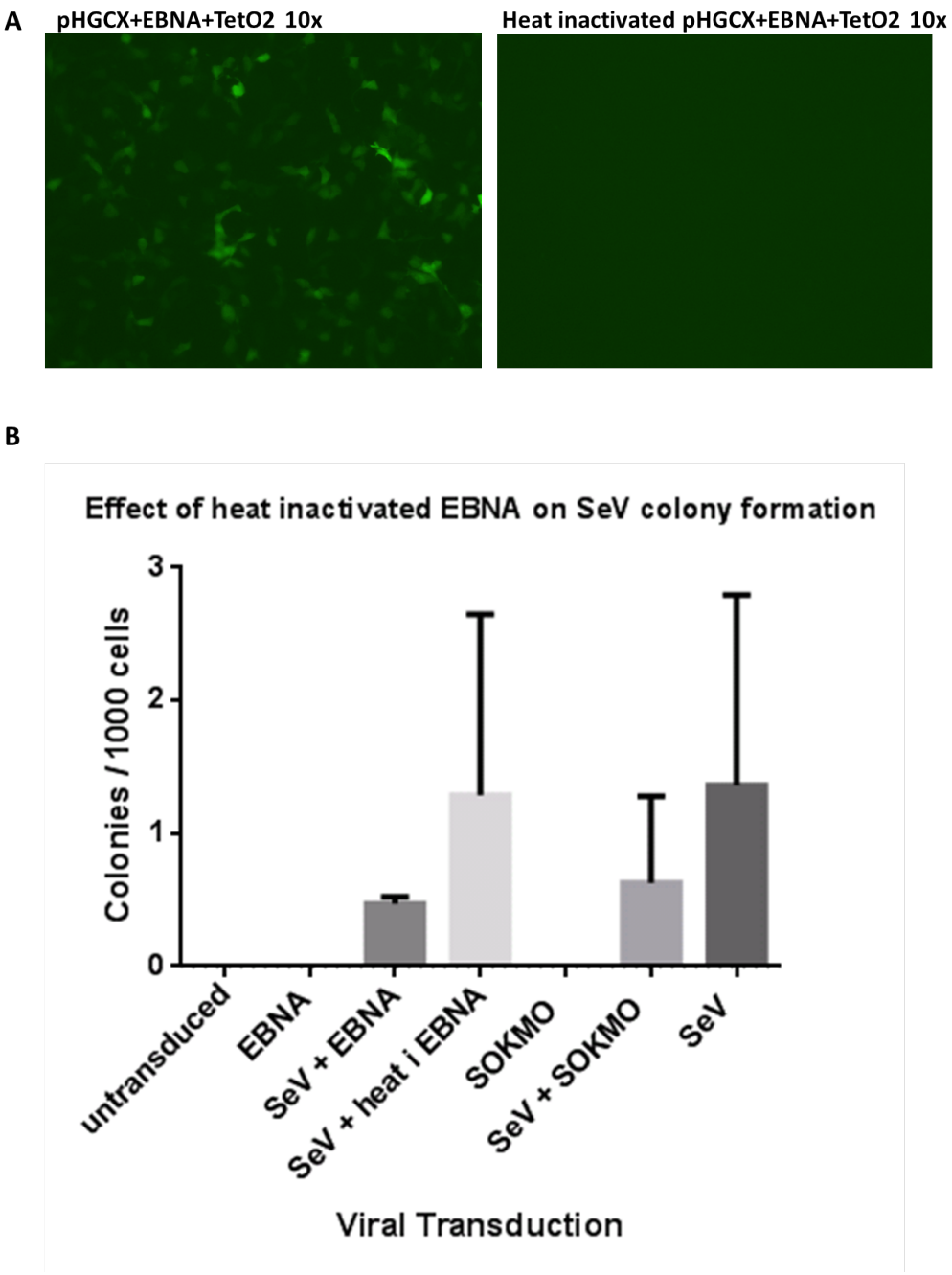


Figure 12 – Heat inactivation of HSV-1 amplicons and their effect on SeV colony formation. A) EGFP expression in G16.9 cells transduced with non-heated EBNA amplicon is shown in the left hand panel and absence of expression in transduction with an equivalent volume of heat inactivated EBNA is shown on the right. **B)** Colony formation in SeV only controls were compared with untransduced, EBNA, SOKMO, SeV + EBNA, SeV +SOKMO and SeV +EBNA heat i (heat inactivated pHGCX+EBNA+TetO2). Colony counts were performed blind by a colleague and analysed by two-way Anova, Dunnet's multiple comparison test. No significant differences were observed, n=3.

4.7 Summary and Conclusions

We successfully generated two new HSV-1 amplicon reprogramming vectors expressing a total of 3x Oct-4, 2x Sox-2, 1x (Klf-4, C-Myc, NANOG and LIN-28) to ensure optimal reprogramming factor stoichiometry. We also generated an alternative vector in parallel expressing an additional copy of Oct-4 via an EGFP-2A-Oct-4 construct. This construct was a safeguard in case the SOKMO polycistronic cassette was unable to support a fifth gene. This vector was not needed as RT-PCR confirmed expression of the final Oct-4 gene in the SOKMO vector. We also confirmed expression of the Oct-4-Sox-2 and Nanog-Lin-28 junction from our second vector pHGCX+OSNL+EBNA+TK+TetO2.

Homologous recombination in bacteria can lead to elimination of repeated sequences by rec-A independent and rec-A dependent mechanisms. Considering that our SOKMO plasmid contains two copies of the Oct-4 gene it is important to consider whether removal of the transgenes by recombination could occur. An analysis of recombination mechanisms in bacteria indicate that direct repeats over 150 bp and interspersed by long sequences are more likely to be eliminated by *rec-A* dependent recombination at a rate of 10^{-3} per generation [224]. Given our Oct-4 sequence is 1057bp in length and the repeats are interspersed by 3 kb of vector sequence, any elimination is likely to be due to a *rec-A* dependent mechanism. Hypothetically if recombination of the two copies of Oct-4 occurred in bacterial cells then the fragment containing the backbone and Sox-2-2A-Oct-4 would remain and the fragment containing Klf-4-2A-C-Myc-2A-Oct-4 would be lost as no origin of replication would be present. We performed multiple digests throughout the construction process of the SOKMO vector and did not detect any

unexpected bands, suggesting that the vector was intact. It is possible that recombination could occur in a small percentage of our plasmids, however if this is the case then the frequency is likely to be below the limit of detection by restriction digest.

It is possible that recombination could occur in transfected or transduced cells either, between the multiple copies of Oct-4 or between multiple copies of the vector within a given cell. In fact our episomal rescue results of the pHGCX+SOKM+EBNA+TK+TetO2 vector from Chapter 3 do suggest several rearrangements within single mammalian clones. This could explain the multiple restriction digest patterns present within many bacterial clones generated from the electroporation of rescued DNA from a single cellular clone. However although recombination events are possible, our WB and RT-PCR data confirm expression of all of our transgenes at similar levels, suggesting that recombination frequency is not high enough to eliminate our transgenes.

We were able to generate eight partially reprogrammed colonies, which were an improvement from the previous vector pHGCX+SOKM+EBNA+TK+TetO2 as they expressed EGFP. However, as before these colonies did not have typical iPS morphology and attempts to expand the colonies by transferring to fresh iMEFs were unsuccessful. Analysis of fourteen pluripotency markers confirmed expression of five markers including endogenous OCT-4 and NANOG, which are typically expressed later on in the reprogramming progress. Expression of hTERT, Cyclin B1 and DPPA4 was weaker than endogenous OCT-4 and NANOG expression however it should be noted that analysis was on a pool of cells

containing 8 partially reprogrammed colonies, un-reprogrammed fibroblasts and irradiated MEFs so this could account for the low expression levels. Expression of hTERT and Nanog was concurrent with the report that these markers are expressed in reprogramming intermediates and we did not observe expression the "true" iPS markers in Rex-1 and DNMT3B. This data supports our hypothesis that the colonies are partially reprogrammed intermediates.

We analysed the effect of HSV-1 amplicons on Sendai virus colony formation and discovered that cells double transduced with Sendai virus plus HSV amplicons compared with cells transduced with Sendai virus alone generated significantly fewer iPS colonies. No differences were observed in cell number prior to seeding cells onto the MEF feeder layer so the difference in colony number is not attributed to the effects of a double viral transduction compared with a single viral transduction. The observation of reduced colony numbers in the pHGCX+EBNA+TetO2 amplicon confirms that the effect is due to the amplicon itself rather than any of the reprogramming factors.

We investigated whether the HSV-1 amplicons were inducing a cellular response that was inhibiting reprogramming. We analysed known reprogramming inhibitors and from semi quantitative PCR experiments we found a trend for increased expression of p21 in amplicon transduced samples (harvested 12 days after transduction) compared to Sendai virus alone. From our qPCR data we found a significant increase in p53 expression in amplicon transduced samples, (harvested 2 days after transduction) compared with samples transduced with Sendai virus alone. In addition p53's primary target p21 was increased in

samples extracted 12 days after transfer however this trend was only significant when normalised to the ACTB reference gene expression. We also observed a relative increase of serine 15 phosphorylated p53/unphosphorylated p53 protein in our amplicon transduced samples compared to SeV transduced and untransduced samples, as analysed by Western blot, n=1. Together these results suggest an induction of the p53/p21 pathway in amplicon transduced cells.

The p53/p21 pathway is a known inhibitor of reprogramming as documented by numerous publications [95, 217, 225]. In addition SV40LT inhibition of p53 was required to sufficiently generate iPS colonies with the Thomson EBNA-1 vectors, a system that is incredibly similar to ours. We tested whether the p53/p21 pathway prevented reprogramming in the amplicon transduced cells by treatment with Pifithrin-α. Although we were able to demonstrate that addition of Pifithrin-α generated a few colonies in Sendai virus plus SOKMO transductions compared to zero colonies generated in the DMSO control, the increase in colony formation was not statistically significant. When we repeated the experiment with an earlier addition of Pifithrin-α, the colony numbers were too low to see a difference in treatments. Future experiments need to be performed on early passage fibroblasts to ensure successful reprogramming of our positive controls, and require treatment with Pifithrin-α at the time of transduction in order to prevent p53 transactivation.

The Sendai virus colony knockdown experiments using heat inactivated amplicon preps show that inactivated virus did not inhibit colony formation, indicating that colony inhibition is most likely due to phospholipids and/or

glycoproteins of the HSV-1 amplicon. Our results were not significantly significant due to low colony numbers so repeats would have to be made to confirm this result. All of our reprogramming experiments were performed using 0.22 micron filtered amplicon preps therefore there should have been minimal contaminants present in all of our experiments.

In conclusion our reprogramming vectors are capable of generating partially reprogrammed colonies. However, HSV-1 amplicons themselves induce p53, which inhibits the reprogramming process causing the cells to senesce. In order to achieve fully reprogrammed colonies the vector would need to be either used in conjunction with a p53 inhibitor such as Pifithrin-α under the appropriate conditions, or re-cloned to include the SV40LT gene to innately inhibit p53. It would be more advantageous however, to identify the p53 inducing component of the amplicon, in order to knock out the gene and make an improved vector without the need for p53 inhibitors.

Chapter 5 - Developing an HSV-1 amplicon vector for direct differentiation

5.1 Introduction

Direct differentiation provides an attractive alternative to cellular reprogramming as it allows you to differentiate your cell type of interest whilst bypassing the pluripotent stem cell stage. We are particularly interested in direct differentiation of fibroblasts to dopaminergic neurons as the process is rapid (2 weeks) and only requires one step [175]. This is a very simple protocol for directly generating DA neurons in comparison to the lengthy process of reprogramming fibroblasts to iPS cells followed by a 4-7 week DA differentiation protocol [173].

Direct conversion of one cell type to another was first achieved in 1979 when mouse fibroblasts were converted to myoblasts following 5-aza-cytidine treatment [226]. A. Lassar and colleagues repeated transdifferentiation of fibroblasts to myoblasts in 1987, by expressing myoblast specific cDNA, which they identified by screening a myocyte cDNA library. The authors successfully transdifferentiated myoblasts from several mouse fibroblast and adipocyte cell lines via the transfection of a single cDNA which was subsequently named myoblast determination gene 1 (MyoD), also known as basic helix loop helix (bHLH) transcription factor [227].

Further studies in MyoD revealed the gene to have a key role in myogenesis. Retroviral delivery of the gene to dermal fibroblasts, chondroblasts, smooth

muscle and retinal pigmented epithelial (RPE) cells converted the cells to striated mononucleated myoblasts and multinucleated myotubes [228]. The four types of converted cells reproduced the temporal sequence of markers characteristic of normal myogenesis with varying efficiency depending on the starting cell type. Whereas the efficiencies of smooth muscle and chondroblasts varied from 5-30% mononucleated myoblasts, fibroblasts and RPE conversion efficiency ranged from 1-5%.

Other examples of transdifferentiation include pancreatic exocrine cell conversion to functional, insulin secreting beta cells and conversion of B-cells to T cells and macrophages. Conversion of pancreatic cells to beta cells *in vitro* was achieved by isolating pancreatic exocrine cells from rats and incubating in media containing the growth factors epidermal growth factor (EGF) and leukemia inhibitory factor (LIF). Within three days the beta cell mass had increased eleven fold and secreted insulin in response to glucose. The cells stained positive for mature beta cell markers and transplantation into diabetic mouse models restored normoglycaemia [229]. D. Melton and colleagues successfully converted exocrine pancreatic cells to beta cells *in vivo* by adenovirus delivery of candidate transcription factors. The combination of the three transcription factors Neurogenin 3 (Ngn3), pancreatic and duodenal homeobox 1 (pdx1) and Musculoaponeurotic Fibrosarcoma Oncogene Homolog A (MafA) successfully generated insulin secreting beta cells in 20% of the infected cells [230].

Conversion of B cells to macrophages *in vitro* and *in vivo* was achieved via retroviral delivery of the transcription factors Ccaat enhancer binding proteins

(C/EBP) α and β. Expression of C/EBPα inhibits Paired box 5 (Pax5, a B cell commitment factor) activity and results in the activation of macrophage specific genes [231]. Deletion of the Pax5 gene from B cells *in vivo* and *in vitro* resulted in dedifferentiation of the B- cells to T- cells when injected into recombination activating gene 2 (Rag2) deficient (B cells and T cells deficient) mice [232].

Early transdifferentiation experiments generated cells that were within the same germ lineage i.e. mesoderm to mesoderm transition seen in fibroblast to myoblast transition and B cell to macrophage transition. In recent years there have been several publications regarding direct conversion of fibroblasts to functional neurons, which requires transcending germ lineages from mesoderm to endoderm [233].

M. Wernig and colleagues successfully generated functional mouse excitatory neurons by screening a pool of nineteen neuronal specific genes. Mouse embryonic fibroblasts derived from Tau-EGFP reporter knock-in mice were infected with lentivirus preparations expressing the 19 neuronal genes. Expression of the neuronal marker beta III tubulin co localised with the EGFP tau reporter expression 32 days after infection, indicative that a combination of genes within the 19 gene pool was sufficient to generate neurons. The three genes Achaete-Scute Complex Homolog 1 (Ascl I), Brain 2 (Brn 2) and Myelin transcription factor 1 (Myt I) were sufficient to generate neurons which co-expressed additional neuronal markers such as Synapsin, Myotubule associated protein 2 (MAP2), gamma-Aminobutyric acid (GABA) and vesicular glutamate transporter 1 (vGLUT 1) within 22 days of lentiviral infection. The neurons also

demonstrated action potentials and spontaneous electrophysiological activity eight days after infection [234].

M. Parmar and colleagues repeated the study in human cells in June 2011. Lentiviral delivery of the same transcription factors to embryonic human fibroblasts and postnatal human foreskin fibroblasts resulted in morphologically and electrophysiologically functional neurons. Further screening of the dopaminergic midbrain markers (Engrailed 1 (En1), forkhead box A2 (FoxA2), GLI family zinc finger 1 (Gli1), LIM homeobox transcription factor 1, alpha and beta (Lmx1a and Lmx1b), Msh homeobox 1 (Msx1), Nuclear receptor related 1 (Nurr1), Orthodenticle Homeobox 2 (Otx2), Paired box 2 and 5 (Pax2 and Pax5) cloned into lentiviral vectors was performed in order to identify factors capable of driving dopaminergic neuron differentiation. The addition of FoxA2 and Lmx1A to the neuronal transcription factor cocktail (Ascl I, Brn2 and Myt I) was sufficient to generate dopaminergic neurons expressing the markers tyrosine hyrodylase (TH), Aromatic L-amino acid decarboxylase (AADC) and Nurr1. Patch clamp recordings confirmed the neurons were capable of induced and spontaneous electrophysiological activity [235].

V. Brocolli and colleagues published similar findings in August 2011. The authors successfully converted both mouse and human fibroblasts to dopaminergic neurons by lentiviral delivery of the three transcription factors Ascl I, Nurr I and Lmx1a. Expression of dopaminergic neuronal markers TH, Vesicular monoamine transporter 2 (VMAT2), Aldehyde dehydrogenase 1(ALDH1A1), calbindin and dopamine transporter (DAT) were detectable at 16

days after infection of MEFs with an efficiency of 18% TH positive cells. Efficiencies were comparatively lower in human embryonic fibroblasts (6% TH positive cells) and human donor fibroblasts (3% TH positive cells). The conversion to dopaminergic neurons was rapid and the resulting neurons were functional and expressed a panel of dopaminergic neuron markers [175].

Direct differentiation of fibroblasts to neurons bypasses the induced pluripotency stage and avoids safety concerns of undifferentiated cells causing teratomas (stem cell derived tumour masses). However, the methods of generating induced dopaminergic (iDA) neurons share the same problems as methods used to generate iPS cells. Lentiviral vectors are integrating and have the potential to cause insertional mutagenesis and the overall efficiency is very low. An alternative adenoviral delivery of the factors Ngn2, Ascl I and Brn2 successfully converts fibroblasts to neurons however the efficiency is much lower than in lentivirus [236].

We have employed the HSV-1 amplicon system to enable the delivery of the three iDA factors Ascl I, Nurr I and Lmx1a in a single polycistronic cassette obtained from V. Brocolli and colleagues. As described previously HSV-1 amplicons are non-integrating, high transgene capacity vectors capable of high transduction efficiency in fibroblasts. The vector also contains the EBNA-1/*oriP* cassette, which enables episomal retention of the vector, as described previously.

5.2 Vector construction

For reference all the vectors used in this chapter, including information on the type of vector, the transcription factors carried and their species origin, the promoter driving the transcription factors and presence of the EBNA-1/oriP and thymidine kinase cassettes are presented in Table 1.

Vectors used in Chapter 5

Vector name	Type of vector	Promoter	Factors	EBNA	TK	Size	Constructed by
pHGCX	HSV-1 amplicon	pCMV	no	no	no	6.7 Kb	R. Wade-Martins
FUW-ANL	Lentiviral	x	mouse ANL	no	no	12.1 Kb	V. Brocolli
pHGCX+EBNA+TetO2	HSV-1 amplicon	pCMVTetO2	no	yes	yes	13.3 Kb	A. Popplestone
pHGCX+ANL+EBNA+TetO2	HSV-1 amplicon	pCMVTetO2	mouse ANL	yes	yes	18.4 Kb	A. Popplestone

Table 1 – Vectors used and constructed in chapter 5. The table indicates the type of vector, promoter used, species of factor and factors carried, presence of EBNA-1/oriP and TK elements, Size (Kb) and who constructed the vector. ANL= Ascl1, Nurr-1 and Lmx1a mouse neuronal transcription factors.

Prior to construction of the HSV-1 iDA amplicon vector the source vector FUW-ANL, obtained from V. Broccolli and colleagues, was sequenced to ensure there were no mutations. Eighteen primers spanning the polycistronic ANL cassette were designed and used in sequencing. The sequence was complete and no mutations were detected. The sequencing primers binding sites are shown in Figure 1.



Figure 1 – FUW-ANL sequence and primer binding sites. The forward (green) and reverse (yellow) primer binding sites are shown on the Ascl I (teal), Nurr I (aqua), Lmx1a (grey) cassette in the FUW-ANL vector. The 2A sequences are shown in red and FUW vector is shown in white.

The HSV-1 amplicon iDA vector was constructed by first isolating the polycistronic ANL cassette by restriction digest of the source vector FUW-ANL with restriction enzymes *Kpn I* and *Eco RV*. The digest was treated with Klenow exonuclease to blunt the restriction site followed by gel extraction and column purification of the 3962 bp fragment. The pHGCX+SOKM+EBNA+TetO2 vector was digested with *Afl II* and *Xba I* to remove the SOKM cassette. The digest products were treated with Klenow to blunt the restriction sites and CIP to prevent self-ligation of the vector. The 13251 bp fragment was gel extracted,

column purified and ligated with the ANL cassette. The cloning strategy and corresponding plasmid maps are shown in Figure 2.

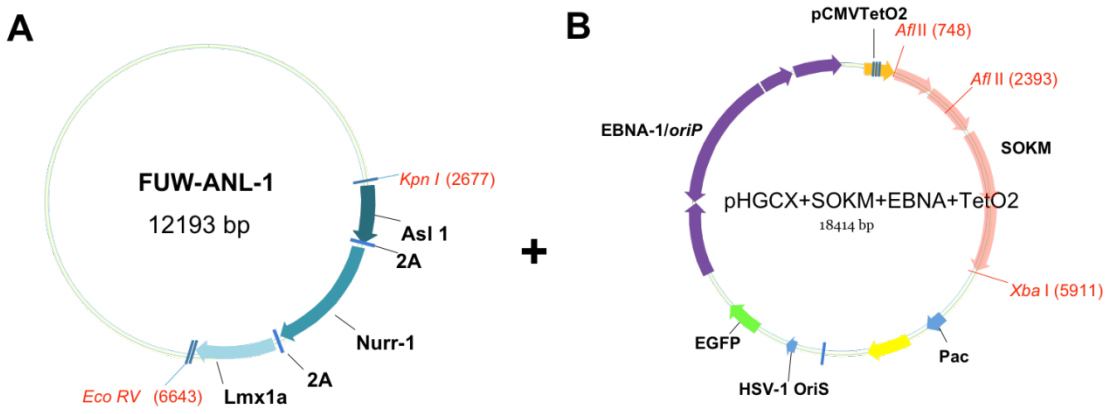


Figure 2 – Construction of HSV-1 amplicon iDA vectors by restriction enzyme digest and ligations. A) The FUW-ANL source vector was digested with *Kpn I* and *Eco RV* and the 3962 bp fragment was gel extracted and column purified**. B)** The pHGCX+SOKM+EBNA vector was digested with *Afl II* and *Xba I* to remove the SOKM construct. The 13251 fragment containing the pHGCX backbone and EBNA-1 cassette was gel extracted. Both fragments were treated with Klenow to blunt the restriction sites and were ligated together.

5.3 Vector confirmation

All ligations were performed alongside vector only ligation controls in order to screen for background ligation products. No colonies were observed in the vector only controls suggesting a low frequency of background ligation products. The pHGCX+EBNA+ANL plasmid was digested with several restriction enzymes to determine whether the insert was present and in the correct orientation. One out of the twenty-four miniprepped plasmids had the correct digest products for all enzymes used. The final plasmid map containing the *Eco RI* restrictions sites and corresponding gel of the correct orientation is shown in Figure 3.

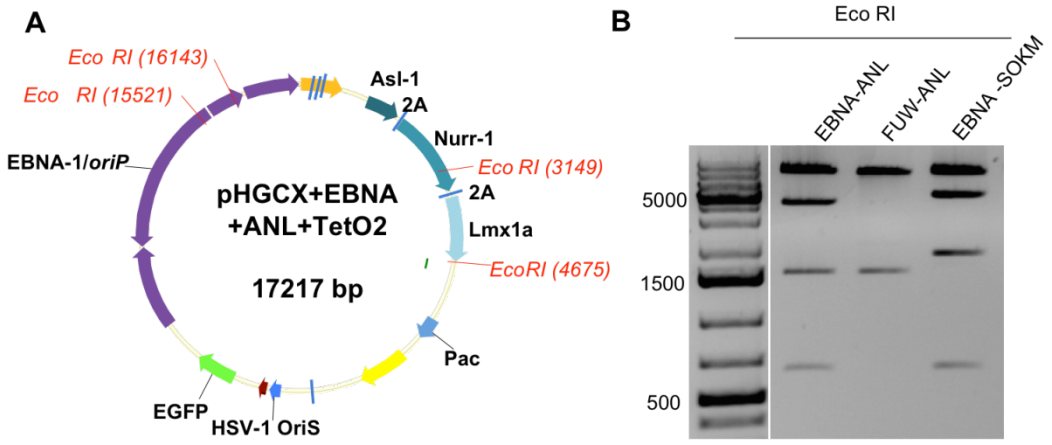


Figure 3 – Restriction enzyme digest analysis of final HSV-1 amplicon iDA vector. Plasmid map of pHGCX+EBNA+ANL+TetO2 (EBNA-ANL) and corresponding Eco RI digest (10858, 4240, 1526, 622) is shown alongside Eco RI digestion of FUW-ANL (10667, 1526) and pHGCX+EBNA+SOKM+TetO2 (10849, 5084, 1859, 622).

5.4 Vector characterisation

The iDA HSV-1 amplicon vector was characterised to confirm functionality of the ANL polycistronic cassette before use in direct differentiation experiments. Confirmation of the three iDA factors protein expression was determined by RT-PCR analysis and western blot analysis of MRC5-V2 cells transfected with the HSV-1 iDA vector pHGCX+ANL+EBNA+TetO2 and the negative control pHGCX. RNA and protein preparations were extracted from cells harvested 48 hours after transfection.

First RNA expression of the iDA factors Ascl I, Nurr I and Lmx1a was confirmed by RT-PCR. Primers were designed to flank the Ascl I-2A-Nurr I and Nurr-1-2A-Lmx1a junctions, resulting in 197 bp and 154 bp PCR products respectively. PCR products of the correct size were observed for both primer pairs whereas no PCR products were observed in the pHGCX transfected controls or non-RT controls

confirming that expression was not due to DNA contamination. RT-PCR gels are shown in Figure 4.

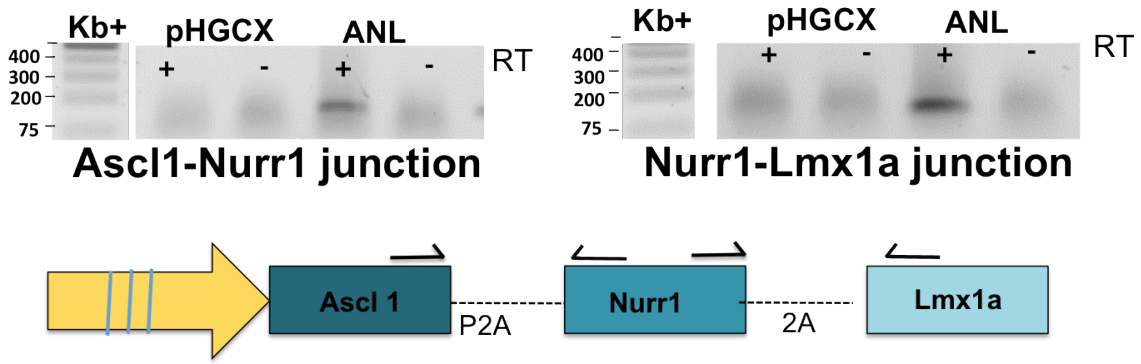


Figure 4 – Confirmation of iDA factor RNA expression in pHGCX+ANL+EBNA+TetO2 transfected MRC5-V2 cells. Confirmation of neuronal transcription factor mRNA expression. Assayed by RT-PCR using primers flanking the Asl I-2A-Nurr I junction and the Nurr I-2A-Lmx1a junction. No expression was detected in the negative control (pHGCX) or non-RT controls (-RT). Schematic indicates primer-binding sites on the polycistronic Ascl1-Nurr1-Lmx1a cassette.

Next protein expression of Ascl I, Nurr I and Lmx1a was analysed by Western blot. We were able to detect the 66.5 kDa and 42.7 kDa molecular weight protein bands of Nurr I and Lmx1a respectively. The corresponding bands were not observed in the pHGCX transfected and untransfected negative controls. We could not detect the predicted 25 kDa Ascl I protein band in our pHGCX+ANL+EBNA+TetO2 transfected samples. We were able to detect multiple protein bands, however these were also observed in our pHGCX transfected negative control sample. Robust expression of the 25 kDa band was observed in the human nigra positive control sample, however transgenic Ascl I originates from mouse. The antibody we used was raised against human Ascl I and according to the data sheet should also bind mouse Ascl I, however in our hands

we were unable to detect Ascl I expression, despite confirmation of expression at the RNA level. The Ascl I, Nurr I and Lmx1a Western blots are shown in Figure 5.

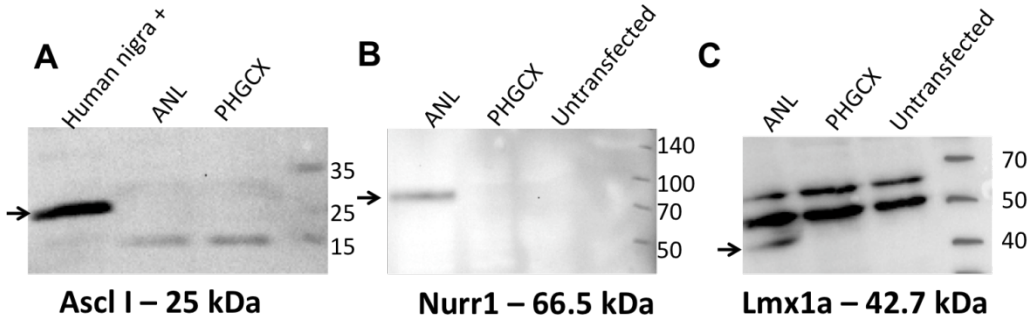


Figure 5 – Confirmation of iDA factor protein expression in pHGCX+ANL+EBNA+TetO2 transfected MRC5-V2 cells. A) Confirmation of Ascl I protein in human nigra control (25 kDa), no expression can be seen in pHGCX+ANL+EBNA+TetO2 transfected cells or pHGCX transfected control. **B)** Confirmation of Nurr I protein expression (66,5 Kda) in pHGCX+ANL+EBNA+TetO2 transfected cells, no expression can be seen in pHGCX transfected or untransfected control. **C)** Confirmation of Lmx1a protein expression (42.7 kDa) in pHGCX+ANL+EBNA+TetO2 transfected cells, no expression can be seen in pHGCX or untransfected controls.

The HSV-1 iDA vectors were packaged into HSV-1 amplicons as described previously by co-transfecting the vector with pcDNA6/TR plasmid and packaging vectors fHSVΔpacΔ27 and ICP27. Viral titres of 10^7 TU/ml were obtained.

5.5 Direct differentiation experiments

The direct differentiation experiments were performed on several cell lines including MRC5 primary fetal lung fibroblasts, control donor fibroblasts obtained from the Oxford Parkinson's Disease Centre (OPDC) and mouse embryonic fibroblasts (MEFs). Images of MRC5 and MEF transduction with pHGCX+ANL+EBNA+TetO2 and pHGCX+EBNA+TetO2 respectively at an MOI of 10 are shown in Figure 6.

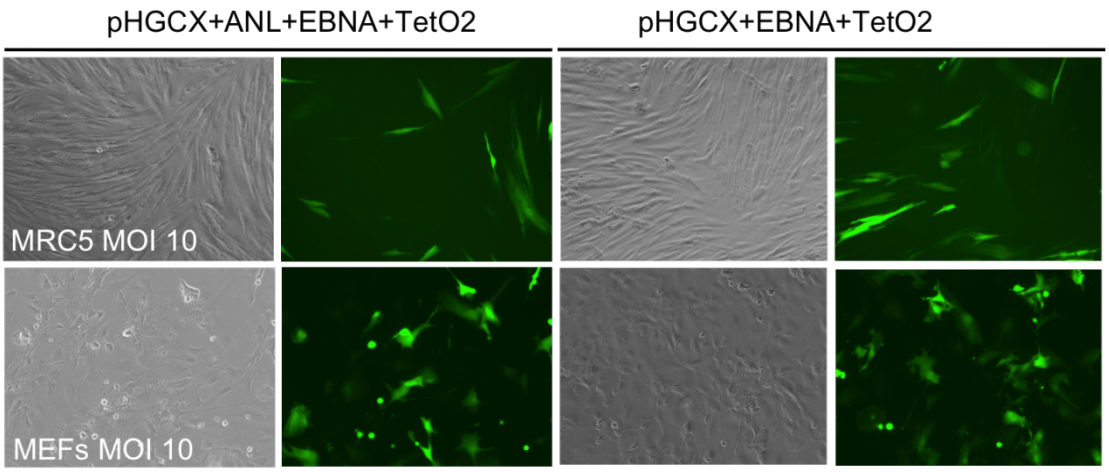


Figure 6 – Transduction of primary fibroblasts (MRC5) and mouse embryonic fibroblasts (MEFs) with HSV-1 amplicons pHGCX+ANL+EBNA+TetO2 and pHGCX. Cells were seeded onto coverslips at 40,000 cells per well and transduced at MOI 10 with HSV-1 iDA amplicons and pHGCX control. Brightfield and fluorescent images are shown.

We followed the direct differentiation protocol as described by V. Brocolli and colleagues. First we seeded 50,000 fibroblasts on matrigel-coated coverslips in a 24 well plate. The next day the cells were transduced with pHGCX+ANL+EBNA+TetO2 or pHGCX+EBNA+TetO2 control in complete DMEM at an MOI of 10. The following day the media was replaced with a neuronal inducing media – DMEM/F12 containing 1% penicillin/streptomycin and 1% N2 supplement (insulin 500 mg/L, transferrin 10,000 mg/L, Sodium Selenate 0.003 mM, progesterone 0.002 mM and puterescine 0.002 mM). A 50% media change was made every 2 days for 22 days and then the cultures were fixed in 4% PFA and stained with the neuronal marker beta tubulin (Btub), dopaminergic neuron marker Tysorosine hydroxylase (TH) and the nuclei stain DAPI.

Weak TH and beta tubulin expression was observed in all culture conditions (pHGCX+ANL+EBNA+TetO2 transduced, pHGCX+EBNA+tetO2 transduced or untransduced) however the morphology remained fibroblast-like. Due to the observation of weak expression in the untransduced control, expression must have either been induced by the neuronal inducing media or was a false positive/ autofluorescence effect. Robust expression of TH was observed in the positive control neuroblastoma cell line (M17), confirming sensitivity of the TH antibody. Quantification of TH and Btub expression was performed by cell counting in triplicate normalised to total cells (DAPI positive cells) in the pHGCX+ANL+EBNA+TetO2 or pHGCX+EBNA+TetO2 transduced cultures. No significant increase in TH or Btub expression was observed in pHGCX+ANL+EBNA+TetO2 transduced cultures compared to the negative control pHGCX+EBNA+tetO2 transduced cultures. Fluorescent images and cell count graphs are shown in Figure 7.

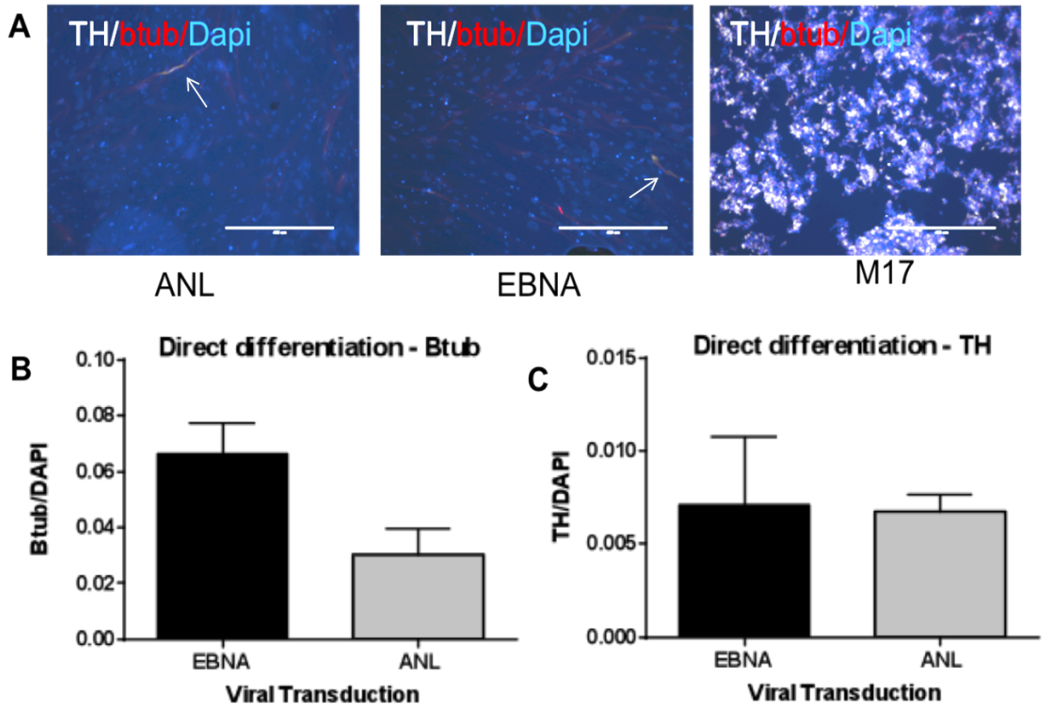


Figure 7 – Immuno staining and quantification of iDA cultures stained with dopaminergic neuron marker Tyrosine hydroxylase (TH) and neuronal marker beta III tubulin (btub). A) Images of pHGCX+ANL+EBNA+TetO2 transduced and negative control pHGCX+EBNA+TetO2 transduced iDA cultures stained with TH (white staining, indicated by white arrows) and Btub (red). The cell line M17 was used as a positive control for TH staining (white). **B)** Quantification of number of btub positive cells normalised to total number of cells (DAPI). No change was seen between ANL and EBNA treated cells. **C)** Quantification of number of TH positive cells normalised to total number of cells (DAPI). A higher number of TH cells were observed in EBNA treated condition however this difference was not significant. Counts were performed in triplicate, n=1 (Unpaired students t-Test).

5.6 Conclusion and summary

We successfully constructed a HSV-1 amplicon vector containing the iDA factors Ascl I, Nurr I and Lmx1a. Sequencing of the FUW-ANL polycistronic cassette and restriction enzyme digests confirm that the cassette was complete and inserted in the correct orientation. RT-PCR using primers spanning the 2A junctions confirmed expression of the iDA factors; no expression was detected in the non-RT control confirming that amplification was from cDNA. Protein expression of Nurr I and Lmx1a was confirmed by Western blot, however we were unable to detect Ascl I by Western blot.

Due to the positioning of Ascl I at the beginning of the polycistronic cassette and the confirmed protein expression of Nurr 1 and Lmx1a it is highly likely that Ascl I was expressed at the protein level. Downstream expression of Nurr I and Lmx1a proteins, which can only happen following upstream translation of Ascl I and ribosomal skipping occurring at the 2A peptide prior to the Nurr I transgene. No fusion proteins were observed on the Nurr-I Western blot and although the protein appears to run at a slightly higher molecular weight of around 70-80 kDa, it is not heavy enough to account for an Ascl I-2A-Nurr-1 fusion protein which has a predicted molecular weight of 102 kDa. Transduction of MRC5-V2 cells with an HSV-1 amplicon containing only the Nurr-1 gene (pHGCX+Nurr-1+EBNA+TetO2) resulted in the same molecular weight protein product.

We were unable to successfully generate dopaminergic neurons using the pHGCX+ANL+EBNA vector. We attempted direct differentiation using several cell lines including the reportedly easier to differentiate mouse embryonic

fibroblasts. We attempted increasing the MOI to 20 and also tried maintaining the cultures for a longer time period of 28 days. We also tried different concentrations of N2 supplement, 1:100, 1:50, 1:20 however no robust TH expression was observed.

Chapter 6 - Delivery of HSV-1 neural transcription factor vectors to enhance dopaminergic differentiation

6.1 Introduction

Embryonic stem cells and induced pluripotent stem cells have the potential to differentiate in to all three germ layers. Cell types differentiated from patient iPS cells provide a valuable cell source for regenerative medicine, drug screening and toxicology and disease modelling. We are interested in the generation of dopaminergic neurons in order to study Parkinson's disease *in vitro.* The aim of this project was to enhance dopaminergic neuron differentiation efficiency by HSV-1 amplicon delivery of neuronal transcription factors.

Early attempts to generate mouse dopaminergic neurons *in vitro* from ES cells relied on co culture with PA6 stromal cells derived from skull bone marrow [237]. Y. Sasai and colleagues co-cultured ES cells on several feeder cell lines and compare expression of the pan-neural marker NCAM. The PA6 induced remarkable expression of NCAM compared to other cell lines with 92% NCAM positive colonies after 12 days [238]. Although the mechanism by which PA6 induce neuronal differentiation was not known at the time the authors identified the factors to be present on the cell surface via fixation experiments. Following investigations identified the initiating factors as stromal cell-derived factor 1 (SDF- 1/CXCL12), pleiotrophin (PTN), insulin-like growth factor 2 (IGF2), and

ephrin B1 (EFNB1) [239]. Later protocols differentiated dopaminergic neurons in stromal free culture conditions [240].

6.1.1 Neurotrophic factors

A. Wobus and colleagues in 2001 further developed mouse ES differentiation protocols by applying several survival promoting and neurotrophic factors to enhance dopaminergic differentiation from mouse ES cells [241]. The authors found that interleukin-1b, glial cell line-derived neurotrophic factor, neurturin, transforming growth factor-β (TGF-β) and dibutyryl-cyclic AMP (cAMP) significantly enhanced the dopaminergic neuronal markers TH and Nurr1 and anti-apoptotic marker bcl-2 mRNA expression.

In 2004 several publications described the differentiation of human ES cells to dopaminergic neurons [240, 242-244]. J. Lim and colleagues compared several neurotrophic factors such as basic fibroblast growth factor (bFGF), transforming growth factor α (TGFα), brain derived neurotrophic factor (BDNF) and retinoic acid (RA) [244]. The authors found that the combination of bFGF and TGFα induced more TH positive neurons compared to other combinations (20% TH+ neurons vs 9-16% TH + neurons). Furthermore in another study, midbrain dopaminergic neurons were established from ES cells following a combination of fibroblast growth factor 8 (FGF8) and Sonic hedgehog (SHH) followed by Ascorbic acid (AA) and BDNF. Neuronal cultures derived using these factors released dopamine, evoked action expressed the midbrain markers PAX2, EN1, ALDH1A1, LMX1B, PITX3, NURR1 and TH, released dopamine and evoked action potentials [243].

6.1.2 SMAD inhibition

Early studies in *Xenopus* development identified that BMP4 – a known promoter of epidermogenesis- inhibited neuronal development [245, 246]. This was confirmed in early mouse ES differentiation studies [238] therefore dopaminergic neuron protocols were improved further by the employment BMP signalling inhibition by Noggin and inhibition of the TGF receptors, alkaline like kinase (ALK) by SB431542. Together the inhibitors induced 80% Pax6 expression compared with 10% in either inhibitor alone. The authors used this approach to derived ES and iPS cells to dopaminergic neurons combined with SHH, FGF8 followed by GDNF, BDNF, TGF-β3 and cyclic AMP (cAMP) [173].

Closer analysis of the mechanism of BMP and TGF inhibitors by L. Iacovitti and colleagues identified their upregulation of SMAD inhibiting protein-1 (SIP1) and Wnt and Lmx1a expression [137]. BMP and TGF inhibition is also accompanied by a downregulation of SHH and Foxa2 so addition of SHH and FGF8a is needed in combination with SMAD inhibition to keep these pathways in equilibrium [137]. In addition high activity forms of SHH in combination with FGF8a and retinoic acid were found to efficiently generate FOXA2 positive ventral midbrain dopamine neurons [247].

6.1.3 Neuronal transcription factors

Several knock out and gain of function studies *in vitro* and *in vivo* have highlighted the importance of neuronal transcription factors in dopaminergic neuron development. Early studies of nuclear receptor related protein 1 (Nurr-

1) mRNA expression in embryonic mice identified a regulatory role for the transcription factors in the nigrostriatal dopamine system [248]. This study was complemented by Nurr-1 null mice lacking midbrain dopaminergic neurons [249]. Transient transfections of wild-type Nurr1 was shown to upregulate aromatic L-amino acid decarboxylase (AADC) and vesicular monoamine transporter-2 (VMAT2) in the dopamine cell line MN9D whereas in the absence of Nurr 1, expression of DA markers such as Pitx3, Lmx1b, En-1, and En-2 are lost later in the differentiation process [250]. In addition retroviral infection of Nurr 1 in adult precursor cells induced endogenous TH expression and footprint analysis identified specific binding of Nurr-1 to the TH promoter at the NBRE consensus sequence [251].

The transcription factor pituitary homeobox-3 (Pitx-3) also plays an important role in dopaminergic neuron differentiation and has been shown to drive TH expression by binding to the TH promoter at a region distinct from the Nurrr-1 binding site [252, 253]. Endogenous TH was confirmed to be upregulated by PitX3 by inducing GFP expression in a TH-GFP promoter-reporter construct [254]. In addition mouse ES cells derived from PitX3 deficient mice resulted in a significant reduction in TH/Map2 positive mature neurons when compared with controls [255].

When expressed in combination with Nurr-1 TH expression was not further enhanced [254] however the late dopaminergic neuron marker Dat was upregulated 3 fold and gel shift assay confirmed co-operative binding of Nurr-1

and Pitx3 to the Dat promoter [256]. Interestingly via Nurr 1 RNA silencing and Nurr-1 overexpression experiments G. Bellenchi and colleagues demonstrated that Nurr-1 regulates Pitx3 expression by binding to the NBRE sequence in the Pitx3 promoter [257].

Other factors important for dopaminergic neuron differentiation include BCLX-2 Lmx1a, Lmx1b, Foxa1, Foxa2, Msx1 and Nngn2 [258, 259]. Numerous studies have highlighted the importance of Lmx1a in dopaminergic neuron differentiation; engineered hES cells expressing LMX1A resulted in a significant upregulation of key DA neuron genes including the A9 marker FOXA2 and mature DA markers DAT and GIRK2 [260]. Knockdown of Lmx1a expression by siRNA resulted in subsequent downregulation of DA-specific genes Aldh1a1 (4-fold), Nurr1 (4-fold), Pitx3 (64-fold), TH (16-fold), dopamine transporter (DAT) (16-fold), and Girk2 (4-fold) compared with controls [137]. Transplantation studies of Lmx1a transfected hES cells resulted in high numbers of TH positive cells within the grafts compared with non transfected controls [261].

FoxA2 and Lmx1a have been shown through conditional and gain of function mouse studies to cooperatively regulate DA differentiation. FoxA2 positively regulates Lmx1a and represses Nkx 2.2, Nkx 6.1 and GABAergic differentiation by repression of the Hert gene. [262, 263]. Foxa2 has also been shown to increase survival and differentiation of A9 DA neurons when retrovirally infected into neural precursors alongside Nurr-1 [264]. Together Foxa2 and Nurr-1 resulted in 37% TH positive cells compared to 2-3% when infected alone. In addition, Foxa2 increased cell survival and resistance to cellular stresses and

toxins such as H_2O_2 and MPP. Midbrain A9 specific markers such as Nurr1, Wnt-3a, Lmx1b, aldehyde dehydrogenase 2 (AHD2), Pitx3 and Corin were also upregulated in response to Foxa2[264].

Recently, V. Brocolli and colleagues have developed a rapid, one step protocol to generate dopaminergic neurons following lentiviral infection of the individual transcription factors ASCL1, NURR1 and LMX1A into iPS cells. Dopaminergic neurons were generated within 21 days and 93% of cells that received all three transcription factors developed into dopaminergic neurons [265].

The enhanced TH populations and more mature dopaminergic neuron phenotypes seen in the combinatorial delivery of transcription factors (FoxA2 and Nurr-1; FoxA2 and Lmx1a; Nurr1 and Pitx3; ASCL1, NURR1 and LMX1A [256, 262-265]) suggest that combinations of transcription factors are key to successful dopaminergic neuron differentiation.

Given this evidence we decided to generate HSV-1 amplicons individually expressing the four neuronal transcription factors Nurr1 (rat), Foxa2 (mouse), PITX-3 (human) and LMX1A (human) to try and enhance the DA neuron population in our differentiation experiments. In addition we also employed the polycistronic ANL vector generated in Chapter 5, for use in these experiments.

6.2 Transduction efficiency of iPS and Neural precursor cells

Before constructing the neuronal transcription factor HSV-1 amplicons we transduced iPS cells and neural precursor cells (NPC) with pHGCX HSV-1 amplicons and analysed by FACS to ensure the transduction efficiency was sufficient. The iPS cells were highly transducible and had an efficiency of 93% and 92% at an MOI of 5 and 10 respectively. The NPCs had a slightly lower transduction efficiency of 61% and 92% at MOI 5 and 10. Fluorescent images and FACs histograms of iPS and NPCs transduced with pHGCX at an MOI of 10 are shown in Figure 1.

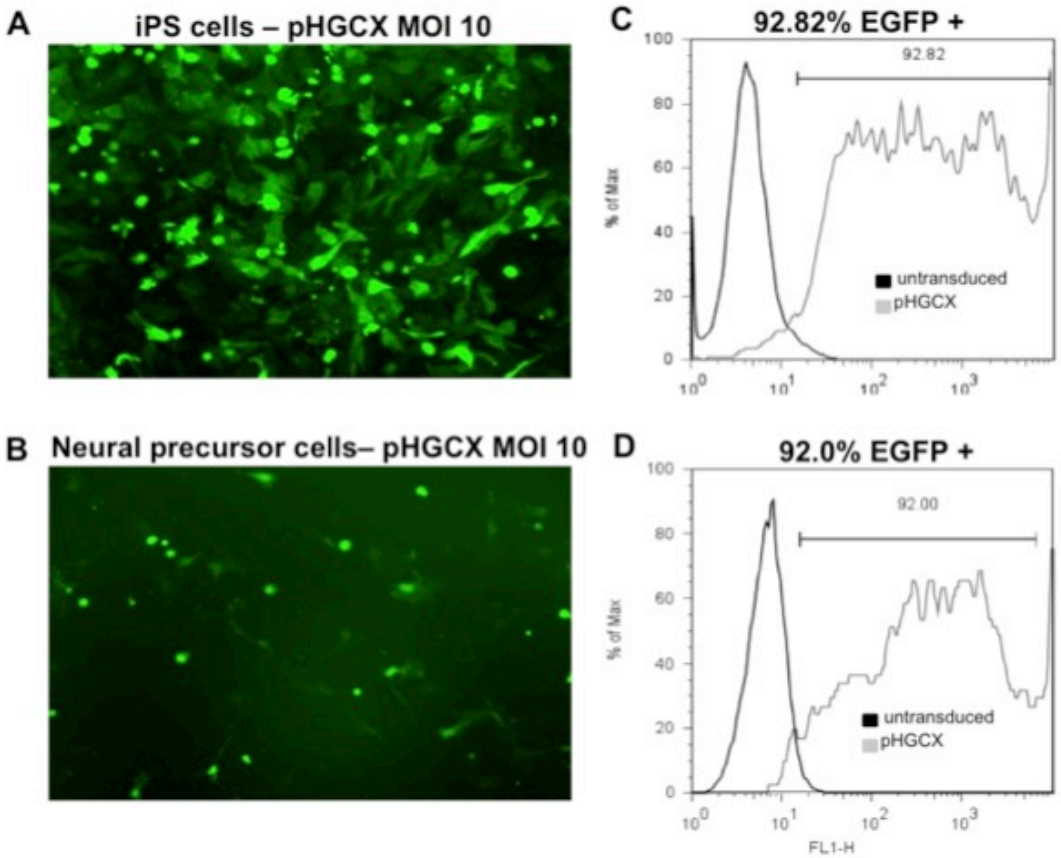


Figure 1 – HSV-1 amplicon transduction of iPS cells and NPCs. **A)** Fluorescent imaging of NHDF-1 iPS cells transduced with pHGCX HSV-1 amplicons at an MOI of 10. **B)** Fluorescent imaging of neural precursor cells (NPCs) (derived from NHDF-1 iPS cells) transduced with pHGCX HSV-1 amplicons at an MOI of 10. **C)** FACs analysis histogram of iPS transduced with pHGCX HSV-1 amplicons at an MOI of 10. **D)** FACs analysis histogram of iPS transduced with pHGCX HSV-1 amplicons at an MOI of 10.

6.3 Vector construction

For reference all the vectors used in this chapter, including information on the type of vector, the transcription factors carried and their species origin, the promoter driving the transcription factors and presence of the EBNA-1/oriP and thymidine kinase cassettes are presented in Table 1.

Vectors used in Chapter 6

Vector name	Type of vector	Promoter	Factors	EBNA	TK	Size	Constructed by
pHGCX	HSV-1 amplicon	pCMV	no	no	no	6.7 Kb	R. Wade-Martins
pRRL-CMV-hLMX1A-iresGFP	lentiviral	pCMV	human LMX1A	no	no	8.7 Kb Kb	M. Caldwell
pRRL-CMV-hPITX3-iresGFP	lentiviral	pCMV	human PITX3	no	no	8.3 Kb	M.Caldwell
Nurr1-EF1a3.1	pUC	EF1a	mouse Nurr1	no	no	7.7 Kb	H. Park
Foxa2(r,ha)-EF6A	pUC	EF1a	rat FoxA2	no	no	7.2 Kb	H. Park
pHGCX+EBNA+TetO2	HSV-1 amplicon	pCMVTetO2	no	yes	yes	13.3 Kb	A. Popplestone
pHGCX+LMX1A+EBNA+TetO2	HSV-1 amplicon	pCMVTetO2	human LMX1A	yes	no	14.4 Kb	A. Popplestone
pHGCX+PITX3+EBNA+TetO2	HSV-1 amplicon	pCMVTetO2	human PITX3	yes	no	14.1 Kb	A. Popplestone
pHGCX+Nurr1+EBNA+TetO2	HSV-1 amplicon	pCMVTetO2	mouse Nurr1	yes	no	14.1 Kb	A. Popplestone
pHGCX+FoxA2+EBNA+TetO2	HSV-1 amplicon	pCMVTetO2	rat FoxA2	yes	no	14.1 Kb	A. Popplestone

Table 1 – Vectors used and constructed in chapter 6. The table indicates the type of vector, promoter used, species of factor and factors carried, presence of EBNA-1/oriP and TK elements, Size (Kb) and who constructed the vector.

The source vectors pRRL-CMV-hLMX1A-iresGFP and pRRL-CMV-hPITX3-iresGFP carrying the human LMX1A and PITX3 neuronal transcription factors (NTF) were obtained from M. Caldwell and colleagues [174]. The source vectors Nurr1-EF1α3.1 and Foxa2(r,ha)-EF6A containing mouse Nurr1 and rat Foxa2 were obtained from S. Lee and colleagues [264] .

LMX1A, PITX3, Nurr1 and Foxa2 were isolated from the source vectors by PCR using primers designed to include restriction digests for direct ligation into the vector. The LMX1A, PITX3 and FoxA2 primers were designed to include the *Not I*

and *Bam HI* restriction sites and primers containing the restriction sites *Afl II* and *Xba I* were used to isolate Nurr1 due to *Not I* cutting within the Nurr1 sequence. The pHGCX+SOKM+EBNA+TetO2 vector was digested with the corresponding restriction enzymes in order to remove the SOKM construct. The digested and purified vector was ligated to purified and digested PCR products resulting in the 4 vectors pHGCX+LMX1A+EBNA+TetO2, pHGCX+PITX3+EBNA+TetO2, pHGCX+Nurr1+EBNA+TetO2 and pHGCX+Foxa2+EBNA+TetO2. The cloning strategy and resulting vectors is shown in Figure 2.

6.4 Vector confirmation

Each of the four NTF vectors were digested with several restriction enzymes to ensure that the factors had been inserted correctly; digestion of pHGCX+Foxa2+EBNA+TetO2, pHGCX+LMX1A+EBNA+TetO2, pHGCX+Nurr1+EBNA+TetO2 and pHGCX+Pitx3+EBNA+TetO2 with *Bst XI, Pvu I, Blp I* and *Eco RI* respectively is shown in Figure 3. The NTF inserts were also sequenced to ensure no errors had been introduced during the PCR amplification. Single transitions were detected in LMX1A and PITX3 and multiple transitions and transversions were detected in Nurr1 however all of the point mutations were silent. No changes were detected in the Foxa2 insert.

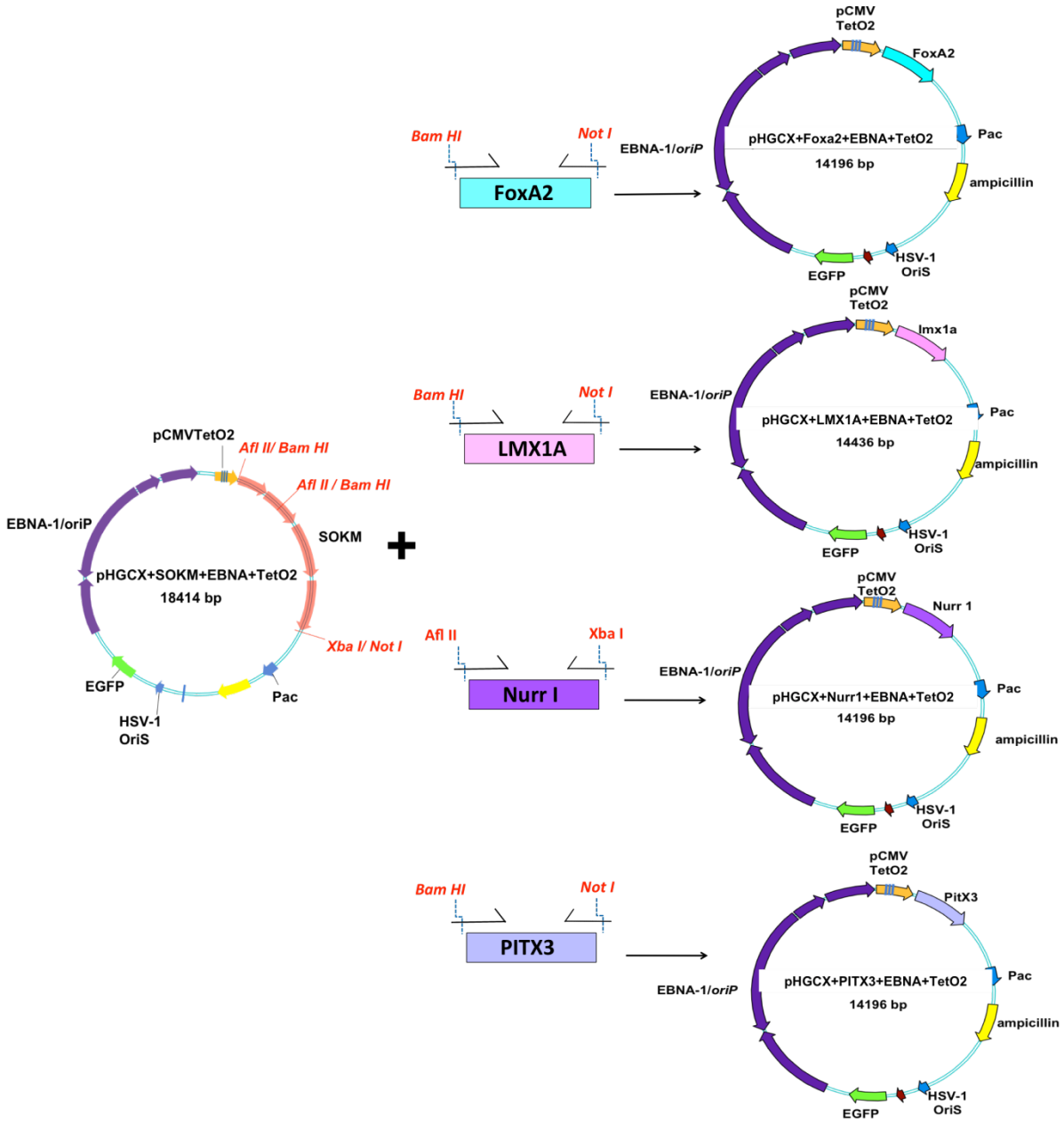


Figure 2 – Vector construction of NTF HSV-1 amplicon vectors by PCR, digest and ligation. The pHGCX+SOKM+EBNA+TetO2 vector was digested with *Afl II/Xba I or Bam HI/Not I.* The four transcription factors Foxa2, LMX1A, Nurr1 and PITX3 were amplified from their source vectors by PCR primers containing the restriction sites *Afl II/ Xba I* or *Bam HI/Not I*. The digested primer products were ligated with the corresponding vector digest to generate the four NTF vectors pHGCX+Foxa2+EBNA+TetO2, pHGCX+LMX1A+EBNA+TetO2, pHGCX+Nurr1+EBNA+Teto2 and pHGCX+Pitx3+EBNA+TetO2.

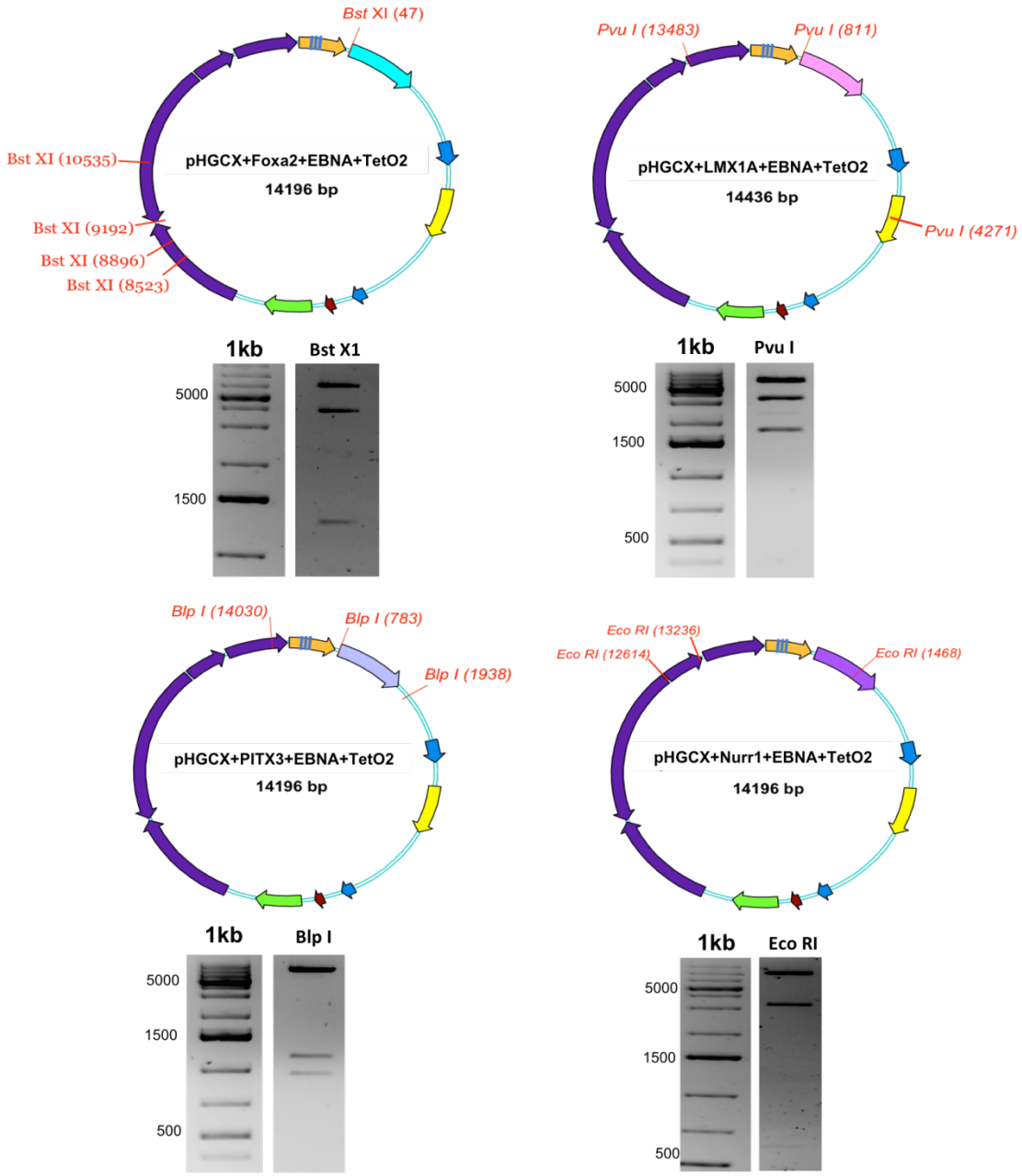


Figure 3 – Restriction enzyme digest analysis and corresponding plasmid maps of pHGCX+FoxA2+EBNA+TetO2, pHGCX+LMX1A+EBNA+TetO2, pHGCX+Nurr1+EBNA+tetO2 and pHGCX+PITX3+EBNA+TetO2. A) pHGCX+FoxA2+EBNA+TetO2- plasmid map indicating the *Bst XI* restriction sites. Gel Electroporation of *Bst XI* digest products (8476, 4176, 1343, 373*, 296*). **B)** pHGCX+LMX1A+EBNA+TetO2 – plasmid maps indicating the *Pvu I* restriction sites. Gel Electroporation of *Pvu I* digest products (9212, 3460, 1764). **C)** pHGCX+PITX3+EBNA+TetO2- plasmid map indicating the *Blp I* restriction sites. Gel Electroporation of *Blp I* digest products (12092, 1155, 949). **D)** pHGCX+Nurr1+EBNA+TetO2- plasmid map indicating the *Eco RI* restriction sites. Gel Electroporation of *Eco RI* digest products (11146, 3286, 622). *bands ran off electrophoresis gel.

6.5 Vector characterisation

The four NTF vectors were transfected into human embryonic kidney (HEK) cells and NTF expression was confirmed by Western blot and by immunocytochemistry. Western blot analysis detected protein bands that were slightly heavier than the expected 43 kDa, 32 kDa, 54 kDa and 72 kDa bands of LMX1A, PITX3, Foxa2 and Nurr 1 respectively. The corresponding band was not observed in the pHGCX transfected controls Figure 4.

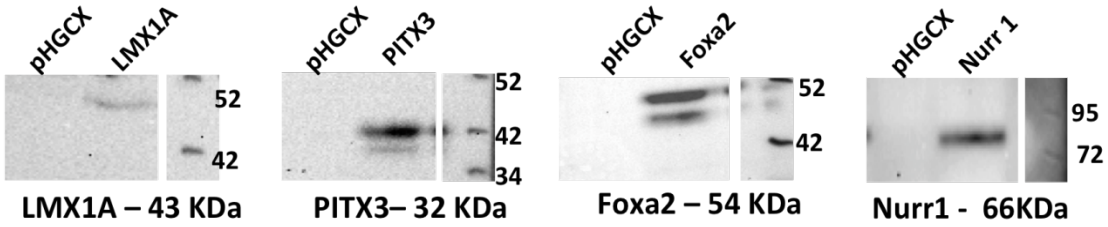


Figure 4 – Confirmation of LMX1A, PITX3, Foxa2 and Nurr1 protein expression in NTF transfected HEK cells. Confirmation of LMX1A, PITX3, Foxa2 and Nurr1 protein in NTF transfected HEKs (43 kDa, 32 kDa, 54 kDa and 66 kDa respectively). No expression can be seen in pHGCX transfected negative controls.

Immunocytochemitry analysis of transfected HEKs confirmed expression of the four transcription factors. The antibodies were labelled with a red secondary antibody and compared with the pHGCX control. Fluorescent imaging of the immuno-stained NTFs and exogenous fluorescence of the GFP reporter is shown in Figure 5.

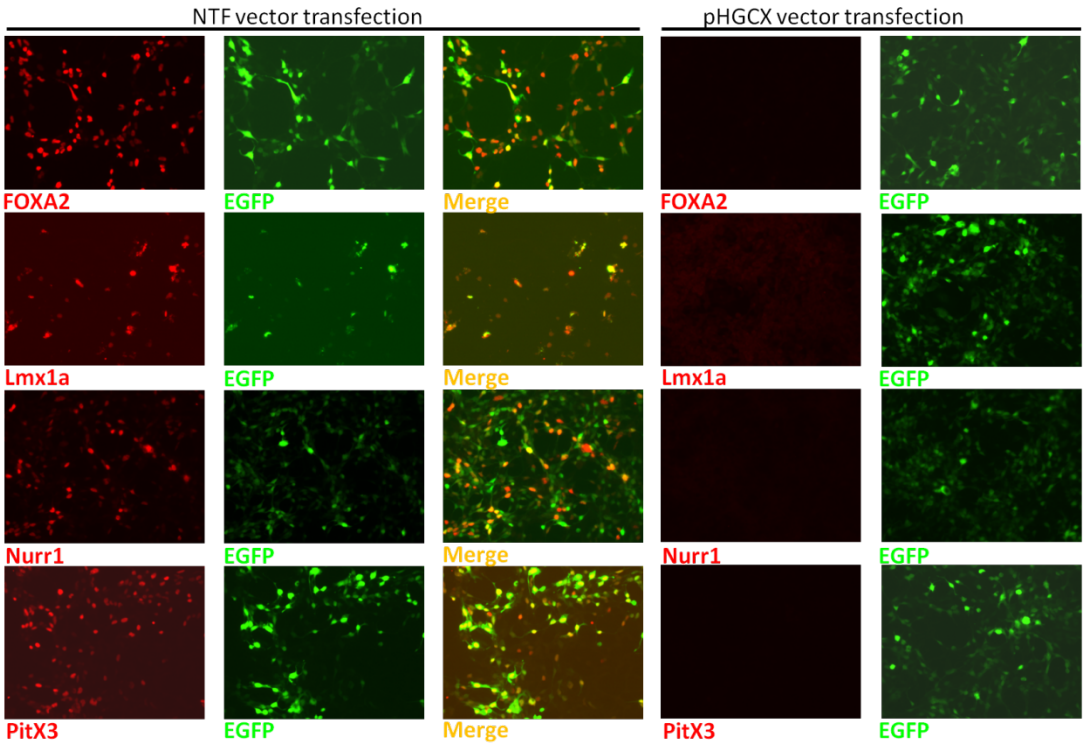


Figure 5 – Immunocytochemistry confirmation of Foxa2, LMX1A, Nurr 1 and PITX3 protein expression in NTF transfected HEK cells. NTF and pHGCX transfected HEKs (green) and immuno staining of Foxa2, LMX1A, Nurr1 and PITX3 (red). Merged images indicating co-localisation of the neuronal transcription factors and EGFP expression are shown in the middle panel.

6.6 NTF vector packaging

Our NTF vectors (pHGCX+Foxa2+EBNA+TetO2, pHGCX+LMX1A+EBNA+TetO2, pHGCX+Nurr1+EBNA+TetO2 and pHGCX+PITX3+EBNA+tetO2) were packaged alongside the polycistronic ANL vector from Chapter 5 (pHGCX+ANL+EbNA+tetO2) and pHGCX+EBNA+TetO2 or pHGCX control vectors for use in dopaminergic neuron differentiation experiments. HSV-1 amplicon titres of 10^7 TU/ml were obtained when packaged alongside the pcDNA6/TR tetracycline repressor plasmid. We did not purify vectors packaged without the repressor however single test plates packaged without the repressor appeared to have fewer replicating foci than plates packaged with the repressor.

6.7 Dopaminergic neuron differentiation protocol

We followed a dopaminergic neuron differentiation protocol adapted in our laboratory by E. Hartfield based on several publications [154, 173, 247, 266]. The protocol employed dual SMAD inhibition followed by SHH and FGF8a to differentiate embryoid bodies to dopaminergic neurons. First we plated embryoid bodies (EBs) derived from either NHDF1 or NHDF2 iPS lines; obtained from Jane Vowles at the Oxford Stem Cell Institute) onto Geltrex-coated 12 well plates at ~12-15 EBs per well. Throughout the protocol the EBs were incubated in a basic neuronal media containing DMEM/F12, L-Glutamine, N2 supplement (insulin, transferrin, sodium selenate, progesterone and puterscine), BSA and anitmyotic/antibiotic and a 50% change was made every 2-3 days. Additional growth factors were added to the basic medium to make the four neural inducing medias; neural induction media 1 (Nim1), Neural induction media 2 (Nim2), BDNF, Ascorbic acid, SHH and FGF8a (BASF) media and final differentiation media.

The EBs were incubated in Nim1, which contained Rho associated kinase (ROCK) inhibitor, and the SMAD inhibitors Noggin and SB431542, which together encourage ectodermal fate and inhibits BMP signalling and endoderm formation. After five days the media was changed to Nim2 containing ROCK inhibitor and high activity form Sonic Hedgehog (SHH), a morphogenic factor which is important in dopaminergic differentiation. On day 10 the media was changed to BASF medium, which contained BDNF, Ascorbic acid, SHH, FGF8a, heparin and ROCK inhibitor. On day 17 the cultures were manually passaged to select neural cultures and replated onto coverslips coated in laminin and Poly-L Lysine. The

dissected cultures were then incubated in a final differentiation media containing BDNF, GDNF, cAMP and ascorbic acid for 2-4 weeks. The protocol timeline including the medias, neuronal images and plating substrates are shown in Figure 6.

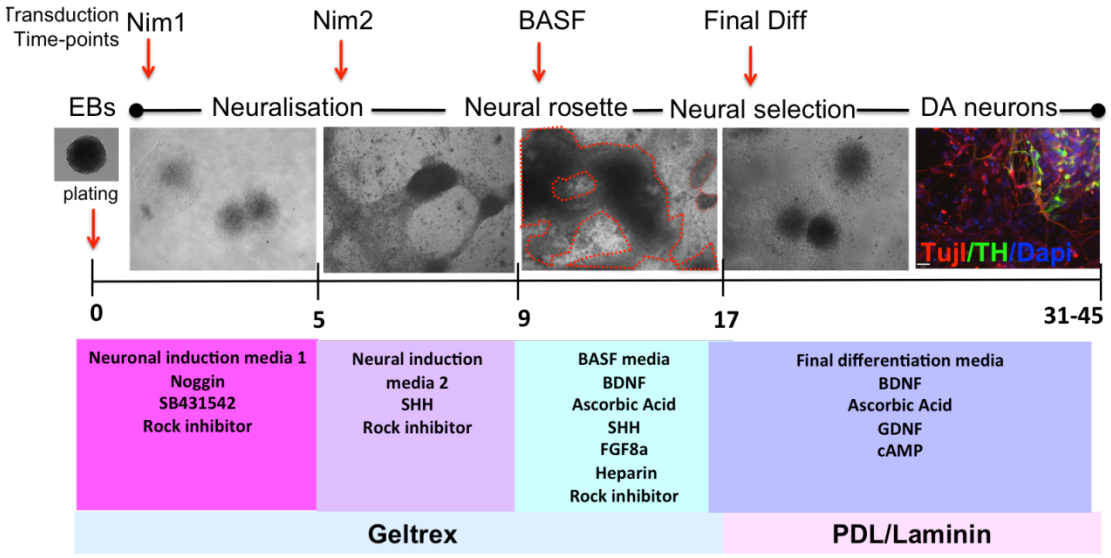


Figure 6 – Dopaminergic differentiation protocol and timeline. Embryoid bodies were plated on Geltrex and incubated in Neural induction media 1 (Nim1) for 5 days followed by Neural induction media 2 (Nim2) on days 5-9 and BASF media on days 9-17. Neural structures were selected (indicated by red dotted line) and replated onto Poly D lysine and laminin coated coverslips and incubated for 2-4 weeks in final differentiation media. The transduction timepoints were Nim1, Nim2, BASF and Final Diff, and are indicated by red arrows.

6.8 DA neuronal cultures HSV-1 amplicon transduction optimisation

Initial neuronal differentiation experiments were conducted to optimise amplicon MOI and confirm viability of our neuronal cultures. An MOI of 20 gave good transduction efficiency and neuronal cultures survived and successfully generated Tuj 1 and TH + neurons. However with a format of 12 EBs per well (~25,000 cells per EB) the number of conditions were limited due to needing an entire prep of amplicons for just one well. Therefore we adapted the protocol to a 96 well format (1 EB per well) to conserve HSV-1 amplicon stocks and reduce variability seen between wells.

The 96 well format (here-on referred to as "undissected") prevented us from dissecting the neural structures which meant that overall efficiency for TH positive cells were very poor with undissected cultures yielding ~1% TH+ cells compared to ~20% TH positive cells routinely obtained by E. Hartfield in our laboratory [267]. This was optimised further by culturing and transducing the EBs in cloning cylinders (1 EB per cyclinder) up until day 17 at which point the cloning cylinders were removed and the neural structures were dissected into 96 well plates for the final 2 weeks of differentiation (here-on referred to as "dissected"). The number of TH positive cells improved under these conditions to 5-12% total cells.

6.9 Dopaminergic neuron differentiation transduction time points

Using the 96 well (undissected) and cylinder (dissected) format we conducted transductions in the iPS cell lines NHDF1 and NHDF2 using a combination of all four of the NTF HSV-1 amplicons (referred to as "All 4", MOI 5 each, total MOI 20) compared with the polycistronic pHGCX+ANL+EBNA+TetO2 (referred to as "ANL", MOI 20) and the control amplicons pHGCX or pHGCX+EBNA+TetO2 (EBNA, MOI 20). Transductions were performed at 4 different time points and were assayed at the end of the differentiation protocol by cell counts and QPCR of TH and PAX6 expression.

Transductions were made 2 days after plating EBs (Nim1), on day 5/6 (Nim2), day 10 (BASF) or 2-3 days after neuronal dissection/change to final differentiation media (final differentiation). Example images demonstrating the transduction efficiency of the cultures when transduced with pHGCX+EBNA+TetO2 (MOI of 20) at the four different time points Nim1, Nim2, BASF and final differentiation are shown in Figure 7. We also performed a double transduction by re-transducing cells that were transduced at Nim1 a second time at Nim2.

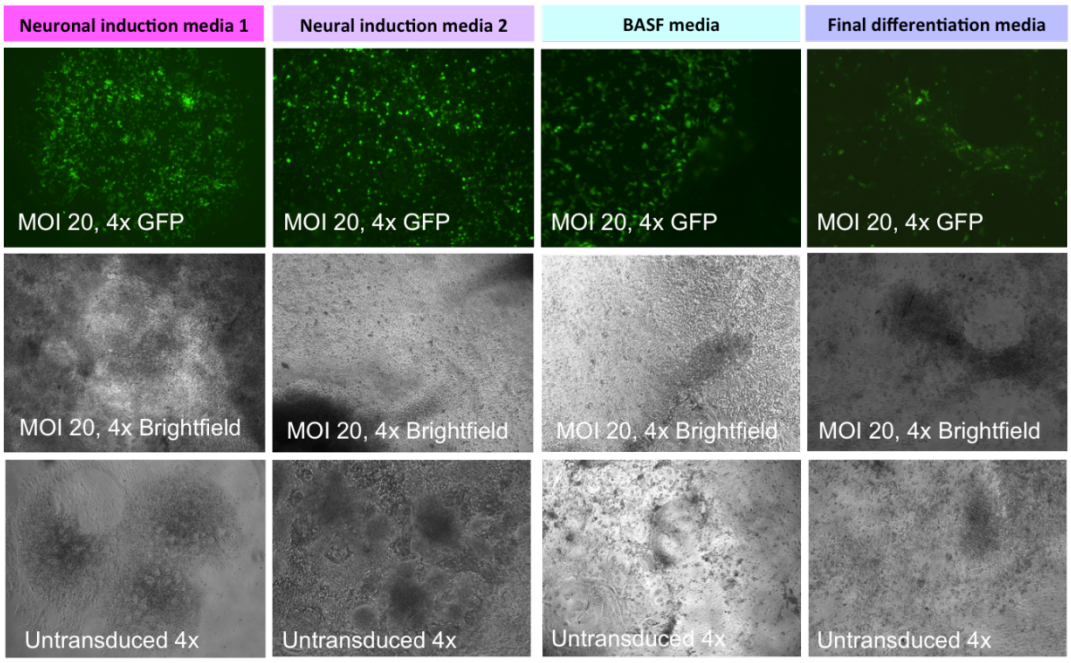


Figure 7 – Transduction of Dopaminergic Neuronal cultures with HSV-1 amplicons. Imaging of single transductions, taken at four different timepoints; Nim1, Nim2, BASF and final differentiation. Fluorescent, and bright field images of pHGCX+EBNA+TetO2 transductions (MOI 20) and untransduced NHDF2 cultures are shown.

At the end of the differentiation the cells were analysed by cell counts and qPCR to compare the four different transduction time points. The NHDF1 line differentiated poorly and was discarded from the analysis. Cells from the NHDF2 line were harvested from non-dissected culture wells for RNA-extraction and subsequent RT-PCR. We analysed expression of a pool of neuronal (PAX6, NESTIN and TUJ 1) and dopaminergic factors (TH, ENGRAILED1, PITX3, GIRK2 and NURR1)and the reference gene GAPDH from single untransduced and transduced wells of a 96 well differentation. Expression of all markers were observed and a representative RT-PCR from untransduced wells are shown, alongside immunostaining of untransduced neuronal cultures (TH and TUJ1)(Figure 8). We were unable to analyse dissected cultures by RT-PCR or

qPCR as the RNA yield from a single well of a 96 well plate following dissection was too low.

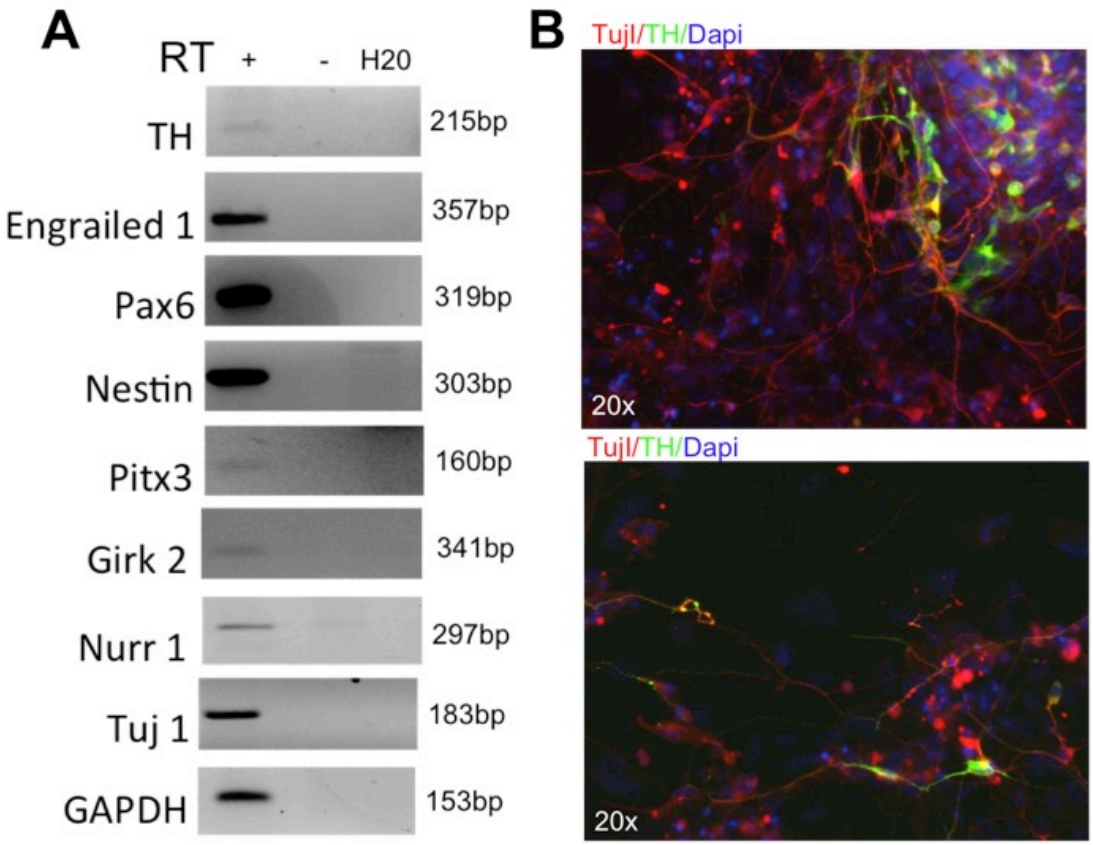


Figure 8 – RT-PCR analysis and immunocytochemistry confirmation of neuronal marker expression in untransduced dopaminergic neuronal cultures. A) Confirmation of TH, EN 1, PAX 6, NESTIN, PITX 3, GIRK 2, NURR 1, TUJ 1 and GAPDH expression in untransduced dopaminergic neuron differentiation cultures. No expression was observed in the negative non-RT control or water controls. **B)** Immunocytochemistry confirmation of dopaminergic marker TH (green) and neuronal marker TUJ 1 (red) expression in untransduced dopaminergic neuron differentiation cultures.

Cells from undissected cultures transduced at time points Nim1, Nim2, double transduced Nim1 and 2 and BASF were harvested for RNA extraction and subsequent qPCR expression. Expression of the dopaminergic markers TH and

the neuroectoderm marker PAX6 were analysed by qPCR normalised to the geometric mean of the three reference genes GAPDH, HPRT and ACTB2. In addition the dissected and undissected cultures were fixed and the number of TH positive cells were quantified by cell counts normalised to DAPI (total cells). All assays were statistically analysed by one-way Anova, Dunnett's multiple comparison test.

6.9.1 Analysis of cultures transduced at Nim1 time point

Cell transduction at the Nim1 time point induced significant upregulation of the dopaminergic neuron marker TH and neuroectoderm marker PAX6 were detected by qRT-PCR. A significant upregulation of TH expression was observed in cultures transduced with all four of the NTF amplicons (All 4) (x 4.72 fold increase, ** $p<0.01$) and ANL amplicons (x3.57 fold increase, * $p<0.05$) in comparison to untransduced cells. Transduction with EBNA control in these cells yielded an x 1.1 fold change however this was not significant. A significant upregulation of general neuroectoderm marker PAX6 was also observed in cultures transduced with ALL4 (x 1.83 fold increase, ** $p<0.01$) and ANL (x 2.59 fold increase, **** $p<0.0001$). Transduction with the EBNA control yielded a 1.2 fold change in expression, which was not significant. Cell counts were not performed at the Nim1 time point due to anti TH antibody failure. The qPCR results are presented in Figure 9.

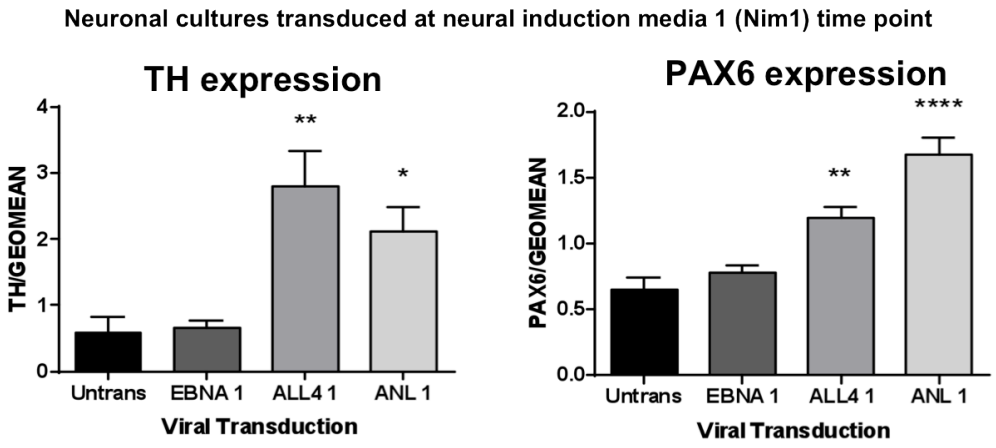


Figure 9 – qPCR analysis of TH and PAX6 expression in neuronal cultures transduced at the Nim1 time point. TH and PAX6 expression was normalised to the geometric mean of the reference genes gapdh, actb2 and hprt. Data was analysed by one-way Anova, Dunnett's multiple comparison test. (* $p<0.05$, ** $p<0.01$, **** $p<0.0001$).

6.9.2 Analysis of cultures transduced at Nim2 time point

Cultures transduced at time point Nim2 were analysed by qPCR of the dopaminergic marker TH and neuroectoderm marker PAX6 and quantification of TH positive cells. A small increase in TH expression was observed in cells transduced with ALL4 and ANL compared with untransduced cultures however the change was not significant. Transduction with the control amplicon EBNA yielded comparatively higher TH expression than the ALL4 and ANL transduced cultures. Expression of PAX6 was ~2 fold higher in ANL transduced cultures compared with untransduced cultures however this change was not significant.

The number of TH positive cells in dissected and undissected cultures were quantified and normalised to total cells (DAPI). The number of TH positive cells was increased in undissected ALL4 and ANL transduced cultures however this change was not significant, consistent with the qPCR data. A similar increase in

the number of TH positive cells was observed in dissected cultures however this increase was also observed in the EBNA transduced control. The results are presented in Figure 10.

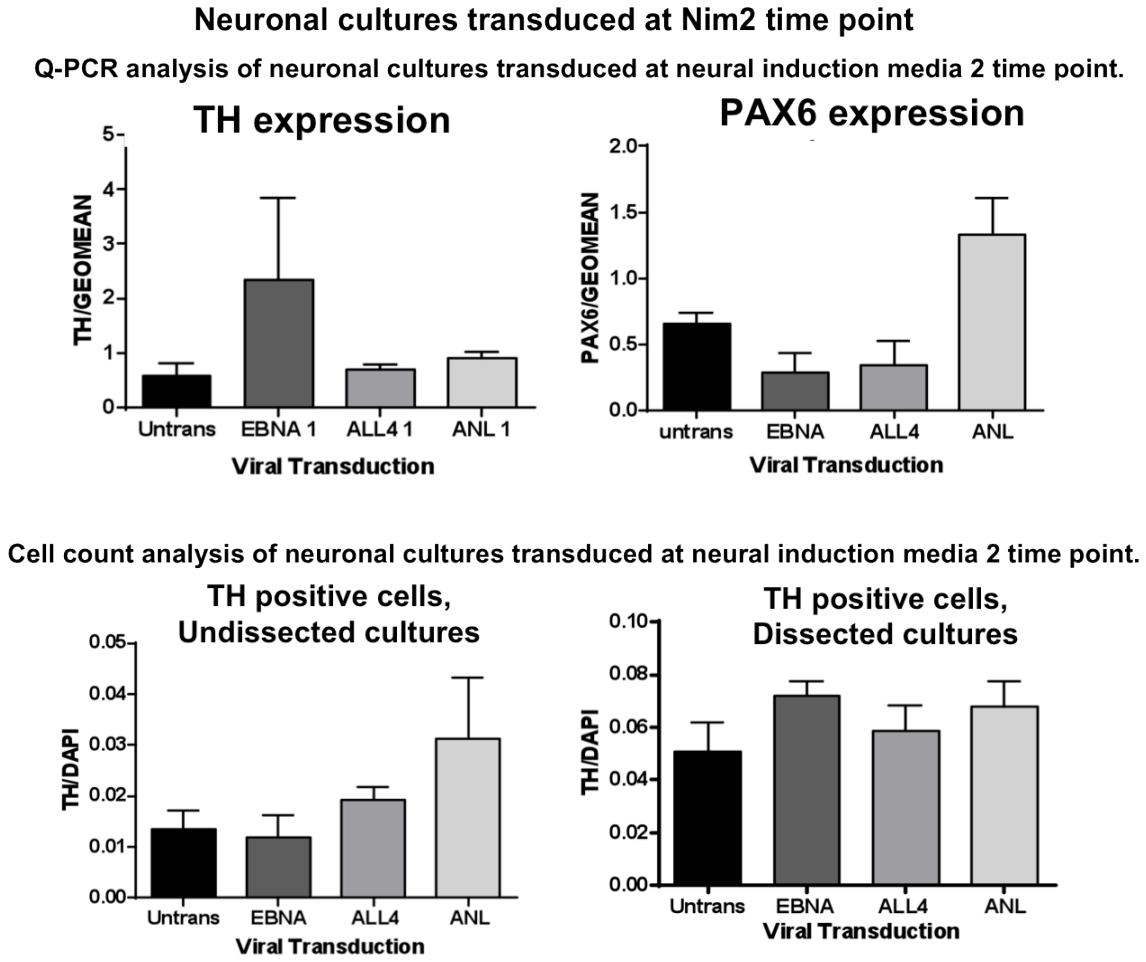


Figure 10 – qPCR analysis of TH and PAX6 expression and quantification of TH positive cells in neuronal cultures transduced at the Nim1 time point. TH and PAX6 expression was normalised to the geometric mean of the reference genes gapdh, actb2 and hprt. Data was analysed by one-way Anova, Dunnett's multiple comparison test. The number of TH positive cells was quantified by cell counts normalised to DAPI (total cells). No significant differences were found.

6.9.3 Analysis of cultures double transduced at Nim1 and Nim2 time points

Double transduced cultures were analysed by qPCR for TH and PAX6 expression. An increase in TH expression was observed in ALL4, ANL and EBNA transduced cultures in comparison to untransduced controls. Whereas the upregulation of TH in ANL transduced cultures were not significant, significant changes were observed in ALL4 (*** $p<0.001$) and EBNA transduced cultures (* $p<0.05$). The expression of the general neuroectodermal marker PAX6 was not upregulated by NTF amplicon transduction. Cell counts were not performed due to technical difficulties with the antibody. The TH and PAX6 qPCR results are presented in Figure 11.

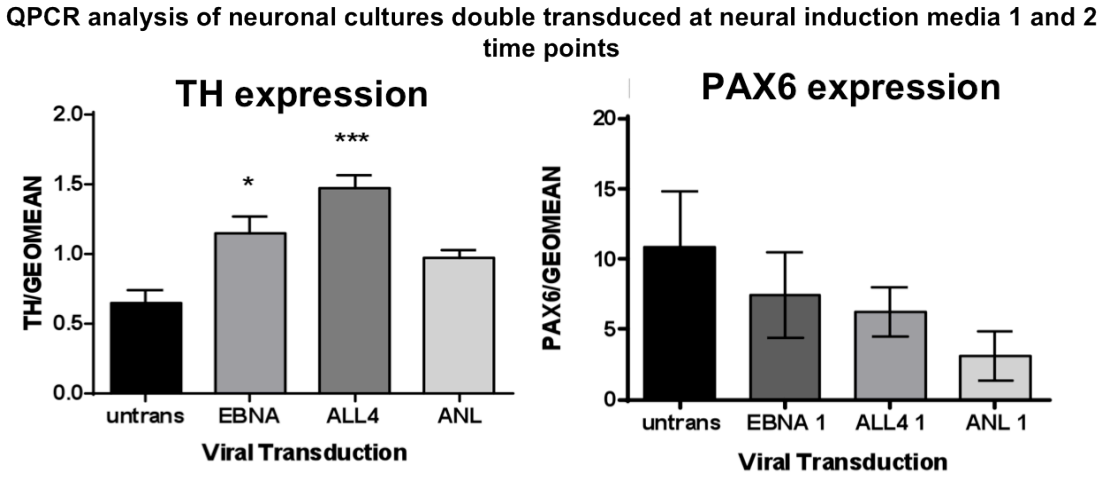


Figure 11 – qPCR analysis of TH and PAX6 expression in neuronal cultures double transduced at the Nim1 and Nim2 time points. TH and PAX6 expression was normalised to the geometric mean of the reference genes gapdh, actb2 and hprt. Data was analysed by one-way Anova, Dunnett's multiple comparison test (* $p<0.05$, ***$p<0.001$).

6.9.4 Analysis of cultures transduced at BASF time point

Cell count analysis of dissected cultures transduced at the BASF time point did not result in increased number of TH positive cells. Increased TH and PAX expression was observed in pHGCX and ALL4 transduced cultures however the changes were not significant. The results are shown in Figure 12.

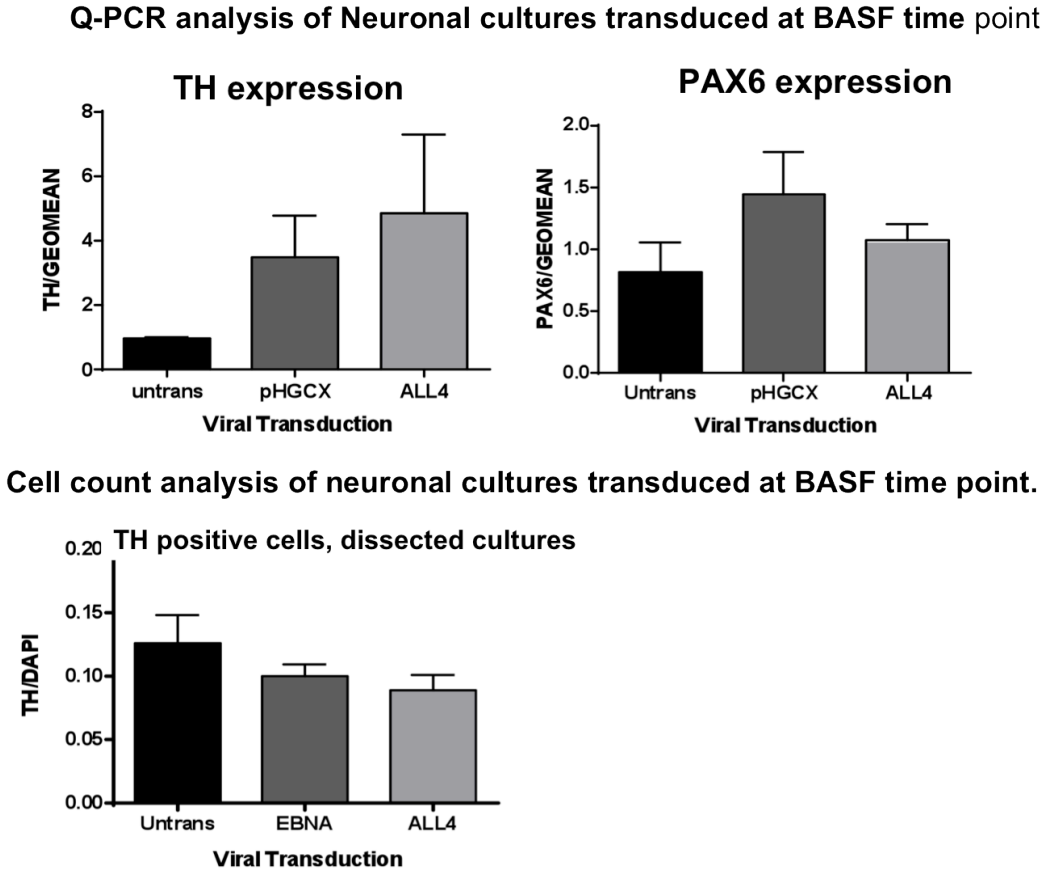


Figure 12 – qPCR analysis of TH and PAX6 expression and quantification of TH positive cells in neuronal cultures transduced at the BASF time point. The number of TH positive cells was quantified by cell counts normalised to DAPI (total cells). TH and PAX6 expression was normalised to the geometric mean of the reference genes gapdh, actb2 and hprt. Data was analysed by one-way Anova, Dunnett's multiple comparison test. No significant differences were found.

6.9.5 Analysis of cultures transduced at final differentiation time point

Analysis of undissected cultures transduced at the final differentiation time point resulted in a x2.39 fold increase in TH expression in ALL4 transduced cultures compared with untransduced cultures. This increase was significant (* $p<0.05$) whereas the x1.6 fold increase seen in pHGCX-transduced cultures was not significant. The results are shown in Figure 13.

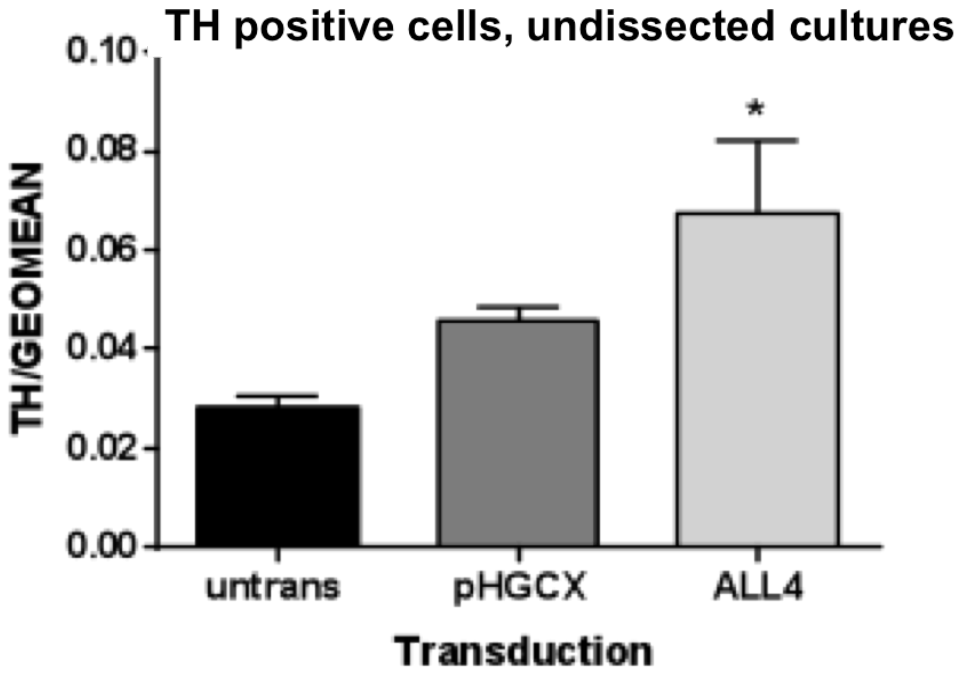


Figure 13 - Quantification of TH positive cells in neuronal cultures transduced at the Final differentiation time point. The number of TH positive cells was quantified by cell counts normalised to DAPI (total cells). Data was analysed by one-way Anova, Dunnett's multiple comparison test (*$p<0.05$)

6.10 Conclusion and summary

We successfully constructed four HSV-1 vectors individually carrying the four neuronal transcription factors (NTF) Foxa2, LMX1A, Nurr1 and PITX3. Sequencing of the neuronal transcription factors and restriction digests confirm that the factors were the correct sequence and inserted in the right orientation. Single base changes were detected in LMX1A, Nurr1 and PITX3 but the mutations were silent. Expression of the four NTFs were confirmed by Western blot and imunocytochemistry of transfected HEK cells and no expression was detected in the pHGCX negative controls as expected. Merged images of the immuno-stained cells indicate colocalisation of the NTFs with the exogenous EGFP reporter. The relative intensity of GFP was variable however we did not use an anti-GFP antibody, and it is possible that the GFP signal could have been quenched during the fixation process. We were able to obtain NTF amplicon titres of 10^7 TU/ml when packaged alongside the PCDNA6/TR plasmid.

Differentiation experiments were initially carried out in the original format of 15 EBs in a 12 well plate however this quickly depleted amplicon stocks. I optimised the protocol to be in 96 well format which allowed efficient transduction of single EBs. However in this format the total number of TH positive cells was around 1%, a lot lower than published efficiencies of 20% TH positive cells. We hypothesised that this decrease in efficiency could be due to omission of the neuronal dissection stage, which discards many of the non-dopaminergic cells, which would dilute out the TH positive population.

To rectify this I devised a way of transducing single EBs in a low volume/surface area but still enabling manual dissection of neuronal structures. This was achieved by plating EBs in cloning cylinders that could be removed following the BASF stage to allow dissection of the neuronal structures. This method improved the total TH efficiency to ~12% TH positive cells however this is still much lower than the expected 20%. This reduced efficiency may be due to the single EB format.

Our differentiating neuronal cultures transduced efficiently at all four time points. We observed significant induction of dopaminergic marker expression when transduced with all four of the NTF HSV-1 amplicons (ALL4) and the polycistronic NTF HSV-1 amplicon vectors (ANL). We saw a significant increase in the dopaminergic marker TH and general neuroectoderm PAX6 expression when transduced with ALL4 or ANL at the early time point Nim1 when compared to untransduced cultures. The increased expression of both the dopaminergic TH and general neuroectormal PAX6 suggests that NTF amplicon transduction at this time point, may generally increase neuronal differentiation. Significant increase in TH expression was also observed in cultures double transduced at time points Nim1 and Nim2 with ALL4 NTF HSV-1 amplicons compared to untransduced controls, indicating that a double amplicon transduction at two time points may specifically increase dopaminergic differentiation, rather than general neuronal differentiation. A significant increase in TH positive cells was also seen in cultures transduced with ALL4 NTF HSV-1 amplicons at the late final differentiation time point in comparison to untransduced cultures. These results indicate that increased dopaminergic

neuron factor induction occurs when the cultures are transduced with neuronal transcription factors at the Nim1 time point, however specificity improves when transduced at the Nim2 time point in addition to the Nim1 timepoint. Transduction at the final differentiation timepoint also results in a significant increase in TH expression however the general marker PAX6 was not analysed when transduced at this time point.

Given that a combination of factors was used, a reasonable explanation for the differences in efficiency at different time points could be that one or some of the factors are effective early in the differentiation protocol and one or some of the factors are effective late in the differentiation protocol. It is known that FOXA2 and LMX1A are expressed early on in neurogenesis compared with PITX3 and NURR1 which act directly on the TH promoter later in the pathway (reviewed in Chapter 1) so this could be a possible explanation for the enhancement of TH expression/TH positive cells at the two different time points.

RT-PCR analysis of neuronal markers such as ENGRAILED1, TUJ1 and PAX6 was performed to confirm that our cultures had a neuronal phenotype. Engrailed 1 is a homeodomain protein, which specifies midbrain development and spatial patterning of Wnt 1, whereas Tuj1 is a general neuronal marker and Pax6 is a general neural ectoderm marker. Dopaminergic markers such as TH, PITX3, GIRK2 and NURR1 confirmed the dopaminergic profile of our cultures. TH is the rate-limiting enzyme in dopamine synthesis and is expressed in midbrain DA neurons and the G-protein–regulated inward-rectifier potassium 2 (GIRK2) channel modulates neuronal excitability and is localised within ventral tier SNC

neurons. PITX3 and NURR1 are DA markers, and we were able to distinguish endogenous expression by using human specific primers that do not detect the mouse PitX3 or rat Nurr1.

Additonal dopaminergic markers such as Nurr1 and PitX3 were not analysed quantitatively by qPCR to determine whether expression of these key markers was increased in our amplicon-transduced cultures. Given that we only analysed one dopaminergic marker (TH) by qPCR in addition to the neuroectoderm marker (PAX6) and general neuronal marker (TUJ1), it would be beneficial to extend this analysis to include other DA markers such as GIRK2 and PITX3. In future the panel of markers to analyse by RT-PCR and qPCR should be expanded to include additional DA markers such as the dopamine transporter (DAT), vesicular monoamine transporters (VMAT), aromatic l-amino acid decarboxylase (AADC) and aldehyde dyhydrogenase 2 (ADH2) may help to determine the maturity of the DA neuron population. DAT, VMAT2 and AADC are direct targets of Nurr1 and ADH2 is direct target of PitX3, therefore analysis of their expression compared to untransduced controls may determine whether Nurr1 and PitX3 are having an effect. Similarily, comparison of expression levels of ASCL1, NGN2, NURR1 and PITX3 may be indicative of LMX1A activation and LMX1A and NURR1 expression may demonstrate FOXA2 activation.

These results show that our HSV-1 NTF amplicons effectively induce dopaminergic neuron differentiation in the iPS line NHDF2 and are capable of enhancing expression of the dopaminergic neuron markers TH and PAX6. These experiments need to be repeated in several iPS lines and in multiple

differentiation experiments in order to confirm the results. In addition different combinations of the factors would need to be made in order to establish which factors were inducing TH expression at the Nim1 timepoint and which factors were inducing TH positive cells in the final differentiation time point.

Finally once time points and factor combinations are established it would be interesting to repeat in a larger scale, i.e. original differentiation protocol conditions of 15 EBs per well of a 12 well plate, to see if the factors could exceed the published efficiencies of ~20% TH positive cells. Given the 2.4 fold increase of TH positive cells seen when transduced at the final differentiation time point, estimated efficiencies when performed on a larger scale would be around 48% TH positive cells.

In conclusion we have developed a set of NTF HSV-1 amplicon vectors, which are capable of enhancing TH population efficiencies in a single iPS line, however more experiments would need to be performed in several cell lines to confirm the results.

Chapter 7 – General Discussion

7.1 Aims

When I started the DPhil there was a distinct lack of efficient, non-integrating methods of deriving iPS cells. Whereas integrating reprogramming methods such as lentiviral delivery were capable of generating iPS cells with an efficiency of around 0.02% [16], non-integrating alternatives were often labor intensive and had a relative reprogramming efficiency of 0.0006% [94]. In addition, although iPS have the potential to generate almost any cell type, the generation of dopaminergic neurons were not very efficient and strategies were needed in order to enhance dopaminergic neuron populations [173]. A third field that has accelerated in recent years is the field of direct differentiation, however similar technical difficulties remain such as the use of integrating vectors and the poor differentiation efficiency [175].

Herpes simplex virus type-1 amplicon vectors provide a promising alternative to integrating vectors due to their large transgene capacity and high transduction efficiency in fibroblasts [196], iPS cells [268] and neuronal precursors. The high transgene capacity allows the insertion of additional elements to allow the episomal retention of the plasmid in dividing cells and the insertion of multiple genes of interest. Using this system our aim was to develop an improved system for the generation and differentiation of iPS cells and the direct differentiation of fibroblasts to dopaminergic neurons.

7.2 Summary of findings

In Chapters 3 and 4 we developed a set of reprogramming vectors expressing multiple reprogramming factors with optimal factor stoichiometry. We successfully generated small EGFP+ colonies with granulated morphology however these colonies did not expand in size or have typical iPS colony morphology of high nucleus to cytoplasm ratio, tightly packed cells and a defined colony edge. Pluripotency marker gene analysis demonstrated that the colonies were partially reprogrammed and expressed five pluripotency markers including the late markers endogenous OCT-4 and endogenous NANOG.

Further reprogramming experiments co transducing fibroblasts with HSV-1 amplicons and the Sendai virus positive control resulted in significantly reduced colony numbers in cultures transduced with both HSV-1 amplicon and Sendai virus compared with cultures transduced with Sendai virus alone. Quantitative RT-PCR analysis of these cultures revealed a significant upregulation of P53 and it's downstream target P21, which are known barriers in cellular reprogramming [225, 269]. Our Western blot data was inconclusive in confirming these findings and unfortunately the pifithrin experiments were unsuccessful, most likely due to the higher passage of our JRO-53 fibroblasts.

In Chapter 5 we successfully generated a tri-cistronic HSV-1 amplicon vector expressing the three neuronal transcription factors Ascl 1, Nurr1 and Lm1xa. Characterisation by Western Blot and RT-PCR confirmed functionality of the vector however we were unable to generate dopaminergic neurons. Some positive staining with βIII tubulin and Tyrosine Hydroxylase (TH) was observed

however the staining was also present in the negative control conditions (untransduced cultures and pHGCX+EBNA+TetO2-transduced cultures).

In Chapter 6 we successfully generated four HSV-1 amplicon vectors individually carrying the four neuronal transcription factors FoxA2, LMX1A, Nurr1 and PITX3. These vectors were confirmed to be functional by Western blot and Immunocytochemistry and sequencing analysis confirmed the transgenes were free of mutations. Differentiating cultures were transduced with the four NTF HSV-1 amplicons or the polycistronic ANL vector at different time points to establish temporal requirements of the transcription factors. Dopaminergic neuron efficiency, analysed by TH positive cell counts and/or quantitative RT-PCR analysis of TH and PAX6, was significantly increased in cultures transduced at the earliest time point (Nim1) or the latest time point (Final differentiation).

7.3 HSV-1 amplicons and reprogramming barriers

The upregulation of p53 in HSV-1 amplicon transduced cultures in Chapter 3 in comparison to untransduced cultures and those transduced with Sendai virus suggest that HSV-1 is inducing p53 expression. In addition, the expression of the p53 downstream target p21 suggests that p53 is transcriptionally activating the p53-p21 senescence pathway, rather than remaining in the inactive form bound to MDM2. Given that p53 activation is a known barrier for reprogramming [218, 225, 269-272], this induction may explain why our reprogramming experiments failed to reach complete pluripotency.

So far there have been no reports of a successful HSV-1 amplicon reprogramming system. However, it is unknown whether this is due to nobody attempting to develop an HSV-1 amplicon reprogramming vector or whether people have tried and failed. Interestingly, there has been one reported attempt at reprogramming of a tumour cell line using a herpes virus family member – herpes virus saimiri based vectors [273]. The authors were able to generate iPS like colonies that exhibited some iPS characteristics such as prolonged culture under stem cell conditions and expression of the pluripotency markers endogenous OCT-4, REX-1 hTERT, AP, SSEA4 and KLF-4. However the lines were only capable differentiation toward the ectodermal lineage, suggestion a multipotent nature. Although this system was more successful than our own HSV-1 amplicon reprogramming, the use of a tumourigenic cell line could be responsible for the improved efficiency, due to likely disruptions in cell cycle regulation.

7.4 HSV-1 amplicons and direct differentiation

Our results from Chapter 4 show that HSV-1 amplicons induce expression of p53 and downstream p21 in transduced fibroblasts. We analysed recent publications of direct differentiation to assess whether p53 acts as barrier in direct differentiation. Although there have been no direct reports of an inhibitory role of p53 on direct differentiation, improvements in direct differentiation efficiency have been achieved by employing small molecule inhibitors (SB-431542, CHIR and dorsomorphin) and enhancers (Forskolin) that indirectly effect p53 regulation [274]. These findings are discussed below.

There have been several publications which have investigated the use of small molecule enhancers and inhibitors to increase direct differentiation efficiency and neuronal differentiation efficiency from iPS cells [274]. O. Brustle and colleagues increased direct differentiation efficiency by employing the small molecules Noggin, SB-431542 (a transforming growth factor-beta receptor type-1 (TGFR-1) inhibitor) and CHIR99021 (a Glycogen synthase kinase-3 beta (GSK3-β) inhibitor). Together the small molecules increased efficiency of neuronal differentiation by 17-fold [275]. This is particularly interesting due to GSK-3β's role as a facilitator of pro-apoptotic factors such as p53. GSK-3β phosphorylates residues in p53 to prevent interaction with MDM2 and subsequent ubiquitination and proteosomal degradation mediated by MDM2. Phophsorylation of p53 thereby stabilises p53 and induces apoptosis. GSK-3β inhibitors sequester GSK-3β, p53 and MDM2 to the cytoplasm where p53 can not act on it's target genes and is coupled with MDM2, preventing apoptosis [276]. The GSK-3β inhibitor alone increased differentiation efficiency by 4 fold suggesting a key role for GSK3 subsequently p53 as negative regulators of trans-differentiation.

The action of the TGFR-1 inhibitor SB-431542 is also interesting as TGFβ is also linked with p53. TGFβ signaling relies on p53 and smad to activate TGFβ transcription. Activation of the target gene p21 requires both TGFβ and p53 binding to induce cell arrest [277] [278]. Thus SB-431542 inhibition of TGFβ also prevents interaction with p53 and downstream activation of p21.

The relationship of TGFβ and GSK3β with p53 and the improved efficiency seen by inhibition of these factors suggest that p53 could have an inhibitory role on trans-differentiation. This is further supported by the study by C. Zhang and colleagues in May 2013 who were able to convert human lung fetal fibroblasts to cholinergic neurons by a combination of the small molecules forskolin and dorsomorphin and the transcription factor neurogenin 2 (Ngn2) [279]. Using Ngn2 as a candidate gene the authors screened a pool of seven small molecules and found that Forskolin induced Tuj1 positive cells 7 days after infection in a dose dependant manner however the cells died before developing into MAP2 positive mature neurons. The addition of dorsomorphin was needed to promote neuron survival. The p53 pathway and its interaction with the genes AMPK. GSKβ, TGFβ and cAMP are shown in Figure 1.

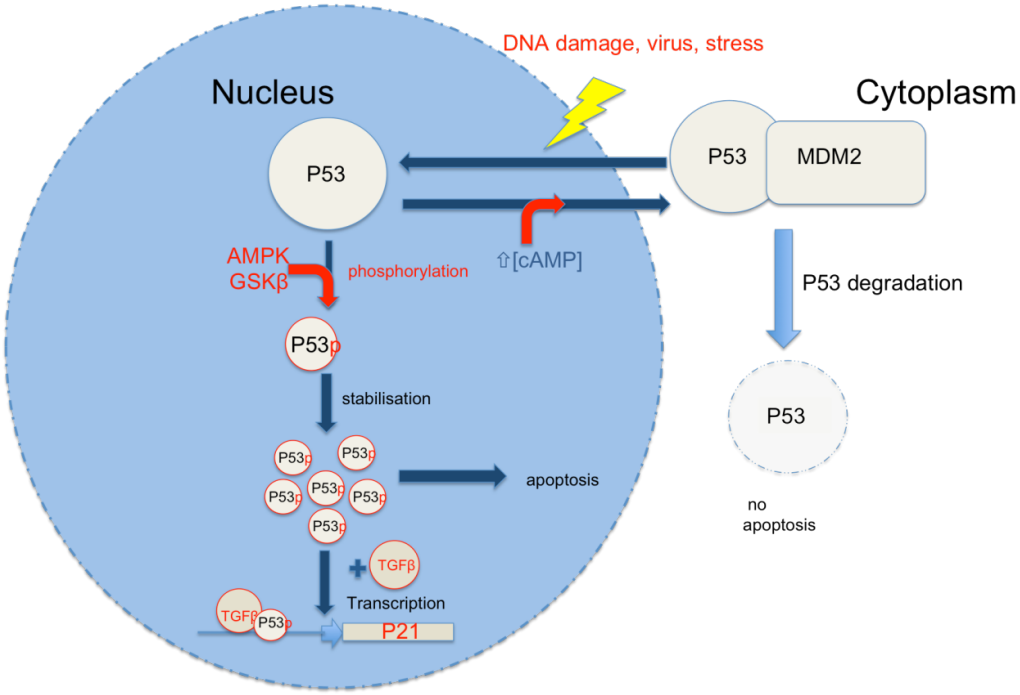


Figure 1 – p53 pathway in response to DNA damage and cellular stress. – In response to DNA damage and stress p53 uncouples from HDM2 in the cytoplasm and relocates to the nucleus where it undergoes post-translational phosphorylation by AMPK and GSKβ, which leads to stabilization of p53 and transcriptional activation of target genes and/or apoptosis. TGFβ is required to transcriptionally activate the gene p21, which induces cell cycle arrest. Increased levels of cAMP induces the p53 to recouple with MDM2.

Forskolin is a cAMP activator. When DNA damage occurs p53 becomes uncoupled from HDM2 and initiates apoptosis, however when cAMP levels are high p53 remains coupled to MDM2 and is degraded [280]. Addition of Forskolin would increase cAMP levels and therefore inhibit p53. Similarly dorsomorphin also inhibits p53 induced apoptosis by preventing phosphorylation by AMPK [281].

These small molecule inhibitors and enhancers have been shown to enhance fibroblast to neuronal transition in direct reprogramming experiments. Each of these small molecules inhibit or enhance factors, which interact with the p53 pathway resulting in an inhibition of p53 phosphorylation and transcriptional

activation of target genes. Together the action of these small molecule inhibitors and enhancers on the p53 pathway suggest a negative role for p53 in transdifferentiation. The action of the small molecule enhancers and inhibitors are shown in Figure 2.

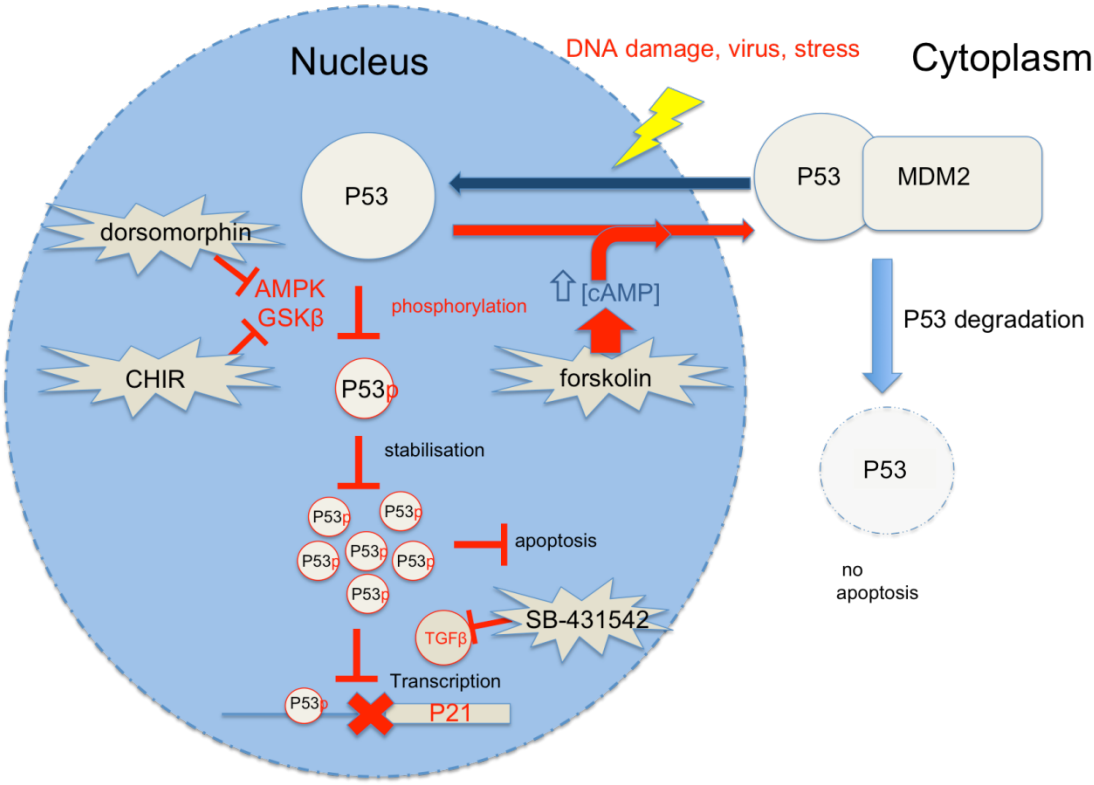


Figure 2 - Action of small molecule inhibitors on p53 homeostasis. The small molecules Dorsomorphin and CHIR inhibit the enzymes AMPK and GSKβ preventing phosphorylation of p53 and subsequent stabilization and of p53 and activation of apoptotic pathways. The small molecule SB-431542 inhibits TGFβ which acts with p53 to transcriptionally activate genes such as p21 and Forskolin activates cAMP, driving p53 to re-couple with MDM2 in the cytoplasm.

Particular compounds such as CHIR, SB-431542, forskolin and dorsomorphin act on genes involved in the p53 pathway, subsequently inhibiting p53 induced apoptosis and transcriptional activation of genes such as p21. Together these results suggest a negative role for p53 on direct differentiation, which is further

supported by the report published in May 2013, which states that p53 inhibition accelerates neurogenesis [282]. Our results from Chapter 4 indicate that HSV-1 amplicon transduction induced p53 and possibly p21 expression in our reprogramming experiments. We hypothesise that this p53 induction is also preventing direct differentiation of fibroblast to dopaminergic neurons.

7.5 HSV-1 amplicons and dopaminergic neuronal differentiation experiments

We were able to improve dopaminergic neuronal differentiation efficiency via the delivery of neuronal transcription factors (NTF) using HSV-1 amplicon transduction. The link between p53 and neuronal differentiation is unclear, and we did not check p53 expression levels in neurons post-transduction in our study. One previous study suggests that p53 $^{(-/-)}$ neural stem cells have accelerated neurogenesis due to BMP/SMAD1 regulation *in vivo* [282]. Conversely, another study suggests that p53 activation in cultured mouse neurons increases neurite outgrowth via the upregulation of the genes Corin1b and Rab13 [283]. That study demonstrated that Corin1b and Rab13 upregulation is induced by post-translational acetylation of serine-320 (which induces cell survival pathways) rather than acetylation of serine 372 (which induces cell death pathways). A third study demonstrated that negative regulation of p53 by SCY1-like 1–binding protein 1 resulted in decreased neurite outgrowth and morphogenesis *in vivo* [284].

It is possible that HSV-1 amplicon induction of p53 may be advantageous to neuronal differentiation if followed by acetylation at serine 320 and subsequent

activation of cell survival pathways. This also may explain the unexpected upregulation in TH when transduced with our control amplicon pHGCX+EBNA+TetO2 (Figure 11, Chapter 6). This is also supported by the known success of HSV-1 delivery and tolerance in postmitotic neurons [285]. It is also possible that upregulation of p53 induced by our amplicons could be counteracted by the presence of the small molecules (SB-431542 and cAMP) in our neuronal culture media or by Nurr1 suppression of p53 transcriptional activity [286].

7.6 Wild type HSV-1 and p53 induction

Experiments using wild-type and mutant HSV-1, as well as HSV-1 amplicons allow us to understand the roles that immediate early genes and tegument proteins play in p53 pathways and cellular response. The structure and gene expression in wild type HSV-1 and HSV-1 amplicons are shown in Figure 3.

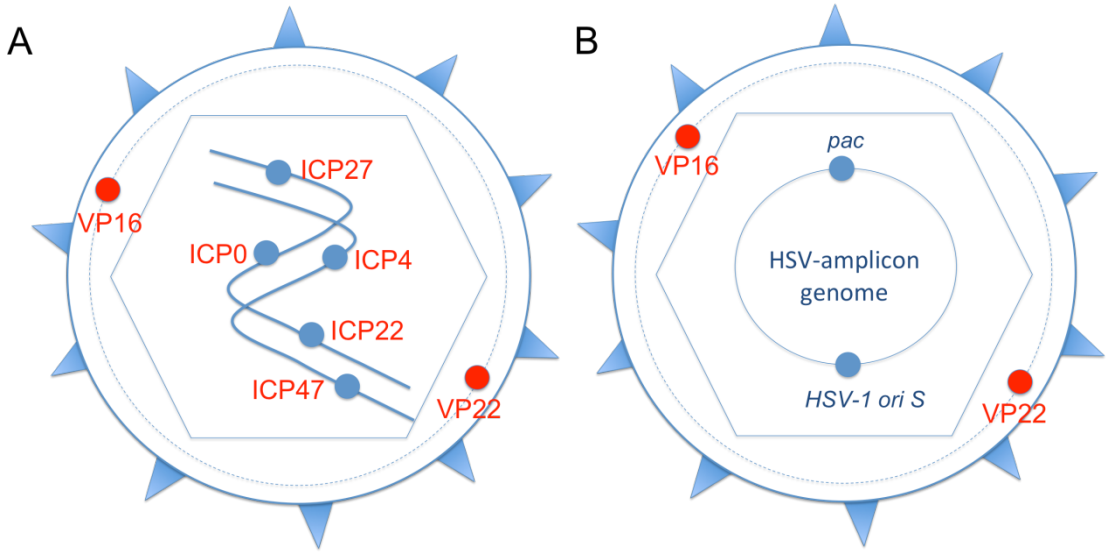


Figure 3– Viral structure and gene expression of A) wild type HSV-1 virions and B) HSV-1 amplicon virions. Both HSV-1 virions are composed of a viral envelope containing 10 glycoproteins to facilitate viral entry. Within the envelope is the tegument, which is composed of many proteins including VP16 and VP22. The HSV-1 viral genome (A) or HAV-1 amplicon genome (B) is enclosed within the viral capsid.

Regulation of p53 expression and post-translational modifications is complex during wild type HSV-1 infection and is subject to various cellular and viral factors. The tumor suppressor gene p53 is involved in numerous cell pathways such as cell cycle regulation, apoptosis, transcriptional activation, DNA repair, autophagy and senescence. Wild-type infection of HSV-1 results in increased levels of cellular p53 due to PI3 kinase phosphorylation of p53 and subsequent stabilization of the protein [287]. Contrary to our own observations using HSV-1 amplicons, no increase in mRNA expression of the gene was observed during wild-type HSV-1 infection. This may be due to expression of the immediate early gene ICP27, which inhibits host protein synthesis [287].

The immediate early protein ICP0 counteracts stabilization of p53 by two mechanisms, the first is by degradation of the catalytic subunit of PI3K, preventing phosphorylation of p53. In addition, ICP0 is a RING finger ubiquitin E3 ligase, which mediates ubiquitination of a subset of p53 molecules and subsequent degradation of the p53 protein, albeit at a lower frequency than the host ubiquitin ligase MDM2 [288]. Expression of ICP0 was able to prevent UV induced apoptosis in U2OS cells, an osteosarcoma cell line, however these results could not be reproduced in hFFF2 cells, a non-transformed human fetal foreskin fibroblasts cell line [288]. Although these findings suggest an inhibitory role for ICP0 on p53 regulation, comparison of the HSV-1 mutant d106 (defective for all viral genes except ICP0) with the mutant d109 (defective for all viral genes) resulted ICP0 dependent cell arrest and p53 independent upregulation of the p53 response genes p21, MDM2 and GADD45 [289].

Further evidence to suggest an HSV-1/host p53 pathway interaction is the finding that ICP0 is targeted for degradation by the gene SIAH-1 [290]. SIAH-1 is the human homologue of *Drosophila seven in absentia* and is a p53-inducible mediator of cell cycle arrest [291]. Interestingly, some evidence suggests that p53 induction plays an anti-apoptotic role during HSV-1 infection and is due to cellular defence against herepes virus dependent apoptosis (HDAP). Nuguyen and colleagues demonstrated in 2007 that this apoptotic balance is maintained by expression of ICP27 and the upregulation of p53 during infection, which prevents apoptosis by inducing cell arrest [292].

The immediate early gene ICP22 has also been demonstrated to be involved in p53 regulation through direct binding of ICP22 with the MDM2 promoter, the negative regulator of p53. Expression of MDM2 is normally controlled by negative feedback regulation of the p53 protein whereby increased p53 levels induce MDM2 expression and subsequent degradation of the p53 protein. Binding of the ICP22 protein to the MDM2 promoter prevents this trans-transcriptional interaction and results in increased p53 levels [293].

A recent study has also demonstrated that ICP22 directly interacts with p53. The role of p53 on viral replication was investigated by directly comparing the effect of p53 on wild type HSV-1 with ICP22 null viruses. The authors found that p53 upregulated ICP27 expression early during infection when expressed in combination with the tegument protein VP16. In addition, p53 was shown to down-regulate ICP0 expression in ICP22 null HSV-1 but not in wild type HSV-1, indicating that ICP22 prevents downregulation of ICP0 by p53 [294].

The observation that p53 can effect regulation of the immediate early genes is supported by the finding that the acidic transcriptional activation domain (TAD) is homologous to the TAD domain of the tegument protein VP16. Both VP16 and p53 have been shown to share binding partners and have been demonstrated to both bind to the same region of the Transcription Factor II Human (TFIIH), which is one of the transcription factors that make up the RNA polymerase II pre-initiation complex [295]. The significance of this finding remains to be seen but suggests that they may share transcriptional targets.

Together these results demonstrate a fine balance between cellular and viral control of p53 degradation, stability and expression. Given that HSV-1 amplicons do not encode the HSV-1 genome, induction of p53 expression is not subject to viral response signals encoded by the immediate early genes. A schematic of p53 regulation in non-stressed cells compared with cells exposed to stresses such as viral infections and DNA damage is shown in Figure 4. The regulation of p53 in wild type HSV-1 infected cells compared with cells transduced with HSV-1 amplicons is shown in Figure 5.

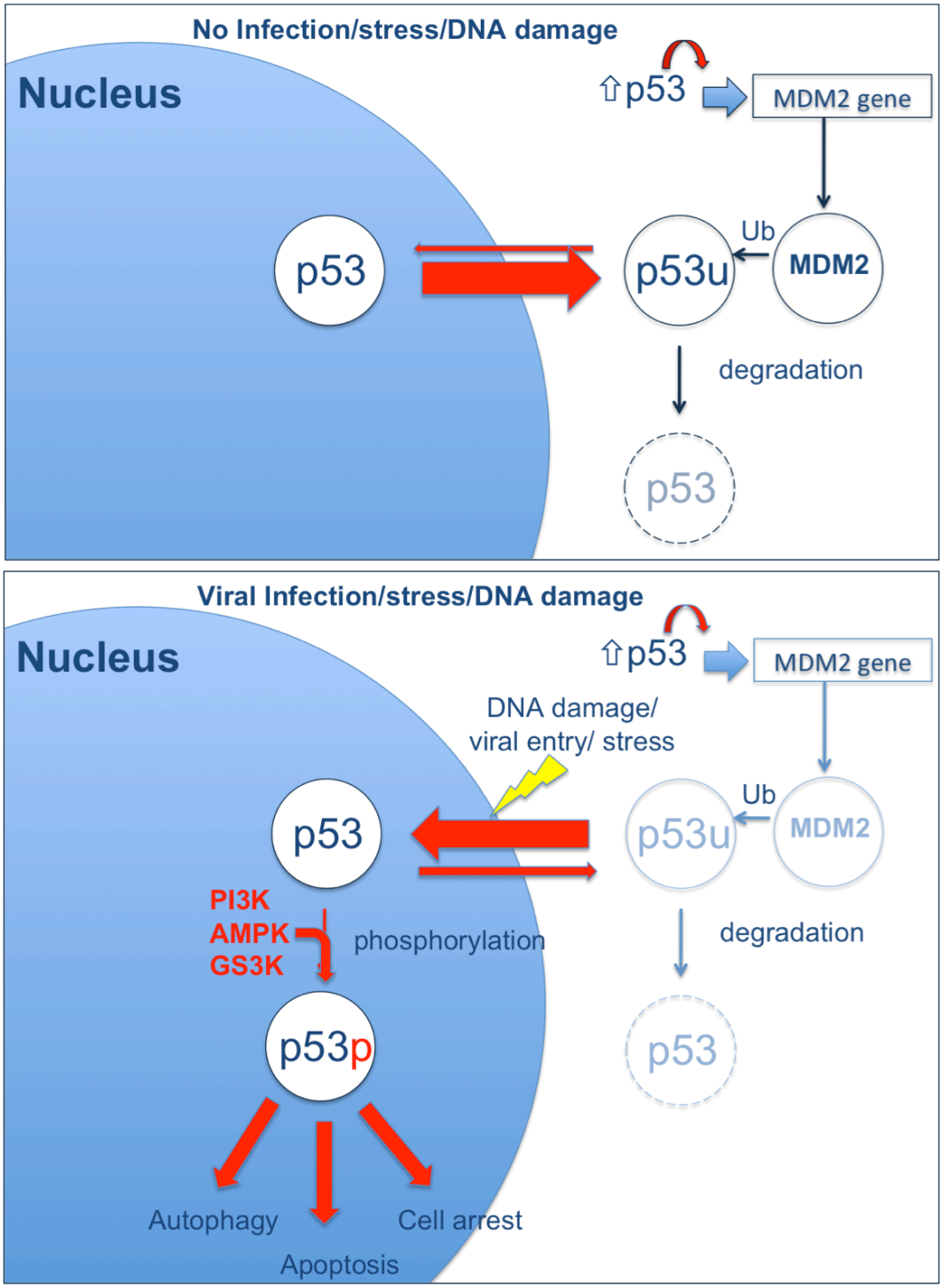


Figure 4 – p53 regulation in stressed and unstressed cells. Under normal conditions p53 levels in the cytoplasm are maintained by a negative feedback loop where by high levels of p53 induce MDM2 gene expression followed by ubiquitination of the p53 protein by MDM2 and p53 degradation. Under times of stress p53 is recruited to the nucleus where it is phosphorylated by kinases such as PI3K and GSK3K and subsequently stabilised for transcriptional activation of downstream targets required for initiation of apoptosis, cell cycle and autophagy pathways.

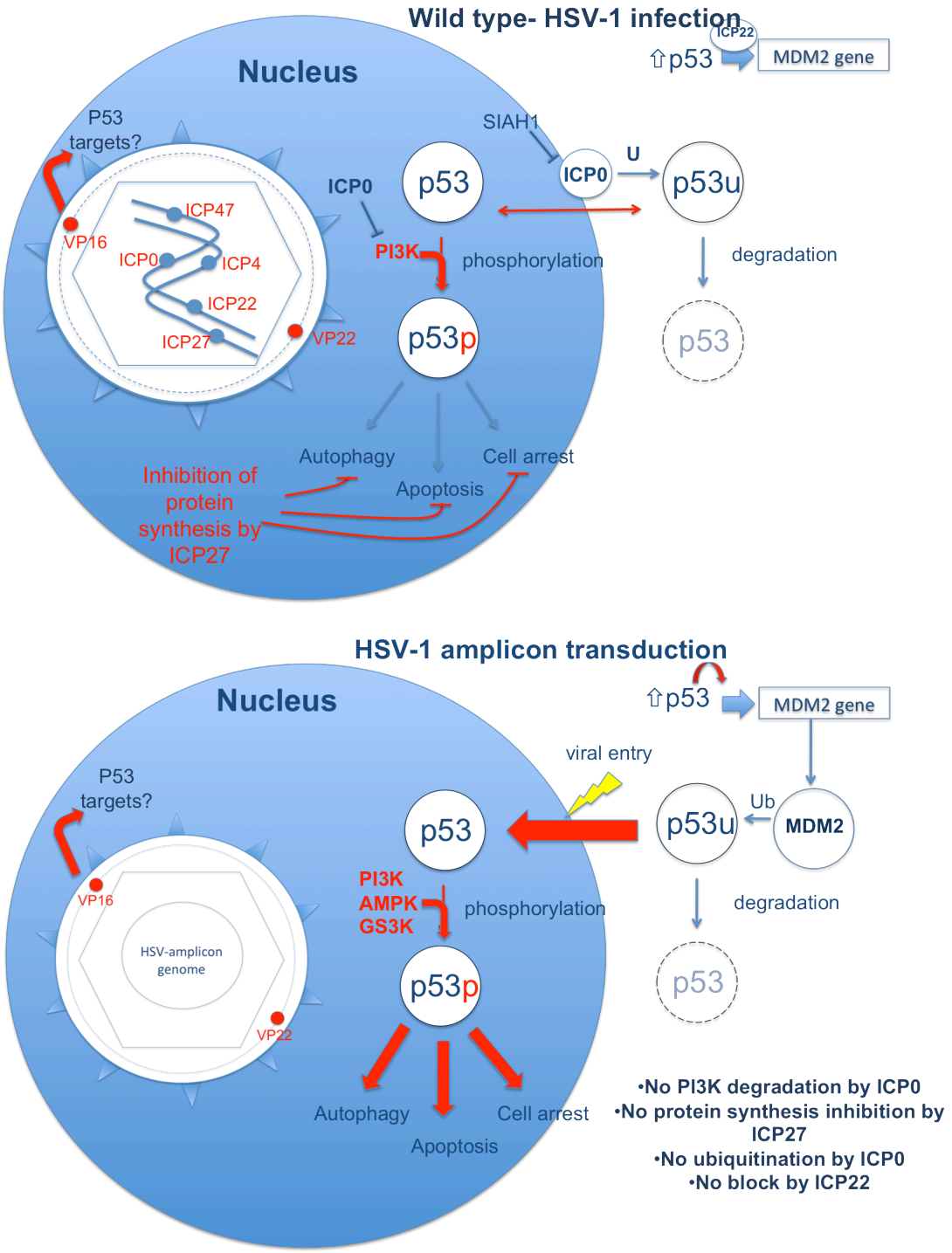


Figure 5 – p53 regulation upon wild type HSV-1 and HSV-1 amplicon transduction. Wild type HSV-1 gene expression induced several effects on p53 regulation including PI3K degradation and ubiquitination of p53 by ICPO. In addition ICP22 blocks the MDM2 promoter to prevent it's regulation by p53. ICP27 inhibits protein synthesis and is upregulated by p53 and VP16. HSV-1 amplicons lack all HSV-1 genes however the tegument protein VP16 is present and may contribute to transcriptional activation of p53 targets.

The induction of p53 expression following HSV-1 amplicon transduction could possibly be avoided by using recombinant HSV-1 viruses which express some but not all of the immediate early genes. The negative regulation exhibited by ICP0 could be employed in order to drive p53 towards the ubiquitination/degradation pathway and inclusion of ICP27 could help to prevent protein synthesis. ICP22 should be avoided due to its negative effect on MDM2 expression. This strategy may offer a safer alternative to p53 inhibition by the transforming gene SV40LT.

7.7 Future of iPS technology

Since iPS technology emerged in 2006, many large scale, collaborative, multi-institutional projects have been established in order to study and understand disease. Locally these programs include the Oxford Parkinson's Disease Centre (OPDC; opdc.medsci.ox.ac.uk), which combines studies on a clinical cohort of 1000 patients (of which 150 iPS cell lines have been generated from 50 patients) with MRI brain imaging and animal models. Over the next five years around 1500 PD patients and 300 age-matched controls are to be recruited to the study. The iPS cell lines are primarily reprogrammed from patient fibroblasts by Sendai virus vectors, followed by subsequent differentiation to dopaminergic fibroblasts. Reprogramming of fibroblasts is conducted by the James Martin Stem Cell Facility, who are also involved in the multidisciplinary StemBANCC project.

The StemBANCC project (stembancc.org) is a European academic-industry consortium that was initiated in October 2012 and aims to generate and characterise 1500 patient iPS lines from 500 patients displaying a wide range of diseases. These lines will be used to study and characterise diseases such as Alzheimer's disease, Parkinson's disease, schizophrenia, bipolar disorder, migraine, neuropathy, and diabetes. The iPS lines will also be used to generate liver, heart, nerve and kidney cells for drug and toxicology screening. This project involves 10 industry partners and 23 Universities with an investment of 55.6 million Euros over the duration of five years. Similar projects are underway at the California Institute of Regenerative Medicine (CIRM; www.cirm.ca.gov) and the Wellcome Trust Cambridge stem cell institute (www.stemcells.cam.ac.uk).

Given the scale and investment involved in these projects the future of iPS technology is an exciting prospect. In the next few years with the availability of multiple lines to researches and industry partners alike will allow the accelerated development of drugs. Patient iPS lines offer a physiological relevant platform to screen drugs and test drug efficacy and toxicology on patient heart and liver cells prior to clinical testing. These "*in vitro* clinical trials" are expected to reduce the failure rate of drugs, which advance to clinical trial stage and reduce development times. In addition the availability of multiple patient lines for studying disease will greatly advance our understanding of multiple diseases and comparison across many lines will allow us to exclude intra-line variation.

Currently these consortiums employ episomal EBNA-1 vectors and Sendai virus reprogramming methods to efficiently generate iPS cells. The success and wide scale use of these reprogramming methods since the beginning of this PhD has effectively removed the need for another non-integrating method, however, should the HSV-1 amplicon be developed in future for successful reprogramming, its large transgene capacity will be a unique feature of the vector.

7.8 Conclusions and future work

This thesis outlines the construction, characterisation and employment of HSV-1 amplicon vectors for use in reprogramming, direct differentiation and dopaminergic neuron differentiation experiments. Further modification of the HSV-1 amplicon vector to include a p53 inhibitor such as SV40LT or the use of a recombinant HSV-1 vector may be required in order to counteract p53 induction and allow successful reprogramming of human fibroblasts. In the immediate future reprogramming experiments could be conducted using the p53 inhibitor Pifithrin-α in order to confirm our p53 hypothesis.

We suspect that p53 induction is also a barrier in the direct differentiation experiments so conducting direct differentiation in the presence of the p53 inhibitor Pifithrin-α and/or the small molecule inhibitors/enhancers outlined in Chapter 5 may confirm this hypothesis. Our dopaminergic neuron differentiation experiments were successful and yielded a significant increase in TH positive neurons/TH expression when transduced at either the early time

point (Nim1) or late time point (Final Diff). Further experiments with different factor combinations at the early and late time points need to be conducted in order to establish which factors are acting at each of the time points. Experiments also need to be confirmed in multiple lines and on a larger scale in order to estimate the improvement in dopaminergic neuron differentiation.

We conclude that we have generated HSV-1 amplicon vectors capable of 1) partially reprogramming fibroblasts to iPS cells and 2) enhancing dopaminergic neuron differentiation. Improvements to the vectors and/or use of a p53 inhibitor such as Pifithrin-α is recommended in order to prevent p53 induction and allow successful reprogramming and direct differentiation free of viral integrations.

References

1. Evans, M.J. and M.H. Kaufman, *Establishment in culture of pluripotential cells from mouse embryos.* Nature, 1981. **292**(5819): p. 154-6.
2. Martin, G.R., *Isolation of a pluripotent cell line from early mouse embryos cultured in medium conditioned by teratocarcinoma stem cells.* Proc Natl Acad Sci U S A, 1981. **78**(12): p. 7634-8.
3. Thomson, J.A., et al., *Embryonic stem cell lines derived from human blastocysts.* Science, 1998. **282**(5391): p. 1145-7.
4. GURDON, J.B., *The developmental capacity of nuclei taken from intestinal epithelium cells of feeding tadpoles.* J Embryol Exp Morphol, 1962. **10**: p. 622-40.
5. Sims, M. and N.L. First, *Production of calves by transfer of nuclei from cultured inner cell mass cells.* Proc Natl Acad Sci U S A, 1994. **91**(13): p. 6143-7.
6. Campbell, K.H., et al., *Sheep cloned by nuclear transfer from a cultured cell line.* Nature, 1996. **380**(6569): p. 64-6.
7. Wilmut, I., et al., *Viable offspring derived from fetal and adult mammalian cells.* Nature, 1997. **385**(6619): p. 810-3.
8. Campbell, K.H., et al., *Cell cycle co-ordination in embryo cloning by nuclear transfer.* Rev Reprod, 1996. **1**(1): p. 40-6.
9. Cheong, H.T., Y. Takahashi, and H. Kanagawa, *Birth of mice after transplantation of early cell-cycle-stage embryonic nuclei into enucleated oocytes.* Biol Reprod, 1993. **48**(5): p. 958-63.
10. Tada, M., et al., *Embryonic germ cells induce epigenetic reprogramming of somatic nucleus in hybrid cells.* EMBO J, 1997. **16**(21): p. 6510-20.
11. Tada, M., et al., *Nuclear reprogramming of somatic cells by in vitro hybridization with ES cells.* Curr Biol, 2001. **11**(19): p. 1553-8.
12. Terada, N., et al., *Bone marrow cells adopt the phenotype of other cells by spontaneous cell fusion.* Nature, 2002. **416**(6880): p. 542-5.
13. Cowan, C.A., et al., *Nuclear reprogramming of somatic cells after fusion with human embryonic stem cells.* Science, 2005. **309**(5739): p. 1369-73.
14. Silva, J., et al., *Nanog promotes transfer of pluripotency after cell fusion.* Nature, 2006. **441**(7096): p. 997-1001.
15. Takahashi, K. and S. Yamanaka, *Induction of pluripotent stem cells from mouse embryonic and adult fibroblast cultures by defined factors.* Cell, 2006. **126**(4): p. 663-76.
16. Takahashi, K., et al., *Induction of pluripotent stem cells from adult human fibroblasts by defined factors.* Cell, 2007. **131**(5): p. 861-72.
17. Yu, J., et al., *Induced pluripotent stem cell lines derived from human somatic cells.* Science, 2007. **318**(5858): p. 1917-20.
18. Avilion, A.A., et al., *Multipotent cell lineages in early mouse development depend on SOX2 function.* Genes Dev, 2003. **17**(1): p. 126-40.
19. Masui, S., et al., *Pluripotency governed by Sox2 via regulation of Oct3/4 expression in mouse embryonic stem cells.* Nat Cell Biol, 2007. **9**(6): p. 625-35.
20. Niwa, H., J. Miyazaki, and A.G. Smith, *Quantitative expression of Oct-3/4 defines differentiation, dedifferentiation or self-renewal of ES cells.* Nat Genet, 2000. **24**(4): p. 372-6.

21. Fong, H., K.A. Hohenstein, and P.J. Donovan, *Regulation of self-renewal and pluripotency by Sox2 in human embryonic stem cells.* Stem Cells, 2008. **26**(8): p. 1931-8.
22. Adachi, K., et al., *Role of SOX2 in maintaining pluripotency of human embryonic stem cells.* Genes Cells, 2010. **15**(5): p. 455-70.
23. Nichols, J., et al., *Formation of pluripotent stem cells in the mammalian embryo depends on the POU transcription factor Oct4.* Cell, 1998. **95**(3): p. 379-91.
24. Li, Y., et al., *Murine embryonic stem cell differentiation is promoted by SOCS-3 and inhibited by the zinc finger transcription factor Klf4.* Blood, 2005. **105**(2): p. 635-7.
25. Nakatake, Y., et al., *Klf4 cooperates with Oct3/4 and Sox2 to activate the Lefty1 core promoter in embryonic stem cells.* Mol Cell Biol, 2006. **26**(20): p. 7772-82.
26. Nakagawa, M., et al., *Generation of induced pluripotent stem cells without Myc from mouse and human fibroblasts.* Nat Biotechnol, 2008. **26**(1): p. 101-6.
27. Huangfu, D., et al., *Induction of pluripotent stem cells by defined factors is greatly improved by small-molecule compounds.* Nat Biotechnol, 2008. **26**(7): p. 795-7.
28. Cartwright, P., et al., *LIF/STAT3 controls ES cell self-renewal and pluripotency by a Myc-dependent mechanism.* Development, 2005. **132**(5): p. 885-96.
29. Lin, C.H., et al., *Myc-regulated microRNAs attenuate embryonic stem cell differentiation.* EMBO J, 2009. **28**(20): p. 3157-70.
30. Mitsui, K., et al., *The homeoprotein Nanog is required for maintenance of pluripotency in mouse epiblast and ES cells.* Cell, 2003. **113**(5): p. 631-42.
31. Chambers, I., et al., *Functional expression cloning of Nanog, a pluripotency sustaining factor in embryonic stem cells.* Cell, 2003. **113**(5): p. 643-55.
32. Chambers, I., et al., *Nanog safeguards pluripotency and mediates germline development.* Nature, 2007. **450**(7173): p. 1230-4.
33. Silva, J., et al., *Nanog is the gateway to the pluripotent ground state.* Cell, 2009. **138**(4): p. 722-37.
34. Aasen, T. and J.C. Izpisúa Belmonte, *Isolation and cultivation of human keratinocytes from skin or plucked hair for the generation of induced pluripotent stem cells.* Nat Protoc, 2010. **5**(2): p. 371-82.
35. Richards, M., et al., *The transcriptome profile of human embryonic stem cells as defined by SAGE.* Stem Cells, 2004. **22**(1): p. 51-64.
36. Xu, B., K. Zhang, and Y. Huang, *Lin28 modulates cell growth and associates with a subset of cell cycle regulator mRNAs in mouse embryonic stem cells.* RNA, 2009. **15**(3): p. 357-61.
37. Qiu, C., et al., *Lin28-mediated post-transcriptional regulation of Oct4 expression in human embryonic stem cells.* Nucleic Acids Res, 2010. **38**(4): p. 1240-8.
38. Serrano, L., B.N. Vazquez, and J. Tischfield, *Chromatin structure, pluripotency and differentiation.* Exp Biol Med (Maywood), 2013. **238**(3): p. 259-70.
39. Jerabek, S., et al., *OCT4: Dynamic DNA binding pioneers stem cell pluripotency.* Biochim Biophys Acta, 2014. **1839**(3): p. 138-154.

40. Boyer, L.A., et al., *Core transcriptional regulatory circuitry in human embryonic stem cells.* Cell, 2005. **122**(6): p. 947-56.
41. Soufi, A., G. Donahue, and K.S. Zaret, *Facilitators and impediments of the pluripotency reprogramming factors' initial engagement with the genome.* Cell, 2012. **151**(5): p. 994-1004.
42. Chan, E.M., et al., *Live cell imaging distinguishes bona fide human iPS cells from partially reprogrammed cells.* Nat Biotechnol, 2009. **27**(11): p. 1033-7.
43. Warlich, E., et al., *Lentiviral vector design and imaging approaches to visualize the early stages of cellular reprogramming.* Mol Ther, 2011. **19**(4): p. 782-9.
44. Megyola, C.M., et al., *Dynamic migration and cell-cell interactions of early reprogramming revealed by high-resolution time-lapse imaging.* Stem Cells, 2013. **31**(5): p. 895-905.
45. Rodriguez-Piza, I., et al., *Reprogramming of Human Fibroblasts to Induced Pluripotent Stem Cells Under Xeno-Free Conditions.* Stem Cells, 2009.
46. Park, I.H., et al., *Reprogramming of human somatic cells to pluripotency with defined factors.* Nature, 2008. **451**(7175): p. 141-6.
47. Takenaka, C., et al., *Effective generation of iPS cells from CD34(+) cord blood cells by inhibition of p53.* Exp Hematol, 2009.
48. Kunisato, A., et al., *Direct generation of induced pluripotent stem cells from human nonmobilized blood.* Stem Cells Dev, 2011. **20**(1): p. 159-68.
49. Carey, B.W., et al., *Reprogramming of murine and human somatic cells using a single polycistronic vector.* Proceedings of the National Academy of Sciences of the United States of America, 2009. **106**(1): p. 157-162.
50. Stadtfeld, M., K. Brennand, and K. Hochedlinger, *Reprogramming of pancreatic beta cells into induced pluripotent stem cells.* Curr Biol, 2008. **18**(12): p. 890-4.
51. Kim, J.B., et al., *Pluripotent stem cells induced from adult neural stem cells by reprogramming with two factors.* Nature, 2008. **454**(7204): p. 646-50.
52. Hacein-Bey-Abina, S., et al., *A serious adverse event after successful gene therapy for X-linked severe combined immunodeficiency.* N Engl J Med, 2003. **348**(3): p. 255-6.
53. Stein, S., et al., *Genomic instability and myelodysplasia with monosomy 7 consequent to EVI1 activation after gene therapy for chronic granulomatous disease.* Nat Med, 2010. **16**(2): p. 198-204.
54. Yu, S.F., et al., *Self-inactivating retroviral vectors designed for transfer of whole genes into mammalian cells.* Proc Natl Acad Sci U S A, 1986. **83**(10): p. 3194-8.
55. Montini, E., et al., *Hematopoietic stem cell gene transfer in a tumor-prone mouse model uncovers low genotoxicity of lentiviral vector integration.* Nat Biotechnol, 2006. **24**(6): p. 687-96.
56. Montini, E., et al., *The genotoxic potential of retroviral vectors is strongly modulated by vector design and integration site selection in a mouse model of HSC gene therapy.* J Clin Invest, 2009. **119**(4): p. 964-75.
57. Modlich, U., et al., *Leukemia induction after a single retroviral vector insertion in Evi1 or Prdm16.* Leukemia, 2008. **22**(8): p. 1519-28.

58. Condiotti, R., et al., *Transduction of fetal mice with a feline lentiviral vector induces liver tumors which exhibit an E2F activation signature.* Mol Ther, 2013.
59. Butler, S.L., E.P. Johnson, and F.D. Bushman, *Human immunodeficiency virus cDNA metabolism: notable stability of two-long terminal repeat circles.* J Virol, 2002. **76**(8): p. 3739-47.
60. Yang, G., et al., *Integration-deficient lentivectors: an effective strategy to purify and differentiate human embryonic stem cell-derived hepatic progenitors.* BMC Biol, 2013. **11**: p. 86.
61. Yáñez-Muñoz, R.J., et al., *Effective gene therapy with nonintegrating lentiviral vectors.* Nat Med, 2006. **12**(3): p. 348-53.
62. Ciuffi, A., et al., *A role for LEDGF/p75 in targeting HIV DNA integration.* Nat Med, 2005. **11**(12): p. 1287-9.
63. Silvers, R.M., et al., *Modification of integration site preferences of an HIV-1-based vector by expression of a novel synthetic protein.* Hum Gene Ther, 2010. **21**(3): p. 337-49.
64. Winkler, T., et al., *No evidence for clonal selection due to lentiviral integration sites in human induced pluripotent stem cells.* Stem Cells, 2010. **28**(4): p. 687-94.
65. Wang, Q., C. Ma, and W. Kemmner, *Wdr66 is a novel marker for risk stratification and involved in epithelial-mesenchymal transition of esophageal squamous cell carcinoma.* BMC Cancer, 2013. **13**: p. 137.
66. Varas, F., et al., *Fibroblast-derived induced pluripotent stem cells show no common retroviral vector insertions.* Stem Cells, 2009. **27**(2): p. 300-6.
67. Okita, K., T. Ichisaka, and S. Yamanaka, *Generation of germline-competent induced pluripotent stem cells.* Nature, 2007. **448**(7151): p. 313-7.
68. Stadtfeld, M., et al., *Induced pluripotent stem cells generated without viral integration.* Science, 2008. **322**(5903): p. 945-9.
69. Zhou, W. and C.R. Freed, *Adenoviral gene delivery can reprogram human fibroblasts to induced pluripotent stem cells.* Stem Cells, 2009. **27**(11): p. 2667-74.
70. Gupta, S., *Hepatic polyploidy and liver growth control.* Semin Cancer Biol, 2000. **10**(3): p. 161-71.
71. Melchiorri, C., et al., *Ploidy and nuclearity of rat hepatocytes after compensatory regeneration or mitogen-induced liver growth.* Carcinogenesis, 1993. **14**(9): p. 1825-30.
72. Fink, K.D., et al., *Survival and Differentiation of Adenovirus-Generated Induced Pluripotent Stem Cells Transplanted into the Rat Striatum.* Cell Transplant, 2013.
73. Nishimura, K., et al., *Development of defective and persistent Sendai virus vector: a unique gene delivery/expression system ideal for cell reprogramming.* J Biol Chem, 2011. **286**(6): p. 4760-71.
74. Li, H.O., et al., *A cytoplasmic RNA vector derived from nontransmissible Sendai virus with efficient gene transfer and expression.* J Virol, 2000. **74**(14): p. 6564-9.
75. Nishimura, K., et al., *Persistent and stable gene expression by a cytoplasmic RNA replicon based on a noncytopathic variant Sendai virus.* J Biol Chem, 2007. **282**(37): p. 27383-91.

76. Yoshizaki, M., et al., *Naked Sendai virus vector lacking all of the envelope-related genes: reduced cytopathogenicity and immunogenicity.* J Gene Med, 2006. **8**(9): p. 1151-9.
77. Fusaki, N., et al., *Efficient induction of transgene-free human pluripotent stem cells using a vector based on Sendai virus, an RNA virus that does not integrate into the host genome.* Proc Jpn Acad Ser B Phys Biol Sci, 2009. **85**(8): p. 348-62.
78. Ban, H., et al., *Efficient generation of transgene-free human induced pluripotent stem cells (iPSCs) by temperature-sensitive Sendai virus vectors.* Proc Natl Acad Sci U S A, 2011. **108**(34): p. 14234-9.
79. Kudva, Y.C., et al., *Transgene-free disease-specific induced pluripotent stem cells from patients with type 1 and type 2 diabetes.* Stem Cells Transl Med, 2012. **1**(6): p. 451-61.
80. Kawagoe, S., et al., *Morphological features of iPS cells generated from Fabry disease skin fibroblasts using Sendai virus vector (SeVdp).* Mol Genet Metab, 2013. **109**(4): p. 386-9.
81. Jin, Z.B., et al., *Integration-free induced pluripotent stem cells derived from retinitis pigmentosa patient for disease modeling.* Stem Cells Transl Med, 2012. **1**(6): p. 503-9.
82. Ye, L., et al., *Blood cell-derived induced pluripotent stem cells free of reprogramming factors generated by Sendai viral vectors.* Stem Cells Transl Med, 2013. **2**(8): p. 558-66.
83. Ono, M., et al., *Generation of induced pluripotent stem cells from human nasal epithelial cells using a Sendai virus vector.* PLoS One, 2012. **7**(8): p. e42855.
84. Soldner, F., et al., *Parkinson's disease patient-derived induced pluripotent stem cells free of viral reprogramming factors.* Cell, 2009. **136**(5): p. 964-77.
85. Sommer, C.A., et al., *Induced pluripotent stem cell generation using a single lentiviral stem cell cassette.* Stem Cells, 2009. **27**(3): p. 543-9.
86. Sommer, C.A., et al., *Excision of reprogramming transgenes improves the differentiation potential of iPS cells generated with a single excisable vector.* Stem Cells, 2010. **28**(1): p. 64-74.
87. Somers, A., et al., *Generation of transgene-free lung disease-specific human induced pluripotent stem cells using a single excisable lentiviral stem cell cassette.* Stem Cells, 2010. **28**(10): p. 1728-40.
88. Awe, J.P., et al., *Generation and characterization of transgene-free human induced pluripotent stem cells and conversion to putative clinical-grade status.* Stem Cell Res Ther, 2013. **4**(4): p. 87.
89. Fan, Y., et al., *Generation of human β-thalassemia induced pluripotent stem cells from amniotic fluid cells using a single excisable lentiviral stem cell cassette.* J Reprod Dev, 2012. **58**(4): p. 404-9.
90. Naldini, L., et al., *In vivo gene delivery and stable transduction of nondividing cells by a lentiviral vector.* Science, 1996. **272**(5259): p. 263-7.
91. Okita, K., et al., *Generation of mouse induced pluripotent stem cells without viral vectors.* Science, 2008. **322**(5903): p. 949-53.
92. Jia, F., et al., *A nonviral minicircle vector for deriving human iPS cells.* Nat Methods, 2010. **7**(3): p. 197-9.

93. Park, H.Y., et al., *Efficient generation of virus-free iPS cells using liposomal magnetofection.* PLoS One, 2012. **7**(9): p. e45812.
94. Yu, J., et al., *Human Induced Pluripotent Stem Cells Free of Vector and Transgene Sequences.* Science, 2009. **324**(5928): p. 797-801.
95. Okita, K., et al., *A more efficient method to generate integration-free human iPS cells.* Nature Methods, 2011. **8**(5): p. 409-412.
96. Chou, B.K., et al., *Efficient human iPS cell derivation by a non-integrating plasmid from blood cells with unique epigenetic and gene expression signatures.* Cell Res, 2011.
97. Cary, L.C., et al., *Transposon mutagenesis of baculoviruses: analysis of Trichoplusia ni transposon IFP2 insertions within the FP-locus of nuclear polyhedrosis viruses.* Virology, 1989. **172**(1): p. 156-69.
98. Ding, S., et al., *Efficient transposition of the piggyBac (PB) transposon in mammalian cells and mice.* Cell, 2005. **122**(3): p. 473-83.
99. Woltjen, K., et al., *piggyBac transposition reprograms fibroblasts to induced pluripotent stem cells.* Nature, 2009. **458**(7239): p. 766-70.
100. Nagy, K., et al., *Induced pluripotent stem cell lines derived from equine fibroblasts.* Stem Cell Rev, 2011. **7**(3): p. 693-702.
101. Mali, P., et al., *Butyrate greatly enhances derivation of human induced pluripotent stem cells by promoting epigenetic remodeling and the expression of pluripotency-associated genes.* Stem Cells, 2010. **28**(4): p. 713-20.
102. Tsukiyama, T., et al., *Simple and efficient method for generation of induced pluripotent stem cells using piggyBac transposition of doxycycline-inducible factors and an EOS reporter system.* Genes Cells, 2011. **16**(7): p. 815-25.
103. Ivics, Z., et al., *Molecular reconstruction of Sleeping Beauty, a Tc1-like transposon from fish, and its transposition in human cells.* Cell, 1997. **91**(4): p. 501-10.
104. Muenthaisong, S., et al., *Generation of mouse induced pluripotent stem cells from different genetic backgrounds using Sleeping beauty transposon mediated gene transfer.* Exp Cell Res, 2012. **318**(19): p. 2482-9.
105. Davis, R.P., et al., *Generation of induced pluripotent stem cells from human foetal fibroblasts using the Sleeping Beauty transposon gene delivery system.* Differentiation, 2013. **86**(1-2): p. 30-37.
106. VandenDriessche, T., et al., *Emerging potential of transposons for gene therapy and generation of induced pluripotent stem cells.* Blood, 2009. **114**(8): p. 1461-8.
107. Mátés, L., et al., *Molecular evolution of a novel hyperactive Sleeping Beauty transposase enables robust stable gene transfer in vertebrates.* Nat Genet, 2009. **41**(6): p. 753-61.
108. Wilson, M.H., C.J. Coates, and A.L. George, *PiggyBac transposon-mediated gene transfer in human cells.* Mol Ther, 2007. **15**(1): p. 139-45.
109. Plews, J.R., et al., *Activation of pluripotency genes in human fibroblast cells by a novel mRNA based approach.* PLoS One, 2010. **5**(12): p. e14397.
110. Angel, M. and M.F. Yanik, *Innate immune suppression enables frequent transfection with RNA encoding reprogramming proteins.* PLoS One, 2010. **5**(7): p. e11756.

111. Warren, L., et al., *Highly efficient reprogramming to pluripotency and directed differentiation of human cells with synthetic modified mRNA.* Cell Stem Cell, 2010. **7**(5): p. 618-30.
112. Kim, D., et al., *Generation of human induced pluripotent stem cells by direct delivery of reprogramming proteins.* Cell Stem Cell, 2009. **4**(6): p. 472-6.
113. Zhou, H., et al., *Generation of induced pluripotent stem cells using recombinant proteins.* Cell Stem Cell, 2009. **4**(5): p. 381-4.
114. Lee, J., et al., *Activation of innate immunity is required for efficient nuclear reprogramming.* Cell, 2012. **151**(3): p. 547-58.
115. Reik, W., *Stability and flexibility of epigenetic gene regulation in mammalian development.* Nature, 2007. **447**(7143): p. 425-32.
116. Lu, J., et al., *Application of epigenome-modifying small molecules in induced pluripotent stem cells.* Med Res Rev, 2013. **33**(4): p. 790-822.
117. Klimasauskas, S., et al., *HhaI methyltransferase flips its target base out of the DNA helix.* Cell, 1994. **76**(2): p. 357-69.
118. Liang, G., et al., *Butyrate promotes induced pluripotent stem cell generation.* J Biol Chem, 2010. **285**(33): p. 25516-21.
119. Shi, Y., et al., *A combined chemical and genetic approach for the generation of induced pluripotent stem cells.* Cell Stem Cell, 2008. **2**(6): p. 525-8.
120. Shi, Y., et al., *Induction of pluripotent stem cells from mouse embryonic fibroblasts by Oct4 and Klf4 with small-molecule compounds.* Cell Stem Cell, 2008. **3**(5): p. 568-74.
121. Ichida, J.K., et al., *A small-molecule inhibitor of tgf-Beta signaling replaces sox2 in reprogramming by inducing nanog.* Cell Stem Cell, 2009. **5**(5): p. 491-503.
122. Yuan, X., et al., *Combined Chemical Treatment Enables Oct4-Induced Reprogramming from Mouse Embryonic Fibroblasts.* Stem Cells, 2011.
123. Li, Y., et al., *Generation of iPSCs from mouse fibroblasts with a single gene, Oct4, and small molecules.* Cell Res, 2011. **21**(1): p. 196-204.
124. Hou, P., et al., *Pluripotent stem cells induced from mouse somatic cells by small-molecule compounds.* Science, 2013. **341**(6146): p. 651-4.
125. de Silva, S. and W.J. Bowers, *Herpes Virus Amplicon Vectors.* Viruses, 2009. **1**(3): p. 594-629.
126. Eidson, K.M., et al., *Expression of herpes simplex virus ICP0 inhibits the induction of interferon-stimulated genes by viral infection.* J Virol, 2002. **76**(5): p. 2180-91.
127. Orvedahl, A., et al., *HSV-1 ICP34.5 confers neurovirulence by targeting the Beclin 1 autophagy protein.* Cell Host Microbe, 2007. **1**(1): p. 23-35.
128. Lussignol, M., et al., *The herpes simplex virus 1 Us11 protein inhibits autophagy through its interaction with the protein kinase PKR.* J Virol, 2013. **87**(2): p. 859-71.
129. Spaete, R.R. and N. Frenkel, *The herpes simplex virus amplicon: a new eucaryotic defective-virus cloning-amplifying vector.* Cell, 1982. **30**(1): p. 295-304.
130. Tsitoura, E., et al., *Infection with herpes simplex type 1-based amplicon vectors results in an IRF3/7-dependent, TLR-independent activation of the innate antiviral response in primary human fibroblasts.* Journal of General Virology, 2009. **90**(9): p. 2209-2220.

131. Suzuki, M., E.A. Chiocca, and Y. Saeki, *Early STAT1 activation after systemic delivery of HSV amplicon vectors suppresses transcription of the vector-encoded transgene.* Mol Ther, 2007. **15**(11): p. 2017-26.
132. Suzuki, M., E.A. Chiocca, and Y. Saeki, *Stable transgene expression from HSV amplicon vectors in the brain: potential involvement of immunoregulatory signals.* Mol Ther, 2008. **16**(10): p. 1727-36.
133. Saeki, Y., et al., *Improved helper virus-free packaging system for HSV amplicon vectors using an ICP27-deleted, oversized HSV-1 DNA in a bacterial artificial chromosome.* Mol Ther, 2001. **3**(4): p. 591-601.
134. McCarthy, A.M., L. McMahan, and P.A. Schaffer, *Herpes simplex virus type 1 ICP27 deletion mutants exhibit altered patterns of transcription and are DNA deficient.* J Virol, 1989. **63**(1): p. 18-27.
135. Byers, B., et al., *SNCA triplication Parkinson's patient's iPSC-derived DA neurons accumulate α-synuclein and are susceptible to oxidative stress.* PLoS One, 2011. **6**(11): p. e26159.
136. Yang, Y.M., et al., *A small molecule screen in stem-cell-derived motor neurons identifies a kinase inhibitor as a candidate therapeutic for ALS.* Cell Stem Cell, 2013. **12**(6): p. 713-26.
137. Cai, J., et al., *The role of Lmx1a in the differentiation of human embryonic stem cells into midbrain dopamine neurons in culture and after transplantation into a Parkinson's disease model.* Stem Cells, 2009. **27**(1): p. 220-9.
138. Park, I.-H., et al., *Disease-Specific Induced Pluripotent Stem Cells.* Cell, 2008. **134**(5): p. 877-886.
139. Jin, Z.B., et al., *Modeling retinal degeneration using patient-specific induced pluripotent stem cells.* PLoS One, 2011. **6**(2): p. e17084.
140. Raya, A., et al., *Disease-corrected haematopoietic progenitors from Fanconi anaemia induced pluripotent stem cells.* Nature, 2009. **460**(7251): p. 53-9.
141. Cooper, O., et al., *Pharmacological rescue of mitochondrial deficits in iPSC-derived neural cells from patients with familial Parkinson's disease.* Sci Transl Med, 2012. **4**(141): p. 141ra90.
142. Kawai, S.I., et al., *Modeling of risk factors for the degeneration of retinal ganglion cells after ischemia/reperfusion in rats: effects of age, caloric restriction, diabetes, pigmentation, and glaucoma.* FASEB J, 2001. **15**(7): p. 1285-7.
143. Simon-Sanchez, J., et al., *Genome-wide association study reveals genetic risk underlying Parkinson's disease.* Nat Genet, 2009. **41**(12): p. 1308-1312.
144. Kitada, T., et al., *Mutations in the parkin gene cause autosomal recessive juvenile parkinsonism.* Nature, 1998. **392**(6676): p. 605-8.
145. Valente, E.M., et al., *Hereditary early-onset Parkinson's disease caused by mutations in PINK1.* Science, 2004. **304**(5674): p. 1158-60.
146. Djarmati, A., et al., *Detection of Parkin (PARK2) and DJ1 (PARK7) mutations in early-onset Parkinson disease: Parkin mutation frequency depends on ethnic origin of patients.* Hum Mutat, 2004. **23**(5): p. 525.
147. Savica, R., W.A. Rocca, and J.E. Ahlskog, *When Does Parkinson Disease Start?* Arch Neurol, 2010. **67**(7): p. 798-801.
148. Fahn, S., *Description of Parkinson's Disease as a Clinical Syndrome.* Annals of the New York Academy of Sciences, 2003. **991**(1): p. 1-14.

149. Braak, H. and E. Braak, *Pathoanatomy of Parkinson's disease.* J Neurol, 2000. **247 Suppl 2**: p. II3-10.
150. Soldner, F., et al., *Generation of isogenic pluripotent stem cells differing exclusively at two early onset Parkinson point mutations.* Cell, 2011. **146**(2): p. 318-31.
151. Nguyen, H.N., et al., *LRRK2 mutant iPSC-derived DA neurons demonstrate increased susceptibility to oxidative stress.* Cell Stem Cell, 2011. **8**(3): p. 267-80.
152. Reinhardt, P., et al., *Genetic correction of a LRRK2 mutation in human iPSCs links parkinsonian neurodegeneration to ERK-dependent changes in gene expression.* Cell Stem Cell, 2013. **12**(3): p. 354-67.
153. Imaizumi, Y., et al., *Mitochondrial dysfunction associated with increased oxidative stress and α-synuclein accumulation in PARK2 iPSC-derived neurons and postmortem brain tissue.* Mol Brain, 2012. **5**: p. 35.
154. Seibler, P., et al., *Mitochondrial Parkin recruitment is impaired in neurons derived from mutant PINK1 induced pluripotent stem cells.* J Neurosci, 2011. **31**(16): p. 5970-6.
155. Xu, X., et al., *Prevention of β-amyloid induced toxicity in human iPS cell-derived neurons by inhibition of Cyclin-dependent kinases and associated cell cycle events.* Stem Cell Res, 2013. **10**(2): p. 213-27.
156. Tanabe, Y. and T.M. Jessell, *Diversity and pattern in the developing spinal cord.* Science, 1996. **274**(5290): p. 1115-23.
157. Briscoe, J. and J. Ericson, *The specification of neuronal identity by graded Sonic Hedgehog signalling.* Semin Cell Dev Biol, 1999. **10**(3): p. 353-62.
158. De Robertis, E.M. and H. Kuroda, *Dorsal-ventral patterning and neural induction in Xenopus embryos.* Annu Rev Cell Dev Biol, 2004. **20**: p. 285-308.
159. Inoue, F., et al., *Gbx2 directly restricts Otx2 expression to forebrain and midbrain, competing with class III POU factors.* Mol Cell Biol, 2012. **32**(13): p. 2618-27.
160. Alexander, T., C. Nolte, and R. Krumlauf, *Hox genes and segmentation of the hindbrain and axial skeleton.* Annu Rev Cell Dev Biol, 2009. **25**: p. 431-56.
161. Gavalas, A., *ArRAnging the hindbrain.* Trends Neurosci, 2002. **25**(2): p. 61-4.
162. Joyner, A.L., *Engrailed, Wnt and Pax genes regulate midbrain--hindbrain development.* Trends Genet, 1996. **12**(1): p. 15-20.
163. Hynes, M. and A. Rosenthal, *Specification of dopaminergic and serotonergic neurons in the vertebrate CNS.* Curr Opin Neurobiol, 1999. **9**(1): p. 26-36.
164. Crossley, P.H., S. Martinez, and G.R. Martin, *Midbrain development induced by FGF8 in the chick embryo.* Nature, 1996. **380**(6569): p. 66-8.
165. Liu, A. and A.L. Joyner, *EN and GBX2 play essential roles downstream of FGF8 in patterning the mouse mid/hindbrain region.* Development, 2001. **128**(2): p. 181-91.
166. Davis, C.A. and A.L. Joyner, *Expression patterns of the homeo box-containing genes En-1 and En-2 and the proto-oncogene int-1 diverge during mouse development.* Genes Dev, 1988. **2**(12B): p. 1736-44.
167. Kim, H.J., *Stem cell potential in Parkinson's disease and molecular factors for the generation of dopamine neurons.* Biochim Biophys Acta, 2011. **1812**(1): p. 1-11.

168. McMahon, A.P., et al., *The midbrain-hindbrain phenotype of Wnt-1-/Wnt-1- mice results from stepwise deletion of engrailed-expressing cells by 9.5 days postcoitum.* Cell, 1992. **69**(4): p. 581-95.
169. Smidt, M.P., et al., *A homeodomain gene Ptx3 has highly restricted brain expression in mesencephalic dopaminergic neurons.* Proc Natl Acad Sci U S A, 1997. **94**(24): p. 13305-10.
170. Smidt, M.P., et al., *A second independent pathway for development of mesencephalic dopaminergic neurons requires Lmx1b.* Nat Neurosci, 2000. **3**(4): p. 337-41.
171. Andersson, E., et al., *Identification of intrinsic determinants of midbrain dopamine neurons.* Cell, 2006. **124**(2): p. 393-405.
172. Ferri, A.L., et al., *Foxa1 and Foxa2 regulate multiple phases of midbrain dopaminergic neuron development in a dosage-dependent manner.* Development, 2007. **134**(15): p. 2761-9.
173. Chambers, S.M., et al., *Highly efficient neural conversion of human ES and iPS cells by dual inhibition of SMAD signaling.* Nat Biotechnol, 2009. **27**(3): p. 275-80.
174. O'Keeffe, F.E., et al., *Induction of A9 dopaminergic neurons from neural stem cells improves motor function in an animal model of Parkinson's disease.* Brain, 2008. **131**(Pt 3): p. 630-41.
175. Caiazzo, M., et al., *Direct generation of functional dopaminergic neurons from mouse and human fibroblasts.* Nature, 2011. **476**(7359): p. 224-7.
176. Hacein-Bey-Abina, S., et al., *A Serious Adverse Event after Successful Gene Therapy for X-Linked Severe Combined Immunodeficiency.* New England Journal of Medicine, 2003. **348**(3): p. 255-256.
177. Epstein, A.L., *HSV-1-derived amplicon vectors: recent technological improvements and remaining difficulties--a review.* Mem Inst Oswaldo Cruz, 2009. **104**(3): p. 399-410.
178. Ryan, M.D., A.M. King, and G.P. Thomas, *Cleavage of foot-and-mouth disease virus polyprotein is mediated by residues located within a 19 amino acid sequence.* J Gen Virol, 1991. **72 (Pt 11)**: p. 2727-32.
179. Ryan, M.D. and J. Drew, *Foot-and-mouth disease virus 2A oligopeptide mediated cleavage of an artificial polyprotein.* EMBO J, 1994. **13**(4): p. 928-33.
180. Donnelly, M.L.L., et al., *Analysis of the aphthovirus 2A/2B polyprotein 'cleavage' mechanism indicates not a proteolytic reaction, but a novel translational effect: a putative ribosomal 'skip'.* J Gen Virol, 2001. **82**(5): p. 1013-1025.
181. Doronina, V.A., et al., *Site-specific release of nascent chains from ribosomes at a sense codon.* Mol Cell Biol, 2008. **28**(13): p. 4227-39.
182. Szymczak-Workman, A.L., K.M. Vignali, and D.A. Vignali, *Design and construction of 2A peptide-linked multicistronic vectors.* Cold Spring Harb Protoc, 2012. **2012**(2): p. 199-204.
183. Boshart, M., et al., *A very strong enhancer is located upstream of an immediate early gene of human cytomegalovirus.* Cell, 1985. **41**(2): p. 521-30.
184. Teschendorf, C., et al., *Comparison of the EF-1 alpha and the CMV promoter for engineering stable tumor cell lines using recombinant adeno-associated virus.* Anticancer Res, 2002. **22**(6A): p. 3325-30.

185. Yao, F., et al., *Tetracycline repressor, tetR, rather than the tetR-mammalian cell transcription factor fusion derivatives, regulates inducible gene expression in mammalian cells.* Hum Gene Ther, 1998. **9**(13): p. 1939-50.
186. Yates, J., et al., *A cis-acting element from the Epstein-Barr viral genome that permits stable replication of recombinant plasmids in latently infected cells.* Proc Natl Acad Sci U S A, 1984. **81**(12): p. 3806-10.
187. Lupton, S. and A.J. Levine, *Mapping genetic elements of Epstein-Barr virus that facilitate extrachromosomal persistence of Epstein-Barr virus-derived plasmids in human cells.* Mol Cell Biol, 1985. **5**(10): p. 2533-42.
188. Rawlins, D.R., et al., *Sequence-specific DNA binding of the Epstein-Barr virus nuclear antigen (EBNA-1) to clustered sites in the plasmid maintenance region.* Cell, 1985. **42**(3): p. 859-68.
189. Lee, M.A., M.E. Diamond, and J.L. Yates, *Genetic evidence that EBNA-1 is needed for efficient, stable latent infection by Epstein-Barr virus.* J Virol, 1999. **73**(4): p. 2974-82.
190. Wade-Martins, R., J. Frampton, and M.R. James, *Long-term stability of large insert genomic DNA episomal shuttle vectors in human cells.* Nucleic Acids Res, 1999. **27**(7): p. 1674-82.
191. Colombo, F., et al., *Combined HSV-TK//IL-2 gene therapy in patients with recurrent glioblastoma multiforme: biological and clinical results.* Cancer Gene Ther, 2005. **12**(10): p. 835-848.
192. Beck, C., et al., *The thymidine kinase/ganciclovir-mediated "suicide" effect is variable in different tumor cells.* Hum Gene Ther, 1995. **6**(12): p. 1525-30.
193. Cheng, F., et al., *Protecting against wayward human induced pluripotent stem cells with a suicide gene.* Biomaterials, 2012. **33**(11): p. 3195-204.
194. Chakraborty, S., et al., *A robust strategy for negative selection of Cre-loxP recombination-based excision of transgenes in induced pluripotent stem cells.* PLoS One, 2013. **8**(5): p. e64342.
195. Reisman, D. and B. Sugden, *trans activation of an Epstein-Barr viral transcriptional enhancer by the Epstein-Barr viral nuclear antigen 1.* Mol Cell Biol, 1986. **6**(11): p. 3838-46.
196. Wade-Martins, R., et al., *An infectious transfer and expression system for genomic DNA loci in human and mouse cells.* Nat Biotech, 2001. **19**(11): p. 1067-1070.
197. Esteban, M.A., et al., *Vitamin C enhances the generation of mouse and human induced pluripotent stem cells.* Cell Stem Cell, 2010. **6**(1): p. 71-9.
198. Esteban, M.A. and D. Pei, *Vitamin C improves the quality of somatic cell reprogramming.* Nat Genet, 2012. **44**(4): p. 366-7.
199. Tiemann, U., et al., *Optimal reprogramming factor stoichiometry increases colony numbers and affects molecular characteristics of murine induced pluripotent stem cells.* Cytometry A, 2011. **79**(6): p. 426-35.
200. Arakawa, T., et al., *Molecular weights of glycosylated and nonglycosylated forms of recombinant human stem cell factor determined by low-angle laser light scattering.* Anal Biochem, 1992. **203**(1): p. 53-7.
201. Gupta, R. and S. Brunak, *Prediction of glycosylation across the human proteome and the correlation to protein function.* Pac Symp Biocomput, 2002: p. 310-22.

202. Jang, H., et al., *O-GlcNAc regulates pluripotency and reprogramming by directly acting on core components of the pluripotency network.* Cell Stem Cell, 2012. **11**(1): p. 62-74.
203. Khidekel, N., et al., *Exploring the O-GlcNAc proteome: direct identification of O-GlcNAc-modified proteins from the brain.* Proc Natl Acad Sci U S A, 2004. **101**(36): p. 13132-7.
204. Kamemura, K., et al., *Dynamic interplay between O-glycosylation and O-phosphorylation of nucleocytoplasmic proteins: alternative glycosylation/phosphorylation of THR-58, a known mutational hot spot of c-Myc in lymphomas, is regulated by mitogens.* J Biol Chem, 2002. **277**(21): p. 19229-35.
205. Zachara, N.E., K. Vosseller, and G.W. Hart, *Detection and analysis of proteins modified by O-linked N-acetylglucosamine.* Curr Protoc Protein Sci, 2011. **Chapter 12**: p. Unit12.8.
206. Papapetrou, E.P., et al., *Stoichiometric and temporal requirements of Oct4, Sox2, Klf4, and c-Myc expression for efficient human iPSC induction and differentiation.* Proceedings of the National Academy of Sciences, 2009. **106**(31): p. 12759-12764.
207. Carey, B., et al., *Reprogramming Factor Stoichiometry Influences the Epigenetic State and Biological Properties of Induced Pluripotent Stem Cells.* Cell Stem Cell, 2011. **9**(6): p. 588-598.
208. Komar, A.A. and M. Hatzoglou, *Cellular IRES-mediated translation: the war of ITAFs in pathophysiological states.* Cell Cycle, 2011. **10**(2): p. 229-40.
209. Jang, S.K., et al., *A segment of the 5' nontranslated region of encephalomyocarditis virus RNA directs internal entry of ribosomes during in vitro translation.* J Virol, 1988. **62**(8): p. 2636-43.
210. Pelletier, J. and N. Sonenberg, *Internal initiation of translation of eukaryotic mRNA directed by a sequence derived from poliovirus RNA.* Nature, 1988. **334**(6180): p. 320-5.
211. Kieft, J.S., *Viral IRES RNA structures and ribosome interactions.* Trends Biochem Sci, 2008. **33**(6): p. 274-83.
212. Chan, H.Y., et al., *Comparison of IRES and F2A-based locus-specific multicistronic expression in stable mouse lines.* PLoS One, 2011. **6**(12): p. e28885.
213. Kuzmich, **A.I.**, et al., *Quantitative comparison of gene co-expression in a bicistronic vector harboring IRES or coding sequence of porcine teschovirus 2A peptide*, **A.V.** Vvedenskii, Editor. 2013, *Russian Journal of Bioorganic Chemistry* p. *pp. 406–416.* .
214. Stadtfeld, M., et al., *Defining molecular cornerstones during fibroblast to iPS cell reprogramming in mouse.* Cell Stem Cell, 2008. **2**(3): p. 230-40.
215. Polo, J., et al., *A Molecular Roadmap of Reprogramming Somatic Cells into iPS Cells.* Cell, 2012. **151**(7): p. 1617-1632.
216. Li, Z. and T. Rana, *A kinase inhibitor screen identifies small-molecule enhancers of reprogramming and iPS cell generation.* Nature Communications, 2012. **3**.
217. Hanna, J., et al., *Direct cell reprogramming is a stochastic process amenable to acceleration.* Nature, 2009. **462**(7273): p. 595-601.
218. Kawamura, T., et al., *Linking the p53 tumour suppressor pathway to somatic cell reprogramming.* Nature, 2009. **460**(7259): p. 1140-U107.

219. Lee, J., et al., *Activation of Innate Immunity Is Required for Efficient Nuclear Reprogramming.* Cell, 2012. **151**(3): p. 547-558.
220. Zhang, Y. and Y. Xiong, *A p53 amino-terminal nuclear export signal inhibited by DNA damage-induced phosphorylation.* Science, 2001. **292**(5523): p. 1910-5.
221. Milczarek, G.J., J. Martinez, and G.T. Bowden, *p53 Phosphorylation: biochemical and functional consequences.* Life Sci, 1997. **60**(1): p. 1-11.
222. Maniscalco, W.M., et al., *Hyperoxic ventilated premature baboons have increased p53, oxidant DNA damage and decreased VEGF expression.* Pediatr Res, 2005. **58**(3): p. 549-56.
223. Komarov, P.G., et al., *A chemical inhibitor of p53 that protects mice from the side effects of cancer therapy.* Science, 1999. **285**(5434): p. 1733-7.
224. Bi, X. and L.F. Liu, *recA-independent and recA-dependent intramolecular plasmid recombination. Differential homology requirement and distance effect.* J Mol Biol, 1994. **235**(2): p. 414-23.
225. Brosh, R., et al., *p53 counteracts reprogramming by inhibiting mesenchymal-to-epithelial transition.* Cell Death Differ, 2013. **20**(2): p. 312-20.
226. Taylor, S.M. and P.A. Jones, *Multiple new phenotypes induced in 10T1/2 and 3T3 cells treated with 5-azacytidine.* Cell, 1979. **17**(4): p. 771-9.
227. Davis, R.L., H. Weintraub, and A.B. Lassar, *Expression of a single transfected cDNA converts fibroblasts to myoblasts.* Cell, 1987. **51**(6): p. 987-1000.
228. Choi, J., et al., *MyoD converts primary dermal fibroblasts, chondroblasts, smooth muscle, and retinal pigmented epithelial cells into striated mononucleated myoblasts and multinucleated myotubes.* Proc Natl Acad Sci U S A, 1990. **87**(20): p. 7988-92.
229. Baeyens, L., et al., *In vitro generation of insulin-producing beta cells from adult exocrine pancreatic cells.* Diabetologia, 2005. **48**(1): p. 49-57.
230. Zhou, Q., et al., *In vivo reprogramming of adult pancreatic exocrine cells to beta-cells.* Nature, 2008. **455**(7213): p. 627-32.
231. Xie, H., et al., *Stepwise reprogramming of B cells into macrophages.* Cell, 2004. **117**(5): p. 663-76.
232. Cobaleda, C., W. Jochum, and M. Busslinger, *Conversion of mature B cells into T cells by dedifferentiation to uncommitted progenitors.* Nature, 2007. **449**(7161): p. 473-7.
233. Caiazzo, M., et al., *Direct generation of functional dopaminergic neurons from mouse and human fibroblasts.* Nature, 2011. **476**(7359): p. 224-227.
234. Vierbuchen, T., et al., *Direct conversion of fibroblasts to functional neurons by defined factors.* Nature, 2010. **463**(7284): p. 1035-1041.
235. Pfisterer, U., et al., *Direct conversion of human fibroblasts to dopaminergic neurons.* Proceedings of the National Academy of Sciences, 2011. **108**(25): p. 10343-10348.
236. Meng, F., et al., *Induction of fibroblasts to neurons through adenoviral gene delivery.* Cell Res, 2012. **22**(2): p. 436-40.
237. Kodama, H., et al., *MC3T3-G2/PA6 preadipocytes support in vitro proliferation of hemopoietic stem cells through a mechanism different from that of interleukin 3.* J Cell Physiol, 1986. **129**(1): p. 20-6.

238. Kawasaki, H., et al., *Induction of midbrain dopaminergic neurons from ES cells by stromal cell-derived inducing activity.* Neuron, 2000. **28**(1): p. 31-40.
239. Vazin, T., et al., *A novel combination of factors, termed SPIE, which promotes dopaminergic neuron differentiation from human embryonic stem cells.* PLoS One, 2009. **4**(8): p. e6606.
240. Schulz, T.C., et al., *Differentiation of human embryonic stem cells to dopaminergic neurons in serum-free suspension culture.* Stem Cells, 2004. **22**(7): p. 1218-38.
241. Rolletschek, A., et al., *Differentiation of embryonic stem cell-derived dopaminergic neurons is enhanced by survival-promoting factors.* Mech Dev, 2001. **105**(1-2): p. 93-104.
242. Zeng, X., et al., *Dopaminergic differentiation of human embryonic stem cells.* Stem Cells, 2004. **22**(6): p. 925-40.
243. Perrier, A.L., et al., *Derivation of midbrain dopamine neurons from human embryonic stem cells.* Proc Natl Acad Sci U S A, 2004. **101**(34): p. 12543-8.
244. Park, S., et al., *Generation of dopaminergic neurons in vitro from human embryonic stem cells treated with neurotrophic factors.* Neurosci Lett, 2004. **359**(1-2): p. 99-103.
245. Sasai, Y., et al., *Regulation of neural induction by the Chd and Bmp-4 antagonistic patterning signals in Xenopus.* Nature, 1995. **377**(6551): p. 757.
246. Steinbeisser, H., et al., *The role of gsc and BMP-4 in dorsal-ventral patterning of the marginal zone in Xenopus: a loss-of-function study using antisense RNA.* EMBO J, 1995. **14**(21): p. 5230-43.
247. Cooper, O., et al., *Differentiation of human ES and Parkinson's disease iPS cells into ventral midbrain dopaminergic neurons requires a high activity form of SHH, FGF8a and specific regionalization by retinoic acid.* Molecular and Cellular Neuroscience. **45**(3): p. 258-266.
248. Zetterström, R.H., et al., *Cellular expression of the immediate early transcription factors Nurr1 and NGFI-B suggests a gene regulatory role in several brain regions including the nigrostriatal dopamine system.* Brain Res Mol Brain Res, 1996. **41**(1-2): p. 111-20.
249. Zetterström, R.H., et al., *Dopamine neuron agenesis in Nurr1-deficient mice.* Science, 1997. **276**(5310): p. 248-50.
250. Hermanson, E., et al., *Nurr1 regulates dopamine synthesis and storage in MN9D dopamine cells.* Exp Cell Res, 2003. **288**(2): p. 324-34.
251. Sakurada, K., et al., *Nurr1, an orphan nuclear receptor, is a transcriptional activator of endogenous tyrosine hydroxylase in neural progenitor cells derived from the adult brain.* Development, 1999. **126**(18): p. 4017-26.
252. Cazorla, P., et al., *A response element for the homeodomain transcription factor Ptx3 in the tyrosine hydroxylase gene promoter.* J Neurochem, 2000. **74**(5): p. 1829-37.
253. Lebel, M., et al., *Pitx3 activates mouse tyrosine hydroxylase promoter via a high-affinity binding site.* J Neurochem, 2001. **77**(2): p. 558-67.
254. Messmer, K., et al., *Induction of tyrosine hydroxylase expression by the transcription factor Pitx3.* Int J Dev Neurosci, 2007. **25**(1): p. 29-37.

255. Papanikolaou, T., et al., *In-vitro analysis of Pitx3 in mesodiencephalic dopaminergic neuron maturation.* Eur J Neurosci, 2009. **29**(12): p. 2264-75.
256. Martinat, C., et al., *Cooperative transcription activation by Nurr1 and Pitx3 induces embryonic stem cell maturation to the midbrain dopamine neuron phenotype.* Proc Natl Acad Sci U S A, 2006. **103**(8): p. 2874-9.
257. Volpicelli, F., et al., *Direct regulation of Pitx3 expression by Nurr1 in culture and in developing mouse midbrain.* PLoS One, 2012. **7**(2): p. e30661.
258. Courtois, E.T., et al., *In vitro and in vivo enhanced generation of human A9 dopamine neurons from neural stem cells by Bcl-XL.* J Biol Chem, 2010. **285**(13): p. 9881-97.
259. Roybon, L., et al., *Effects on differentiation of embryonic ventral midbrain progenitors by Lmx1a, Msx1, Ngn2, and Pitx3.* J Neurosci, 2008. **28**(14): p. 3644-56.
260. Sánchez-Danés, A., et al., *Efficient generation of A9 midbrain dopaminergic neurons by lentiviral delivery of LMX1A in human embryonic stem cells and induced pluripotent stem cells.* Hum Gene Ther, 2012. **23**(1): p. 56-69.
261. Friling, S., et al., *Efficient production of mesencephalic dopamine neurons by Lmx1a expression in embryonic stem cells.* Proc Natl Acad Sci U S A, 2009. **106**(18): p. 7613-8.
262. Lin, W., et al., *Foxa1 and Foxa2 function both upstream of and cooperatively with Lmx1a and Lmx1b in a feedforward loop promoting mesodiencephalic dopaminergic neuron development.* Dev Biol, 2009. **333**(2): p. 386-96.
263. Nakatani, T., et al., *Lmx1a and Lmx1b cooperate with Foxa2 to coordinate the specification of dopaminergic neurons and control of floor plate cell differentiation in the developing mesencephalon.* Dev Biol, 2010. **339**(1): p. 101-13.
264. Lee, H.S., et al., *Foxa2 and Nurr1 synergistically yield A9 nigral dopamine neurons exhibiting improved differentiation, function, and cell survival.* Stem Cells, 2010. **28**(3): p. 501-12.
265. Theka, I., et al., *Rapid generation of functional dopaminergic neurons from human induced pluripotent stem cells through a single-step procedure using cell lineage transcription factors.* Stem Cells Transl Med, 2013. **2**(6): p. 473-9.
266. Schneider, B.L., et al., *Over-expression of alpha-synuclein in human neural progenitors leads to specific changes in fate and differentiation.* Hum Mol Genet, 2007. **16**(6): p. 651-66.
267. Hartfield, E.M., et al., *Physiological Characterisation of Human iPS-Derived Dopaminergic Neurons.* PLoS One, 2014. **9**(2): p. e87388.
268. Lufino, M.M., et al., *Episomal transgene expression in pluripotent stem cells.* Methods Mol Biol, 2011. **767**: p. 369-87.
269. Banito, A., et al., *Senescence impairs successful reprogramming to pluripotent stem cells.* Genes Dev, 2009. **23**(18): p. 2134-9.
270. Feng, B., *Molecules that Promote or Enhance Reprogramming of Somatic Cells to Induced Pluripotent Stem Cells.* 2009.
271. Hong, H., et al., *Suppression of induced pluripotent stem cell generation by the p53-p21 pathway.* Nature, 2009. **460**(7259): p. 1132-5.
272. Okita, K., et al., *A more efficient method to generate integration-free human iPS cells.* Nat Methods, 2011. **8**(5): p. 409-12.

273. Brown, H.F., C. Unger, and A. Whitehouse, *Potential of herpesvirus saimiri-based vectors to reprogram a somatic Ewing's sarcoma family tumor cell line.* J Virol, 2013. **87**(12): p. 7127-39.
274. Alexanian, A.R., Q.S. Liu, and Z. Zhang, *Enhancing the efficiency of direct reprogramming of human mesenchymal stem cells into mature neuronal-like cells with the combination of small molecule modulators of chromatin modifying enzymes, SMAD signaling and cyclic adenosine monophosphate levels.* Int J Biochem Cell Biol, 2013. **45**(8): p. 1633-8.
275. Ladewig, J., et al., *Small molecules enable highly efficient neuronal conversion of human fibroblasts.* Nat Methods, 2012. **9**(6): p. 575-8.
276. Jacobs, K.M., et al., *GSK-3β: A Bifunctional Role in Cell Death Pathways.* Int J Cell Biol, 2012. **2012**: p. 930710.
277. Cordenonsi, M., et al., *Links between tumor suppressors: p53 is required for TGF-beta gene responses by cooperating with Smads.* Cell, 2003. **113**(3): p. 301-14.
278. Cordenonsi, M., et al., *Integration of TGF-beta and Ras/MAPK signaling through p53 phosphorylation.* Science, 2007. **315**(5813): p. 840-3.
279. Liu, M.L., et al., *Small molecules enable neurogenin 2 to efficiently convert human fibroblasts into cholinergic neurons.* Nat Commun, 2013. **4**: p. 2183.
280. Naderi, E.H., et al., *Activation of cAMP signaling interferes with stress-induced p53 accumulation in ALL-derived cells by promoting the interaction between p53 and HDM2.* Neoplasia, 2011. **13**(7): p. 653-63.
281. Maclaine, N.J. and T.R. Hupp, *The regulation of p53 by phosphorylation: a model for how distinct signals integrate into the p53 pathway.* Aging (Albany NY), 2009. **1**(5): p. 490-502.
282. Liu, H., et al., *p53 regulates neural stem cell proliferation and differentiation via BMP-Smad1 signaling and Id1.* Stem Cells Dev, 2013. **22**(6): p. 913-27.
283. Di Giovanni, S., et al., *The tumor suppressor protein p53 is required for neurite outgrowth and axon regeneration.* EMBO J, 2006. **25**(17): p. 4084-96.
284. Liu, Y., et al., *SCYL1BP1 modulates neurite outgrowth and regeneration by regulating the Mdm2/p53 pathway.* Mol Biol Cell, 2012. **23**(23): p. 4506-14.
285. Krisky, D.M., et al., *Deletion of multiple immediate-early genes from herpes simplex virus reduces cytotoxicity and permits long-term gene expression in neurons.* Gene Ther, 1998. **5**(12): p. 1593-603.
286. Zhang, T., et al., *NGFI-B nuclear orphan receptor Nurr1 interacts with p53 and suppresses its transcriptional activity.* Mol Cancer Res, 2009. **7**(8): p. 1408-15.
287. Boutell, C. and R.D. Everett, *Herpes simplex virus type 1 infection induces the stabilization of p53 in a USP7- and ATM-independent manner.* J Virol, 2004. **78**(15): p. 8068-77.
288. Boutell, C. and R.D. Everett, *The herpes simplex virus type 1 (HSV-1) regulatory protein ICP0 interacts with and Ubiquitinates p53.* J Biol Chem, 2003. **278**(38): p. 36596-602.
289. Hobbs, W.E. and N.A. DeLuca, *Perturbation of cell cycle progression and cellular gene expression as a function of herpes simplex virus ICP0.* J Virol, 1999. **73**(10): p. 8245-55.

290. Nagel, C.H., et al., *Herpes simplex virus immediate-early protein ICP0 is targeted by SIAH-1 for proteasomal degradation.* J Virol, 2011. **85**(15): p. 7644-57.
291. Liu, J., et al., *Siah-1 mediates a novel beta-catenin degradation pathway linking p53 to the adenomatous polyposis coli protein.* Mol Cell, 2001. **7**(5): p. 927-36.
292. Nguyen, M.L., et al., *p53 and hTERT determine sensitivity to viral apoptosis.* J Virol, 2007. **81**(23): p. 12985-95.
293. Guo, H., et al., *Immediate-early gene product ICP22 inhibits the trans-transcription activating function of P53-mdm-2.* Sci China C Life Sci, 2007. **50**(4): p. 473-8.
294. Maruzuru, Y., et al., *Roles of p53 in herpes simplex virus 1 replication.* J Virol, 2013. **87**(16): p. 9323-32.
295. Langlois, C., et al., *NMR structure of the complex between the Tfb1 subunit of TFIIH and the activation domain of VP16: structural similarities between VP16 and p53.* J Am Chem Soc, 2008. **130**(32): p. 10596-604.